

# **STUDY OF RHEOLOGICAL BEHAVIOR OF HIGH- PERFORMANCE CONCRETE**

*A Thesis Submitted*

in Partial Fulfillment of the Requirements  
for the Degree of

**DOCTOR OF PHILOSOPHY**

By

Aminul Islam Laskar

Roll No. 05610406



CIVIL ENGINEERING DEPARTMENT  
INDIAN INSTITUTE OF TECHNOLOGY GUWAHATI  
GUWAHATI-781039, INDIA  
MARCH, 2008

## CERTIFICATE

This is to certify that the thesis entitled “Study of Rheological Behavior of High-Performance Concrete” submitted by Aminul Islam Laskar, Roll No. 05610406 to the Indian Institute of Technology, Guwahati for the degree of Doctor of Philosophy in Civil Engineering is a record of bonafide research work carried out by him under my supervision and guidance. The thesis work, in my opinion, has reached the requisite standard fulfilling the requirement for the degree of Doctor of Philosophy.

The results contained in this thesis have not been submitted in part or full to any other University or Institute for award of any degree or diploma.

(Dr. Sudip Talukdar)

Professor,

Dept of Civil Engineering,

Indian Institute of Technology,

Guwahati-781039. INDIA.

## ACKNOWLEDGEMENT

This thesis is the result of the experimental investigation carried out at the department of Civil Engineering at Indian Institute of Technology, Guwahati, India. At the outset, I would like to express my gratitude to my supervisor, Dr. Sudip Talukdar for initiating an interesting and innovative research topic and for his personal commitment, interesting discussion and valuable advice. I appreciate the opportunities I got to develop myself in a new area of concrete technology. He has been continuously encouraging throughout the work and contributed with valuable guidance and supervision.

Majority portion of this thesis was to carry out experiments. This would not have been possible without the support of technical staff of Concrete Laboratory of IIT Guwahati. I will express my gratitude to Dr. Arun Chandra Borsaikia, Scientific Officer, for his earnest effort to procure materials required for the experiment like cement, sand, coarse aggregate, super-plasticizer and steel fibers from time to time at the earliest. I want to thank Mr. Nripen Kalita, technical staff of Concrete laboratory, for his continuous help and ideas about carrying out the experiments.

I would also like to thank Scientific Officers of Central Instrumentation Facility and Chemical Engineering Department of IIT, Guwahati for carrying out SEM-EDX analysis and HAAKE RS1 respectively on my behalf.

Thanks are also due to Prof. Anjan Dutta, Prof. Sajal Kanti Deb and Prof U. S. Dixit who were the members of my doctoral committee and who contributed with valuable remarks and ideas to obtain the final results of this research work.

I would like to acknowledge the suggestions and comments I received via E-mail from Dr. F de Larrard of LCPC (France), Prof PFG Banfill of Heriot-Watt University (UK)

and Prof AK Tamimi of American University of Sharjah (UAE) at various occasions whenever I sought clarification of any doubts.

I would like to thank the Director, National Institute of Technology, Silchar, India for deputing me to pursue the PhD degree under Quality Improvement Program. Finally, I want to thank Elkem (India) Private limited and Fosroc (India) Private limited for providing condensed silica fume and super-plasticizer respectively free of cost.

Besides works, I had a good time with colleagues from Civil Engineering Department Office of IIT Guwahati who helped me a lot at various occasions. I want to thank my parents, wife, children, other family members and friends for their support, encouragement and patience during the period of my research work.

*Aminul Islam Laskar*

**Roll No. 05610406**

*IIT, Guwahati (India)*

*March , 2008.*

# CONTENTS

	LIST OF TABLES	ix
	LIST OF FIGURES	x
	LIST OF SYMBOLS AND ABBREVIATIONS	xiv
	<b>ABSTRACT</b>	xvii
<b>CHAPTER 1</b>	<b>INTRODUCTION</b>	1
1.1	Introduction	1
1.2	Literature Review	4
1.2.1	Workability Tests and Effect of Different Parameters on Workability	5
1.2.2	Rheological Tests and Effect of Different Parameters on Rheology	8
1.2.3	Rheology of High-Performance Concrete (HPC)	13
1.2.4	Some Special Topics on Rheology	30
1.3	Scope and Objective of the Present Study	36
1.4	Organization of the Thesis	39
1.5	Closure	39
<b>CHAPTER 2</b>	<b>DESIGN OF A CONCRETE RHEOMETER</b>	41
2.1	Introduction	41
2.2	Rheological Models	41
2.3	Design of Concrete Rheometer	43
2.3.1	Conceptual Design	43
2.3.2	Actual Design and Construction	45
2.3.3	Governing Equation	48
2.3.4	Calibration of Torque	58
2.4	Validation of Present Rheometer	60
2.5	Testing Procedure for Rheological Measurements	62

	2.6	Repeatability Analysis	63
	2.6.1	Concrete Mix Used	63
	2.6.2	Material Properties	66
	2.6.3	Mixing Procedure	67
	2.6.4	Repeatability	67
	2.7	Effect of Wall Resistance on Rheological Parameters	71
	2.8	Closure	71
<b>CHAPTER</b>	<b>3</b>	<b>RHEOLOGICAL BEHAVIOR OF HIGH-PERFORMANCE CONCRETE WITHOUT MINERAL ADMIXTURES</b>	<b>97</b>
	3.1	Introduction	77
	3.2	Experimental Program	77
	3.2.1	Slump and Slump Flow Test	77
	3.2.2	Density of Fresh Concrete	79
	3.2.3	Bulk Density and Packing Density of Aggregates	79
	3.2.4	Other Tests	79
	3.2.5	Stability by Visual Observation	79
	3.2.6	Rheological Test	80
	3.3	Results and Discussion	81
	3.3.1	Effect of Percentage Sand	81
	3.3.2	Effect of Sand Gradation	82
	3.3.3	Effect of Maximum Size of Coarse Aggregate	82
	3.3.4	Effect of Single Size Coarse Aggregates	83
	3.3.5	Effect of HRWRA Dosage	83
	3.3.6	Effect of Cement Paste to Aggregate Volume Ratio on Bingham Parameters	84
	3.3.7	Effect of Elapsed Time	84
	3.4	Correlation Between Conventional Workability Tests and Rheological Parameters	94

	3.4.1	Slump Test and Rheological Parameters	94
	3.4.2	Slump Flow, Flow time and Rheological Parameters	95
	3.5	Closure	96
<b>CHAPTER</b>	<b>4</b>	<b>RHEOLOGICAL BEHAVIOR OF HIGH PERFORMANCE CONCRETE WITH MINERAL ADMIXTURES AND STEEL FIBERS</b>	<b>101</b>
	4.1	Introduction	101
	4.2	Study with Mineral Admixtures	101
	4.2.1	Scanning Electron Microscopy	101
	4.2.2	X-ray Diffraction Analysis	109
	4.2.3	Experimental Program	110
	4.2.4	Results and Discussion	112
	4.3	Study of Ternary Blends	118
	4.4	Study with Round Steel Fibers	120
	4.4.1	Experimental Program	120
	4.4.2	Results and Discussion	121
	4.5	Correlation of Vebe Time and Percent Flow with Rheological Parameters	126
	4.5.1	Vebe Test	126
	4.5.2	Flow Test	126
	4.5.3	Testing Procedure	127
	4.5.4	Results and Discussion	128
	4.6	Closure	133
<b>CHAPTER</b>	<b>5</b>	<b>MIX DESIGN PROCEDURE OF HIGH PERFORMANCE CONCRETE</b>	<b>134</b>
	5.1	Objective of Mix Design of HPC	134
	5.2	Background of Mix Design of HPC	134
	5.2.1	Water Binder Ratio	135
	5.2.2	Cementitious Materials Content	135

	5.2.3	Mineral Admixtures	135
	5.2.4	Super-plasticizers	135
	5.2.5	Aggregates	136
	5.3	Proposed Method of Mix Design Procedure	137
	5.3.1	IS Code Method of Mix Design Procedure	137
	5.3.2	Steps to Arrive at Mix Proportions	139
	5.4	Examples of Mix Design of HPC Using Proposed Method	144
	5.5	Closure	146
<b>CHAPTER</b>	<b>6</b>	<b>CHARACTERIZATION OF WORKABILITY OF HIGH PERFORMANCE CONCRETE</b>	<b>155</b>
	6.1	Introduction	155
	6.2	Experimental Program	155
	6.3	Results and Discussion	158
	6.4	Closure	160
<b>CHAPTER</b>	<b>7</b>	<b>SUMMARY AND CONCLUSION</b>	<b>163</b>
	7.1	Summary of Investigation	163
	7.2	Major Findings	164
	7.3	Scope for Future Work	167
	7.4	Concluding Remarks	167
<b>REFERENCE</b>			<b>169</b>
<b>APPENDIX-I</b>		Some Basic Principles of Statistics	<b>180</b>

## LIST OF TABLES

Table 1.1	Shear rates in various operations	36
Table 2.1	Preliminary design requirements	46
Table 2.2	Mix proportions and mix designations	63
Table 2.3.	Sieve Analysis of Sand	68
Table 2.4.	Sieve Analysis of Coarse Aggregate	68
Table 2.5.	Sample size for Yield stress ( $\tau_0$ ) and Plastic Viscosity ( $\mu$ )	72
Table 2.6	Comparison of rheological parameters with and without wall resistance	72
Table 3.1.	Mix proportions and mix designations	78
Table 3.2	Mix proportions used for slump and slump flow tests	96
Table 4.1	Chemical composition of cement and other additives	111
Table 4.2	Mix proportions and mix designations	111
Table 4.3	Mix proportions and mix designations	121
Table 4.4	Mix proportions for studying Vebe and % flow	129
Table 5.1	Approximate sand and water content for w/c=0.35; CF=0.80	139
Table 5.2	Adjustment of values in water content and %sand for other conditions	139
Table 5.3	Mixtures containing PC as HRWRA	152
Table 5.4	Mixtures containing SN as HRWRA	153
Table 5.5	Correction factors for $\tau_0$	154
Table 5.6	Correction factors for $\mu$	154
Table 6.1	Mixtures containing PC as HRWRA	156
Table 6.2	Mixtures containing SN as HRWRA	157

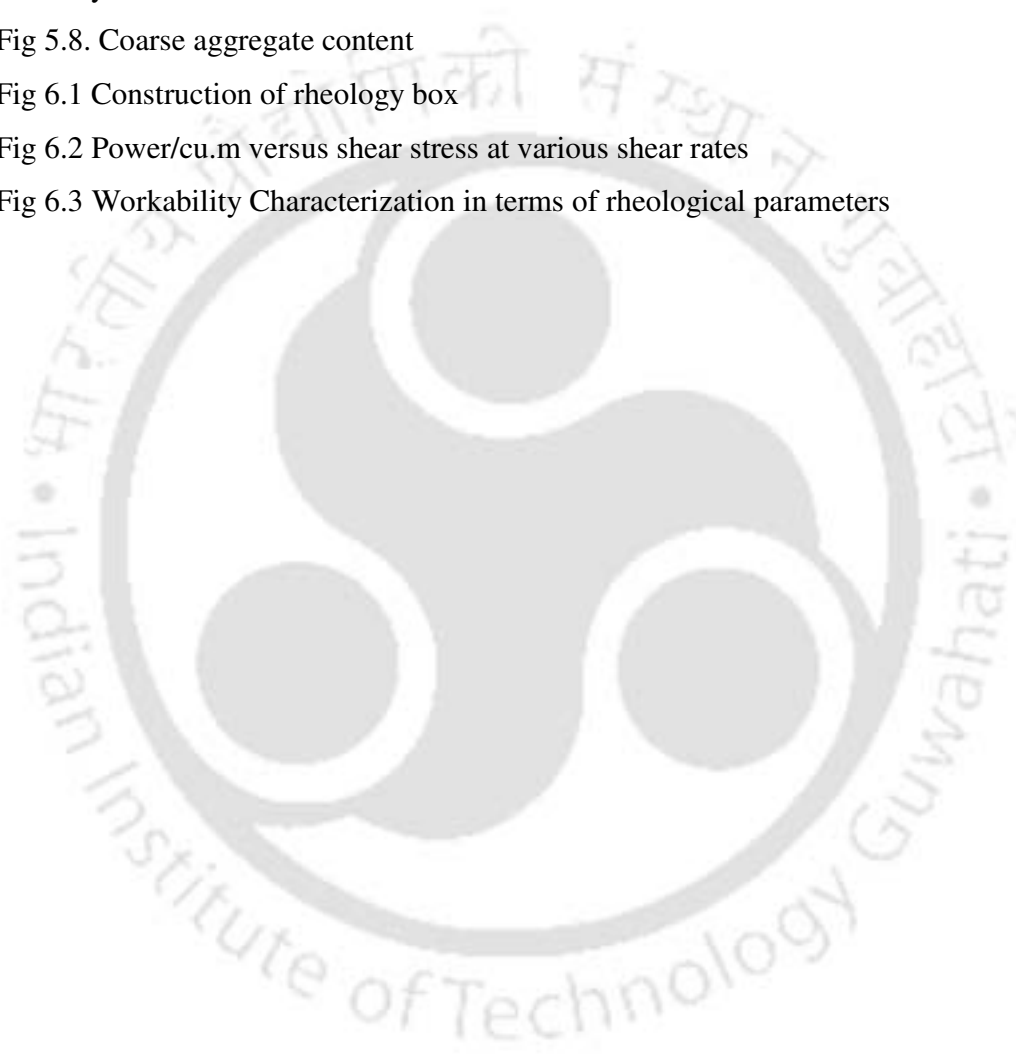
## LIST OF FIGURES

Fig 1.1	Representation of Bingham's model	3
Fig1.2	Rheology of fresh concrete	4
Fig 1.3.	Equivalence of rheology and workability	5
Fig 2.1	Principle of available parallel plate rheometers (Velocity profiles are all at the surface)	45
Fig 2.2	(a) Impeller (b) Cylindrical container of present rheometer	50
Fig 2.3	Schematic diagram of present rheometer	50
Fig 2.4.	Photograph of present rheometer	51
Fig 2.5.	Flow of concrete below vane plate	53
Fig 2.6	Flow of concrete in the annulus	54
Fig 2.7	Velocity profile at mid-height (a)on horizontal plane (b) sectional elevation	57
Fig 2.8.	Calibration Chart for Torque	64
Fig 2.9.	HAAKE RS1 rheometer	64
Fig 2.10.	Visco-elastic measurement of MR fluid with HAAKE RS1 at shear rate 30 per sec	65
Fig 2.11.	Validation of torque using MR fluid	65
Fig 2.12:	Plug flow correction	66
Fig 2.13	Flow curve of Mix A1	73
Fig 2.14	Flow curve of Mix A2	73
Fig 2.15.	Histogram of Yield stress (Mix A1)	74
Fig 2.16.	Histogram of Plastic Viscosity (Mix A1)	74
Fig 2.17.	Histogram of Yield stress (Mix A2)	75
Fig 2.18.	Histogram of Plastic Viscosity (Mix A2)	75
Fig. 2.19.	Flow curve of Mix A1 with and without wall resistance	76
Fig 3.1	Slump and slump flow test	78
Fig 3.2	No segregation after slump flow	80
Fig 3.3	No segregation even though slight halo present	81
Fig 3.4	Segregation due to large mortar halo and aggregate piling at centre	81

Fig 3.5 Effect of % sand on rheological parameters (a) Effect on yield stress (b) Effect on plastic viscosity	86
Fig 3.6 Effect of sand zone on rheological parameters (a) Effect on yield stress (b) Effect on plastic viscosity	87
Fig 3.7 Effect of maximum size of coarse aggregate on rheological parameters (a) Effect on yield stress (b) Effect on plastic viscosity	88
Fig 3.8 Effect of average coarse aggregate size on rheological parameters (a) Effect on yield stress (b) Effect on plastic viscosity	89
Fig 3.9 Effect of HRWRA dose on rheological parameters (a) Effect on yield stress (b) Effect on plastic viscosity	90
Fig 3.10 Effect of cement paste/aggregate volume ratio (a) Effect on yield stress (b) Effect on plastic viscosity	91
Fig 3.11 Effect of cement paste/aggregate volume ratio and w/c ratio (a) Effect on yield stress (b) Effect on plastic viscosity	92
Fig 3.12. Effect of elapsed time on rheological parameters (a) Effect on yield stress (b) Effect on plastic viscosity	93
Fig 3.13 Relationship between rheological parameters and slump (a) yield stress (b) Plastic viscosity	98
Fig 3.14 Relationship between rheological parameters and slump (a) yield stress (b) Plastic viscosity	99
Fig 3.15 Relationship between rheological parameters and slump (a) yield stress (b) Plastic viscosity	100
Fig 4.1. Mineral admixtures used in the present study (a) Condensed silica fume (b) Fly ash (c) Rice husk ash	102
Fig 4.2. Scanning electron microscope used in the present study	102
Fig 4.3. SEM images of fly ash	104
Fig 4.4. SEM images of RHA	105
Fig 4.5 SEM images of CSF	106
Fig 4.6 EDX patterns of CSF at two spots	107
Fig 4.7 EDX pattern of PFA at two spots	108
Fig 4.8 EDXA of RHA	109

Fig 4.9 XRD pattern of RHA	109
Fig 4.10 XRD pattern of CSF	110
Fig 4.11 Effect of PFA replacement on rheological parameters (a) Effect on yield stress (b) Effect on plastic viscosity	115
Fig. 4.12 Effect of CSF replacement on rheological parameters (a) Effect on yield stress (b) Effect on plastic viscosity	116
Fig. 4.13 Effect of RHA replacement on rheological parameters (a) Effect on yield stress (b) Effect on plastic viscosity	117
Fig 4.14 Effect of ternary blends on rheological parameters (a) Effect on yield stress (b) Effect on plastic viscosity	119
Fig 4.15 Effect of fiber volume fraction on Bingham parameters (a) Effect on yield stress (b) Effect on plastic viscosity	123
Fig 4.16. Effect of aspect ratio of fiber on rheological parameters (a) Effect on yield stress (b) Effect on plastic viscosity	124
Fig 4.17. Effect of fiber diameter on Bingham parameters (a) Effect on yield stress (b) Effect on plastic viscosity	125
Fig 4.18 Vebe test	127
Fig 4.19 Flow test	128
Fig 4.20. Flow test of FRC (a) After lifting the cone (b) After jolting the flow table	153
Fig 4.21: Variation of rheological parameters with Vebe time (a) Yield stress (b) Plastic viscosity	131
Fig 4.22. Variation of percentage flow with rheological parameters (a) yield stress (b) plastic viscosity	132
Fig 5.1. Variation of compressive strength with yield stress (Mixes with PC)	148
Fig 5.2. Variation of compressive strength with plastic viscosity (Mixes with PC)	148
Fig 5.3 Variation of compressive strength with plastic viscosity (Mixes with SN)	149
Fig 5.4. Variation of compressive strength with yield value (Mixes with	149

SN)	
Fig 5.5. Variation of compressive strength with rheological parameters (with SN)	150
Fig 5.6 Variation of aggregate volume/paste volume ratio with yield stress	150
Fig 5.7 Variation of aggregate volume/paste volume ratio with plastic viscosity	151
Fig 5.8. Coarse aggregate content	151
Fig 6.1 Construction of rheology box	161
Fig 6.2 Power/cu.m versus shear stress at various shear rates	161
Fig 6.3 Workability Characterization in terms of rheological parameters	162



## LIST OF SYMBOLS AND ABBREVIATIONS

<b>Symbols</b>	<b>Meaning</b>
$V$	Absolute volume of fresh concrete
$W$	Mass of water per cu.m of concrete
$C$	Mass of cement per cu.m of concrete
$S_c$	Specific gravity of cement
$p$	% sand
$f_a$	Total mass of fine aggregates
$C_a$	Total mass of coarse aggregates
$S_{fa}$	Specific gravity of fine aggregates
$S_{ca}$	Specific gravity of coarse aggregates
$\tau_o$	Yield stress, Pa
$\mu$	Plastic viscosity, Pa.s
$\tau$	Shear stress, Pa
$\dot{\nu}$	Shear strain rate, Per sec
$\tau_{o,i}$	Interfacial yield stress;
$\eta_o$	Interfacial viscous constant (Pa.s/m)
$v_g$	Sliding velocity (m/s)
$\omega$	Angular velocity, rad/sec
$\tau_r$	Resting yield stress
$\tilde{\tau}_o$	Yield stress related to reversible coagulation state
$\tilde{\mu}$	Plastic viscosity related to reversible coagulation state
$N$	Rotational frequency in revolution per minute
$d$	Diameter of the vane plate
$h$	Effective gap between bottom of the vane plate and the bottom of the cylinder
$t$	Height of the ribs of vane plate
$g$	Effective gap of the annulus

$E_{20}$	Induced emf in rotor winding when the stator is at standstill
$N_r$	Rotor speed, rpm
$N_s$	Speed of flux cutting
$V_1$	Stator applied voltage,
$\phi_2$	Phase difference between rotor current, $I_2$ and rotor voltage $E_2$ ,
$X_{20}$	Leakage reactance of rotor winding when rotor is at standstill,
$I_{20}$	Rotor current at standstill
$I_2$	Rotor current at slip $S$
$S$	Slip
$E_2$	Rotor voltage
$T$	Mechanical torque developed by the rotor
$V_1$	Stator applied voltage
$a$	No. of class intervals
$\bar{x}$	Sample mean
$m$	Population mean
$s$	Sample standard deviation
$t_I$	Tabulated Student's t value
$n$	Sample size to be predicted
$E$	Permissible error
$\beta$	Packing density,
$\rho$	Density of particles
$\gamma_b$	Bulk density of particles
$D_{av}$	Weighted mean size
$M_i$	% retained on the $i$ th sieve
$D_i$	Size of particular $i$ -th sieve
$\Phi$	Volume concentration
$\Phi^*$	Maximum packing density
$S_f$	Slump flow

$S$	Slump
$S_t$	Slump time in seconds
$\dot{E}$	Energy dissipation rate per unit volume

<b>Abbreviations</b>	<b>Meaning</b>
HPC	High Performance Concrete
HRWRA	High Range Water Reducing Admixtures
SP	Super-plasticizer
FMS	Melamine formaldehyde sulfonate
VMA	Viscosity modifying admixtures
pfa or PFA	Pulverized fuel ash
CSF	Condensed Silica fume
RHA	Rice Husk Ash
FRC	Fiber Reinforced Concrete
SFRC	Steel fiber reinforced concrete
SSM	Solid Suspension Model
SN	Sulphonated Naphthalene formaldehyde
PC	Poly-carboxylic ether polymer
emf	Electro-magnetic field
MRF	Magneto-rheological fluid
OPC	Ordinary Portland cement
COV	Coefficient of variation
SEM	Scanning electron microscopy
EDX	Energy dispersive X-ray analyzer
XRD	X-ray diffraction analysis
HSC	High strength concrete
w/c	Water cement ratio
M <sub>sa</sub>	Nominal maximum size of aggregate

## ABSTRACT

High performance concrete has become indispensable in construction of modern high rise buildings, long span bridges, nuclear structures, off shore structures and in many other applications. This is generally preferred for high strength and high durability. To achieve these objectives, production of concrete should be given due consideration in terms of proper workability. Principles of fluid rheology have been found to describe workability of high performance concrete in a more scientific way than conventional empirical rules do. Rheology of fresh concrete is recognized as difficult subject due to the fact that concrete is a complex material with time dependent properties and includes wide range of particle sizes. It has been found that concrete can be considered as Bingham fluid with good accuracy where flow is described by two parameters: yield stress and plastic viscosity. Two types of rheometers viz. coaxial and parallel plate type are in use to determine rheological parameters of cementitious materials and concrete. While the rheometers for cement pastes and cementitious material are more or less established in terms of its functioning, concrete rheometers still today present challenge in design and operation because of large size of coarse aggregate.

The present study undertakes the design and construction of a new rheometer with parallel plate geometry. Frictional resistance between concrete and vertical wall of cylindrical container has been taken into account while deriving expression for total torque. Measures have been taken to prevent wall slip by providing ribs in the cylindrical container of the rheometer. Concrete is subjected to torsion where the shear rate is not uniform in all areas of material. This non-uniform variation of shear rate has been taken

in to account while deriving the expression for the torque. For practical use, shear stress versus torque and overall shear strain rate versus rotational frequency relationships have been established for the given geometry of the rheometer.

Calibration of torque in the present rheometer has been performed by rotor blocking method. Calibration of torque was validated by testing a magneto-rheological fluid (MRF 132DG) with the present rheometer and comparing these test results with the results independently obtained by HAAKE RS1 rheometer. It was observed that measured values of MRF properties by the present rheometer and HAAKE RS1 are comparable. Repeatability of the tests has been judged by statistical approach.

The presently developed rheometer has been used to investigate rheology of high performance concrete without using any mineral admixtures and then using different mineral admixtures and steel fibers. In concrete without mineral admixtures, experiments have been conducted to examine the influence of some basic parameters such as percentage sand, aggregate gradation, chemical admixture dosage and elapsed time on rheological properties of high performance concrete (HPC). It was observed that different parameters affected rheological parameters in different manners. Optimum values exist for percent sand, sand zone and HRWRA dose. It was also observed that, in addition to water-cement ratio, cement paste volume/aggregate volume ratio affect the rheological parameters of concrete.

In the next step, a study has been conducted employing three different mineral admixtures such as pozzolanic fly ash (PFA), condensed silica fume (CSF) and rice husk ash (RHA). Individual use of these admixtures and ternary blends has been included in the experimental program. Morphology has been studied by scanning electron

microscope to better interpret the effect of admixtures on workability. It has been observed that yield stress decreases as the replacement level of rice husk ash and fly ash increases. On the other hand, silica fume seems to be a better material for moderate plastic viscosity needed for the design of high performance concrete. For low yield stress and moderate plastic viscosity, blending of equal masses of silica fume and rice husk ash seems to be suitable admixture at different replacement levels.

Fibers are used in concrete to increase toughness and ductility. The addition of steel fibers to concrete tremendously decreases workability. Further experiments have been conducted using round steel fibers of various aspect ratios, different diameters and volume fractions. Decrease in workability of fibers reinforced concrete has been observed in rheological tests. Experimental investigations have been carried out to correlate conventional workability tests such as slump and slump flow test to the rheological parameters determined with the present rheometer. Variation of yield stress and plastic viscosity of steel fiber reinforced concrete with percent flow and Vebe time were also investigated.

Compressive strength is greatly influenced by the performance of concrete in its fresh stage such as uniform mixing, proper compaction, resistance to segregation during transporting and placing. Attempt has, therefore, been made to correlate compressive strength to the rheological behavior of high performance concrete. It has been observed that compressive strength increases steeply as the yield stress increases up to a certain level. Plastic viscosity, however, shows optimum value for maximum compressive strength.

It is found that mix design procedure of high performance concrete is not well established since the water-cement ratio is not a very good predictor of compressive strength in case of high performance concrete. A mix design procedure of high performance concrete has been proposed based on rheological parameters. Correction factors for yield stress and plastic viscosity have been found out for different sand zones and maximum aggregate size for working out mix proportions.

Finally, a power based scale of workability combining three parameters namely yield stress, plastic viscosity and shear strain rate has been developed. It is possible to assess the workability category with this new scale of energy dissipation rate of concrete flow. Shear rate plays a critical role in workability characterization of high performance concrete in addition to yield stress and plastic viscosity.

# **CHAPTER 1**

## **INTRODUCTION AND LITERATURE REVIEW**

### **1.1. INTRODUCTION**

Concrete has become the most widely used structural material today. Concrete has two distinct stages- fresh and hardened stage. Hardened concrete should possess definite shape, good appearance, adequate strength and durability. To achieve these, the fresh concrete should have a suitable composition in terms of quality and quantity of cement, aggregates and admixtures. In addition, concrete should satisfy a number of requirements from mixing stage till it is transported, placed in forms and compacted. One should be able to produce a homogeneous fresh concrete from the constituent materials of the batch under the action of mixing forces. A less mixable concrete mix requires more time to produce a homogeneous and uniform mix. This property is termed as mixability. The mix should be stable such that it should not segregate during transportation and placing. Any segregation caused during transportation operation does not correct during remaining operations to follow. The tendency of bleeding should be minimized. The mix need be cohesive and sufficiently mobile to be placed in the form around the reinforcement and should be able to cast into the required shape without losing continuity or homogeneity. This property is termed as flowability or mobility. The mix should be amenable to proper and thorough compaction into dense and compact concrete with minimum voids. This property is termed as compactability. It should be possible to attain a satisfactory surface finish without honeycombing or blowing holes from formwork and on free surface by trowelling and other processes. This capability is termed as finishability.

The diverse requirements of mixability, stability, placeability, mobility, compactability, and finishability of fresh concrete are collectively referred to as “workability” of concrete. The workability of fresh concrete is thus a composite property. It is difficult to define precisely all the aspects of workability in a single definition. ACI 116R-90 defines workability as that property of freshly mixed concrete or mortar, which determines the ease and homogeneity with which it can be mixed, placed, compacted and finished. The Indian Standard Code of Practice (IS: 6461-1973) defines workability as that property of

freshly mixed concrete or mortar, which determines the ease and the homogeneity with which it can be mixed, placed, compacted and finished. The American Standards of Testing Materials (ASTM C 125-93) defines workability as that property of determining the effort required to manipulate a freshly mixed quantity of concrete with minimum loss of homogeneity.

The workability of fresh concrete is a critical property that has a direct impact on strength, durability, appearance and cost of concrete. In construction field, terms like workability, flowability and cohesion are used, sometimes interchangeably to describe behavior of concrete under flow. The definitions of these terms are quite subjective and no agreement can be found among the definitions. All the terms used are defined according to the feeling of the persons and are not based from the physical behavior of the material. During the course of time, workability tests of different types and quality have been developed and used, to give some kind of description of the fresh concrete. It is pointed out that all empirical workability tests are single-point tests, i.e. the result is a single number. No workability test is able to provide adequate information of fresh concrete properties.

In recent years, high performance concrete (HPC) mixes are in demand for the construction of critical structures like high rise buildings, long span bridges, nuclear structures, offshore structures in environmentally unfavorable situation. The term HPC is applied to concrete mixtures possessing three characteristics: high workability, high strength, and high durability. The significance of high workability is obvious. It is one of the key factors that affect the constructability. A concrete mixture that cannot be placed easily or compacted fully is not likely to yield the expected strength and durability characteristics. High performance concrete must be able to flow into corners of the formwork to fill it completely. Concrete of unsuitable consistency results in honeycombed and non-homogeneous mass. This may often lead to strength degradation, loss of serviceability and aesthetics. To avoid such adverse things, sufficient care should be taken to provide concrete of suitable “workability”.

There is increasing pressure on engineers to ensure high workability while at the same time maintain the structural properties necessary to meet design specifications. Researchers treat fresh concrete as fluid and use fluid rheology methods to describe

concrete behavior. Concrete as a fluid is most often assumed to behave like a Bingham fluid with good accuracy. In Bingham model, flow is defined by two parameters: yield stress and plastic viscosity. Yield stress gives the quantitative measure of initial resistance of concrete to flow and plastic viscosity governs the flow after it is initiated. Yield stress is the contribution of the skeleton i.e. it is a manifestation of friction among solid particles. It is the result of an accumulation of contributions of each granular class, these contributions involving size and roughness of particles and their affinity for High Range Water Reducing Admixtures (HRWRA). Plastic viscosity is the contribution of suspending liquid that results from viscous dissipation due to the movement of water in the sheared material. Plastic viscosity appears to be controlled essentially by the ratio of solid volume to the packing density of granular mixture, including aggregates and cement. To determine the Bingham parameters with a rheometer, fresh concrete is sheared at high rate before the rheological test. Then, shear rate is decreased gradually and stress is measured. The relationship between shear stress and shear rate is plotted as flow curve [Fig 1.1]. The intercept at zero shear rate is yield stress,  $\tau_o$ , while the slope of the flow curve is plastic viscosity  $\mu$ .

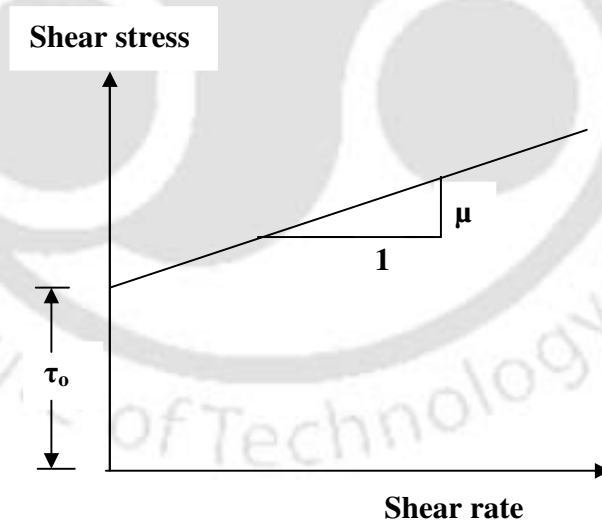


**Fig 1.1** Representation of Bingham's model

Nevertheless, the most commonly used tests to describe concrete flow are limited to the measurement of only one parameter, often directly not related to either of the Bingham

parameters. For advancements to be made in understanding and controlling the workability of fresh concrete, testing procedures and Standards must move to a more fundamental quantitative basis. Accordingly, workability should be defined in terms of established measurable parameters such as yield stress and plastic viscosity. Today, through the use of rheometers, concrete rheology has emerged as a viable technique for characterizing workability of cementitious materials.

Relationship between rheology and workability of fresh concrete is shown in **Fig 1.2**.

Equivalence of parameters defining rheology and workability is presented in **Fig 1.3**.

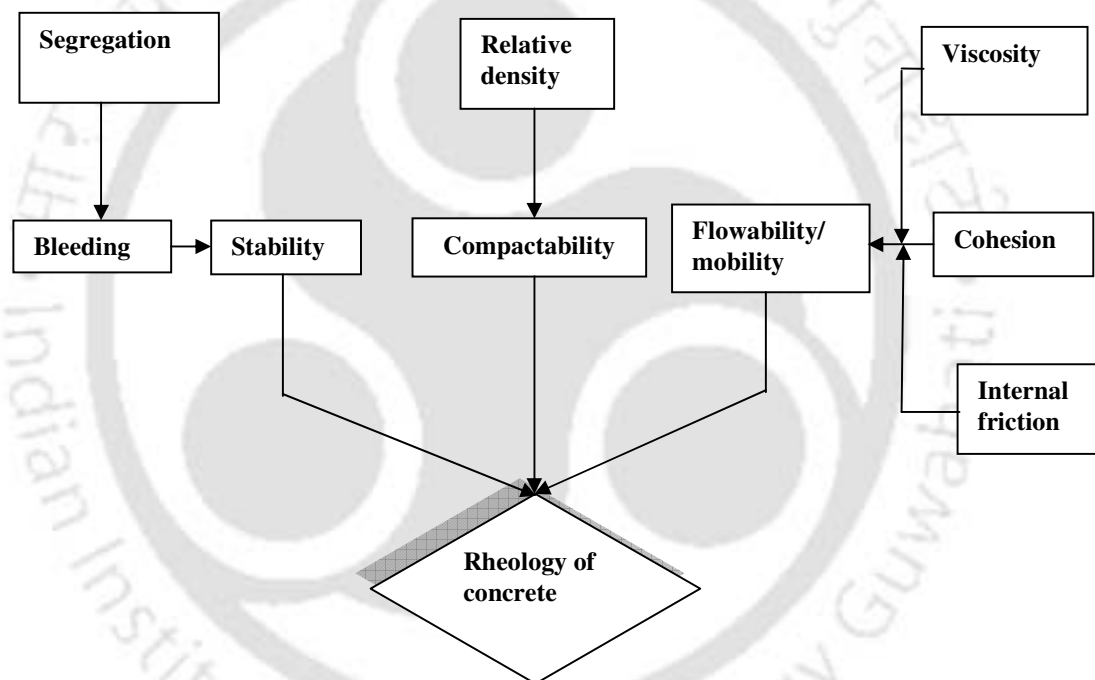


**Fig1.2** Rheology of fresh concrete

## 1.2. LITERATURE REVIEW

Literature on the properties of fresh concrete rheology is abundant. A detailed survey has been carried out to find out the research aim. In this section, works carried out by the past authors has been discussed and inadequacy or shortfall of the earlier studies has been pointed out. Review presented in this section has been grouped into four different topics:

- i) Workability tests and effect of different parameters on workability
- ii) Rheological tests and effect of different parameters on rheology
- iii) Rheology of high-performance concrete (HPC)
- iv) Some special topics on rheology

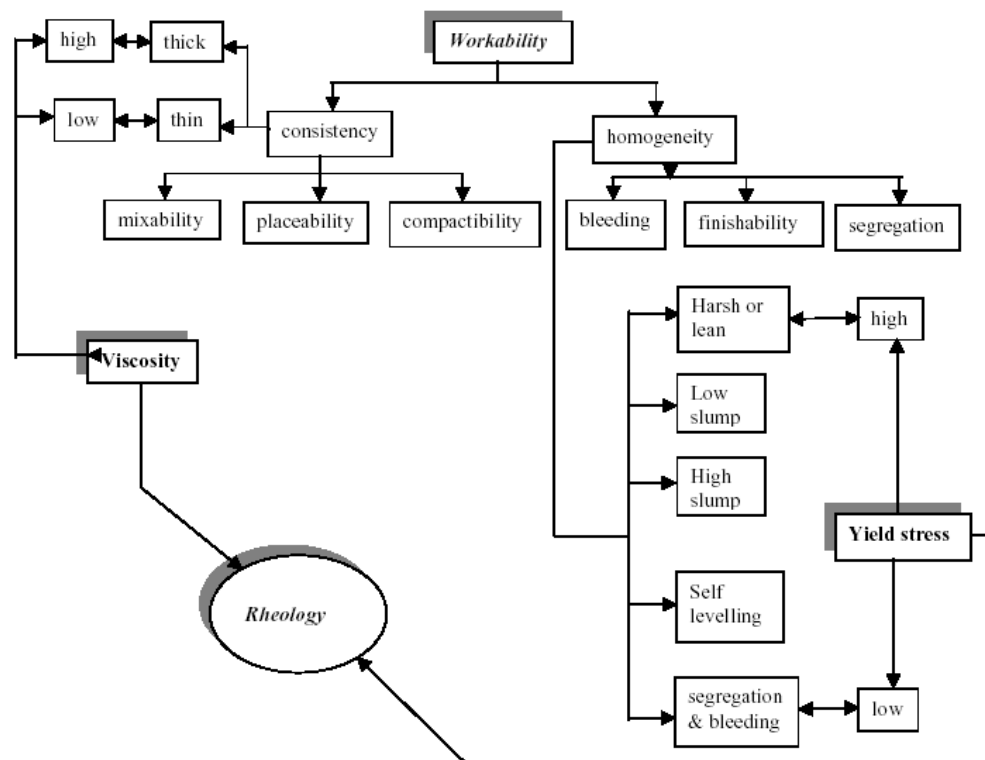


Fig 1.3. Equivalence of rheology and workability

### 1.2.1. Workability Tests and Effect of Different Parameters on Workability

Scanlon [1994] presents a comprehensive review of the test procedures and factors influencing concrete workability. The workability of concrete mixtures is affected by water content, cement content, aggregate grading and admixtures.

A large number of workability test have been developed so far and a good review have been done by Koehler and Fowler [2003] and Ferraris [1996]. One of the most famous, oldest and most widely used empirical tests is the slump test. Slump test has been prescribed by various Standards all over the world. The slump test does not measure the workability of concrete, although ACI 116R-90 describes it as a measure of consistency. With different aggregates, same slump can be recorded for different workability. Slump test does not reflect behavior under dynamic condition such as vibration, finishing, pumping and moving through a tremie.

After the invention of slump test, other workability tests have been developed like flow table test, compacting factor test, Vebe test, ball penetration test etc [Neville, 2003]. Compacting factor test is more sensitive at the low workability end of the scale than at high workability. Vebe is a good laboratory test for dry mixes and it has the advantage that the treatment of concrete during the test is comparatively related to the method of placing in practice. Flow test has become more widely used in recent years as it is considered appropriate for concrete of high and very high workability which would exhibit a collapse slump.

ACI 211.1: Standard Practice for Proportioning Concrete Mixtures assumes that for a given maximum size of coarse aggregate, the slump or consistency of concrete is a direct function of the water content; that is, within limits it is independent of other factors such as aggregate grading and cement content. It is to be mentioned that in predicting the influence of mixture proportions on workability, among the factors water content, cement content and aggregate grading, only two have been reported to be independent [Mehta and Monteiro, 2006]. When the aggregate-cement ratio is reduced at constant water cement ratio, the water content and hence workability increases. Concrete mixtures with high water content tend to segregate and bleed thereby adversely affecting the workability. Mixtures with too low water content may be difficult to place and compact and the coarse aggregate may segregate on placement.

Workability is affected by cement content also. Mehta and Monteiro, [2006] in their text book reported that with conventional Portland cement concrete, at given water content, a drastic reduction of cement content would produce a harsh mixture with poor finishability. Concrete mixtures containing very high cement content or high proportion

of fine particles show excellent cohesiveness but tend to be sticky. In the same text book, effect of particle size of coarse aggregate on the water requirement for a given consistency was discussed. Very fine sand or angular sand requires more water for a given consistency. They will produce harsh and unworkable mixtures at the water content that might have been adequate with coarse or well-rounded sand. The authors also discussed how the addition of chemical admixture increases workability of concrete without changing water content.

Neville, [2003] reported that pozzolanic admixtures tend to reduce the bleeding and improve the cohesiveness of concrete. Fly ash, when used as partial replacement for fine aggregate, generally increases the workability at given water content.

The concrete industry has changed significantly over last century, but the slump test has remained unchanged due to its simplicity. Attempt has been made by researchers to correlate slump to rheological parameters. Morinaga [1973] found an inverse relationship between slump and yield stress determined by concentric cylinder rheometer.

Murata [1984] confirmed the results of Morinaga using normal and light-weight concrete and suggested that slump is not influenced by plastic viscosity. Christensen [1991] corrected integration error in original Murata's model and converted the units to dimensional quantities.

Pashias et al [1996] adopted dimensionless slump model for cylindrical geometries and found excellent agreement between predicted and measured yield stress and plastic viscosity.

Tanigawa and Mori [1989], Tanigawa et al [1991] performed measurements of slump as a function of time and found that both yield stress and plastic viscosity could be related to slump-time curve.

Ferraris and de Larrard [1998] developed a modified slump cone and observed that slump and slump time could be correlated to yield stress and plastic viscosity. Wallevick [2003] demonstrated that there exists a good relationship between slump and yield stress; however, it was concluded that the relationship between plastic viscosity and slump is poor.

Tattersall [1991], Tattersall and Banfill [1983], Tattersall and Bloomer [1989] criticized conventional workability tests on the grounds that they measure only one parameter. The

single-point tests nowadays are considered as incapable of providing an adequate characterization of workability of today's much more advanced concrete mixtures. National Ready Mixed Association Survey identified the need for better method to characterize workability of HPC [Ferraris and Lobo, 1998].

Ferraris et al [2001] listed most common tests with their limitations and it was mentioned that fresh concrete behaves in different way under the applied stress field. The stress to which fresh concrete is subjected during testing influences the particular aspects of workability that can be measured by the test. For example, gravitational stress is predominant in slump test, turning tube viscometer, k-slump, flow cone and slump drop test. Slump values give indication of yield stress of concrete. K-slump values are related to segregation. Flow cone test results measure the ability of concrete to flow through openings. Turning tube viscometers are useful to obtain information about viscosity. In Vebe and LCL apparatus, workability is measured under the action of vibrational stress. Vebe tests are found suitable for measuring workability of concrete with high yield stress. The vibrational tests are actually useful to determine the time required to achieve compaction, an important aspect of workability of fresh concrete.

### **1.2.2. Rheological Tests and Effect of Different Parameters on Rheology**

Rheology is the scientific study of the flow and deformation of the matter. In context of concrete, rheology is used to describe workability of fresh concrete in a quantitative manner. Rheological tests are "two-point" tests meaning that they measure two parameters: yield stress and plastic viscosity. Yield stress represents threshold value for the flow to start whereas plastic viscosity reflects the increase in shear stress with increase in rate of shear.

There are two types of concrete rheometers: rotational and capillary tube rheometers. Hackley and Ferraris, [2001] reported that rotational methods are generally better than capillary methods for concentrated suspension, gel and pastes. Rotational methods offer the advantage of being able to shear a sample indefinitely in order to achieve equilibrium and to monitor changes over time. For non-Newtonian fluids, the distribution of shear stress and shear rate is typically better defined in a rotational device. The rheometers that are commonly available today are: BML (Iceland) [Wallewick, Gjorv,1990], BTRHEOM

(France)[de Larrard et al, 1993; de Larrard et al, 1996], CEMAGREF-IMG (France)[Hu, 1995], IBB (Canada)[Beaupre, 1994], Two-point test (UK) [Tattersal, 1976; Domone et al, 1999] , UIUC rheometer [Szecsy, 1997], ICAR rheometer [Koehler and Fowler, 2004].

### Two-point Test

This is the most widely known instrument for measuring the flow properties of concrete. A vane of special geometry or impeller is lowered into the sample. The vane starts rotating and the resistance on the impeller due to concrete is measured. The planetary motion of the impeller is a standard feature of commercially available Mk apparatus. Torque is measured indirectly through oil pressure in the drive unit. A relationship between oil pressure and torque is to be obtained by prior calibration. Tattersall [1976] designed the first instrument, known as Mk I apparatus. Wallewick and Gjorv [1988], Beaupre [1994] have improved and commercialized it. The test was further modified by Domone, Xu and Banfill [1999]. Based on additional research, Mk I apparatus was later replaced by Mk II for high workability mixes and Mk III for low to medium workability mixes. Ferraris and Browner [2001] criticized Two-point test on the ground that the flow pattern in the instrument is too complicated to allow a calculation of instrument constants. The main difficulty is that no standard granular material was recommended for calibration of the equipment.

### IBB Rheometer

This apparatus is the automated version of the existing apparatus developed by Tattersall [1976]. It was modified in Canada by Beaupre [1994] to study the behavior of high performance shotcrete. The shape of the impeller is H-shaped and has a planetary motion in addition to axial rotation. The concrete bowl leaves a 50 mm gap between the impeller and the bowl. The recommended maximum aggregate size is 25 mm and sample volume is 21 liters. Bartos et al [2002] reported that this instrument can be used to test concrete with slump ranging from 40 mm to 300 mm.

### CEMAGREF-IMG Rheometer

CEMAGREF-IMG is a large coaxial-cylinder rheometer that contains 500 liters of concrete. The outer wall is serrated and the inner one is equipped with metallic grip to check wall slip. The radii of outer and inner cylinder are 120 mm and 76 mm. The height of the sample is 900 mm. Tests are carried out by manual control of the engine power. A rubber seal is fitted to the base of the inner cylinder to avoid any material leakage between the cylinder and the container bottom. The rotational movement is transmitted from motor axis to the inner cylinder through two mechanical linkages, both of which include a load cell that measure the torque transmitted to concrete. Rotation is measured by a dynamo, the axis of which is connected by a wheel to the cap of rotating inner cylinder.

### BML Rheometer

This is a coaxial cylinder rheometer based on the Couette rheometer principle [Tattersal and Banfill, 1983] where the inner cylinder measures torque as the outer cylinder rotates at variable rpm. Several versions have been designed so far from the basic instrument. BML is user friendly, fully automated and is controlled by software called FRESHWIN. Each test takes about 3-5 minutes. During testing the material is sheared for about 1 min. The radii of outer and inner cylinders are 145 mm and 100 mm respectively. The height of the specimen is 150 mm and the volume is about 17 L. Both the cylinders contain ribs parallel to vertical axis. An external load cell and a stopwatch perform the calibration of torque and angular speed. The measured values are inserted in the software that calculates calibration constants.

### BTRHEOM

It is a parallel plate rheometer for soft to fluid concrete (slump > 100 mm) with a maximum size of aggregate up to 25 mm and  $\dot{\gamma}$  ranging 0.5-8 s<sup>-1</sup> [de Larrard et al, 1997]. The rheometer is designed so that concrete having the shape of a hollow cylinder is sheared between a fixed base and a ribbed top section that is rotated around the vertical axis. The motor is housed below the container and is connected to the top blade through a 40 mm diameter shaft that extends through the center of the container. The radii of outer

and inner cylinders are 120 mm and 20 mm. The height of the specimen is 100 mm. The rpm can be varied from 6 to 60. The maximum torque that can be measured is 14 N-m. The limitation of this instrument is that concrete with high plastic viscosity and high yield stress cannot be sheared. There is always a possibility of segregation especially under vibration. The seals are required to be replaced very frequently.

#### UIUC Rheometer

The UIUC concrete rheometer was built at the University of Illinois at Urbana-Champaign (UIUC) by modifying the frame of the Two-point Test [Szecsy, 1997]. The design of this rheometer was based on the BTHREOM, with major changes to reduce the difficulties involved in the installation and cleaning of the apparatus during the experiments. It can be idealized as a pseudo parallel-plate rheometer with additional sidewalls. The radius of the rotating plate is about 120 mm and the gap between two shear plates is about 90 mm.

#### ICAR Rheometer

International Centre for Aggregate Research at the University of Texas at Austin [Koehler and Fowler, 2004] developed a field rheometer that uses the principle of soil vane shear. Rotation speed is measured with an incremental optical encoder mounted to the end of the motor. A non-contact inline torque transducer is connected with couplings between the gearbox and the keyless chuck. This set-up is rugged, portable for use on a jobsite and is commercially available nowadays. But additional work is needed to determine the distribution of shear stress and strain rate within the material. Analytical methods or numerical simulation is required to derive the expression for total torque.

#### Comparison of Rheometers

International tests were conducted in two phases, one at Nantes, France (Ferraris et al, 2001), and the other at Cleveland, USA (Ferraris et al, 2004) to compare the rheometers. It was observed that the rheometers gave different values of the rheological parameters but the degree of correlation of both the parameters between any pair of rheometers was good. Differences in absolute values were attributed to several factors like wall slip,

particle interference and use of different materials for calibration. Thus it was realized that no rheometer was likely to make true fundamental measurements and that additional effort would be required to compare results from one rheometer to another.

### Some Artifacts in Rheological Measurements

With granular suspensions like concrete, an interfacial layer of mortar forms spontaneously in the vicinity of the wall, owing to the exclusion of coarse aggregates, which makes the material more fluid than the bulk of suspension. Ferraris and Browner [2001] described this phenomenon as “wall effect”. It is possible to reduce the slippage due to wall effect by roughening rheometer walls to allow improved packing. Kaplan [2000] reported that for a coaxial rheometer having a mean distance of 100 mm between inner and outer cylinder, and no roughness to avoid slippage, an error of more than 50% can occur in the experimental assessment of Bingham parameters.

Saak et al (2001) studied influence of wall slip on yield stress and viscoelastic measurements using coaxial rheometer and confirmed that slip layer develops when shear stress approaches yield stress. They concluded that slip is not prevalent in measurements below yield stress.

For fluids with a yield stress, the range of shear stresses present in the annulus may not be sufficient to cause all materials to flow. The results are a dead zone where no flow occurs. In concrete literature, this is often referred to as plug flow. In coaxial rheometers, plug flow can be eliminated by increasing rpm, reducing the radii ratio of outer to inner cylinder, and reducing the ratio of yield stress and plastic viscosity. The yield stress and viscosity depend on material being tested while rpm is determined from the desired shear rate; therefore the radii ratio is the parameter that can be controlled. Tattersal and Banfill [1983] as well as Ferraris [1999] suggested that limiting value of ratio of outer to inner cylinder radius shall not be greater than 1.1 or 1.2 to reduce the plug flow.

Wallewick [2003] found that ignoring the plug flow results in an underestimate of yield stress and overestimate of viscosity. Various methods for taking plug flow into consideration have been suggested. Wallewick [2003] suggested successive iteration of Reiner-Riwlin equation.

Koehler and Fowler [2004] recommended point elimination method or effective annulus method. True velocity profile is difficult to assume. Raynud et al [2002] has adopted Magnetic Resonance Imaging.

Ferraris and Brower [2001] reviewed critically the rheometers in view of the artifacts. These are summarized as follows:

- (i) In BML, slip risks are minimal. The main critical issue lies in the fact that gap between the cylinders is only 2-3 times the maximum aggregate size. Whereas to eliminate particle interference, this gap should be within the range 3-10 times the maximum size of aggregates [Banfill, 2003; Ferraris et al, 2001].
- (ii) In BTRHEOM, wall slip is also minimal and the chance of particle interference is little.
- (iii) In CEMAGREF-IMG, there is no particle interference and the slip risk is medium.
- (iv) In IBB and Two-point test, slip risk is very high. The gap between the sheared surfaces is very small and therefore, there is a chance of particle interference.

### **1.2.3 Rheology of High-Performance Concrete (HPC)**

HPC is designed to give optimized performance characteristics for a given set of materials, usage, exposure conditions consistent with strength, durability, workability and service life. The major difference between conventional concrete and HPC is essentially the use of chemical and mineral admixtures.

The principal factors affecting rheology of high performance concrete are composition of concrete including chemical and mineral admixtures dosage and type; gradation, shape and type of aggregates; water content and cement characteristics. The same mixture design can result in different flow properties if secondary factors are not taken into account. These are: Mixer type: pan, truck, and so on [Chang and Peng, 2001], Mixing sequence [Chang and Peng, 2001], Mixing duration and Temperature. A review of literatures on the various factors influencing rheology of HPC is presented here.

#### Effect of Cement Content and Cement Characteristics

An increase in the cement content, at a constant water-to-cement ratio, provides more paste to coat aggregates and to fill the spaces between aggregates, resulting in improved

workability. Smeplass (1994) found that an increase in cementitious materials content (cement with 5% silica fume) relative to aggregate volume resulted in a decrease in both yield stress and plastic viscosity.

The chemical composition and physical characteristics of cement can significantly influence workability. Even for a single type of cement, as defined by ASTM C 150 or ASTM C 1157, the changes in cement characteristics can be consequential. Hope and Rose (1990) examined the effects of cement composition on the water demand required for a constant slump. Although the correlations between composition and water demand varied between different aggregates and mixture proportions, the authors were able to draw several conclusions. The water demand increased for cements with high  $Al_2O_3$  or  $C_2S$  contents and decreased for cements with high loss on ignition, high carbonate addition, or high  $C_3S$  content. The particle size distribution of the cement was found to be significant for concrete made with angular aggregate and less pronounced for concrete made with rounded aggregate. For the concrete with angular aggregate, the cements with a higher portion of material smaller than  $10\ \mu m$  exhibited higher water demand. The specific surface, however, had minimal influence on water demand.

Vom Berg (1979) determined that increasing cement fineness resulted in exponential increases in both yield stress and plastic viscosity for cement pastes.

Mork and Gjoerv (1997) found that the ratio of gypsum-to-hemihydrate in cement could influence concrete rheology. For a cement with high contents of  $C_3A$  and alkalis, a reduction in the gypsum-to-hemihydrate ratio resulted in a decrease in yield stress but little change in plastic viscosity. When a melamine based HRWR was used, the trend was reversed, with a lower gypsum-to-hemihydrate ratio resulting in an increase in yield stress. For cement with lower contents of  $C_3A$  and alkalis, the effects of the gypsum-to-hemihydrate ratio were less pronounced. Further, a reduction in the sulfate content from 3% to 1% resulted in a decrease in both the yield stress and plastic viscosity.

#### Effect of Water Content

Mork (1996) investigated the effect of water-to-cementitious materials on rheological parameters of HPC. It was observed that an increase in the water-to-cementitious materials ratio in either concrete or cement paste results in reductions in both yield stress

and plastic viscosity. The same trend was observed by Tattersall and Banfill (1983) and Tattersall (1991).

Szecszy (1997) reported that the addition of water reduces the solids concentration, resulting in less resistance to flow. Workability is improved with increasing water-to-cementitious materials ratios up to a certain point, after which segregation can become a problem.

Banfill (1994) studied effect of water-cement ratio on rheological parameters of cementitious materials and observed that both yield stress and plastic viscosity decreases exponentially with the increase in water-cement ratio.

Hu and de Larrard (1996) investigated effect of water content on rheological parameters of high performance concrete. It was observed that yield stress decreases rapidly with increase in water-cement ratio. Plastic viscosity also decreases with the increase in water content but the decrement rate is less compared to that of yield stress.

#### Effect of Aggregate

The relationship between solids volume concentration and viscosity is well established for concentrated suspensions (Barnes et al, 1989). Szecszy (1997) reported that an increase in the total volume fraction of aggregate in concrete results in increases in yield stress and plastic viscosity. Higher volume fractions of aggregates result in reduced spacing between aggregates and, thus, greater resistance to flow.

Workability can be improved by optimizing the sand-to-aggregate ratio (S/A). Tattersall, (1991) reported that optimum values of S/A exist for minimizing yield stress and plastic viscosity. An optimum S/A for yield stress may not be optimum for plastic viscosity. Increasing or decreasing the S/A from its optimum value results in increases in yield stress or plastic viscosity. At high values of S/A, an increase in sand content results in a increase in the surface area of aggregates that must be coated with cement paste and, thus, an increase in the resistance to flow. When the sand content is reduced below the optimum value, the result is a lack of fine aggregates to fill the voids between coarse aggregates and, thus, increased resistance to flow. For tests reported by Tattersall (1991), the minimum value of yield stress occurred at an S/A of about 0.33, while the minimum

value of plastic viscosity was reached at an S/A of approximately 0.40. The exact value was a function of water-to-cement ratio.

Szecsy (1997), when testing crushed limestone and river gravel coarse aggregates, found that the minimum yield stress was achieved at an S/A of approximately 0.40 while plastic viscosity was minimized at an S/A of approximately 0.30. In comparison, S/A values of approximately 0.50 are typical for self-consolidating concrete.

Quiroga (2003) found that aggregates with spherical, cubical, or rounded shapes and smooth textures required less cement and water to achieve the same slump as aggregates with flat, elongated, or angular shapes and rough textures. It was also observed that when gradation was held constant, aggregates with greater packing density, which is related to shape and texture, produced higher slumps.

Tattersall (1991) studied effect of shapes of coarse aggregate on rheological behavior of concrete and observed that spherical shapes are preferable because they more readily flow past each other and have reduced specific surface area. It was also observed that particle shape has a greater influence on plastic viscosity than on yield stress and that texture has no significant effect on rheology.

Barnes et al. (1989) studied the effect of the gradation on rheology of concrete and observed that particle size distribution of aggregate plays a critical role in the workability and rheology of concrete. Barnes et al are of the opinion that the gradation should take into account all materials, including the cementitious materials and aggregates. In concentrated suspensions, increasing the poly-dispersity, or spread of sizes, decreases viscosity concretes produced with gap-graded aggregates, which intentionally omit certain size fractions. This can be harsh and more susceptible to segregation.

Banfill (1994) investigated effect of particle size distribution on rheological behavior of mortar at constant water-cement ratio and cement –sand ratio. It was observed that finer the sand, more are the values of yield stress and plastic viscosity. When the percentage sand fraction passing 170 micron and retained 100 micron is increased, yield stress and plastic viscosity increases sharply. The increase is more pronounced in mix having low water-cement ratio.

Quiroga (2003) found that uniform aggregate particle size distributions required less water for a given slump than other gradations. In designing a concrete mixture, the

gradation can be optimized for a variety of objectives, such as slump, packing density, uniformity, or plastic viscosity. It was found that mixtures optimized for maximum packing density or slump produced harsh mixtures with poor workability and high susceptibility to segregation. Concrete mixtures above the line on the 0.45 power chart resulted in stiff mixtures, while mixes below the line resulted in harsh, segregating mixtures. It was therefore, recommended that gradation should be such that there is a balance between high packing density and uniform grading.

The addition of microfines can improve or reduce workability depending on the quantity and characteristics of the microfines, as well as the composition of the rest of the concrete mixture. Ho et al. (2002) evaluated the addition of either limestone or granite powder in a cement paste intended for use in self-consolidating concrete. The limestone powder and granite powder had approximately 80% and 75% passing the #200 sieve, respectively, and were obtained as dust from the aggregate crushing process. In general, the replacement of cement with the inert powders at rates up to 55% reduced cement paste yield stress and plastic viscosity. All cement paste samples incorporated one of two different high-range water-reducing admixtures and maintained a constant water-to-powder ratio (cement and filler). The reduction in Bingham parameters was less pronounced for the granite powder, which tended to have flakey and elongated shapes.

Ghezal and Khayat (2002) examined the use of a limestone filler material with a Blaine fineness of 565 m<sup>2</sup>/kg and 97.2% of particles smaller than 45 μm. When used in self-consolidating concrete mixtures at rates up to 100 kg/m<sup>3</sup> with a constant water-to-powder ratio, the limestone filler resulted in decreases in yield stress and plastic viscosity. The change was most pronounced at low cement levels. The use of limestone filler also enhanced the stability of the concrete mixtures.

#### Effect of Chemical Admixtures

Water-reducing admixtures enhance workability by reducing the water-to cementitious materials ratio needed to achieve a given slump. Alternatively, they can be used to increase slump for a given water-to-cementitious materials ratio, reduce cement content while keeping the water-to-cementitious materials ratio constant, or some combination of the above applications.

Mork (1996) suggests that, in general, low-range water reducers decrease yield stress and plastic viscosity, while high-range water reducers decrease yield stress and increased plastic viscosity. For both types of admixtures, the changes in plastic viscosity are most pronounced at high admixture dosages.

Smeplass (1994) found that the use of high-range water reducer in concrete mainly reduced yield stress but had little impact on plastic viscosity.

For cement paste, Ho et al. (2002) found that high-range water reducers decreased yield stress, but resulted in minimal decreases in plastic viscosity.

Tattersall (1991) reported that the use of a lignosulphonate-based low range water-reducing admixture in concrete resulted in a reduction in both yield stress and plastic viscosity, although the effect on yield stress was more pronounced. The decrease in these values was considerable at low dosages and without much effect at higher dosages. In contrast, the use of melamine sulphonate-, naphthalene sulphonate-, and lignosulphonate-based high-range water-reducing admixtures in concrete all resulted in dramatic reductions in yield stress but little change in plastic viscosity. He also presented data showing that the addition of a high range water-reducing admixture resulted in an increase in viscosity when used in a concrete with a low sand content ( $S/A = 0.35$ ), but a decrease in viscosity when used in a concrete with a high sand content ( $S/A = 0.45$ ). The change in yield stress was approximately the same regardless of the sand content. According to Tattersall (1991) the effects of naphthalene- and melamine based high-range water reducers depend on cement characteristics. Further, increasing the cement content increases the potency of high-range water-reducing admixtures.

Tattersall and Banfill (1983) suggested that at low sand contents, the flocculated cement paste separates coarse particles; therefore, when the cement is deflocculated, the coarse particles come closer together and generate greater resistance to flow. The result is an increase in plastic viscosity of the concrete in spite of the decrease in viscosity of the cement. In mixes with a high sand content, the sand fills more of the space between coarse particles. As a result, a reduction in viscosity of the paste results in a reduction in the viscosity of the concrete because the coarse particles do not move sufficiently closer together.

Billberg et al (1996) used melamine and naphthalene based high-range water-reducing admixtures and found a reduction in both yield stress and plastic viscosity. The concrete tested had an S/A ratio of 0.57 and a maximum aggregate size of 16 mm. The reduction in yield stress was greater in percentage terms—whereas the yield stress was reduced from 600 Pa to approximately 100 to 200 Pa, the plastic viscosity was reduced from 30 Pa.s to 15 - 20 Pa.S.

Faroug et al al (1999) found that the effects of naphthalene- and melamine-based high-range water reducers were most pronounced at low water-to-cement ratios. The use of both types of high-range water reducers in concrete resulted in decreases in yield stress and plastic viscosity. The admixtures had essentially no effect on plastic viscosity above a water-to-cement ratio of 0.40 or on yield stress above a water-to-cement ratio of 0.50. Hu and de Larrard (1996) studied the effect of super-plasticizer on rheological parameters of HPC. It was observed that yield stress decreases very rapidly up to a super-plasticizer (SP) dosage 1.3% by weight of cement and then remains unchanged. Plastic viscosity decreases initially up to 1.3% and again increases with the increase in SP dosage.

Kong et al (2006) studied the effect of Melamine formaldehyde sulfonate (FMS) on cementitious materials. It was concluded that FMS inverts the sign of surface potential on cement particles from positive to negative. This sign inversion causes electrostatically flocculated cement particles to be electrostatically dispersed. Consequently, there is a reduction of shear viscosity. Higher dosages of FMS concentration leads to increase in high shear viscosity indicating depletion of flocculation caused by excess MFS in solution. These results illustrate the importance of determining optimal concentration of a SP to achieve fluidity and cohesiveness of in a cement suspension.

Faroug et al [1999] studied the influence of different super plasticizers on rheological properties of concrete. It was observed that better workability is obtained as a result of decrease of yield stress and plastic viscosity. The range of the change depends on w/c ratio, superplasticizer type and dosage. The lower the w/c ratio, the more effective is the superplasticizer at constant dosage. At high w/c ratio, SP becomes ineffective and segregation may occur. It was also observed that between naphthalene formaldehyde and melamine formaldehyde, naphthalene formaldehyde compounds are more effective in reducing yield stress and plastic viscosity.

Kosmatka et al [2002] observed that air-entraining agents improve workability, particularly for lean or harsh mixtures or mixtures with angular or poorly graded aggregates. The presence of entrained air results in a concrete that is more cohesive; however, excessive entrained air contents can make concrete sticky and difficult to finish. Air entrainment also reduces segregation and bleeding.

Tattersall (1991) showed that the use of air-entraining agent in concrete reduced plastic viscosity to a much greater extent than yield stress. The change in plastic viscosity was essentially zero above an air content of 5%, although the yield stress continued to decrease at higher air contents.

Tattersall and Banfill (1983) reported that in cement paste, air entrainment can increase yield stress. This increase is thought to be due to the apparent negative charge imparted on the air bubbles by the air entrainment agent. This negative charge can attract hydrating cement grains, resulting in the formation of bridges between the cement grains. In concrete, the reduction in plastic viscosity is likely due to the “ball bearing” effect of the spherical air bubbles. The yield stress of the concrete is not decreased as significantly as the viscosity due to the increase in yield stress of the cement paste.

Viscosity modifying admixtures (VMAs), also known as anti-washout admixtures, are typically used in self-consolidating concrete or for placing concrete underwater. For self-consolidating concrete, VMAs are used to improve stability by reducing segregation, surface settlement, and bleeding. In underwater concrete, VMAs reduce the washout mass loss. VMAs increase both the yield stress and plastic viscosity. A thorough overview of VMAs and their effects on concrete is provided by Khayat (1998). A range of VMAs with various chemical compositions is commercially available. VMAs used for concrete typically consist of water-soluble polymers, such as welan gum or cellulose derivatives. Typically, these VMAs increase the viscosity of the mixing water through a variety of mechanisms, with the precise mode of action depending on the type of polymer.

The use of a VMA results in shear-thinning, or pseudo-plastic, behavior in cement pastes or mortars. This behavior is advantageous for concrete because the relatively high viscosity at low shear rates prevents segregation of aggregates while the relatively low

viscosity at higher shear rates ensures excellent deformability during mixing, pumping, and placing operations. VMAs also increase thixotropy.

Sonebi (2006) investigated the influence of dosage of second generation VMA on rheological parameters of cement based materials grout compared to welan gum. It was observed that increase in the dosage of both the VMAs for a given dose of SP increases significantly yield value, apparent and plastic viscosity. With an increase in dosage of SP, apparent viscosity at low shear rate decreases dramatically than that at high rate of shear due to pseudo-plastic rheology of grouts containing VMA. Both VMAs exhibited high apparent viscosity at low shear rates which were attributed to entanglement and intertwining of VMA polymer chains at low shear rates and association of water between adjacent chains. Second generation VMA gives higher values of yield stress and plastic viscosity compared to welan gum.

#### Effect of Time and Temperature

The effect of elapsed time on rheology of concrete was studied by Hu and de Larrard [1996]. The process of loss of workability is generally reflected by an increase in yield stress; however, in most cases plastic viscosity is nearly constant during the test period (generally less than 90 min).

Punkki et al (1996) studied the effects of different mixing procedures (delayed addition of portion of water and delayed addition of superplasticizer) and elapsed time on yield stress and plastic viscosity. Both yield stress and plastic viscosity increased with the elapsed time after mixing. When the superplasticizer was added simultaneously with water, increase in yield stress was very high while increase in viscosity was insignificant. When SP was added after water, in two increments, increase in yield stress was the lowest and increase in plastic viscosity was also the lowest.

Beaupre [1994] also made the same observation for pseudo yield stress and pseudo plastic viscosity, measured with a two-point rheometer. It is noteworthy that different SP does not lead to same effect on rheological properties of HPC.

Li et al [2004] investigated flow performance of HPC using a special type of fabricated shear box apparatus and observed that for a given stress rate, shear strain rate increases

with temperature up to a certain limit and then decreases. He concluded that up to certain limit, flow performance improves because of the decrease of viscosity of water.

Banfill (1994) studied effect of time on rheological properties of mortar. It was observed that yield stress increases as the elapsed time increases. For mortar with higher water-cement ratio, the increase is, however, insignificant. Plastic viscosity decreases initially and after that it attains a constant value.

Petit et al (2006) investigated coupled effect of time and temperature on yield stress of flowable mortar with different types of HRWRA. Test results showed that yield stress varies linearly with the coupled effect of time and temperature during dormant period for mixtures made with poly-naphthalene Sulfonated based HRWRA. Such changes are found to depend on mixture temperature for mixtures made with poly-carboxylic based HRWRA. The threshold temperature of mixtures made with poly-carboxylic compound is shown to vary with mixture composition. Below a given threshold temperature, mix exhibits a considerable degree of retention of yield value over 30% of dormant period. Above the threshold temperature, yield value is shown to increase linearly with time.

#### Effect of Mineral Admixtures

##### *Fly Ash*

Fly ash, also known as pulverized fuel ash (pfa or PFA), is the ash precipitated electrostatically or mechanically from the exhaust gases of coal fired power stations. Fly ash particles are spherical in shape and have very high fineness: vast majority of particles have a diameter between less than 1 micron and 100 micron and the specific surface area is usually between 250 m<sup>2</sup>/kg and 600 m<sup>2</sup>/kg [Neville, 2003]. India produces about 75 million tons of PFA every year the disposal of which has become a serious environmental issue. The effective use of PFA in India is only 5% of the total production [Shetty, 2004]. The effective use of PFA in concrete industry is therefore attracting serious considerations and the use needs to be popularized.

ASTM C 618-94a classifies fly ash into three categories depending on the type of coal from which the ash originates. The most common fly ash derived from bituminous coal is known as class F fly ash that is mainly siliceous. Sub-bituminous coal and lignite result in high lime ash (class C). High lime ash has some hydraulic properties of its own but there

will be less of these compounds to react with the lime liberated by hydration of cement. The MgO content can be high and some of the MgO and some of the lime can lead to deleterious expansion.

During early 1980s, several investigators attempted to elucidate effect of fly ash on the flow behavior of concrete in terms of fundamental rheological properties [Hobbs,1980; Ivanov et al,1980; Banfill, 1982; Ellis,1982]. The results obtained in the studies showed wide disparity, raising serious doubts on whether this type of approach can describe the mechanism of PFA contribution to workability of concrete. Indeed, it has been pointed out that the flow behavior of cement paste system and its relationship to concrete workability is complex, and even for the simplest Portland cement-water system the published data showed no general agreement.

Tattersall (1991) showed that the use of a mass replacement of fly ash in concrete mixtures resulted in a reduction of yield stress, while the plastic viscosity decreased only slightly. The magnitude of reduction in yield stress depended on the initial cement content, with fly ash having the greatest improvement at lower initial cement contents. When fly ash was replaced on a volume basis instead of a mass basis, the changes in yield stress and plastic viscosity were doubled, suggesting that the increased surface area played a larger role in the incremental difference in volume between the mass and volume replacements.

Szecszy (1997) found that a 10% fly ash mass replacement level in concrete mixtures resulted in an increase in yield stress. From 10% to 20%, the use of fly ash reduced the yield stress. The use of 5% fly ash resulted in a reduction of plastic viscosity; however, further replacement of cement with fly ash at rates up to 20% resulted in little additional change in plastic viscosity.

Grzeszczyk et al [1997] studied rheological properties of high calcium fly ash cement pastes. An increase in both yield stress and plastic viscosity with PFA content was observed. An important relation was shown between fine fraction (less than 24 micron) content and degree of fluidity rather than specific surface area versus fluidity. The grinding of high calcium PFA brought about the rheological properties improvement. The effect was negligible at lower PFA content but becomes significant at higher contents.

Cyr et al [2000] studied shear thickening of cement paste containing PFA and other mineral additives. It was observed that mineral additives as replacement of different amount of cements modify the intensity of shear thickening. The phenomenon is unchanged due to addition of PFA.

Ferraris et al [2001] investigated the influence of different types of PFA such as coarse, fine and ultra fine on rheology of cement paste and concrete. It was determined that mixtures with ultrafine PFA represent the best rheological improvements.

Park et al [2005] studied rheological properties of cementitious materials containing mineral admixtures. Sample without PFA shows little bit yield stress than the sample with PFA. Yield stress slightly increases as PFA amount increases. Plastic viscosity also increases slightly with increasing PFA.

Sonebi (2006) investigated effect of PFA on rheological behavior of cement grout containing VMA and observed that for a given dosage of VMA and SP, incorporation of PFA resulted in decrease in yield stress and plastic viscosity. For a given replacement level of PFA, a greater reduction of yield value was observed when welan gum was used in the mix. With second generation VMA, incorporation of PFA led a slight reduction in yield value compared to welan gum.

### *Silica Fume*

Condensed silica fume (CSF) is a byproduct from electric arc furnaces used in manufacture of silicon metal or silicon alloys. The material that contains more than 80% silica in non crystalline state and in the form of extremely fine particles (0.1micron average diameter) is highly pozzolanic [Nawy, 2000]. Being a waste product with relative ease in collection compared to PFA, CSF has gained rapid popularity in construction industry.

Silica fume is highly reactive and the smallness of the particles speeds up the reaction with calcium hydroxide produced by the hydration process. The very small particles can enter the spaces between the particles of cement and thus improves packing. Silica fume is at present available in four different forms. It can be bought as collected in the 'baghouse' where its bulk unit weight ranges from 200 kg/cu.m to 250 kg/cu.m. Silica fume is also available more commonly in a 'densified' form. In this case, the bulk density

can vary from 400 to 500 kg/cu.m. Silica fume is also available in slurry form in which solid content is around 50%. At the present time, silica fume available is blended directly with OPC. In any case, choice of the form in which silica fume will be used is usually limited by availability, economics, and service considerations.

The effect of CSF on the rheology of fresh concrete is generally viewed as a 'stabilizing effect' in the sense that addition of very fine particles to concrete mixture tends to reduce segregation and bleeding tendencies. Swamy [1986] reported that due to increase in the number of solid-to-solid contact points, the cohesiveness of concrete is greatly improved when CSF is added. This makes the material highly attractive for use in shotcreting, pumping and tremie operations. In fact, use of too much CSF makes the concrete mixture sticky.

The use of silica fume can improve workability when used at low replacement rates but can reduce workability when added at higher replacement rates. The addition of 2% to 3% silica fume by mass of cement can be used as a pumping aid for concrete (Tattersall 1991). Like fly ash, the spherical shape of silica fume particles is advantageous for workability; however, the small diameter of silica fume particles can significantly increase the surface area that must be wetted. According to Tattersall (1991) and Mork (1996), a threshold value of the silica fume replacement level exists for concrete mixtures, such that below the threshold value, the use of silica fume reduces plastic viscosity but produces little change in yield stress. Above the threshold value, both yield stress and plastic viscosity increase with increasing levels of silica fume replacement.

Faroug et al (1999) measured the rheology of concrete with the silica fume used as either a replacement or addition to cement. When used as a replacement, the yield stress increased with increasing replacement levels up to 20%, above which further silica fume replacement resulted in a reduction in yield stress. The plastic viscosity decreased at up to a 10% replacement rate, but then began increasing at higher replacement rates so that the plastic viscosity was approximately unchanged from the control at a 15% replacement rate and higher than the control at further replacement rates up to 30%. When used as an admixture at levels up to 10%, silica fume resulted in increased yield stress across the tested range. Plastic viscosity increased at addition levels up to 7.5%, above which it began to decrease.

Shi et al (2002) tested mortar mixtures and found that the addition of silica fume resulted in a reduction in both yield stress and plastic viscosity at replacement rates up to 6% and 9%, respectively. At higher rates, yield stress and plastic viscosity increased, such that at a 12% replacement rate, both yield stress and plastic viscosity were higher than the control mixture.

Cyr et al [2000] conducted rheological tests to point out the conditions of occurrence of shear thickening in cement paste, varying nature of super plasticizer (SP), and observed that shear thickening reduces with the introduction of CSF.

Park et al (2005) observed that yield stress and plastic viscosity steeply increase with the increase in CSF until 15% by weight even if replacement is very low. It was concluded that since CSF has very high surface area and fineness, it absorbs SP molecules with multilayer. As replacement level increases, quantity of SP decreases. As a result, yield stress and plastic viscosity steeply increases as CSF increases.

#### *Rice Husk Ash*

Rice milling generates a by-product known as husk. While they are utilized as fuel in some regions, in others they are waste product causing pollution and problem with disposal. When burnt under controlled temperature, rice husk ash (RHA) generated is highly pozzolanic and suitable for Portland cement replacement.

One ton of rice yield 200 kg of husk and 40 kg of ash [Swamy1986]. India occupies the second position in the production list of rice. About 4.88 million tons of rice husks are produced alone in India annually. Largest producers of rice are the developing countries: China 1<sup>st</sup>, Indonesia 3<sup>rd</sup>, and Bangladesh 4<sup>th</sup>. There is a good potential to make use of RHA as a valuable pozzolanic material in these countries.

Research on RHA that can be used in concrete is not new. Mehta in 1973 investigated the effect of pyro-processing on pozzolanic reactivity of RHA [cited by Swamy,1986]. Zhang and Malhotra [1996] found that it is possible to produce HSC using fine enough RHA and an optimum % replacement of cement. The fineness of RHA is an important factor that affects the strength of concrete. RHA particles have complex shape reflecting

their plant origin and they therefore have high super-plasticizer demand. Reported work on the effect of RHA on rheological parameters such as yield stress and plastic viscosity of HPC is not known.

### Effect of Fiber

Fiber reinforced concrete (FRC) is defined as concrete made with hydraulic cement, containing fine or fine and coarse aggregate and discontinuous discrete fibers. For structural applications, steel fibers are used as complementary reinforcement to increase the cracking resistance, flexural and shear strength, impact resistance and ductility of RCC elements. Fibres are used in cementitious materials in order to improve the characteristics in the hardening or the hardened state. Their effect on workability is mainly due to four reasons: First, the shape of the fibers is more elongated compared with aggregates; the surface area at the same volume is higher. Second, stiff fibers change the structure of the granular skeleton, while flexible fibers fill the space between them. Stiff fibers push apart particles that are relatively large compared with the fiber length. The porosity of the granular skeleton thus, increases. Third, surface characteristics of fibers differ from that of cement and aggregates, e.g. plastic fibers might be hydrophilic or hydrophobic. Finally, steel fibers often are deformed (e.g. have hooked ends or are wave-shaped) to improve the anchorage between a fiber and the surrounding matrix. The friction between hooked-end steel fibers and aggregates is higher compared with straight steel fibers.

Nawy [2001] pointed out that factors affecting the properties of fresh concrete are [Nawy, 2001] aspect ratio, volume percentage of fibers, coarse aggregate size, gradation and quantity, water-cement ratio and method of mixing.

Johnston [2001] reported that steel fiber reinforced concrete (SFRC) appears stiffer (lower slump) compared with conventional concrete without fibers even when the workability (judged by any test using vibration) is the same. He suggested that initial slump of plain concrete should be 50-75 mm more than the desired final slump and adjustment to be done by adding superplasticizer, not by additional water. SFRC tends to 'hang' together. Vibration is encouraged to increase the density, to decrease the air void content and to improve the bond with reinforcement bars.

Swamy [1975] concluded that size, the shape and the content of the coarse aggregates as well as the geometry and the volume fraction of steel fibers affect the workability of concrete. At a given fiber diameter and volume fraction, compactability was linearly related with the aspect ratio of the fibers. The relative fiber to coarse aggregate volume and the 'balling up' phenomenon govern the maximum possible content of steel fibers [Swamy & Mangat, 1974]. The maximum fiber content is the critical fiber content at which the compactability drastically decreases. Fiber balling already might occur before the fibers are included into the concrete and a maximum of 2% volume of steel fibers (1% at a high aspect ratio) is considered as a maximum [ACI 544, 1993].

Edgington et al. [1978] performed tests on the effect of the aspect ratio and the fiber concentration on the Vebe-time. Mixtures without fibers were used as a reference. The reference mortar contained aggregates with a maximum size of 5 mm. To obtain the same Vebe-time, the maximum fiber volume fraction had to be decreased. In the same study, different reference mixtures were tested [Edgington et al., 1978], which differed in the maximum aggregate size (20, 10, 5 mm and cement paste). One type of steel fiber was applied; the aspect ratio was kept constant at 100. The larger the maximum aggregate size, the higher the Vebe-time was for certain steel fiber content. The difference between the cement paste and a 5 mm-mortar was rather small; the aggregates were relatively small compared with the fiber length. An increase of the maximum aggregate size usually implies that the aggregate content is higher, since less paste is required to fill the interstices of the granular skeleton.

Narayanan et al [1982] found that the 'optimum fiber content' increased at increasing percentage sand of total aggregate; both parameters were linearly correlated. The 'optimum fiber content' was defined as the content of the steel fibers beyond which fiber balling took place. The maximum aggregate size of the coarse aggregates was 14 mm (sand: 3 mm). Different steel fiber types with length between 25-43 mm were tested. The established relation was independent of the ratios of aggregate to cement and water to cement, which means that balling occurred at a given fiber content no matter what was the composition of the concrete.

Hoy [1998] performed experimental and numerical studies on the packing density of the granular skeleton of SFRC. To include steel fibers into the Solid Suspension Model

(SSM), which is a packing program developed by de Larrard & Sedran [1994], various methods were tested. Hoy assumed that the most workable mixture would be that with the highest packing density. He obtained the optimum composition of the granular skeleton from simulations with the SSM. Input parameters of simulations were the characteristics of the components (steel fibers, sand and coarse aggregate). It was observed that higher the content of the steel fibers, the higher was the required optimum sand content. At a defined content of the steel fibers, the higher the aspect ratio was, the higher was sand to total aggregate ratio. Practical considerations limit the applicability of steel fiber contents larger than 2.0% volume fraction because a significant decrease of workability takes place.

The effect of flexible fibers differs from that of stiff fibers; they fill the interstices between the aggregates rather than pushing the aggregates apart. The surface area of flexible fibers often is much higher compared with that of the steel fibers. Plastic fibers having the same surface area might affect the workability to different degrees; the fibers might be either hydrophobic or hydrophilic. The flow of cement-based matrices also depends on the surface area of the fibers. Ando et. al. [1990] showed that a linear correlation exists between the flow spread and the fiber content (specific surface area) of a carbon fiber- reinforced cement paste.

Tattersall (1991) showed that increasing the content of steel and synthetic fibers resulted in increases in both yield stress and plastic viscosity. For the steel fibers, increasing the fiber length resulted mainly in an increase in yield stress but little change in plastic viscosity.

Grunewald et al [2003] observed in SCC that in spite of addition of steel fibers, yield stress does not differ significantly until a threshold value of slump flow is reached. Plastic viscosity is more affected by the addition of steel fibers and higher the volume percentage, more is the plastic viscosity.

Bui et al [2003] reports the results of the experimental program on fiber-reinforced mortars. The effect of fiber volume and surface area has been discussed. It is seen that higher volume fraction, ratio of fiber volume fraction and maximum packing density lead to greater yield stress and plastic viscosity. There are other possible factors that influence the rheological properties of FRC. These are: total surface area of fibers, modulus of

elasticity of fibers, rheological properties of mortar without fibers, and processing techniques.

Kuder et al [2007] investigated the effect of steel fiber-reinforced cement paste for various volume fractions. It was observed that yield stress decreases until a critical volume fraction is reached and then increases. The viscosity decrease until reaching a critical point; however, the decrease for stiffer mix is much greater. The trend in yield stress and plastic viscosity has been explained by a coupling effect between structural breakdown of the material that occurs at low fiber volume and mechanical interlocking which occurs at higher volume fractions.

ACI Committee: 544 (1978) has recommended the use of inverted slump cone for measurement of workability. The test measures the time to empty the steel fiber concrete mix from an inverted slump cone resting 75 mm above the bottom of a 9 liters bucket, after a 25- 30 mm diameter vibrator probe has been inserted. The probe is allowed to fall and touch the bottom of the bucket. The time recorded in the range of 11- 28 seconds indicates good workability. This test has not been fully evaluated and is somewhat cumbersome. Tattersall and Banfill [1983] criticized inverted slump cone test for FRC as empirical and arbitrary test for workability.

#### **1.2.4. Some Special Topics on Rheology**

##### Suspensions

Suspensions of solid particles in a liquid generally behave like a fluid and it is often useful to characterize their rheological behavior. Two key factors affect this behavior: volume fraction of solid particles in the suspension and the extent to which the particles are agglomerated or flocculated [Ramachandran and Beaudoin, 2006]. Increasing volume fraction of solid ( $\phi$ ) causes a considerable increase in viscosity.

The other factor affecting flow behavior is the extent to which particles are flocculated or dispersed. Flocculation is particularly important for colloidal particles (less than 1 micron) which may flocculate spontaneously. Flocculated particles either form discrete aggregate or gel. The forces are often fairly weak and easily broken by shear and suspension begins to flow. The stress at which such a breakdown occurs is called yield stress and flocculation produces plastic behavior.

Zukoski and Strubble [1993] have described the flocculation process by means of simple equation relating yield stress to solid volume fraction in the form of power law.

### Thixotropy

Cement paste is a concentrated suspension of cement particles in water. As the mean size of cement particles is of the order of microns, inter-particle forces and gravity forces are of the same order of magnitude and both types of forces play an important role concerning the macroscopic characteristics of such suspension. Inter-particle forces are two types: Vander Waal force and electrical double layer interaction. Whatever is the liquid, Vander Waal force is always positive. Electrical double layer have their origin in the surface electric charge that appears for most substances in contact with aqueous medium.

It was established that electrical double layer at oxide-water interface is related to unequal adsorption of  $\text{OH}^-$  ions and  $\text{H}^+$  ions. Between two particles, the double layer can be attractive or repulsive depending on the sign of each particle. Suspensions are stable when repulsive double layer interaction is larger than Vander Waal forces and there is flocculation in opposite case. That is to say, suspensions have good flowing properties (deflocculated) when repulsive inter-particle forces dominate. When repulsive double layer forces are smaller, the solid particles form a solid structure inside the liquid and the suspension is very cohesive and has very poor flowing properties. The more the suspension is agitated during the experiment, the more fluid it is. This phenomenon is called thixotropy. The solid structure reappears when suspension is at rest.

However, in case of cementitious materials, things are not simple as the hydration process starts. The apparent viscosity of the material is permanently evolving as described by Banfill and Saunders [1981]. Recently, Jarney et al [2005] have shown using Magnetic Resonance Imaging velocimetry that over short time scale, flocculation and de-flocculation process dominate which leads to rapid thixotropic effect. Over larger time scale, hydration process dominates that leads to irreversible evolution of the behavior of the fluid. These two effects might act at any time but they appear to have different characteristic time. Roussel [2006] concluded that it seems possible to model

thixotropy on short period of time (not more than 30 minutes as an order of magnitude) during which irregular evolution of concrete can be neglected.

Mewis [1979] used the term thixotropy to describe an isothermal gel-sol transition due to mechanical agitation. Barnes et al [1989] has given a comprehensive review of the topic and described thixotropy as a decrease of the apparent viscosity under constant shear stress or shear rate, followed by a gradual recovery when stress or shear rate is removed. The effect is time dependent. An approach to measure the degree of thixotropy by finding area under hysteresis loop was described. In a thixotropic sample, hysteresis loop is obtained when torque is measured under linear increase and then decrease in rotational frequency.

While hysteresis loops are useful as a preliminary indicator of behavior, they do not provide a good basis for quantitative treatments [Tattersall and Banfill 1983]. Wallewick [2003] investigated thixotropic behavior of cementitious materials. He presented two types of yield stress:  $\tau_o$  and  $\tilde{\tau}_o$ .  $\tau_o$  is related to permanent coagulation state of cement particles, while  $\tilde{\tau}_o$  is related to reversible coagulation state. The same type of relationship was also presented for plastic viscosity,  $\mu$  and thixotropic counterpart,  $\tilde{\mu}$ . Wallewick also observed that thixotropy is governed by a combination of reversible coagulation, dispersion, re-coagulation of cement particles and super-plasticizer type.

From practical point of view, an important effect of thixotropy of concrete is a large increase of yield stress during resting. This phenomenon was observed by Hu and de Larrard [1996]. The resting yield stress  $\tau_r$  is distinguished from the shear yield stress  $\tau_o$  measured in a steady state. In fact, for concrete after a period of rest it is the resting yield stress that characterizes such properties as capacity to hold a slope and facility to be “finished”. The resting yield stress  $\tau_r$  can be obtained by performing a controlled yield stress test [de Larrard et al 1997]. They demonstrated that  $\tau_r$  can be several times greater than  $\tau_o$ . Measurements under vibration showed little difference between  $\tau_o$  and  $\tau_r$ , which means that applied vibration cancelled thixotropy of concrete.

### Dilatancy

Dilatancy is the increase in volume of a fluid during shearing. In concentrated suspension, particles sliding past each other lead to such an expansion in volume [Koehler and Fowler, 2004].

Hu and de Larrard [1996] found that no relationship exists between dilatancy and Bingham parameters. Dilatancy seems to be more noticeable for concrete in which maximum size of aggregate is greater. Concrete with crushed aggregates show more dilatancy concrete with rounded aggregates. Increase of the volume of fines (less than 400 micron) limit dilatancy.

Dilatancy should not be confused with shear thickening [Whorlow, 1992; Hackley and Ferraris, 2001]. The shear thickening behavior was first associated and even confused with the phenomenon of volumetric dilatancy of coarse aggregate, originally described by Reynold. All kinds of suspensions of solid particles in a fluid can show a shear thickening behavior [Barnes, 1989; Hoffman, 1998], if they present two particularities: volume fraction of solids in the suspension must be very high and the suspension must be non-flocculated. This requires that particles are mutually repelling due to Vander Waal forces and electrostatic forces as in some colloidal suspensions.

According to Barnes [1989], shear thickening behavior is mostly controlled by particle shape, size and distribution. Various attempts have been made to provide assumptions explaining this behavior. Among them, Hoffman's [1998] order-disorder transition theory and Bossis and Brady's clustering theory are emerging [Brady and Bossis, 1985]. It is difficult to directly transpose these theories to the cementitious materials. The use of super plasticizer makes it possible, owing to its dispersing action, the existence of concentrated dispersed suspension and so the occurrence of shear thickening. According to Barnes [1989], the gradual occurrence of shear thickening could be due to highly poly-dispersity of particles.

### Particle Sedimentation

Settling of particles during a rheological test is a function of liquid viscosity, liquid density, particle diameter, particle shape, particle density and fractional volume concentration of the dispersed particles [Chhabra, 1993]. Particle sedimentation would be

more significant in case of parallel plate compared to that in coaxial cylinders rheometers. Sedimentation or “creaming” in rheometers can result in an increase in the indicated viscosity [Barnes, 2000]. However, in most rheological setups, particle settling leads to a decreasing torque with time and leads to misleading results.

Banfill [1990] showed that in cement pastes, it is necessary to keep water-cement ratio below 0.4 for coaxial cylinder tests to avoid creating a vertical concentration gradient in the tested specimen that can affect the validity of results.

### Particle Migration

Fresh concrete is a coarse particle suspension, where it is the gravel particles that can be modeled as suspended particles and with mortar as the surrounding matrix. Barnes [1989], Leighton and Acrivos [1987] reported that there is a migration of suspended particles from the region of high shear rate to the region of low shear rate. They explained the reason for this phenomenon is related to a certain kind of diffuse process, induced by shearing.

Wallevick [2003] studied particle migration by numerical simulation and observed that gravel particles are pushed by collisions away from the region of highest collision rate to other region of the rheometer, leaving a concrete that is very rich in mortar. Another physical phenomenon could be present at the same time, also responsible for particle migration. This is the effect of dilatancy. In a suspension of densely packed suspended particles, the gravel distribution must change to permit gravel particles to flow past one another. This means a withdrawal of matrix from the region of smallest deformation into the region of largest deformation and hence the change in gravel concentration in the process.

Wallevick [2003] observed that particle migration is also dependent on the ratio of yield stress to plastic viscosity for coaxial rheometer. When this ratio is very low, such as in SCC, it is possible to solve the problem of gravel migration. A third physical phenomenon could also be accountable for particle migration, called confinement effect [Wallevick, 2003] and becomes apparent at low ratio of  $D_{flow}/D_{max}$ , where  $D_{flow}$  is the effective width of flow and  $D_{max}$  is the maximum size of aggregate. With relative small gap system such as  $D_{flow}/D_{max}=3$ , gravel particles could collide more strongly with each

other due to their lack of motional freedom in avoiding such a direct and strong mechanical interaction. This could result in a stronger pushing mechanism. The potential for gravel migration could be reduced by reducing maximum value of the rotational frequency. However, in making this step care must be taken to ensure that the smallest possible time passes between the end of mixing and start of measurement. If not, thixotropic effect could affect the result. Moreover, reduction of rotational frequency may cause plug flow. Wallewick [2003] concluded that plug flow is not a problem and can be accounted for and compensated. The error due to particle migration is a worse type of error because of its unknown magnitude.

### Shear Rate

The range of the shear rate generated in a rheometer for a given mix should be similar to the rates present in actual field conditions. Due to the possibility of nonlinearity in the flow curve, selection of a proper range of shear rate will ensure that the results are relevant to the given application. According to Schramm [1994], shear rate for a given application can be estimated as the maximum speed of fluid as it flows through a gap divided by the gap size. On a jobsite, the speed with which concrete flows through a pump, down a chute, or through space between reinforcing bars could be determined to calculate shear rate. During casting it is not unexpected if about 5 cm thick layer of concrete is flowing with the speed ranging from about 0.1 m/s to 0.5 m/s. with this, shear rate is in the order of magnitude  $2 \text{ sec}^{-1}$  to  $10 \text{ sec}^{-1}$ . Szecsy [1997] suggests without any data that  $\dot{\gamma}=10 \text{ sec}^{-1}$  is a maximum practical rate in the field. However, reports are also available where shear rate more than  $10 \text{ sec}^{-1}$  have been used [Westerholm et al, 2003; Esping, 2003], particularly in SCC. Roussel [2006] listed maximum shear rates in various flow patterns that are presented in **Table 1.1**

It is to be observed that de-flocculated state is reached during mixing. None of the rheometers are able to break completely flocculation state of the material after a resting period and shear rate they can apply is always less than that during mixing. This means that rheological behavior that is measured immediately after mixing will never be measured again if the sample stays in a rheometer. Because of the limitation of rotation

speed of the rheometers, this state and apparent irreversible evolution of the material that is not due to hydration process but due to rheometers limitation will be measured.

**Table 1.1:** Shear rates in various operations

<b>Flow pattern</b>	<b>Approx. maximum shear rate, /sec</b>
Mixing	10-60
Mixing truck	10
Pumping	20-40
Casting	10
Two-point test (MK III)	5
BML	10
BTREHEOM	15

### **1.3. SCOPE AND OBJECTIVE OF THE PRESENT STUDY**

Literature survey shows that although extensive works have been carried out to explain the rheological behavior of fresh cement mortar or concrete, more research is needed to improve the existing techniques of measurement and to examine the influence of materials, admixtures and their blending, mixing methods and measurement techniques on the rheological properties of high performance concrete. Rheometers have been developed and commercially made available to find out the workability of fresh concrete in terms of yield stress and plastic viscosity. However, direct measurement of these parameters are not possible and therefore, mathematical relationships were derived based on the principles of fluid rheology. The relationships were derived based on many simplifying assumptions such as ignoring frictional resistance between the side of the cylindrical wall and concrete. It may be emphasized that due to presence of coarse aggregate, the concrete rheometers are different from the rheometers used for cement paste or mortar. Geometrical requirement of every rheometer are different so that test results are widely variable. Moreover, concrete rheometers are less used compared to those developed for cement paste. Cleaning of the rheometer after test is very important

and existing rheometers present some inconvenience in cleaning because of non attachable parts.

In recent years, use of high performance concrete is in demand for increased strength, durability and appearance. The structural and architectural considerations necessitate slender and thin element, high rise construction, long span bridges for which high strength, dense, flowable concrete are essential. In case of structural component congested with reinforcement, proper adjustment of the properties of fresh concrete is highly significant for the performance of structure. The tests performed in the field are not adequate to describe all components of workability. Therefore, need arises for the proper judgment of the properties of fresh concrete by rheological tests. A new workability scale based on rheological parameters is essential for proper control of concrete mix. Observing the practical significance of the research on concrete rheology and inadequacies/ inconvenience of the existing methods, the main objectives of the present study are:

- To design a rheometer with parallel plate geometry for high performance concrete and to fabricate it.
- To establish a relationships between shear stress versus torque and overall shear strain rate versus rotational frequency in terms of the equipment geometrics and directly observed parameter to obtain flow curves for determination of yield stress and plastic viscosity. The frictional resistance between the cylindrical wall of the container and concrete which was ignored in earlier studies will be considered in the present case.
- To calibrate the equipment and validate by measuring the properties of a viscous fluid independently with the newly developed rheometer and available fluid rheometer.
- To perform the repeatability check of the new rheometer

Nearly every aspect of mixture proportion, material characteristics and construction conditions influences the rheology of concrete. After developing the rheometer and validating the new equipment, further works are planned

- To experimentally investigate the effect of all possible factors such as sand, percentage sand, coarse aggregate size and distribution, HRWRA dosage, elapsed

time, water-cement ratio and paste volume-aggregate volume ratio on the rheological properties of HPC.

It has been found mineral admixtures are invariably used in HPC, which improves properties of fresh and hardened concrete. The role of mineral admixtures such as condensed silica fumes (CSF), rice husk ash (RHA) and pulverized fuel ash (pfa) on the rheological properties of fresh concrete need to be investigated. Steel fibers are added to concrete to reduce the chance of cracking. It may be noted investigation on the rheology of HPC with RHA was not reported in the literature and also no attention was paid to investigate the effect of blending of different mineral admixtures on the rheological properties of concrete. Hence the present study aims at

- Investigating the rheological properties of concrete with individual use of CSF, RHA and PFA and also with their blending
- Investigating effect of steel fibers on rheological behavior of high performance concrete.

From different experimental results in the present study, it is desired

- To find a correlation between conventional workability tests results (slump, slump flow, flow values, Vebe in case of fiber reinforced concrete) and rheological parameters (yield stress and plastic viscosity)
- To propose a new workability scale based on rheological parameters.

It is also found that mix design of high performance concrete is based on trials. The main difficulty is in finding out suitable water-cement ratio to match target strength as the existing water-cement ratio versus compressive strength relationship is not suitable for high performance concrete. Hence, the final aim of the present study is

- To propose a mix design for high performance concrete based on rheological parameters. Correlation between rheological parameters and compressive strength is to be investigated and the information will be used in proposed mix design. Proposed design aims to combine empirical results with mathematical calculations based on absolute volume method.

#### **1.4. ORGANIZATION OF THE THESIS**

The thesis is split into 7 chapters. Introduction, literature review, objective and scope are presented in **Chapter 1**. **Chapter 2** provides a full description of a parallel plate concrete rheometer including conceptual design, actual design, calibration, validation and repeatability. Methods are indicated to account for uncertainty so as to appreciate validity and limitations of experimental results. In **Chapter 3**, experimental investigation of rheological behavior of HPC without any mineral additives has been presented. Attempt has been made to correlate rheological parameters and slump, slump flow and slump flow time. In **Chapter 4**, results of the experimental investigation to examine the effect of fly ash, silica fume, rice husk ash, ternary additives and steel fibers on rheological properties has been presented. Experimental results on the effect of yield stress and plastic viscosity on Vebe time, % flow of fiber reinforced concrete have also been presented in this chapter. In **Chapter 5**, a new method of mix design procedure for HPC has been discussed. Correlations between compressive strength and rheological parameters, paste volume to aggregate volume ratio versus rheological parameters have been presented which are used in the mix design calculations. **Chapter 6** presents rheology based approach for characterization of workability of high performance concrete. Analysis and discussion has been presented to categorize workability combining yield stress, plastic viscosity and shear strain rate together into a single parameter, the energy dissipation rate per unit volume, which was used to develop a new workability scale. **Chapter 7** presents the general conclusion of the total experimental program and scope for future work. List of references are given in “**Reference**”. Basic statistical principles used in the analysis of experimental results are given in “**Appendix-I**”.

#### **1.5 CLOSURE**

The study of rheology of cement based materials goes back to 1910 with slump test. Since then, a large amount of discovery, suggestions failures and improvements have been made. In the present chapter, significance of the control of properties of fresh concrete has been discussed and provisions of different codes for defining workability has been mentioned. An extensive literature review has been presented in this chapter. For convenience, literatures have been grouped into three main divisions-(i) workability

tests and effect of different parameters on workability (ii) rheological tests and effect of different parameters on rheology (iii) rheology of high performance concrete and (iv) some special topics on rheology. In the literature review, readers are introduced with different commercially available rheometers and comparison of their performance. Observing various shortfall and inadequacies of the earlier studies, finally the scope and objectives of the present study have been listed.



## **CHAPTER 2**

### **DESIGN OF A CONCRETE RHEOMETER**

#### **2.1 INTRODUCTION**

“Rheology” is the scientific study of the deformation and flow of matter. The devices which use principle of fluid rheology to measure the shear stresses of fluid at varying shear rates are called rheometers. Concrete rheometers are of two types: capillary and rotational. Capillary methods are more precise in measuring viscosity where yield stress is negligible or very small. Rotational methods are better for concentrated suspension like concrete because concrete can be sheared continuously to achieve equilibrium in such rheometers and changes of shear stress over time can be monitored. The primary components of a rotational rheometer are a motor, optical encoder or tachometer, torque-sensing mechanism and a means of applying torque along the rotor axis.

Although, fresh concrete can be considered as fluid, the design of concrete rheometer is difficult due to the presence of large size coarse aggregate. Concrete rheometer differs from other rheometers in geometrical requirements such as gap between shearing surfaces and radii of cylinders. The range of shear rate in concrete rheometer is also much less. Over and above, thixotropy, particle migration and particle sedimentation makes the design more complicated. Particle migration and particle sedimentation, in particular, are not a very common problem in cement paste or mortar rheometers.

The objective of this chapter is to design a parallel plate concrete rheometer taking into considerations the above challenges, obviating common artifacts and analytical drawbacks of existing rheometers.

#### **2.2 RHEOLOGICAL MODELS**

Rheological study aims to determine the deformation and flow of matter under the influence of an applied stress. The materials may range from elastic solids to viscous liquids but in rheology, interest is usually focused on those materials that possess both elastic and viscous properties. In practice, rheology has usually been restricted to the

study of the fundamental relations, called constitutive relations, between force and deformation in materials, primarily liquid.

Conventional rheological models in widespread use include the Bingham's model, Power-law, and Newtonian models [Hackley and Ferraris, 2001; Ramachandran and Beaudoin, 2006]. Of these, the Bingham model is advantageous because it includes a yield point and may be applied to cementitious materials. More recently, the Herschel-Bulkley model has been widely used because it accommodates the existence of a yield point (Bingham plastic) as well as the nonlinearity of the relationship of shear stress to shear rate (Power-law). Herschel-Bulkley model is used to describe the flow behavior of self compacting concrete.

A fluid that has a constant viscosity at all shear rates at a constant temperature and pressure is called a Newtonian fluid. Also, it can be described by a one parameter rheological model. An equation describing a Newtonian fluid is given below:

$$\tau = \mu \dot{\nu} \quad (2.1)$$

where the  $\tau$  is the shear stress,  $\dot{\nu}$  is the shear rate,  $\mu$  is the viscosity.

The Bingham plastic model was the first two-parameter model that gained widespread acceptance in fluid rheology and is simple to visualize. The model is given by

$$\tau = \tau_o + \mu \dot{\nu} \quad (2.2)$$

where  $\tau_o$  is the yield stress and  $\mu$  is the plastic viscosity.

The Herschel-Bulkley model defines a fluid by three-parameter and can be described mathematically as follows:

$$\tau = \tau_o + \mu \dot{\nu}^n \quad (2.3)$$

where  $n$  is the power index which represents the deviation from linear behavior and it can be greater or less than 1. When  $n$  is equal to 1, Herschel-Bulkley model becomes a Bingham equation.

Casson's model described the flow of viscoelastic fluids. This model is used by petroleum engineers in the characterization of cement slurry and is better for predicting high shear-rate viscosities when only low and intermediate shear-rate data are available. The Casson model is more accurate at both very high and very low shear rate and is given by the following equation:

$$\sqrt{\tau} = \sqrt{\tau_o} + \sqrt{\mu \dot{\nu}} \quad (2.4)$$

Concrete as a fluid is most often assumed to behave like a Bingham fluid with good accuracy. In Bingham model, flow is defined by two parameters: yield stress and plastic viscosity as mentioned earlier. Yield stress gives the quantitative measure of initial resistance of concrete to flow and plastic viscosity governs the flow after it is initiated. To determine the Bingham parameters with a rheometer, fresh concrete is sheared at high rate before the rheological test. Then, shear rate is decreased gradually and stress is measured. The relationship between shear stress and shear rate is plotted as flow curve. The intercept at zero shear rate is yield stress,  $\tau_o$  while the slope of the flow curve is plastic viscosity  $\mu$ .

## **2.3. DESIGN OF CONCRETE RHEOMETER**

### **2.3.1. Conceptual Design**

Design of a concrete rheometer is a challenge due to the nature and composition of concrete and the main problem with properly characterizing the rheology of concrete is the large size of coarse aggregates. The general rule for rheometers is that gap size should be in the range 3 to 10 times the maximum size of aggregate [Ferraris 1999; Banfill 2003]. This is important to minimize the effect of change in particle packing near walls. Rheological measurement of same concrete will vary among the rheometers due to differences in geometry, particularly ratio of outer to inner diameters in case of coaxial rheometers. For concrete, maximum value of this radii ratio has been suggested as 1.2 [Tattersall and Banfill 1983] or 1.1 [Ferraris 1999] to ensure small variation in shear rate across the gap and to minimize the speed range at which plug flow occurs. In case of parallel plate rheometer, however, radii ratio does not intervene. Ignoring plug flow results in an underestimate of yield stress and overestimate of plastic viscosity. The height-radius ratio should not be less than 1.0 to minimize the contribution of the bottom of the cylinder. A common problem for a rheometer is the slippage that occurs at the walls due to wall effect [Ferraris and Browner 2001]. It is possible to reduce or prevent slippage by roughening the rheometer walls or by providing ribs.

Tattersall and Banfill [1983] reports that if a rheometer were constructed based on the requirements stated above, the volume of such a rheometer would be 2.6 cubic meter. Therefore, in commonly available rheometers, some compromise is made and hence the dimensions provided do not exactly satisfy the theoretical requirements.

Concrete rheometers have been used by the researchers over the years. Parallel plate has the advantage over the coaxial rheometer that the gap between shearing surfaces can be adjusted. In parallel plate rheometers like BTRHEOM and UIUC, it is assumed that frictional resistance between concrete and vertical wall of cylindrical container is negligible due to formation of a layer of water and fine particles [Fig 2.1]. In some investigation, this frictional resistance has been found to be small compared to yield stress of concrete [Hu et al, 1996]. It has also been reported that there are difficulties involved in cleaning the parallel plate rheometers during the experiment [Ferraris and Brower (Ed), 2004]. In case of UIUC rheometer, adjustments are to be made to the rheometer to reduce error in measurement, because material may enter the gap between lower plate and side wall. It produces extra torque and makes the estimation of shear stress more difficult [Szecsy, 1997].

In view of the above, the present study undertakes the design of a new rheometer for concrete with parallel plate geometry. Frictional resistance between concrete and vertical wall of the cylindrical container has been taken into account. There are difficulties to take shear stress of the mortar into account in existing parallel plate rheometers. First, the exact shear rate variation near the wall is not known i.e. whether there is slip, no-slip or partial slip at the wall [Fig 2.1]. Secondly, even if the shear rate field is known, one has to determine the rheological parameters of mortar near the wall which makes the situation more complex. In the present study, this problem has been solved in the simplest but still in the most effective way. The diameter of the shearing plate has been kept smaller than the cylindrical container so that in the annulus one has concrete under investigation. The difference in diameters satisfies criteria of the gap/maximum size of aggregate ratio when end effect of vane plate is considered up to 20 mm coarse aggregate size. Concrete in the annulus between surface passing through vane plate and vertical wall of cylindrical container is sheared and has been considered in deriving expression of total torque. The arrangement also provides convenience in cleaning.

### 2.3.2. Actual Design and Construction

As a first step, preliminary minimum design requirements were developed for the rheometer. These requirements were based on the expected operating range of the rheometer and the operating characteristics of existing rheometers. These requirements are listed in **Table 2.1**.

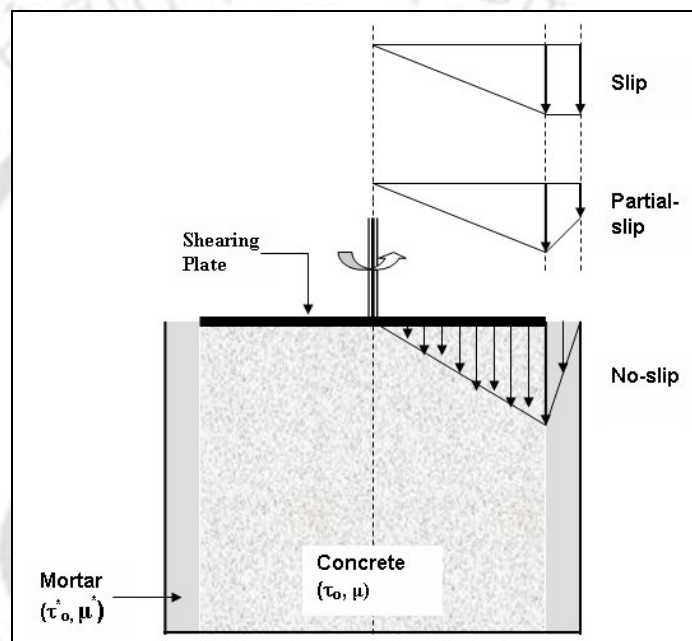


**Fig 2.1** Principle of available parallel plate rheometers (Velocity profiles are all at the surface)

The development of present rheometer consisted of three major aspects: the selection of motor and gear box, development of control system and impeller. The motor should be able to provide sufficient torque to turn an impeller in concrete. Motors that are able to provide necessary torque may have very large rpm that may not be within the limit for concrete rheology. Size of high hp motor is also prohibitive in a rheometer. Shear rate setting on a motor within desirable torque range is difficult that is necessary for a flow curve measurement. In the present case, 1 HP motor with different rated revolutions

were used with different impeller sizes as discussed in detail in next paragraph for selection of motor.

**Table 2.1** Preliminary design requirements

Particulars	Design Requirements
Maximum expected torque	25 N-m
Maximum shear strain rate	40 per sec
Size	As compact as possible
Control	Operations to be controlled by electrical appliances
Impeller	As small as possible while still generating representative flow and minimizing segregation.

The impeller size should be such that gap sizes are a proper multiple of maximum aggregate size and that increment of torque generated at each higher speed increment can be measured accurately. Still, torque generated should not be too large in order to avoid unreasonably large size motor. In order to select impeller size, it was necessary to test experimentally impellers of several diameters. It is also useful to consider total torque generated after structural breakdown. If the torque measured by the impeller is too low, the resolution in torque measurements may be insufficient for accurate flow curve measurement. Further, low torque may be an indication that only a small portion of material is flowing. If the torque is too high, the range of concrete workability that can be measured will be limited. Based on series of tests of 75 mm, 125 mm, 150 mm and 175 mm impellers, the vane plate having diameter 150 mm was selected for use in the present case. **Fig 2.2(a) & (b)** shows the photograph of impeller and cylindrical container of presently designed and fabricated rheometer. The amount of torque generated by the impeller was acceptable for providing adequate torque resolution while not exceeding maximum torque capacity of rheometer during structural breakdown stage. Small size impellers can easily shear stiff mixes but the sensitivity is less for high slump concrete.

Tests were conducted with 1 HP-1425 rpm motor and 150 mm diameter vane plate to arrive at the gear ratio of gear box for optimum speed to be used to measure yield stress. If the speed is too low, structure of concrete may reform due to flocculation before the yield stress is reached and there may be possibility of plug flow during rheological measurements. If the speed is too high, there may be possibility of particle migration. For the purpose of optimum speed, several gear boxes were fabricated with gear ratios 5, 7 and 10. Gear ratio 7 was found suitable and finally selected keeping in mind the design requirements listed in **Table 2.1**.

A schematic diagram of the proposed parallel plate rheometer is shown in **Fig 2.3** to describe its components and working principle. It consists of a 150 mm diameter flat circular vane plate driven by an induction motor through a gear box. The gear box reduces the rpm and at the same time it increases the torque. The thickness of the vane plate is 20 mm and it is mounted coaxially with a cylindrical container of effective diameter 270 mm (total diameter being 310 mm) with sleeve and bearing arrangement to ensure accurate alignment. The torque and speed of rotation of the motor and hence the vane plate is controlled manually by varying input voltage with a 10 ampere AC variac. Variac is a type of auto-transformer. An auto-transformer is a one-winding transformer. The same winding acts as the primary and a part of it as the secondary. The winding is tapped at a suitable point to obtain the desired output voltage across the secondary. In an auto-transformer, the smaller the ratio of primary to secondary voltage, the smaller is the amount of power transformed and hence larger is the amount of power conducted from primary to the load. A variac has a winding wound around on a toroidal core. A thick carbon brush makes contact with the winding in the desired position. The output voltage can be varied from zero to 120% of the input voltage. Variacs are mainly used for making available variable AC voltage from fixed supply voltage.

The number of revolution of the vane plate is measured automatically with a non-contact infrared digital tachometer, by focusing at the retro-reflective tape glued to the spindle or shaft. The contact type tachometer cannot be used in the present case because at low voltages, spindle cannot rotate once the tachometer is pressed against the shaft. Thus, one cannot measure the shear rate at low voltages with contact type tachometer.

The cylindrical container is provided with vertical ribs of 20 mm projection at a pitch of 60 mm along the circumference. A circular vane plate of diameter 310 mm and thickness 20 mm is also welded to the bottom of the cylinder. The effective gap between the bottom and the shearing surface is 75 mm. The effective concrete height above the vane plate is also 75 mm. The no-slip condition of flow at top of the cylinder is achieved by providing 20 mm high mesh of blades. The mesh can be detached for convenient cleaning as and when necessary. The spindle has a pulley welded to it at its mid height that is used for calibration purpose only. The photograph of the built up rheometer used in the present study to measure rheological parameters of HPC has been shown in **Fig 2.4**.

### 2.3.3. Governing Equation

Following cases are considered to derive the governing equation leading to the estimate of Bingham parameters.

#### Case (a): Actual Flow Considering Resistance at Vertical Wall

In order to calculate yield stress and plastic viscosity from torque and tachometer readings, it is necessary to consider analytically the distribution and magnitude of shear stress acting on the side of the vane plate, top and bottom of the vane plate. From equilibrium, total torque acting on the vane plate is equal to sum of the resisting torques offered by concrete at side, top and bottom. The torque attributed to the side of the vane plate can easily be determined. However, the stress distribution above and below the vane plate is not uniform that poses difficulty in deriving expression for total torque.

Nguyen and Boger (1985) performed experimental measurements for such a case of a vane rheometer with three different methods to calculate shear stress. The torque attributed to side ( $T_s$ ) was assumed equal to shear resistance offered when the material just yields, as usually assumed in soil vane shear. The deduced expression of  $T_s$  is given by

$$T_s = \left(\frac{\pi}{2} d^2 t\right) \tau_s \quad (2.5)$$

where  $\tau_s$  is the shear stress acting on side,  $d$  is the diameter, and  $t$  is the height of vane. The distribution of stress below the vane was represented with an integral in terms of an unknown function of bottom shear stress,  $\tau_b(r)$  at any radius  $r$  as shown below:

$$T_b = 2\pi \int_0^{d/2} \tau_b(r) r^2 .dr \quad (2.6)$$

so that total torque,  $T=T_s + 2T_b$ . (2.7)

To solve the above equation, additional assumptions were made by Nguyen and Boger (1985) for three different conditions which are as follows:

(I): In the first method, shear stresses on the side, top and bottom are assumed to be evenly distributed and are equal to yield stress when maximum torque is reached. Total torque at yielding is thus given by:

$$T = \frac{\pi d^3}{2} \left( \frac{t}{d} + \frac{1}{3} \right) \tau_o \quad (2.8)$$

(II): In the second method, shear stresses on top and bottom are assumed to vary with radius based on a power law relationship. While the shear stress along the side of vane is equal to yield stress, shear stresses at top and bottom vary from zero at the centre to the yield stress at tip. The shear stress at top or bottom may be expressed based on the following equation:

$$\tau_b(r) = \left( \frac{2r}{d} \right)^m \tau_s \text{ for } 0 \leq r \leq \frac{d}{2} \quad (2.9)$$

Total torque is given by

$$T = \frac{\pi d^3}{2} \left( \frac{t}{d} + \frac{1}{m+3} \right) \tau_o \quad (2.10)$$

To solve for two unknowns  $m$  and  $\tau_o$  of the above equation, two measurements with different values of  $t/d$  may be performed.

(III): In this method, no assumption is made about the distribution of shear stress on the top and bottom of vane. Instead, the equation (2.6) is considered a function of  $t$ . The intercept of the line is equal to total torque acting on the top (and bottom) of the vane. By making measurements with at least two vanes of different heights slope can be determined and used to calculate yield stress.



Fig 2.2 (a) Impeller (b) Cylindrical container of present rheometer

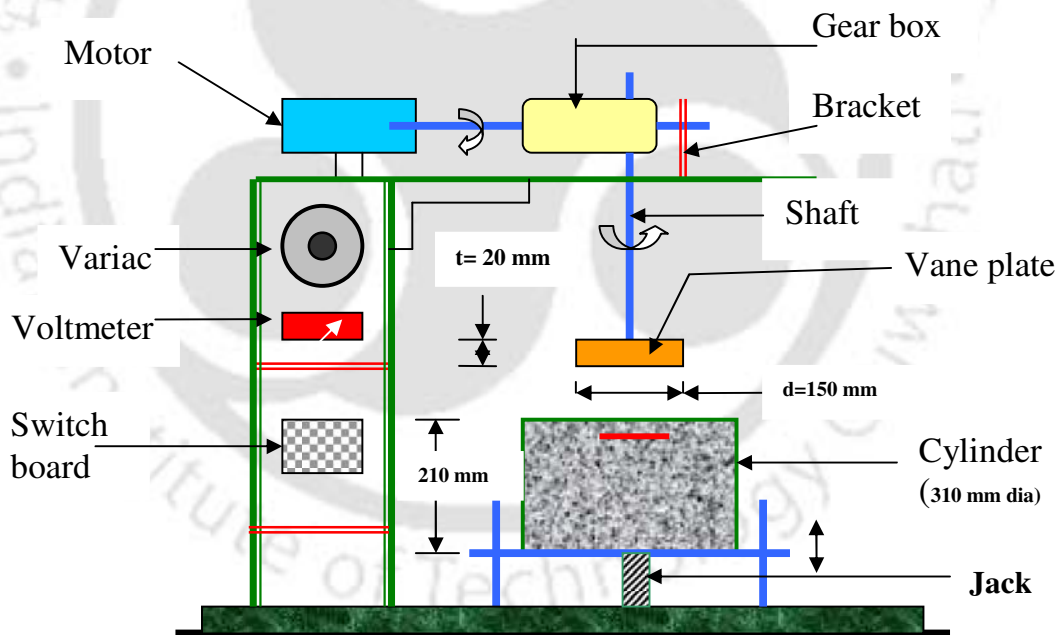


Fig 2.3. Schematic diagram of present rheometer



**Fig 2.4. Photograph of present rheometer**

The limitation of above three cases is that the expressions only contain yield stress and not plastic viscosity and the equilibrium conditions were derived on the onset of yielding. But concrete is a Bingham material that cannot be treated as a material like pure clayey soil.

Browne and Bamforth (1977) considered the flow in the annulus of a vane rheometer in presence of a cylindrical container in a different manner. They proposed a model to describe the shear stress as follows:

$$\tau = \tau_{o,i} + \eta_o v_g \quad (2.11)$$

where,  $\tau_{o,i}$  = interfacial yield stress;

$\eta_o$  = interfacial viscous constant (Pa.s/m)

$v_g$  = sliding velocity (m/s).

However, an assumption was made regarding the distribution of  $v_g$  along the gap. It was assumed that  $v_g$  was linearly distributed along the gap. The above equation was then expressed as:

$$\frac{T_s}{\frac{2}{3}\pi R^3} = \frac{3h}{R}\tau_{o,i} + \frac{3h\eta_o}{2}\omega \quad (2.12)$$

where  $R$  is the radius of the vane  $h$  is the gap between bottom of vane and cylindrical container.

Kuder et al (2007) ignored the resistance offered by the side and deduced the resistant torque at bottom as follows:

$$\frac{T_b}{\frac{2}{3}\pi R^3} = \tau_o + \left(\frac{3R}{4h}\omega\right)\mu \quad (2.13)$$

The above two expressions for  $T_s$  and  $T_b$  which were deduced independently ignoring the material response at the interface were simply added by Kuder et al (2007) to obtain total torque from bottom and side as follows:

$$\frac{T}{\frac{2}{3}\pi R^3} = \left(\tau_o + \frac{3h}{R}\tau_{o,i}\right) + \left(\frac{3R}{4h}\omega\right)\left(\mu + \frac{2\eta_o h^2}{R}\right) \quad (2.14)$$

$\omega$  is the angular velocity of circular vane.

The existing equations were based on simplifying assumptions as discussed above. In the present study, the actual non-uniform distribution of shear rate across the material was considered as it were without any assumption or simplification. Material response at the interface of bottom and side of vane plate were taken into account by considering the compatibility condition of equal deformation. The non-uniformity was taken care of by considering infinitesimal strips of material and integrating over the specified domain. The deduction for total torque is as follows:

Consider an element  $dr$  of the vane plate at a radial distance  $r$  and let  $h$  be the effective gap between bottom of the vane plate and the bottom of the cylindrical container (**Fig 2.5**).

Linear velocity at this radius =  $r\omega$ ;  $\omega$  = angular velocity of the plate in radian/sec.

Shear strain rate,  $\dot{\gamma} = \omega r/h$

Torque on this elemental disc is expressed as

$$dT = (\tau_0 + \mu\dot{\gamma})2\pi r^2 dr$$

$$\text{Total torque, } T_1 = \int_0^{d/2} dT = \frac{\pi d^3}{12} \tau_0 + \frac{\pi d^4 \omega}{32h} \mu \quad (2.15)$$

The above expression takes into account the effect of shear on the concrete just below the vane plate, that is, sample contained in cylinder ABCD. This surface ABCD also shears concrete contained in the annulus and can be calculated as follows.

Consider an elemental layer of thickness  $dz$  at a height  $z$  from bottom on the cylindrical surface ABCD [Fig 2.6]. The velocity along the radial direction on the surface of ABCD is given by

$$v_r = \frac{z \omega d}{h \cdot 2} = \frac{vz}{h} \quad (2.16)$$

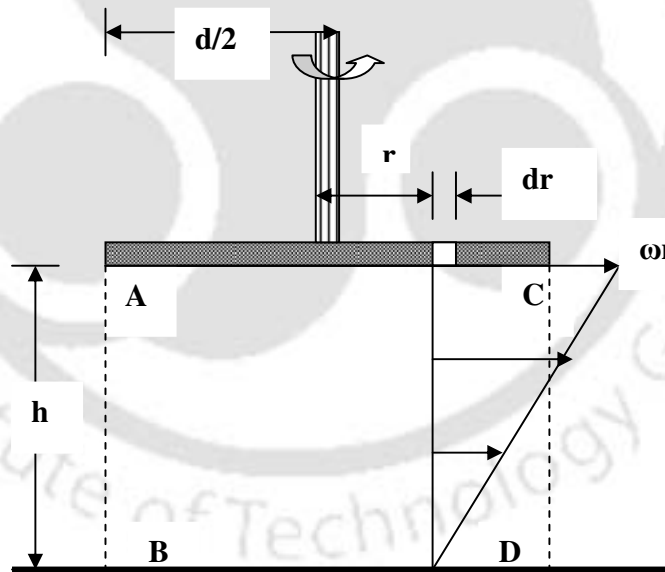


**Fig 2.5.** Flow of concrete below vane plate

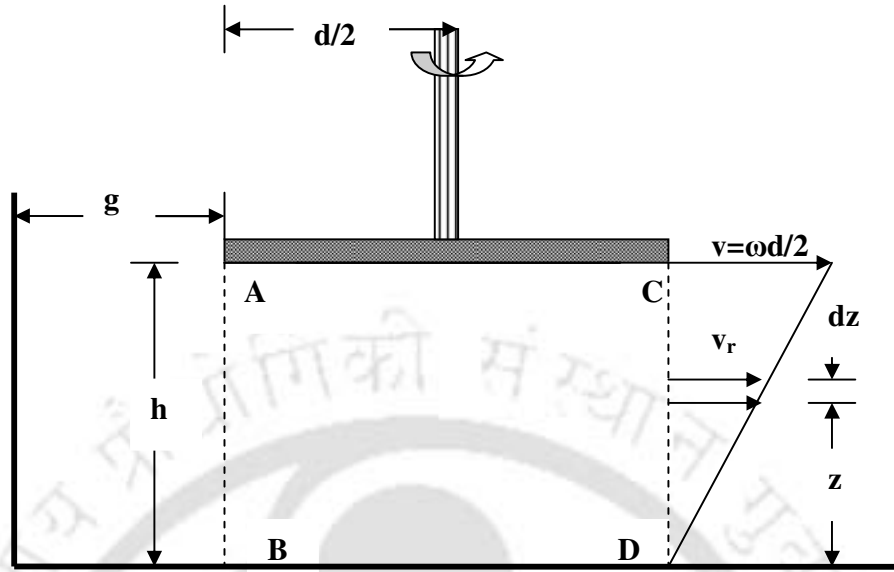


**Fig 2.6** Flow of concrete in the annulus

Therefore, at a height  $z$  from bottom shear stress  $\tau_r = \tau_o + \mu \frac{vz}{hg}$ ,  
 where  $g$  is the effective gap of the annulus.

Force on this elemental area,  $dF = [\tau_o + \mu \frac{vz}{hg}] \pi d \cdot dz$

$$\text{Total force} = \int_0^h dF = \pi d [\tau_o + \frac{\mu v}{2g}] h$$

$$\text{Total torque, } T_2 = \frac{\pi d^2}{2} h [\tau_o + \frac{\mu \omega d}{2g}] \quad (2.17)$$

Next, consider the end effect of the ribs of the vane plate. Let  $t$  be the height of the ribs. Velocity and shear rate are given by  $v = \omega(d/2)$  and  $v/g$  respectively.

$$\text{Torque, } T_3 = (\tau_o + \mu \frac{v}{g}) \pi d \cdot t \cdot \frac{d}{2}. \quad (2.18)$$

For concrete above the vane plate, similar expressions for torques  $T_4$  and  $T_5$  for material above the vane plate and in the annulus respectively may be deduced. During shearing of concrete in rheometer, deformations at the common boundaries (shown by dotted lines in **Fig 2.5**) are exactly same for two adjacent parts due to compatibility condition and have

been taken into account while deriving total torque. It is to be emphasized here that equal deformation at common boundary does not necessarily mean equal shear strain rate and shear stress in two adjacent parts.

Torques  $T_1$  to  $T_5$  are all directed towards longitudinal axis of the shaft. The magnitude of the resultant torque is, therefore, algebraic addition of magnitude of the component torques. Thus total torque ( $T$ ) is given by

$$T = \sum_{k=1}^5 T_k \quad (2.19)$$

which can be expressed in the form  $T = A + BN$  (2.20)

In the equation (2.20),  $N$  is the rotational frequency in revolution per minute (rpm),  $A$  and  $B$  are constants. Thus equation for torque is a linear function of rpm. The above expression can also be rearranged in the following form after substituting expressions for  $T_1$  to  $T_5$ .

$$\frac{T}{\left(\frac{\pi d^2}{2}(2h+t+\frac{d}{3})\right)} = \tau_0 + \left(\frac{\frac{d}{2h} + \frac{2(h+t)}{g}}{2h+t+\frac{d}{3}} \frac{\pi N d}{120}\right) \mu \quad (2.21)$$

where,  $N$  is the rotational frequency in revolution per minute (rpm). In the present equipment,  $d$  (diameter of the vane plate) = 0.150 m;  $h$  (effective gap between bottom of the vane plate and the bottom of the cylinder) = 0.075 m;  $t$  (height of the ribs of vane plate) = 0.025 m and  $g$  (effective gap of the annulus) = 0.060 m. Substituting these in equation (2.21), one has

$$125.75T = \tau_0 + 0.08N\mu \quad (2.22)$$

The above equation (2.22) is in Bingham's form. Comparing equation (2.22) with Bingham's equation, total shear stress (Pa) in terms of torque (N.m) can be expressed as

$$\tau = 125.75T \quad (2.23)$$

The overall shear strain rate (per sec) in terms of rotational frequency (rpm) can be written as

$$\dot{\gamma} = 0.08N \quad (2.24)$$

Both the quantities  $\dot{\gamma}$  and  $\tau$  can be observed during the experiment. By plotting the values of  $(\dot{\gamma}, \tau)$ , one has the flow curve from which  $\tau_0$  and  $\mu$  can be obtained.

It is to be mentioned here that concrete for rheological measurement can be taken up to the level of vane plate. In that case, only  $T_1$ ,  $T_2$ ,  $T_3$  will contribute to the total torque. In the present case, concrete is placed above the vane plate. This is done to avoid formation of gap, if any, below vane plate that may not have filled with concrete during shearing, particularly in low slump concrete. This is as per available literature on rheological measurements where unconsolidated concrete needs to be tested in a rheometer [Koehler and Fowler, 2004]. Consolidation starts once concrete is sheared in a rheometer. In case of highly flowable mix, material has a tendency to flow away from the bottom of the vane plate. Therefore, vane plate is totally immersed in concrete.

#### Case (b): Flow Neglecting Resistance at Vertical Wall

If resistance offered by the vertical wall of the cylindrical container is neglected, no-slip condition of flow of concrete during shearing is not achieved. The tangential velocity of the material in the annulus at the mid-height of the cylindrical container is constant and is equal to  $(\omega d / 2)$  [Fig 2.7]. Thus, there is a linear decrease of velocity from mid-height to the bottom (and to the top) of the cylindrical container.

Shear strain rate between mid-height and bottom of material in the annulus is given by

$$\dot{\gamma} = \frac{\omega d}{2h+t} \quad (2.25)$$

$$\text{Shear force} = \text{Shear stress} \times \text{area} = \left( \tau_o + \mu \frac{\omega d}{2h+t} \right) \left( \frac{\pi}{4} (D^2 - d^2) \right)$$

The torque due to the material in the annulus is given by

$$T_2' = T_4' = \left( \tau_o + \mu \frac{\omega d}{2h+t} \right) \left( \frac{\pi}{4} (D^2 - d^2) \right) \left( \frac{d+g}{2} \right) \quad (2.26)$$

where  $T_2'$  and  $T_4'$  are the torque components due to material in the annulus below and above the vane plate respectively.

In this case, torque components  $T_2, T_3, T_4$  will be non-existing as found in case (a). Torque  $T_1$  and  $T_5$  will be given by equation (2.15).

Total torque thus can be written as

$$T = T_1 + T_5 + T_2' + T_4' \quad (2.27)$$

where  $T_1 = T_5 = \left( \frac{\pi d^3}{12} \tau_o + \frac{\pi d^4 \omega}{32h} \mu \right)$  and  $D =$  diameter of the cylindrical container.

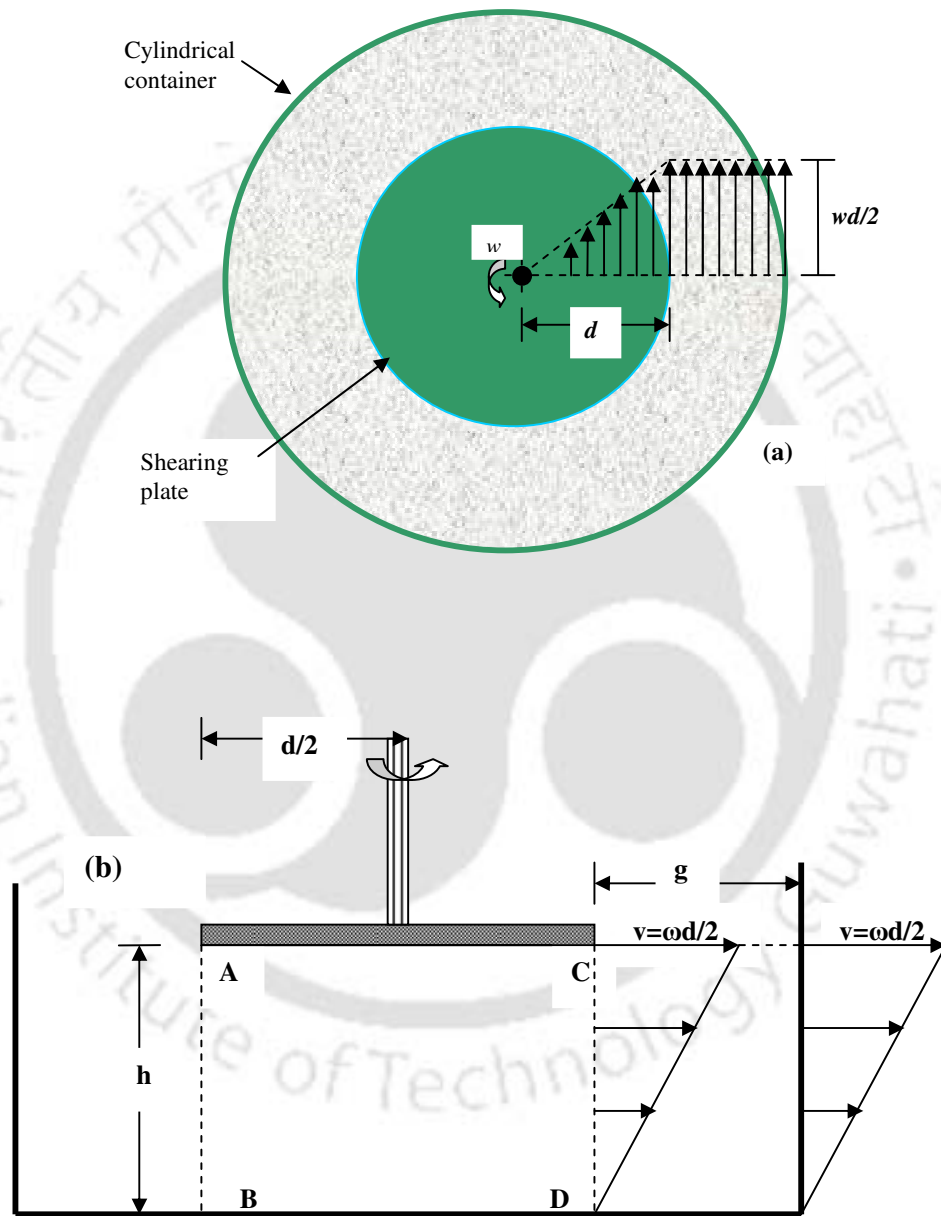


**Fig 2.7** Velocity profile at mid-height (a) Horizontal Plane (b) Sectional Elevation

Substituting the values of d, t, g, h as before, one has the simplified equation in the following form:

$$136.57T = \tau_o + (0.132N)\mu \quad (2.28)$$

The above equation (2.28) is in Bingham's form. Comparing equation (2.28) with Bingham's equation, total shear stress (Pa) in terms of torque (N.m) can be expressed as

$$\tau = 136.57T \quad (2.29)$$

The overall shear strain rate (per sec) in terms of rotational frequency (rpm) can be written as

$$\dot{\gamma} = 0.132N \quad (2.30)$$

Equation (2.28) can be used to draw the flow curves to determine yield stress and plastic viscosity. The comparison of the rheological parameters obtained using equation (2.22) and equation (2.28) has been discussed in **section 2.7**.

### 2.3.4. Calibration of Torque

The torque in the present rheometer was calibrated by electro-mechanical method. A brief theoretical background of torque and induced emf of induction motor is presented in subsequent paragraphs, the details of which are available in Bhattacharya (1990).

#### Rotor Induced Emf

The rotating magnetic field produced by the stator of an induction motor will induce emf in both stator and rotor windings. The induced emf will depend upon the magnitude of rotating flux and the speed at which this flux cuts the stator and rotor conductors. When the rotor is stationary, the stator flux cuts the rotor conductors at a speed  $N_s$ .

Let  $E_{20}$  be the induced emf in rotor winding when the stator is at standstill. When the rotor starts rotating at a speed  $N_r$ , the rotating field cuts the rotor conductors at the speed  $(N_s - N_r)$  rpm. Since at  $N_s$  speed of flux cutting, induced emf in rotor is  $E_{20}$ , at  $(N_s - N_r)$  speed of flux cutting, induced emf in rotor will be  $SE_{20}$  where  $S = (N_s - N_r) / N_s$  is called slip.

Let  $V_1$  = stator applied voltage,

$\phi_2$  = phase difference between rotor current,  $I_2$  and rotor voltage  $E_2$ ,

$X_{20}$  = leakage reactance of rotor winding when rotor is at standstill,

$I_{20}$  = rotor current at standstill,

$I_2$  = rotor current at slip  $S$ ,

It can be shown that  $I_{20}$ , or  $I_2$  and  $\phi_2$  is given by

$$I_{20} = \frac{E_{20}}{\sqrt{R_2^2 + X_{20}^2}} \quad (2.31)$$

$$I_2 = \frac{SE_{20}}{\sqrt{R_2^2 + (SX_{20})^2}} \quad (2.32)$$

$$\cos \phi_2 = \frac{R_2}{\sqrt{R_2^2 + (SX_{20})^2}} \quad (2.33)$$

#### Torque in a Single Phase Induction Motor

Electrical power generated in single phase induction motor is equal to  $E_2 I_2 \cos \phi_2$ . This electrical power is lost as  $I^2 R$  loss in the rotor circuit and is given by [Bhattacharya, 1990]

$$I^2 R \text{ loss in the rotor} = \frac{S^2 E_{20}^2 R_2}{R_2^2 + S^2 X_{20}^2} \quad (2.34)$$

Again  $I^2 R$  loss in the rotor =  $S \times$  rotor input

$$= S \times S \frac{2\pi T N_s}{60} \quad (2.35)$$

where  $T$  = mechanical torque developed by the rotor. Equating above two expressions, one has

$$T = \frac{60}{2\pi N_s} \frac{SE_{20}^2}{R_2^2 + S^2 X_{20}^2} R_2 \quad (2.36)$$

Now,  $E_{20}$  is proportional to air gap  $\phi$ , and therefore  $T \propto \frac{S\phi^2 R_2}{R_2^2 + S^2 X_{20}^2}$ . (2.37)

Since flux produced in the air gap is approximately proportional to supply voltage to the stator, from the above expression it can be seen that torque on rotor is proportional to square of the stator applied voltage,  $V_1$ .

$$\text{That is, } T \propto V_1^2. \quad (2.38)$$

#### Calibration Procedure and Preparation of Calibration Chart

The circuit for the purpose of calibration consists of wattmeter, voltmeter, ammeter and a 10 ampere variac. A spring balance anchored to a fixed object is fitted to the pulley of the spindle. When the motor is switched on, the spring balance blocks its rotor and the spring balance reading is noted. This arrangement gives the braking torques at different voltages. Thus for a set of voltages, braking forces or torques can be obtained. In the present case, two spring balances were used: 20 kg up to 65 volts and 100 kg for above. The spring balances were again calibrated using an accurate digital balance. Finally, braking torque was plotted against volt and watt. Calibration charts were obtained using regression analysis. The  $R^2$  value of Torque-Volt curve is much higher than that of Torque-Watt curve and hence it was used as the calibration chart for torque throughout the experiment (**Fig 2.8**). Banfill [1991] adopted such rotor blocking method in one of his rheometer designed for cement mortar.

It is to be mentioned that iron loss, winding loss are constants losses in case of AC induction motors. They are same at any load and are dependent on the supply voltage and speed and not dependent on load on the motor [Bhattacharya 1990]. The gear box was well lubricated before testing and lubrication was maintained at regular intervals. Therefore, the mechanical loss, if any, may be considered as insignificant. As mentioned earlier in previous section, torque is proportional to square of the stator-applied voltage. However, **Fig 2.8** shows that torque is a second order polynomial of input voltage due to the presence of gear box.

#### **2.4. VALIDATION OF PRESENT RHEOMETER**

Calibration of torque was checked by testing a magneto-rheological fluid (MRF 132DG) supplied by LORD Corporation. The MR Fluid (magneto-rheological fluid) is a suspension of micron sized magnetizable particles in a carrier fluid (density=2980-3180

kg/cu.m; solid content by weight=80.98%; operating temperature= -40 to +130 °C). The fluid can be used in a shear mode [<http://www.lord.com>]. It responds to an applied magnetic field with a change in rheological behavior. This property enables MR fluid to find its use in various control devices such as brakes and clutches, dampers, shock absorbers etc. In many engineering applications, Bingham model can be effectively used to describe essential fluid properties [Yang et.al, 2002]. MR fluid, however exhibits Newtonian properties when no magnetic field is applied. It may be mentioned that Banfill (1991) used heavy Newtonian fluid for calibrating a rheometer designed for cement mortar.

This fluid has been used for validation purpose because it was readily available in the laboratory which has been brought for other purpose. The fluid is heavy and non-homogeneous like concrete. Rheological tests were carried out with the proposed rheometer at room temperature (20°C) to draw the flow curve of the MR fluid. No magnetic field was applied during the measurement. MR fluid has also been tested by HAAKE RS1 coaxial rheometer with plate and cone arrangement (rotor C35/1 attachment) to obtain the flow curve with RheoWin 323 software. RS1 is a research grade rheometer for all types of measurements in rotation and oscillation [Fig 2.9]. It can be equipped with a wide range of different temperature control and measuring systems. The use of sophisticated air bearing and digital signal processing technology allows extremely accurate measurements of viscoelastic and viscous properties. The fluid was sheared at each shear rate for 30 seconds and the measurements were obtained at 10, 20, 30, 40 per sec. Typical measurement at shear rate 30 per sec with RS1 is presented in Fig 2.10. Temperature was maintained 20.6°C during the experiment. The values of shear stresses exactly at 30<sup>th</sup> second at each shear rate were used to draw the flow curve. Fig 2.11 compares the flow curves of MR fluid obtained independently by two different rheometers namely HAAKE RS1 and present rheometer for the range of shear strain rate 10-40 per sec. It may be observed that the deviation of shear stresses obtained with the present rheometer from that of HAAKE RS1 vary between -6% to +21% within the range of shear rates under consideration. The reason for observed variation, however, may be attributed to the geometrical requirements such as gap size that are provided in present rheometer for concrete containing large size aggregate. In case of MR Fluid, maximum

size of particles is of the order of microns. Also, vane plate and ribs at wall creates local turbulence in the fluid at high shear rate resulting in a quite different rate field that is not accounted for while deriving expression for total torque.

## **2.5. TESTING PROCEDURE FOR RHEOLOGICAL MEASUREMENTS**

The measured rheological properties are, besides the material and geometrical configuration of the rheometer, affected by measuring procedure [Bager et al, 2001; Geiker et al, 2002]. The so-called *relaxation period* needed to obtain steady state flow should be taken into account in the selection of measuring procedure. Starting at high rotational speed, non-steady state is likely to cause overestimation of plastic viscosity and underestimate of yield stress. Furthermore, lack of steady state may indicate an apparent shear thickening behavior. The phenomenon was explained by particle suspension of colloidal particles exhibiting structural breakdown and recoagulation when subjected to increase or decrease in shear rate. Wallewick [2003] showed that coagulation rate is not only dependent on chemical composition of the mix but also on shear rate. The total time at each shear should be long enough to obtain steady state but short enough to limit segregation. The effect of measuring procedure is particularly pronounced for concretes with low water content [Geiker, 2003]. Wallewick [2003] used stepwise increasing shear rate sequence between 0-25 s followed by stepwise decreasing shear rate sequence between 25-40 s. Nedhi and Rehman [2004] while testing cement paste, pre-sheared for 2 minutes by applying a shear rate sweep from 0-70/sec. Then sample was sheared from 0-50/sec within 90 sec to procure up-curve. After allowing an equilibrium time of 15 sec, the sample was sheared 50-0/sec within 90 sec to produce down curve. Westerholm and Lagerblad [2003], Shienn and Tam [2003] considered third down curve to evaluate Bingham parameters.

Shear history of the sample can have significant influence on test results. One option to reduce variability in shear history would be to consolidate concrete fully by rodding or by vibration [Koehler and Fowler, 2004]. Of the existing rheometers only BTRHEOM includes a vibrator. Lack of full consolidation likely leads to additional variability in the test results. The measurement of concrete after full consolidation is disadvantageous because concrete at sites flows in unconsolidated state and is not fully consolidated until

it reaches its final location. Therefore flow of fully consolidated concrete is not relevant to construction operation.

In the present study, stepwise increasing shear stress sequence followed by a decreasing shear stress sequence has been used and the down curve has been taken to draw the flow curve. Concrete was sheared at each shear stress for 30 sec and readings were taken at the end of each period. Care was taken during the measurements so that shear strain rate did not exceed  $10 \text{ sec}^{-1}$  in any case [Roussel 2006; Szecsy 1997]. Otherwise particle migration of unknown magnitude may affect the test results. Any flow curve giving negative value of yield stress and  $R^2$  value less than 0.98 was rejected and repeated with a new batch. Plug flow, if any, is corrected graphically as explained below.

**Fig 2.12** shows a typical flow curve during rheological measurement. The curve has two parts: non-linear portion at lower shear rates that does not follow Bingham equation and a linear portion that actually follows Bingham equation. The non-linear portion is due to plug flow. If initial non-linear portion is considered, there is an over estimation of plastic viscosity (given by slope) and under-estimation of yield stress. Therefore, points corresponding to high shear rates were considered. In case of any deviation from linearity, those points were omitted during regression analysis.

## 2.6. REPEATABILITY ANALYSIS

### 2.6.1. Concrete Mix Used

For repeatability analysis, two different HPC mixes were prepared in the laboratory using the same materials but with different mix proportions. The mix proportions and mix designations are presented in **Table 2.2**. The physical properties of the ingredient materials are presented in the subsequent sections.

**Table 2.2** Mix proportions and mix designations (Quantities in  $\text{kg/m}^3$  of concrete)

Mix	Cement	Sand	Coarse Aggregate	Water	HRWRA	HRWRA Type
A1	531.7	516.3	1033	195.9	7.44	PC
A2	504.7	491	1114	176.3	10.1	SN

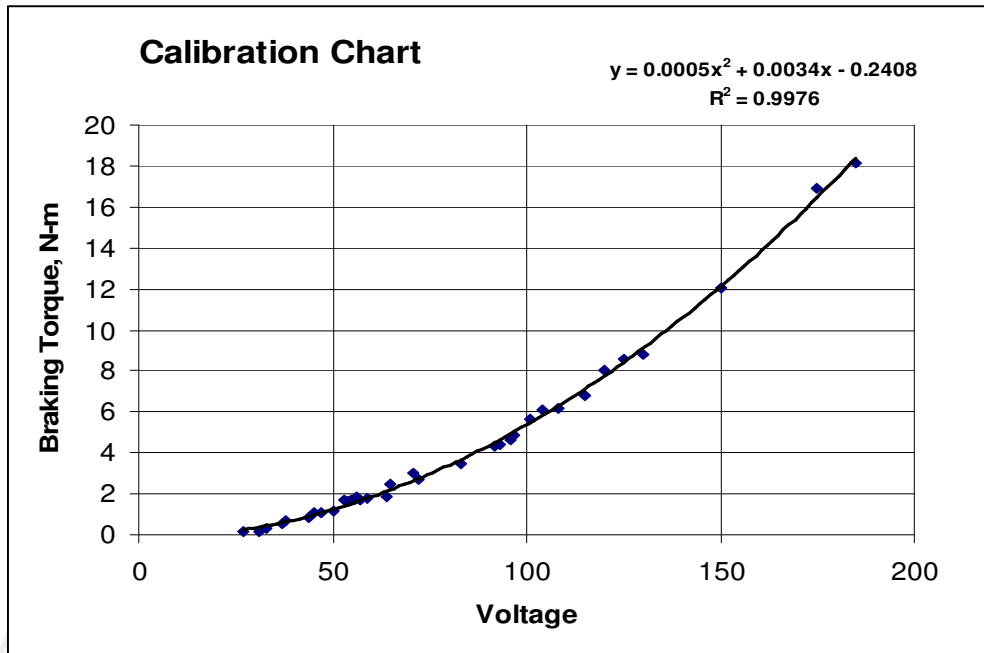
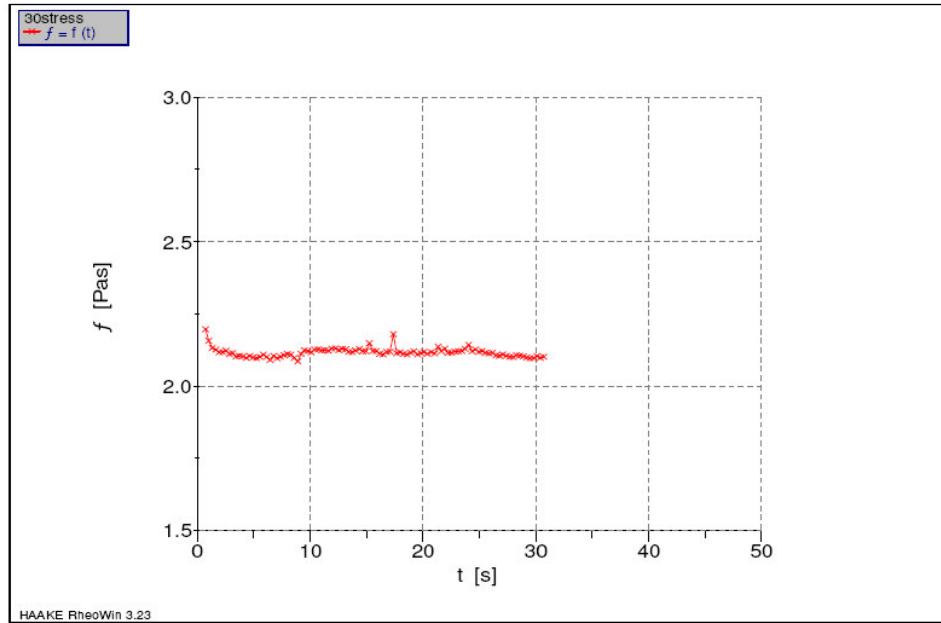


**Fig 2.8.** Calibration Chart for Torque



**Fig 2.9.** HAAKE RS1 Rheometer



1: C:\Documents and Settings\kaustav\Desktop\civil\30stress.rwd  
Company / Operator: IIT / IIT  
Date / Time / Version: 25.10.2007 / 11:05:27 AM / HAAKE RheoWin 323  
Substance / Sample no: MRF-132DG / 1

**Fig 2.10.** Visco-elastic measurement of MR fluid with HAAKE RS1 at shear rate 30 per sec

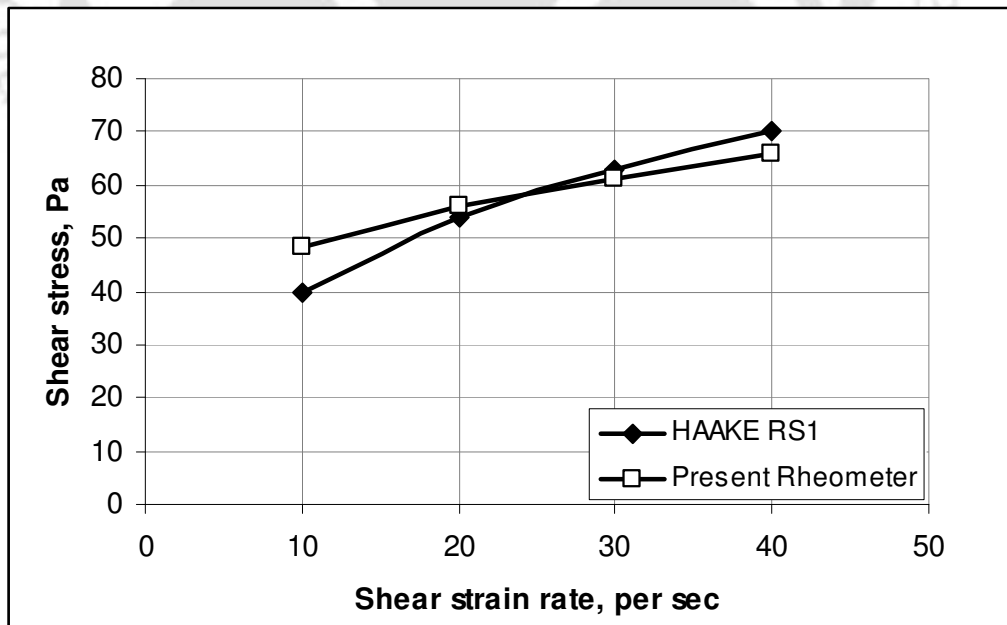


**Fig 2.11.** Validation of torque using MR fluid

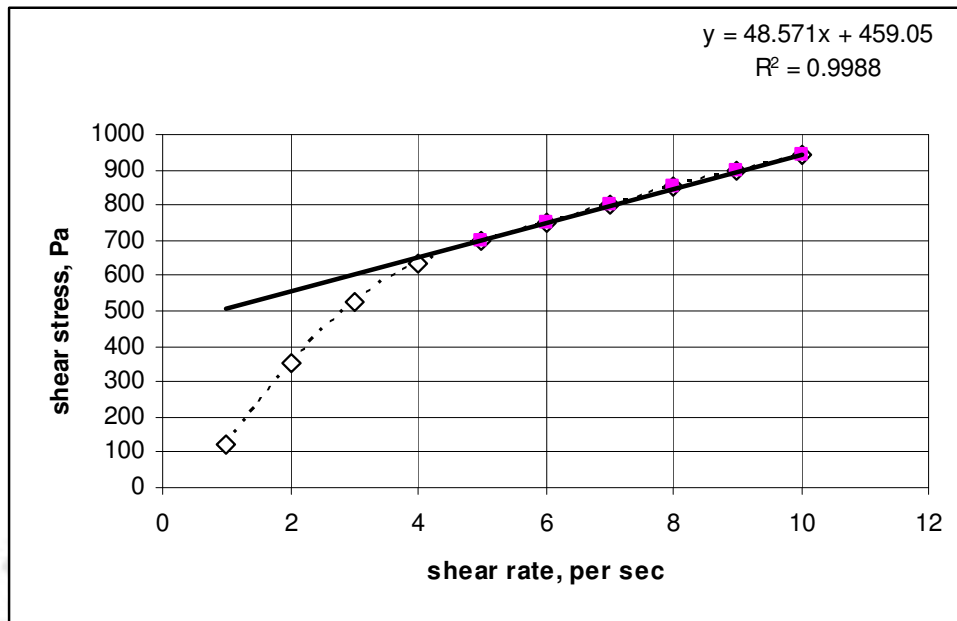


**Fig 2.12:** Plug flow correction

## 2.6.2 Material Properties

### Cement

The cement used throughout the experiment was Ordinary Portland Cement (OPC). The physical properties of cement determined as per Indian Standard Code Practice IS: 12269-1987 are as follows:

Specific gravity= 3.10

Standard consistency=29%

Initial setting time=55 minutes and final setting time=6 hours

28 day compressive strength=50.2 N/mm<sup>2</sup>

### Sand

Locally available alluvial sand (specific gravity=2.6) from a same pit was used. Sieve analysis, specific gravity, moisture content, water absorption, bulk density was determined as per relevant Indian Standard code (IS: 2386). The particle size distribution is shown in **Table 2.3**. Sand was stored inside the laboratory throughout the experimental investigation.

### Coarse Aggregate

Graded crushed stone aggregate (specific gravity=2.6; aggregate crushing value=20%) of maximum size 16 mm was stored in the laboratory. The physical properties were determined as per the code stated above. The particle size distribution is presented in **Table 2.4**. Aggregates were not sieved and were used as received.

### Chemical Admixtures

High range water reducing admixture (HRWRA) with set retarding effect was used as chemical admixture. Two types of HRWRA were used: Poly-carboxylic ether polymer (PC) for Mix A1 and Sulfonated Naphthalene Polymer (SN) for Mix A2. Ordinary tap water was used for all the mixes to prepare fresh concrete.

#### **2.6.3. Mixing Procedure**

Concrete was mixed in a tilting mixer (laboratory type). Mixing sequence was as follows:

- Mix coarse aggregate, fine aggregate and cement for one minute;
- Add water during mixing and mix for two minutes;
- Stop mixing for one minute;
- Add admixture to the mix and mix for three minutes;
- Pour the concrete mix.

The prepared concrete was transferred to the cylinder with a trowel from same height every time. The rheological test was carried out exactly after 15 minutes from the addition of water. Each time new batch of concrete with the same composition for a particular mix was prepared. The mixing sequence and the time at which the rheological test was performed were identical for each batch and for all mixes.

#### **2.6.4. Repeatability**

Potential source of errors in the measurement of rheological properties using new rheometer could be variations in mixing procedure, variations of materials used and measurement procedure.

Koehler and Fowler (2004) repeated the test on a same mix twice and compared the values of  $R^2$  values of flow curves. It was observed that  $R^2$  values were above 0.90 and it was concluded that repeatability was good as because testing variances were low.

**Table 2.3. Sieve Analysis of Sand**

Sieve size, mm	% Passing
4.75	98.2
2.36	96.5
1.70	94.6
1.18	91.2
0.60	66.3
0.30	20.3
0.15	1.6

**Table 2.4. Sieve Analysis of Coarse Aggregate**

Sieve size, mm	% Passing
16	100
12.5	42.20
10	31.80
6.3	25.0
4.75	0.9

Ferraris and Brower (2004) repeated testing three times on mixes and observed that coefficient of variation (COV) was very high. Most of the time, COV was higher than 10% and even as high as 166% in some cases. Ferraris and Brower (2004) stated, “These repeatability data are disappointing and it is not clear how to proceed, as the non-repeatability sheds a light of great uncertainty on all the data and correction factors.”

Wallewick (2003) measured rheological parameters of the same mix four times at different time intervals and computed the COV. It was observed that for measured values of yield stress and plastic viscosity, COV was 10%- 20% and repeatability was reported to be good.

In the present work, thirty observations were taken for each mix. The reason for choosing 30 is that Chi-square test [Chapra and Canale, 2002] is appropriate for class intervals

greater than 5 and can be obtained using the relation given by Ranganathan [1999] as follows:

$$a = 1 + 3.3 \log_{10} N \quad (2.39)$$

where, a=no of class intervals

N=total number of observations taken.

The other reason for taking N=30 is that Standard Normal Distribution provides a good approximation to Student-t distribution when the total sample size is 30 or more. For repeatability, each time new batch of concrete with same composition for a particular mix was prepared. Mixing sequence and the time at which test was performed were identical for each observation. Rheological tests were performed as per the procedure outlined before.  $(\tau_o, \mu)$  for mixes were calculated from flow curves using least square method. Thus for each mix, thirty values of  $(\tau_o, \mu)$  were obtained. Typical flow curves are shown in **Fig 2.13** and **Fig 2.14**. The raw data for  $(\tau_o, \mu)$  were grouped to draw histograms [**Fig 2.15- Fig 2.18**].

Assuming the distribution to be Normal, “goodness of fit” was tested by Chi-square test. It was observed that the distributions of  $(\tau_o, \mu)$  fitted normal distribution at 5% significance level for both the mixes under consideration. Since the number of observations in this case was only 30, distribution cannot be considered as population. In fact, it is sample distribution in the present case. When one uses sample mean ( $\bar{x}$ ) to population mean ( $m$ ), it is known that the chances are slim or virtually non-existent that the estimate is exactly equal to population mean. Hence it would seem desirable to accompany such a point estimate of population mean with some statement as to how close one might reasonably expect the estimate to be. The error,  $(\bar{x} - m)$  is the difference between estimated and true value. To examine this error, one can make use of the fact that  $(\bar{x} - m)/(s/\sqrt{N})$  is a value of the variate having Student-t distribution [Chapra and Canale, 2002] with (N-1) degrees of freedom. Consequently, one can assert with a probability of  $(1-\alpha)$  such that

$$\begin{aligned} -t_{\alpha/2} &\leq (\bar{x} - m)/(s/\sqrt{N}) \leq t_{\alpha/2} \\ \text{or } N &= \left[ \frac{s}{E} t_{\alpha/2} \right]^2 \end{aligned} \quad (2.40)$$

where  $E=(\bar{x} -m)$ ,  $s$ =sample standard deviation and  $t_{\alpha/2}$  is such that area to its right is equal to  $\alpha/2$ . The above expression requires the knowledge of population mean. Sample mean and sample standard deviation as obtained cannot be used to calculate the minimum number of times samples to be repeated or tested (i.e. the sample size) for some permissible error at some confidence level. Stein's two-stage formula [Steel and Torrie1980] was therefore used in the present study to predict the sample size given by

$$n = \left[ \frac{t_1}{D} s \right]^2 \quad (2.41)$$

where  $t_1$ =tabulated Student's t value,

$s$ =sample standard deviation and

$D$ =half width of the confidence interval and is calculated as the product of permissible error and sample mean.

The basic principles of statistics used in the repeatability analysis are given in Appendix-I of the thesis.

Typical calculation of n-value is as follows:

For **Mix:A1**,  $\bar{x} = 170.3$ ,  $s = 9.03$ .

Here  $N=30$  and thus  $\text{dof} = N-1=29$ .

Confidence interval= 95%, level of significance= 5%.

Permissible error  $E= 15\%$ .

As per Steel and Torrie (1980),  $D$  is calculated as the product of permissible error and sample mean i.e.  $D=E \cdot \bar{x} = 0.15 \times 170.3 = 25.55$  in the present case.

For  $\text{dof}=29$ , tabulated  $t_1 = 2.045$ ; [Miller and Freund, 1991].

Therefore,  $n = \left[ \frac{2.045 \times 9.03}{25.55} \right]^2 = 0.52 \cong 1$ .

The results of the statistical analysis are presented in **Table 2.5**. Definitions of the statistical terms and expressions are given in Appendix. The predicted sample size is one for both the rheological parameters. However, it is always desirable to have more than one reading for practical application.

## 2.7 EFFECT OF WALL RESISTANCE ON RHEOLOGICAL PARAMETERS

Most of the earlier studies neglected frictional resistance between wall of the cylindrical container and concrete. In the present study, frictional resistance was considered and comparison of results without frictional resistance has been presented in this section.

Rheological tests were carried out for Mixes A1 and A2 and the values of rotational frequency in rpm and input voltages were recorded to draw the flow curves in accordance with the procedure outlined in **section 2.6**. Flow curves were drawn for the cases when wall resistance is considered and when wall resistance is neglected using equations (2.22) and (2.28) respectively. The results have been presented in **Table 2.6**. Flow curves using the two cases are presented in **Fig 2.19**.

It may be observed from **Table 2.6** that there is a deviation of -37% and -41% of yield stress and plastic viscosity respectively from the actual rheological parameters when flow curve is drawn using equation (2.28), with the assumption that resistance offered by the vertical wall of the cylindrical container is negligible. Thus, the present study reveals that there is an underestimation of yield stress and plastic viscosity of significant amount if wall resistance is not taken into account.

## 2.8 CLOSURE

In this chapter, design of a rheometer for concrete has been presented. The concept and working principle have been discussed. The rheometer so designed has been fabricated in the laboratory and made ready to measure the rheological parameters of high-performance concrete. The calibration of the instrument, validation and repeatability check has been performed. An expression for total shear stress has been derived from where shear stress versus torque and overall shear strain rate versus rotational frequency relationship have been established for the designed geometry of the present rheometer. For deriving the desired relationship, resistance offered by vertical wall of cylindrical container to concrete during shear has been taken into account. The study also showed that negligence of wall friction underestimates yield stress by 37% and plastic viscosity by 41%.

**Table 2.5. Sample Size for Yield stress ( $\tau_0$ ) and Plastic Viscosity ( $\mu$ )** [Confidence interval=95%; permissible error=15%]

Particulars	Mix A1		Mix A2	
	Yield stress (Pa)	Plastic Viscosity, (Pa s)	Yield stress (Pa)	Plastic Viscosity, (Pa s)
Mean	170.3	51	175.1	70.1
SD	9.03	3.47	8.76	4.84
COV	5.3%	6.8%	5.0%	6.9%
n	1	1	1	1

**Table 2.6:** Comparison of rheological parameters with and without wall resistance

Mix	Actual flow considering wall friction [case(a)]		Flow neglecting wall friction [case(b)]		Deviation from actual	
	$\tau_0$ , Pa	$\mu$ , Pa.s	$\tau_0$ , Pa	$\mu$ , Pa.s	$\tau_0$ , Pa	$\mu$ , Pa.s
<b>A1</b>	164.2	49.2	103.4	28.8	-37%	-41%
<b>A2</b>	171	71.6	107.7	42.2		

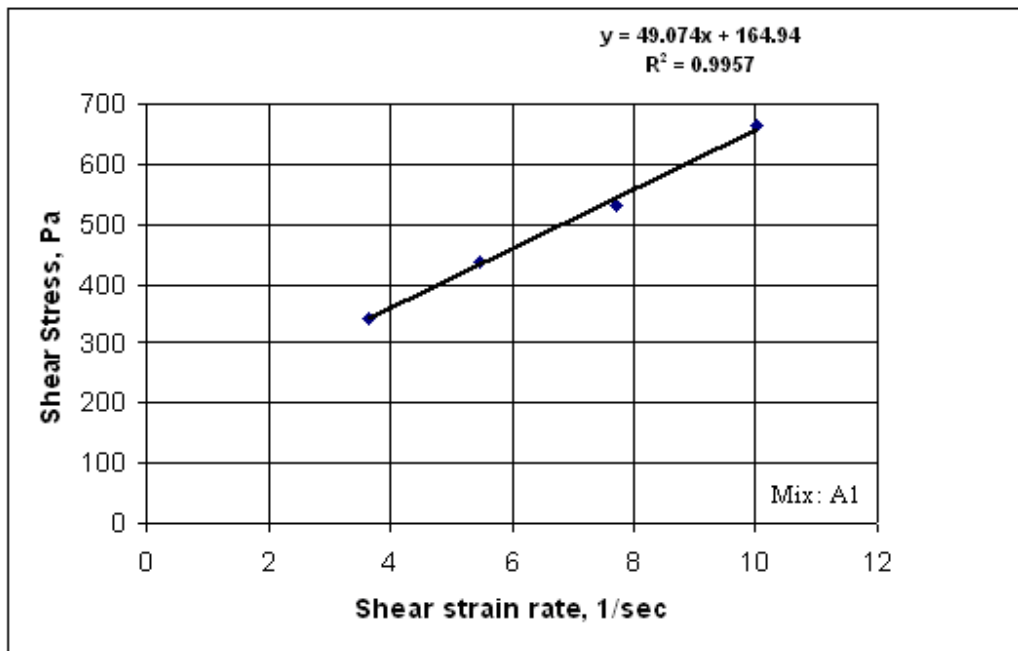


**Fig 2.13** Flow curve of Mix A1

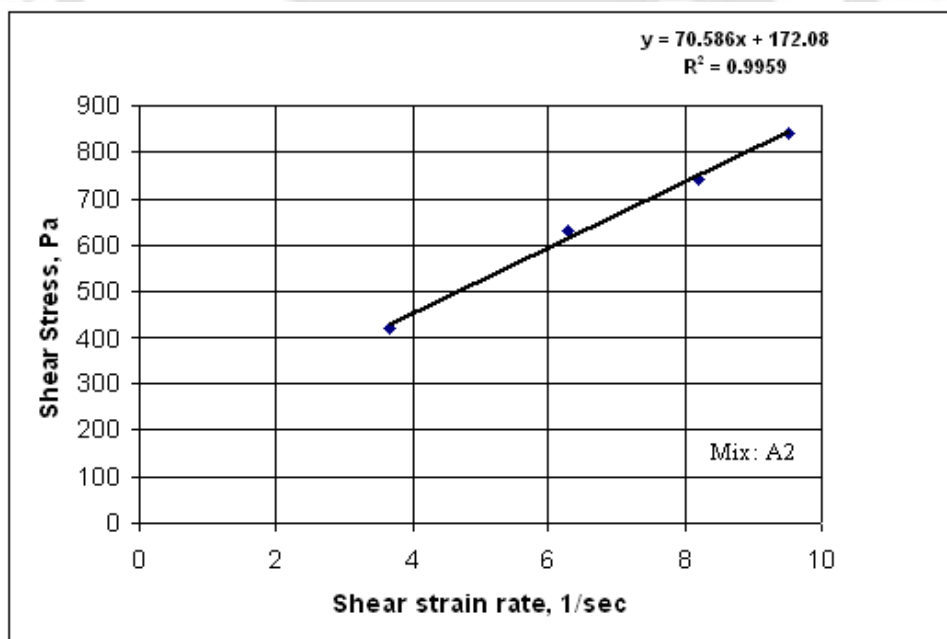


**Fig2.14.** Flow curve of Mix A2

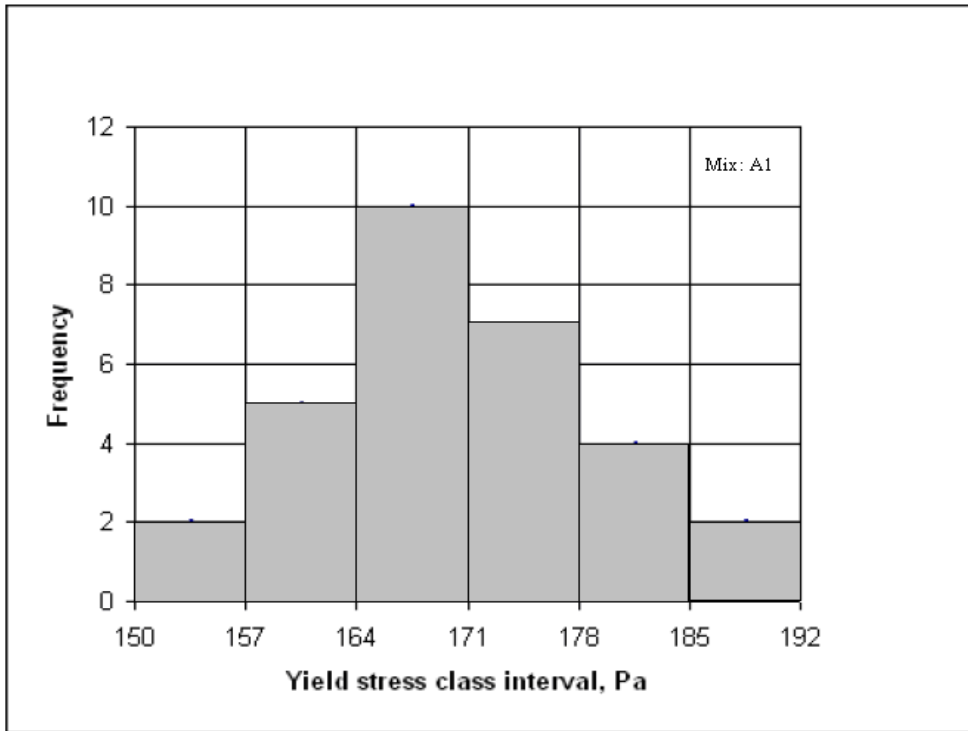


**Fig 2.15.** Histogram of Yield stress (Mix A1)

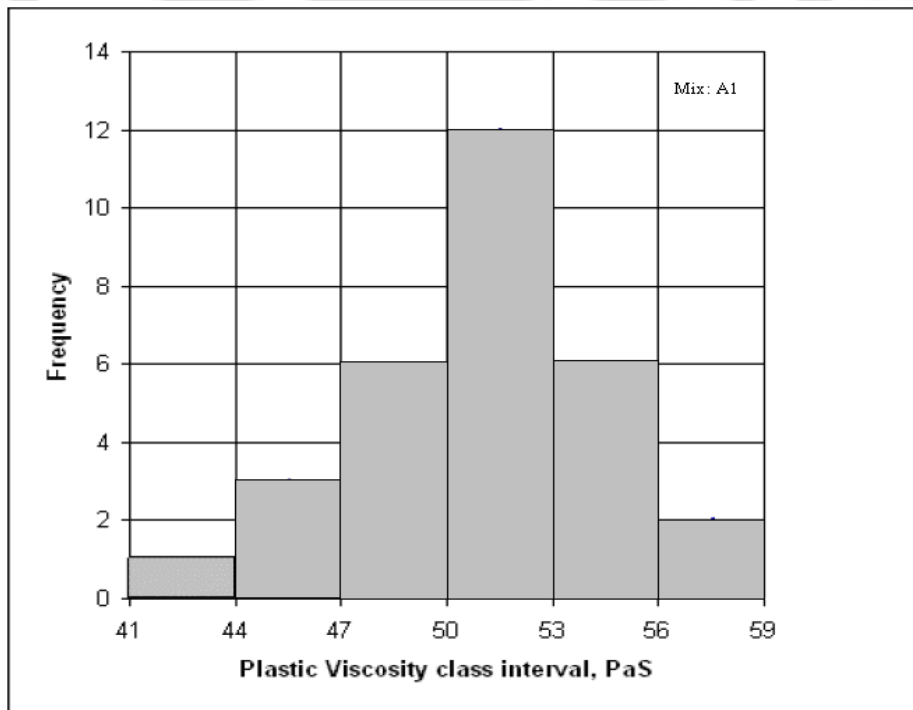


**Fig 2.16.** Histogram of Plastic Viscosity (Mix A1)

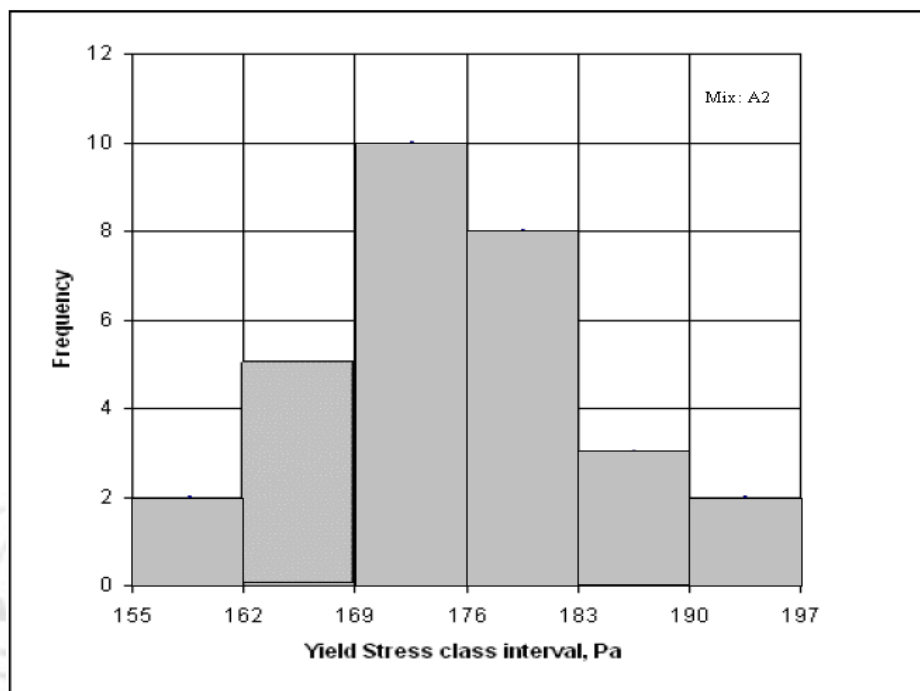


**Fig 2.17.** Histogram of Yield stress (Mix A2)

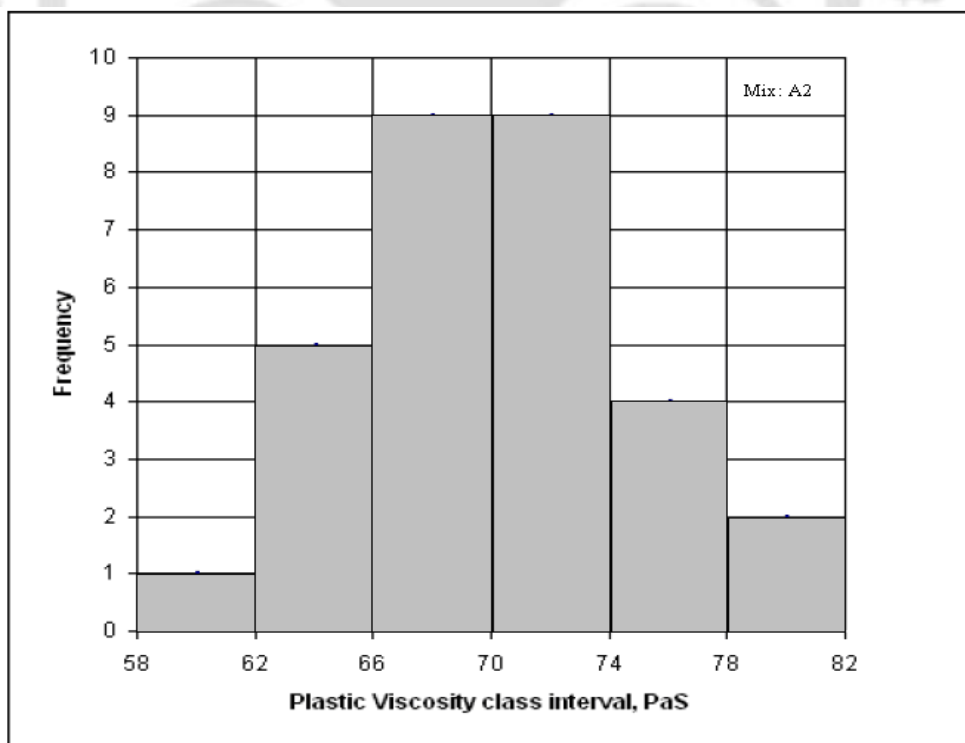


**Fig 2.18.** Histogram of Plastic Viscosity (Mix A2)

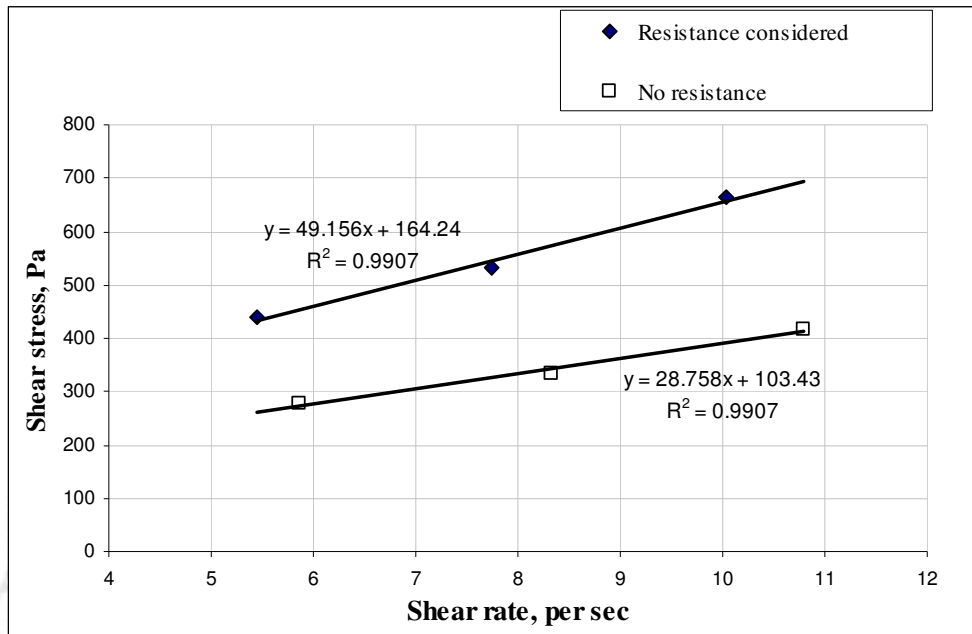


**FIG. 2.19.** Flow curve of Mix A1 with and without wall resistance

# CHAPTER 3

## RHEOLOGICAL BEHAVIOR OF HIGH-PERFORMANCE CONCRETE WITHOUT MINERAL ADMIXTURES

### 3.1. INTRODUCTION

Rheological behavior of concrete has been found significant to quantify the workability parameters. More investigations are needed to establish the role played by constituent materials, their properties and composition. Experiments were conducted to investigate the effect of sand content, gradation of aggregates, maximum size of coarse aggregate, average size of coarse aggregate and high range water reducing admixture (HRWRA) dosage and type on the rheological behavior of HPC.

### 3.2. EXPERIMENTAL PROGRAM

Five different HPC mixes were prepared in the laboratory for this purpose using the same materials but with different mix proportions. Mix proportions for different mixes were obtained by trial and adjustment so as to have different slump values. While arriving at the mix proportions, care has been exercised so that slump values were more than 100 mm. The mix proportions and mix designations are presented in **Table 3.1**. The constituent materials, mixing sequence were the same as described in section 2.6.2 and section 2.6.3 of Chapter 2 respectively.

#### 3.2.1 Slump and Slump Flow Test

Slump test was performed in a standard manner as specified in Indian standard code of practice IS: 7320-1974. As shown in **Fig 3.1(a)**, the apparatus consist of a mould in the shape of a truncated metal cone, open at both ends. The internal diameter of the slump cone is 200 mm at the base, 100 mm diameter at the top and has a height of 300 mm. This device is usually provided with foot pieces and handles. **Fig 3.1(b)** demonstrates how the slump is measured. Basically the procedure consists of filling the metal cone with concrete in three layers and each layer is compacted 25 times by a 16 mm rod. Thereafter,

the metal cone is lifted, leaving the concrete sample behind, which slumps down by the action of gravity.

<b>Particulars</b>	<b>Mix: B1</b>	<b>Mix B2</b>	<b>Mix B3</b>	<b>Mix B4</b>	<b>Mix B5</b>
Cement	503	558.7	531.7	504.7	422.8
Sand	660	444	516.3	491	676.5
Coarse Aggregate	1040	1085	1033	1114	1027.6
Water	186	193.5	195.9	176.3	173.3
HRWRA	7.07	7.71	7.44	10.1	8.27
HRWRA type	PC	PC	PC	SN	SN
Density, kg/cu.m.	2394	2372	2377	2328	2303
Slump, mm	187	180	170	128	75

Slump flow test is an alternative test for highly workable mixes and has been incorporated in Japanese Standard [JSCE-F503]. Slump flow is simply the measurement of the diameter of concrete after subsidence in conventional slump test [Fig 3.1(b)]. This test has the advantage that when testing a concrete whose workability is such that it is difficult to determine in advance if the concrete will flow, the value of either slump or slump flow as appropriate can be recorded.

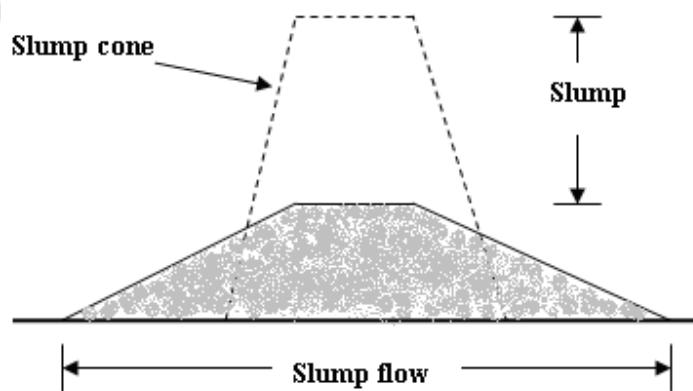


**Fig 3.1** (a) Slump test apparatus (b) slump and slump flow

### 3.2.2 Density of Fresh Concrete

Density of fresh concrete was determined by placing concrete in a 3 liter cylindrical mould in three equal layers and each layer was compacted 25 times by a 16 mm diameter rod. The weight of the concrete in the mould gave fresh concrete density.

### 3.2.3 Bulk Density and Packing Density of Aggregates

Packing density was determined as per IS: 2386 (Part-3)-1990. The packing of an aggregate for concrete is the degree of how good the solid particles of aggregate would fill up the volume of the concrete. For a given mix proportion, workability of a mix decreases as the void ratio [defined as  $1 - \text{packing density}$ ] increases. The packing density of individual particles is determined from its bulk density as follows:

$$\beta = \frac{\gamma_b}{\rho} \quad (3.1)$$

where  $\beta$ =packing density,

$\gamma_b$ =bulk density of particles,

$\rho$ = density of particles.

For determination of bulk density, the aggregates are filled in the container and compacted in a standard manner. The weight of the aggregate gives the bulk density in kg/cu.m. For sand and coarse aggregates, 3 liters and 15 liters nominal capacity containers respectively were used.

### 3.2.4 Other Tests

Specific gravity of coarse and fine aggregates were determined as per IS: 2386 (Part-3)-1990 using wire basket and pycnometer respectively. Water absorption and moisture content of aggregates were also determined in a standard manner.

### 3.2.5 Stability by Visual Observation

Before conducting workability and rheological tests, the stability of the prepared mixes against segregation has been visually examined and observations have been documented. Any trial mix that segregated during mixing in the mixer and during slump and rheological tests were discarded and not reported in this thesis. The same is true for all

the mixes containing mineral admixtures and round steel fibers which are reported in subsequent chapters. Mixtures were considered stable against segregation and bleeding if the following criteria, set by Daczko (2003) were satisfied.

- i) No evidence of segregation in slump or slump flow or in mixer drum.
- ii) No or slight mortar halo or aggregate pile in slump or slump flow patty but some slight bleed or air popping on the surface of the concrete in mixer drum.

The result of a typical slump flow test of a mix is shown in **Fig 3.2**. It is to be observed that no halo exists at the edge of the concrete and the aggregates are more or less uniformly distributed throughout the mass. In **Fig 3.3**, a slight halo is present at the edge of the concrete but it was also considered stable against segregation. The mix shown in **Fig 3.4** showed segregation because there was aggregate piling at the centre and there existed a large mortar halo at the edge of the mix.

### 3.2.6 Rheological Test

The prepared concrete was transferred to the cylinder with a trowel from the same height every time. The rheological test was carried out with the present rheometer exactly after 15 minutes from addition of water. Stepwise increasing shear stress sequence followed by a decreasing shear stress was used and the down curve was taken to draw the flow curve. Concrete was sheared at each step for 30 sec and readings were taken at the end of each period. The mixing sequence and the time at which the rheological test was performed were same for all mixes.



**Fig 3.2** No segregation after slump flow



**Fig 3.3.** No segregation even though slight halo present



**Fig 3.4** Segregation due to large mortar halo and aggregate piling at centre

### **3.3. RESULTS AND DISCUSSION**

#### **3.3.1. Effect of Percentage Sand**

Sand ratio, expressed as the percentage of total aggregate volume, has a significant influence on rheological parameters. Varying the percentage sand from 25%-55% in mixes, plastic viscosity and yield stress of concrete mixes have been obtained and their variation with percentage sand has been shown in **Fig 3.5**. It may be observed that there exists an optimum sand content lying between 30%-40% for minimum yield stress and plastic viscosity. Beyond the optimum, more sand indicates larger surface to be wetted and hence more resistance to flow would be required. On the other hand, less sand below

the optimum sand content makes the mix harsh. It is to be emphasized here that optimum sand content for different mixes are not the same and optimum values for yield stress and plastic viscosity for a particular mix are not necessarily equal.

### 3.3.2. Effect of Sand Gradation

**Fig 3.6** shows the systematic effect of different zones of sand on the rheological parameters. Indian Standard Code IS: 2386-1992 classifies coarse sand as Zone I, medium as Zone II, fine as Zone III and very fine as Zone IV. Sieving of sand was carried out and percentage passing through some sieves was adjusted either by addition or by removal of particles to conform the grading requirements of the code. Rheological parameters were plotted against the weighted mean size ( $D_{av}$ ) of sand zone.  $D_{av}$  for sand in five different mixes were calculated as follows [Tangtermsirikul, 2004]:

$$D_{av} = \frac{\sum M_i D_i}{\sum M_i} \quad (3.2)$$

where  $D_{av}$  is the average size group computed from average of sizes of the considered sieve and next larger sieve,  $D_i$  is the size of particular  $i$ -th sieve,  $M_i$  is the % retained on the  $i$  th sieve.

Here the volume concentration  $\Phi$  of sand is same for all the zones. However, maximum packing density of sand  $\Phi^*$  as determined in the laboratory, improves continuously from Zone IV to Zone I. It is known that more the  $\Phi^*$ , more is the workability [Kwan and Mora, 2001] for a given  $\Phi$ . But it is not the case as evident from **Fig 3.6**. There exists an optimum  $D_{av}$  for both the rheological parameters. When sand is fine, more surface area is to be wetted and when it is coarse, mix becomes harsh due to particle interference of coarse particles thereby increasing the resistance of flow.

### 3.3.3 Effect of Maximum Size of Coarse Aggregate

The effect of maximum size of coarse aggregate on yield stress and plastic viscosity is shown in **Fig 3.7**. Coarse aggregate passing through 16 mm sieve was considered as 16 mm maximum size and so on. Plastic viscosity and yield stress decrease as maximum

size of coarse aggregate increases because of the improvement of  $\Phi^*$ . However, the change is not very significant in most of the cases.

### **3.3.4 Effect of Single Size Coarse Aggregates**

The rheological behavior of mixes with respect to mean size of coarse aggregate is shown in **Fig 3.8**. Coarse aggregates were separated into different sieve sizes by sieving. Average coarse aggregate size was considered as the mean of sieve size passing and sieve size retained for a particular sieve class. In the present case, average size used were the averages of 16 mm-12.5 mm, 12.5 mm-10 mm, 10 mm-6.3 mm for coarse aggregates in five different mixes. Yield stress is found to decrease with the increase in mean size. The reason is the same as described in connection with **Fig 3.7**. There is insignificant change in plastic viscosity without a particular trend in variation for different mixes.

### **3.3.5 Effect of HRWRA Dosage**

**Fig 3.9** shows the variation of rheological parameters with HRWRA dosage. Both the rheological parameters initially decrease with the addition of HRWRA dosage. Portland cement being in fine state of division has a tendency to flocculate in wet concrete. This flocculation always entraps some water and therefore all water is not available to lubricate the mix. When HRWRA is used in the mix, they get adsorbed on the surface of cement particles. The adsorption of charged polymer creates particle-to-particle repulsive forces (called Zeta Potential) which overcome the attractive forces. Consequently cement particles are de-flocculated and dispersed. Water trapped inside the flocs gets released and becomes available for lubrication. However, plastic viscosity again increases beyond a certain dosage level plastic viscosity. Tattersall [1991], Hu et al [1996] observed similar behavior and suggested that plastic viscosity increases when it reaches its saturation concentration.

### 3.3.6 Effect of Cement Paste to Aggregate Volume Ratio on Bingham Parameters

Considering mix proportions of concretes listed in **Table 3.1** as the mixtures to start with, various mixtures were prepared by changing cement paste content. Quantities of other ingredients such as sand and coarse aggregate were adjusted so that total volume was  $1.0 \text{ m}^3$ . However, % sand, gradation of coarse and fine aggregates was kept constant for each mix of a particular designation shown in **Table 3.1**.

**Fig. 3.10** shows the variation of yield stress and plastic viscosity with cement paste volume to aggregate volume. Cement paste volume was calculated as the total volume of cement, water, and air content. Air content was assumed to be 2.5% in all cases as per IS 10262: 1982. It may be observed that as the relative volume of cement paste to aggregate increases, yield stress decreases sharply. The decrease in yield stress is due to availability of more cement paste for lubrication. However, in mixes containing SN as HRWRA, yield stress shows optimum value beyond which there is an increase in yield stress with the increase in cement paste to aggregate volume ratio. This is due to the fact that mix becomes sticky due to excessive cohesion at higher cement paste volumes. Plastic viscosity increases gradually in mixtures containing PC as HRWRA due to increase in volume concentration of cement. In mixtures containing SN, optimum value of cement paste to aggregate volume ratio exists beyond which there is an increase in plastic viscosity.

**Fig 3.11** shows the effect of cement paste to aggregate volume ratio at different water-cement ratios. A gradual decrease in Bingham parameters have been noted with increase in cement paste volume to aggregate ratio for obvious reasons. The sensitivity of curves is different for different water-cement ratios. It may also be observed that lower values of yield stress and plastic viscosity are possible even at lower water-cement ratio. In fact, in addition to water-cement ratio, rheological parameters are very much affected by cement paste to aggregate volume ratio.

### 3.3.7 Effect of Elapsed Time

To examine the effect of elapsed time on rheological parameters of concrete, concrete mixes Mix#B1 and Mix#B3 of **Table 3.1** was selected. The mixing sequence of

ingredients was same as described in **Section 2.6.3**. The measuring procedure for this section was as follows:

- T=15 min: rheological measurements with concrete rheometer.
- T=24 min: remixing of concrete for 2 minutes in the concrete mixer.
- T=30 min: rheological measurements with concrete rheometer.
- T=44 min: remixing of concrete for 2 minutes in the concrete mixer.
- T=50 min: rheological measurements with concrete rheometer.
- T=74 min: remixing of concrete for 2 minutes in the concrete mixer.
- T=80 min: rheological measurements with concrete rheometer.
- T=124 min: remixing of concrete for 2 minutes in the concrete mixer.
- T=130 min: rheological measurements with concrete rheometer.

After each measurement, concrete was placed back into the mixer to rest there. Care was taken to prevent moisture loss due to evaporation. Mixer was covered with plastic bags for that purpose. Concrete was transferred manually to the rheometer. This applied to all the measurements taken thereafter.

After each measurement, a rough cleaning procedure was applied to the cylindrical container. This consisted of removing the remaining concrete manually. Thereafter, cylindrical container and the impeller were covered with plastic bags to prevent moisture loss from remaining fine mortar stuck to the container and impeller. The results of the effect of elapsed time on rheological parameters are presented in **Fig 3.12**. It may be observed from **Fig 3.12** that plastic viscosity more or less remains uniform with time. Change in yield stress is insignificant up to 50 minutes and thereafter it steadily increases. With increasing time, number of free particles decreases as a result of their coagulation and therefore, plastic viscosity slightly decreases after 30 minutes of time, though the decrease is very small. Yield stress increases because of the increase in phase volume of cement paste and surface roughness due to hydration.

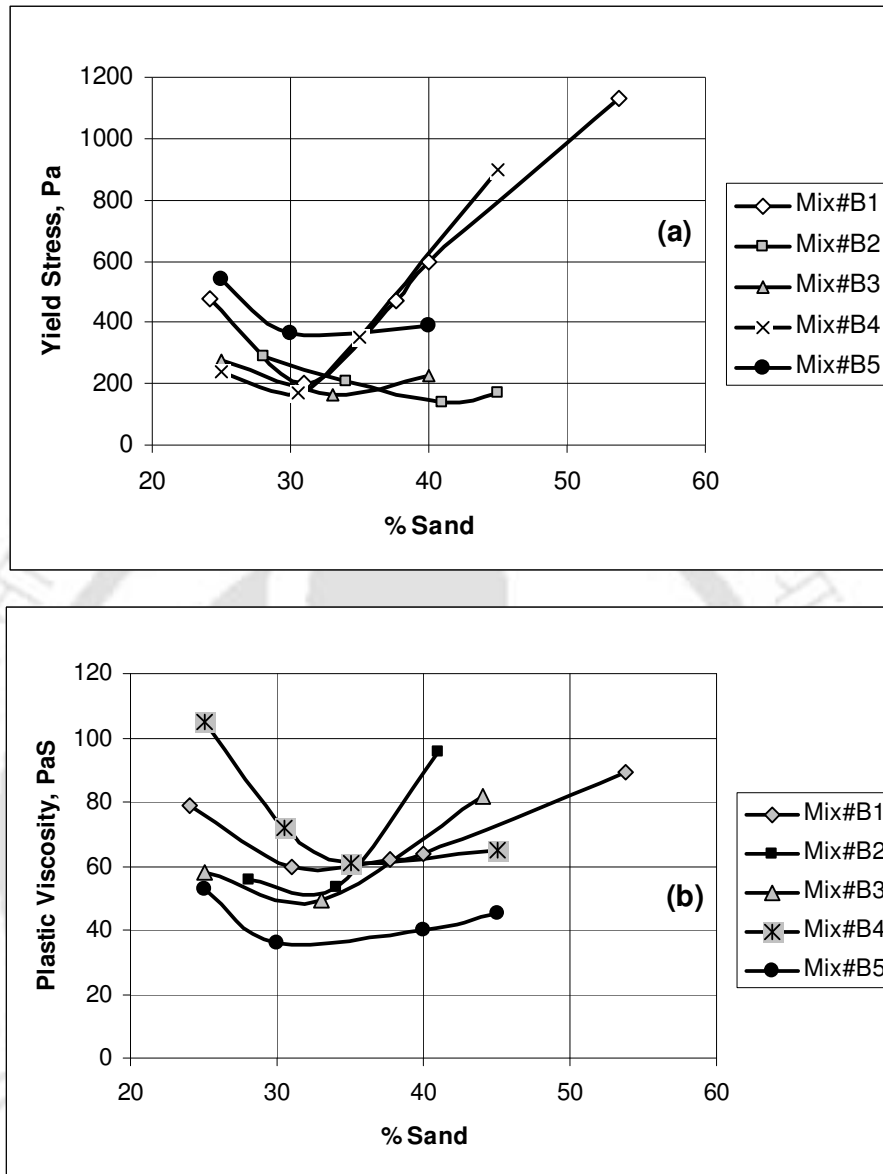


**Fig 3.5** Effect of % sand on rheological parameters (a) Effect on yield stress (b) Effect on plastic viscosity

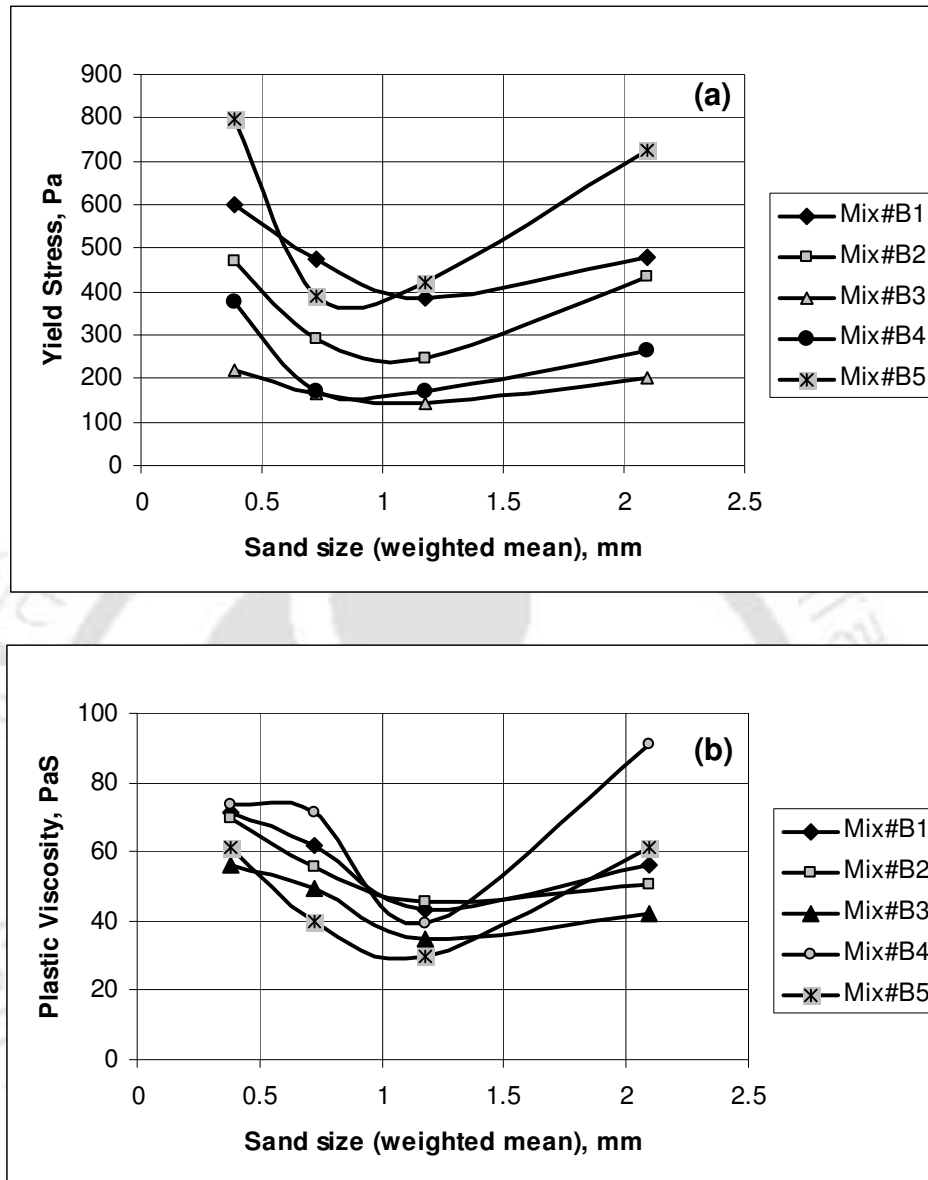


**Fig 3.6** Effect of sand zone on rheological parameters (a) Effect on yield stress (b) Effect on plastic viscosity

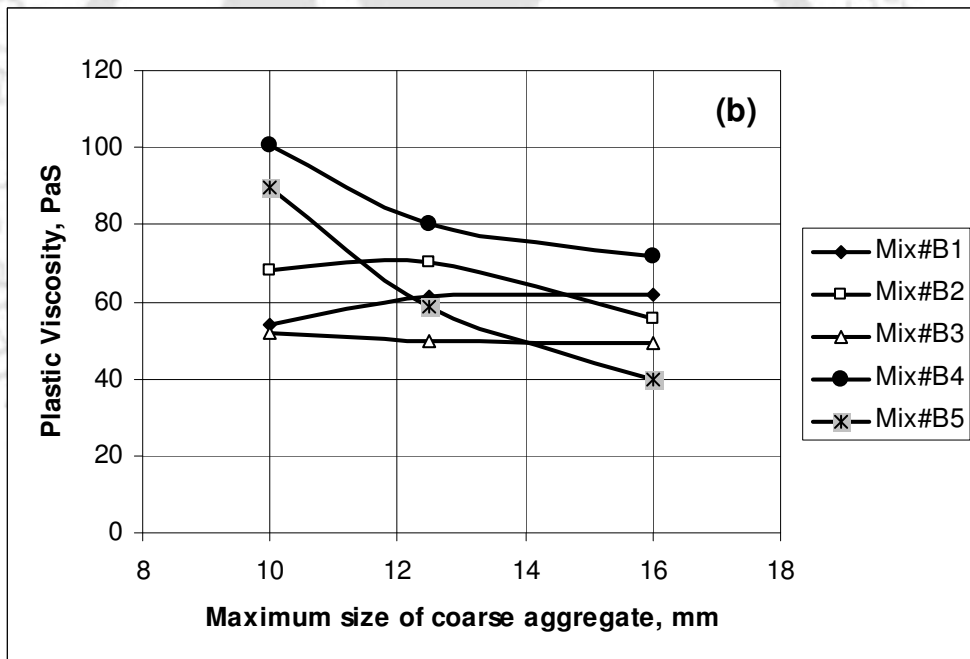
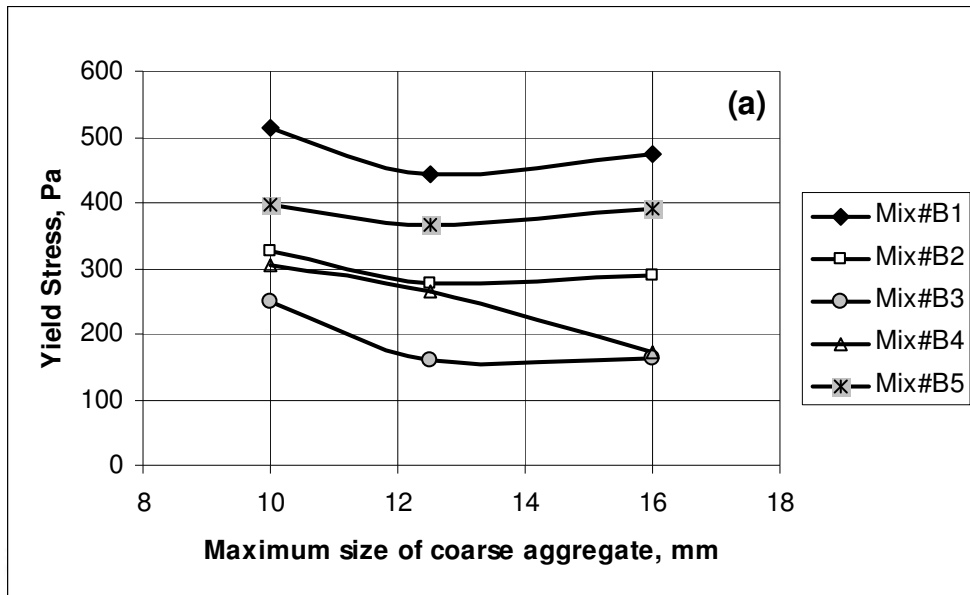


**Fig 3.7** Effect of maximum size of coarse aggregate on rheological parameters (a) Effect on yield stress (b) Effect on plastic viscosity

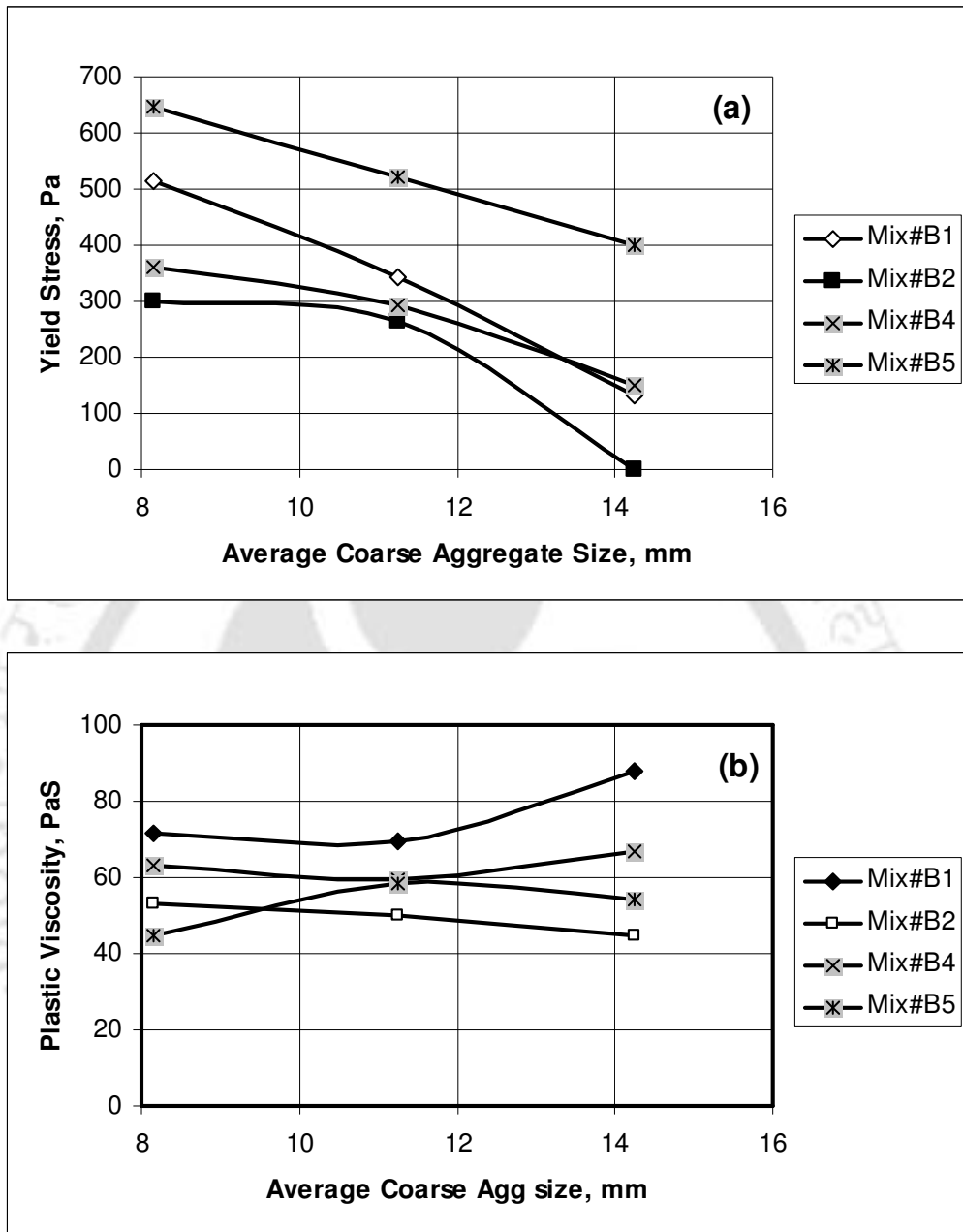


**Fig 3.8** Effect of average coarse aggregate size on rheological parameters (a) Effect on yield stress (b) Effect on plastic viscosity

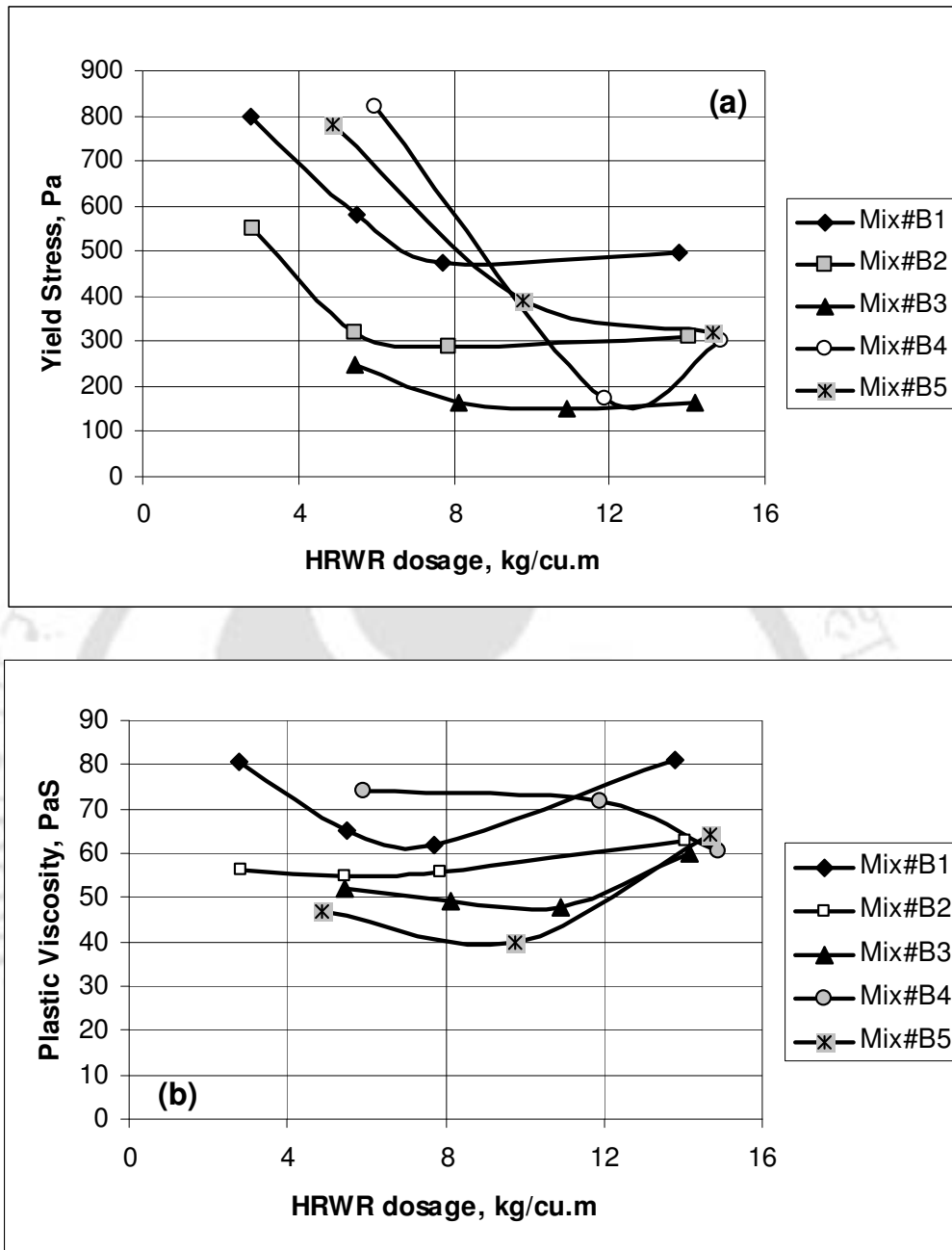


**Fig 3.9** Effect of HRWRA dose on rheological parameters (a) Effect on yield stress (b) Effect on plastic viscosity

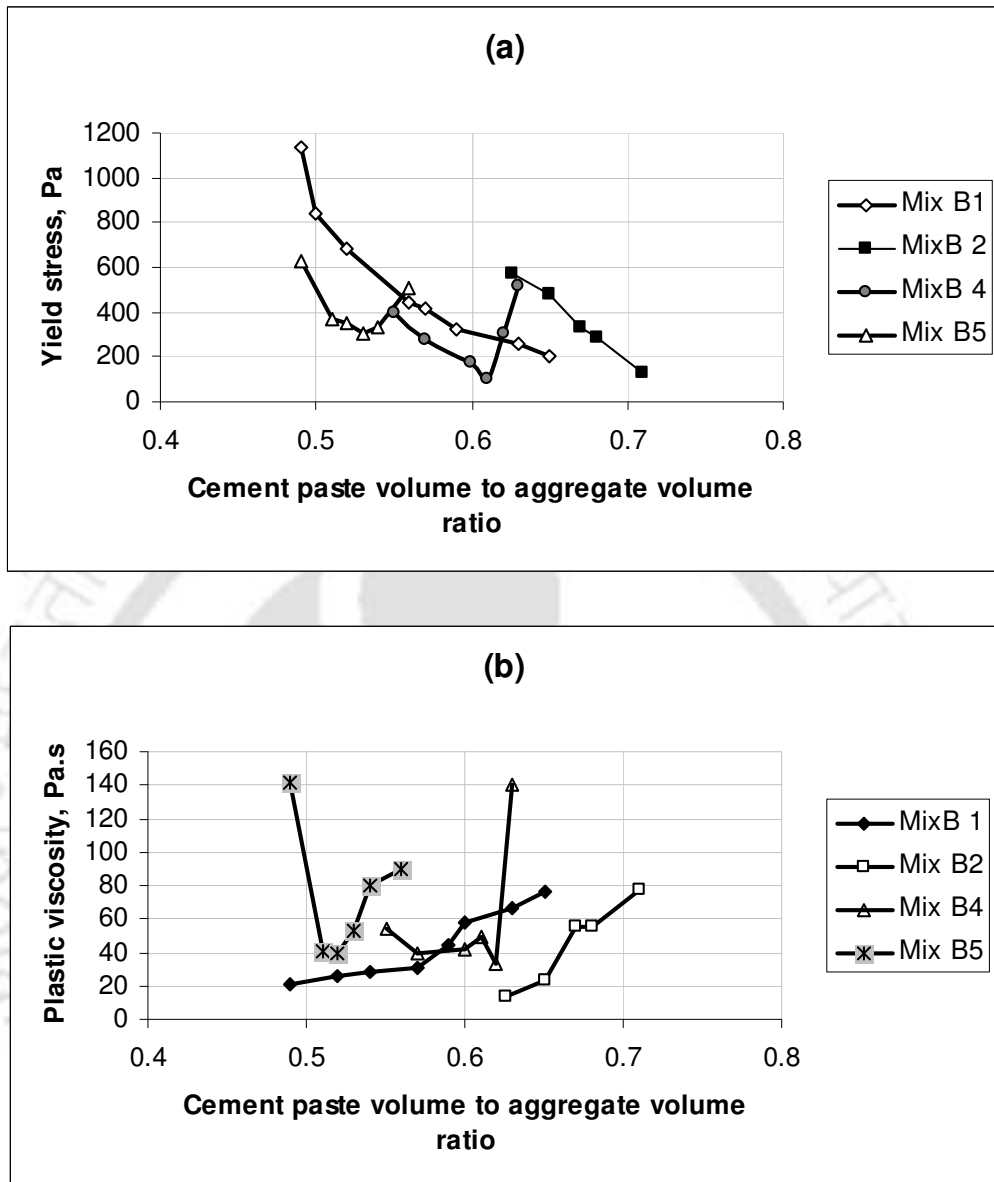


**Fig 3.10** Effect of cement paste/aggregate volume ratio (a) Effect on yield stress (b) Effect on plastic viscosity

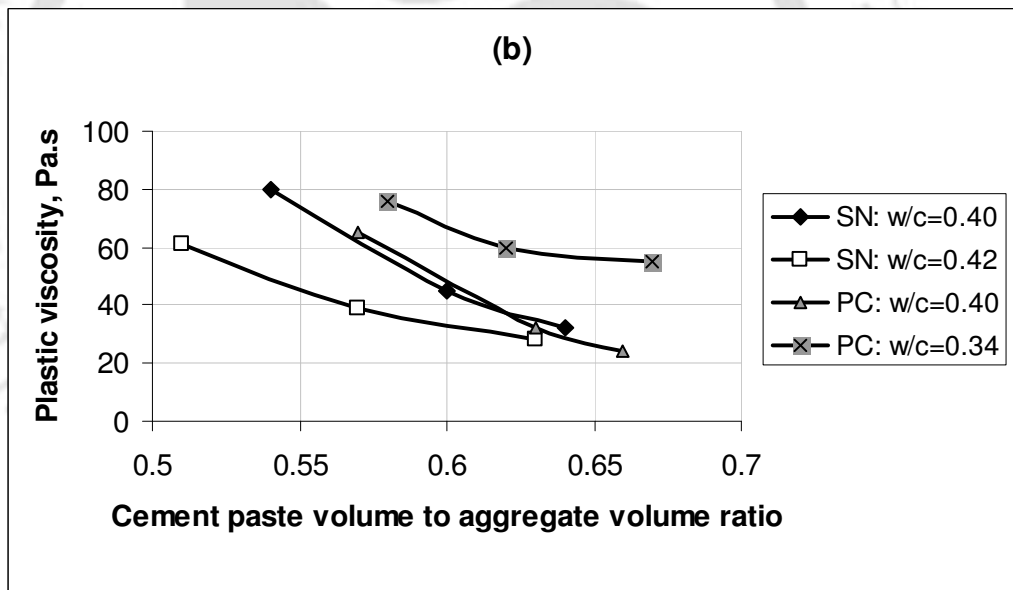
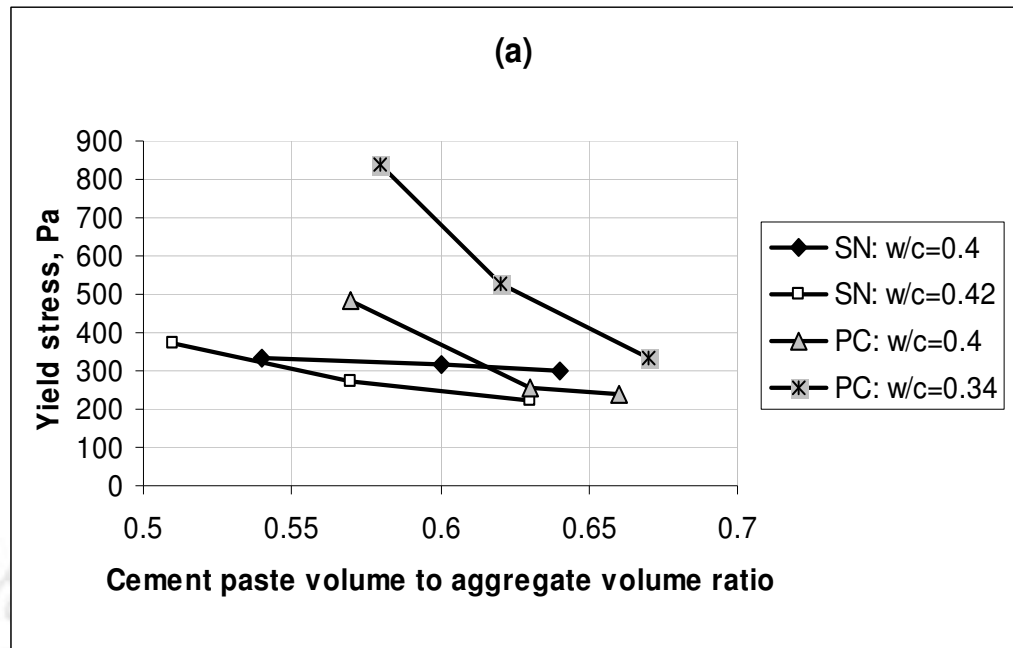


**Fig 3.11** Effect of cement paste/aggregate volume ratio and w/c ratio (a) Effect on yield stress (b) Effect on plastic viscosity

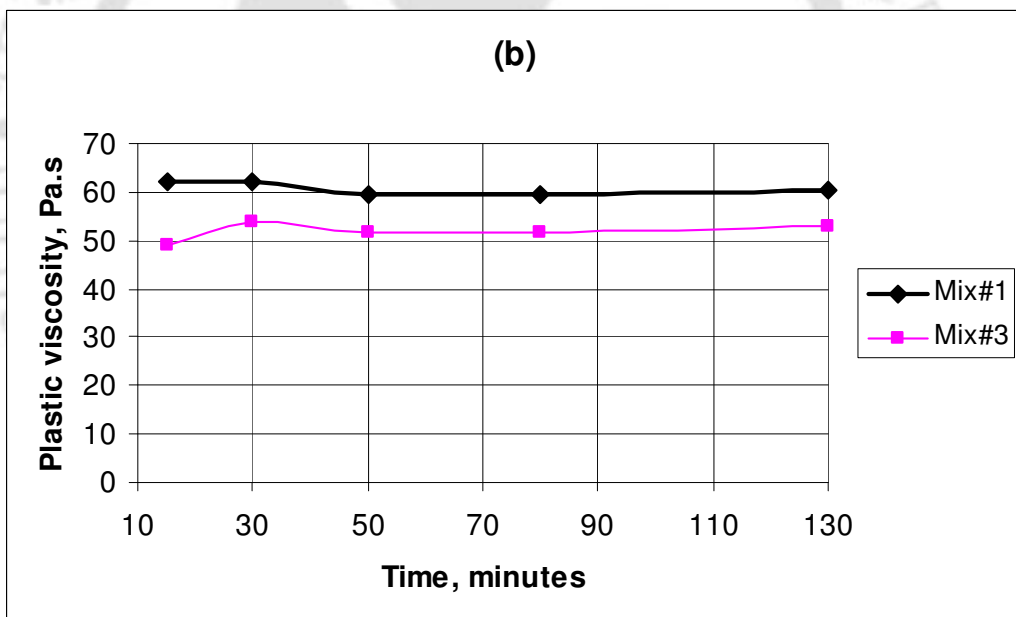
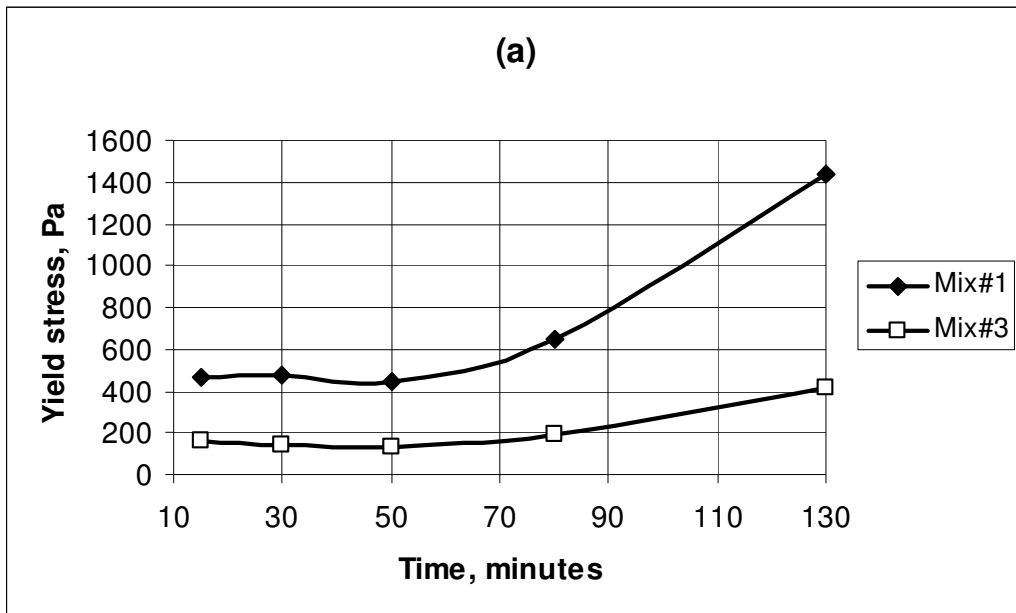


**Fig 3.12.** Effect of elapsed time on rheological parameters (a) Effect on yield stress (b) Effect on plastic viscosity

### 3.4 CORRELATION BETWEEN CONVENTIONAL WORKABILITY TESTS AND RHEOLOGICAL PARAMETERS

#### 3.4.1 Slump Test and Rheological Parameters

In the present study, correlation between slump values and yield stress and plastic viscosity determined by the present rheometer has been studied. The rheological data have been extracted from the observations as in **section 3.3** of this chapter. Different mixes used for the present section has been shown in **Table 3.2**. Immediately after the rheological test for each sample, concrete was transferred to the mixer. Leftover concrete in the cylindrical container was cleaned manually so that all the mortar is taken in the mixture. Concrete was mixed again for two minutes and transferred for subsequent testing. Slump test was performed after 30 minutes from the addition of water. It may be mentioned that similar procedure was adopted by Wallewick [2003]. Moreover, it has already been demonstrated that there is no significant change on rheological parameters up to 70 minutes from addition of water [Fig 3.10].

The variation of slump with yield stress and plastic viscosity is presented in **Fig 3.13**. In **Fig 3.13**, slump is plotted against  $(\tau_o / \rho g)$ , because it was shown by dimensional analysis that slump is governed by this quantity [de Larrard, 1999]. Here  $\rho$  is the density of fresh concrete in  $\text{kg/m}^3$ ,  $g$  is the gravitational constant. It may be observed that there exists a linear relationship between slump and yield stress of concrete. As yield stress increases, slump value decreases and vice versa. The following empirical relation may be obtained by least square regression:

$$S = 0.21 - 2.87 \left( \frac{\tau_o}{\rho g} \right) \quad (3.3)$$

where  $\tau_o$  is Pa,  $\rho$  is in  $\text{kg/m}^3$ ,  $g$  is in  $\text{m}^2/\text{sec}$ ,  $S$  is in meter.

It may also be observed from **Fig 3.13** that there also exists a good relationship between plastic viscosity and slump value. Initially when plastic viscosity increases, slump value also increases up to a value 60-80 Pa.s and then decreases with further increases in plastic viscosity. Thus, there exists an optimum plastic viscosity at which slump value is the maximum. The following empirical relation may be obtained by least square regression:

$$S = -0.048\mu^2 + 6.63\mu - 46.1 \quad \text{where } \mu \text{ is in Pa.s and } S \text{ is in mm.} \quad (3.4)$$

For design of HPC, moderate value of plastic viscosity is necessary which is indirectly related to slump as depicted in Fig.3.13 showing optimum plastic viscosity at particular slump.

### 3.4.2 Slump Flow, Flow Time and Rheological Parameters

In addition to slump test, slump flow value and slump flow time were recorded from the same slump test. In the present study, slump flow was the average of two measurements at right angles to each other after removal of cone. Slump time was the time recorded from the removal of cone up to the instant at which the flow of concrete completely stopped that was judged visually and was recorded with a digital stop watch. The variation of slump flow with rheological properties is shown in **Fig 3.14(a) & (b)**. It may be observed from **Fig 3.14** that as yield stress increases slump flow decreases linearly. For plastic viscosity, there exists an optimum value (60- 80 Pa.s) beyond which any increases in it indicates a decrease in slump flow. Similarly, below the optimum value, decreases in plastic viscosity means decreases in slump flow. The following empirical relations may be derived by least square regression:

$$S_f = 655 - 0.238\tau_o \quad (3.5)$$

$$S_f = -0.085\mu^2 + 12.11\mu + 161 \quad (3.6)$$

where  $S_f$  is the slump flow in mm,  $\tau_o$  is Pa and  $\mu$  is in Pa.s.

The relationship between slump time and rheological parameters is presented in **Fig 3.15(a) & (b)**. From **Fig 3.15(b)**, it may be observed that there is a good correlation between slump time and plastic viscosity. As plastic viscosity increases, slump time also increases initially. It shows a peak and then decreases gradually with further increases in plastic viscosity. The optimum range of plastic viscosity is again 60-80 Pa.s for maximum slump time. Yield stress shows no correlation with the slump time for the experimental data considered in the study. The following empirical relation between slump time and plastic viscosity can be derived by least square regression:

$$S_t = -0.0152\mu^2 + 2.55\mu - 32 \quad (3.7)$$

where  $S_t$  is slump time in seconds and  $\mu$  is in Pa.s.

### 3.5 CLOSURE

Effect of various factors on rheological parameters of concrete without mineral admixture and fiber has been investigated experimentally. Coarse and fine aggregate gradation and size have significant influence on yield stress and plastic viscosity. Optimum values exist for percentage sand, mean sand size, and HRWRA dosage. In addition to water cement ratio, ratio of cement paste volume to aggregate volume affect yield stress and plastic volume significantly.

Good correlation between yield stress and slump, yield stress and slump flow was observed in high performance concrete. Yield stress decreases linearly as either slump or slump flow increases. A relationship also exists between plastic viscosity and slump, plastic viscosity and slump flow, plastic viscosity and slump time. The optimum plastic viscosity is 60- 80 Pa.s for maximum slump, maximum slump flow and maximum slump time. No correlation exists between yield stress and slump flow time for the concrete studied.

**Table 3.2:** Mix proportions used for slump and slump flow tests

Sl no.	Cement	Sand	Coarse aggregate	HRWRA (PC)	Water	Remarks
1	503	660	1040	7.7	183	
2	558	444	1085	7.9	192	
3	532	516	1033	8.1	193	
4	505	491	1114	11.9	176	
5	423	677	1028	8.3	173	
6	300	647	1020	7.6	182	
7	343	637	1004	7.4	180	
8	385	627	988	7.3	177	
9	427	618	973	7.2	174	
10	466	610	960	7.0	171	
11	505	672	932	7.1	186	
12	588	590	930	8.8	202	

13	503	660	1040	2.78	209.8	
14	503	660	1040	13.9	198.7	
15	503	660	1040	7.7	183	Coarse sand
16	503	660	1040	7.7	183	Fine sand
17	503	660	1040	7.7	183	CA passing 12.5 mm
18	503	660	1040	7.7	183	CA passing 10 mm
19	503	660	1040	7.7	183	CA:10-6.3 mm
20	503	660	1040	7.7	183	CA: 12.5-10 mm
21	503	660	1040	7.7	183	CA: 16-12.5 mm
22	484	705	940	6.8	178	
23	514	452	1105	7.4	197	
24	471	460	1125	7.5	200	
25	600	440	1075	7.2	191	
26	570	453	1107	7.3	178	
27	563	448	1095	7.2	185	
28	560	536	996	7.2	183	
29	555	660	909	7.0	173	
30	518	535	1070	7.1	186	
31	485	505	1140	7.1	175	

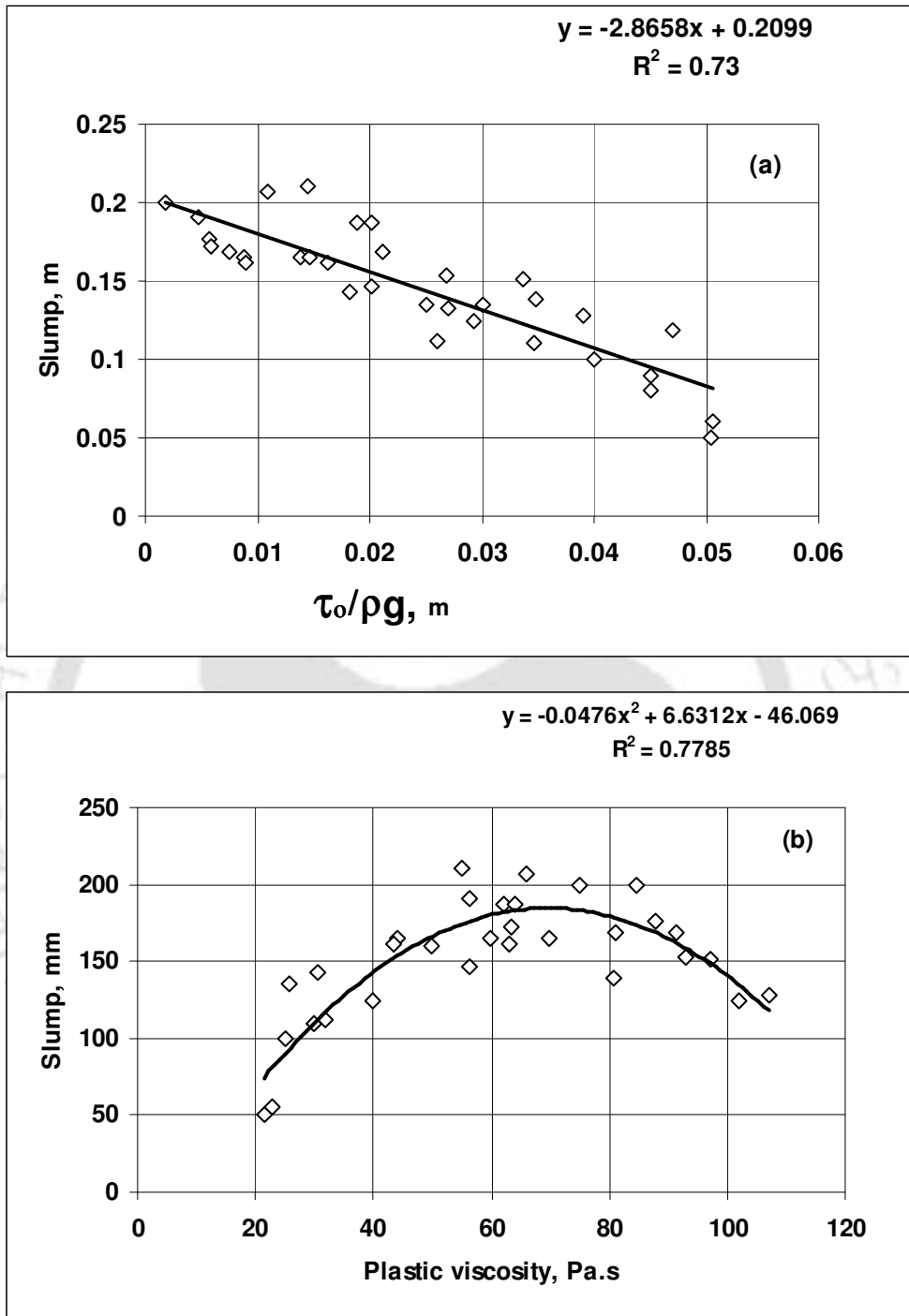


**Fig 3.13** Relationship between rheological parameters and slump (a) yield stress (b) Plastic viscosity

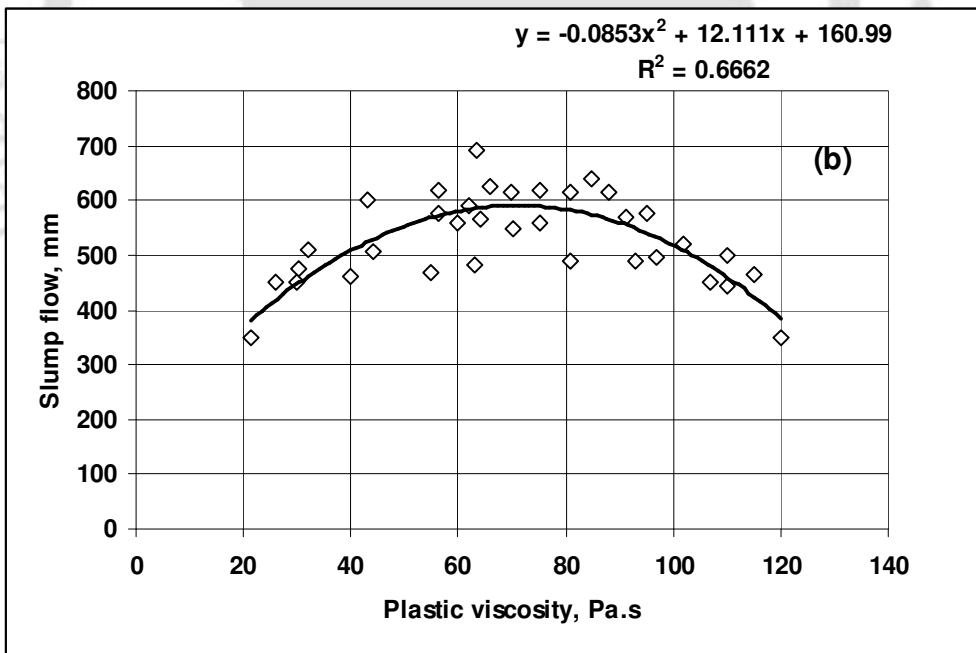
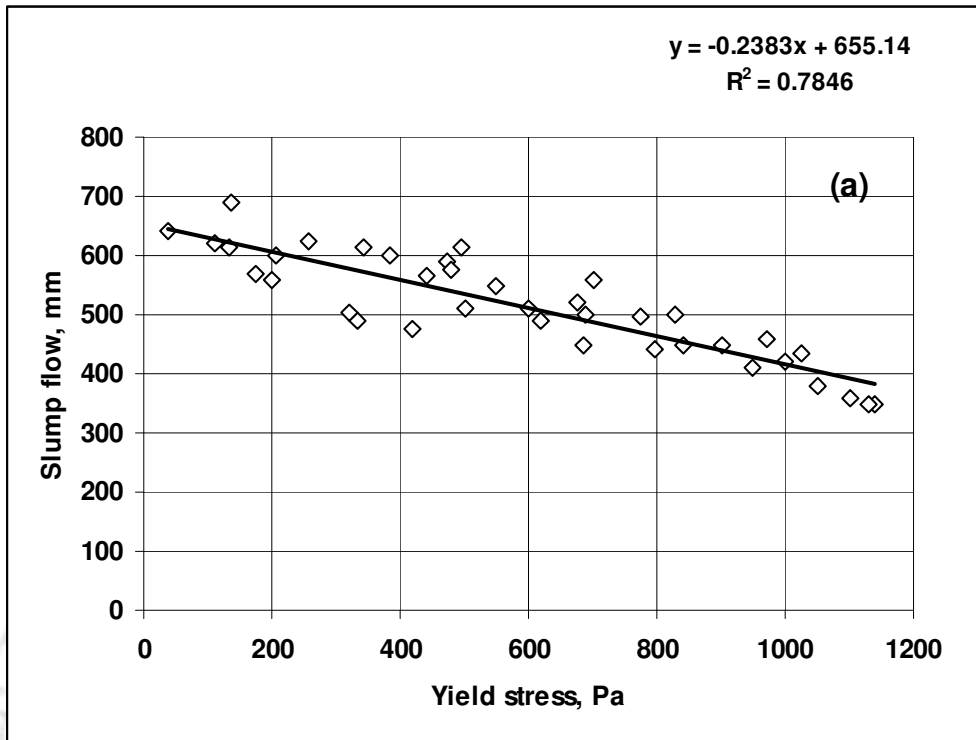


**Fig 3.14** Relationship between rheological parameters and slump flow (a) yield stress (b) Plastic viscosity

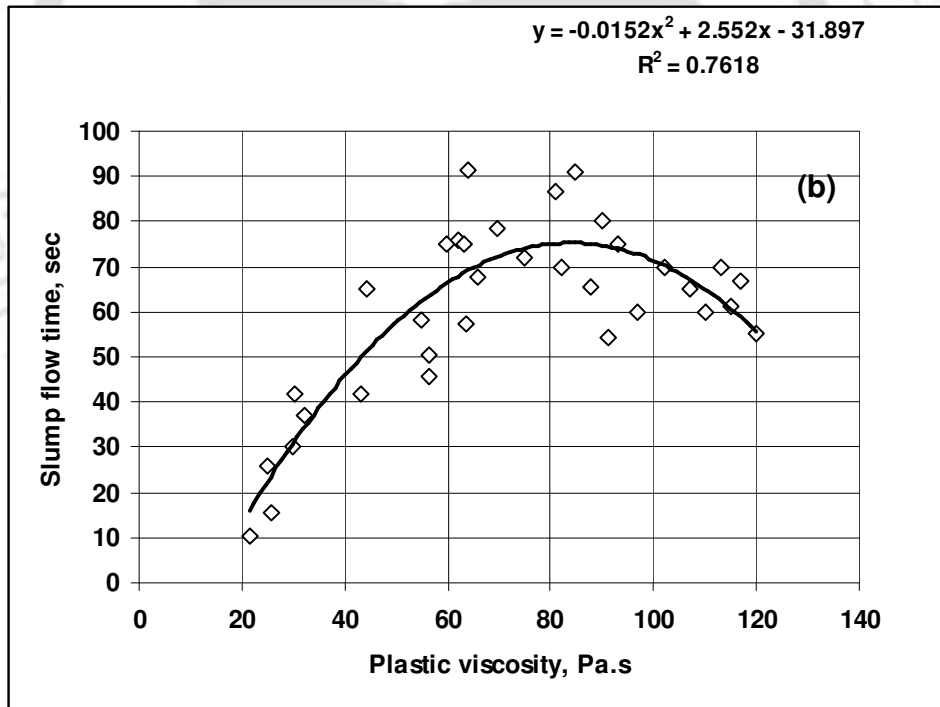
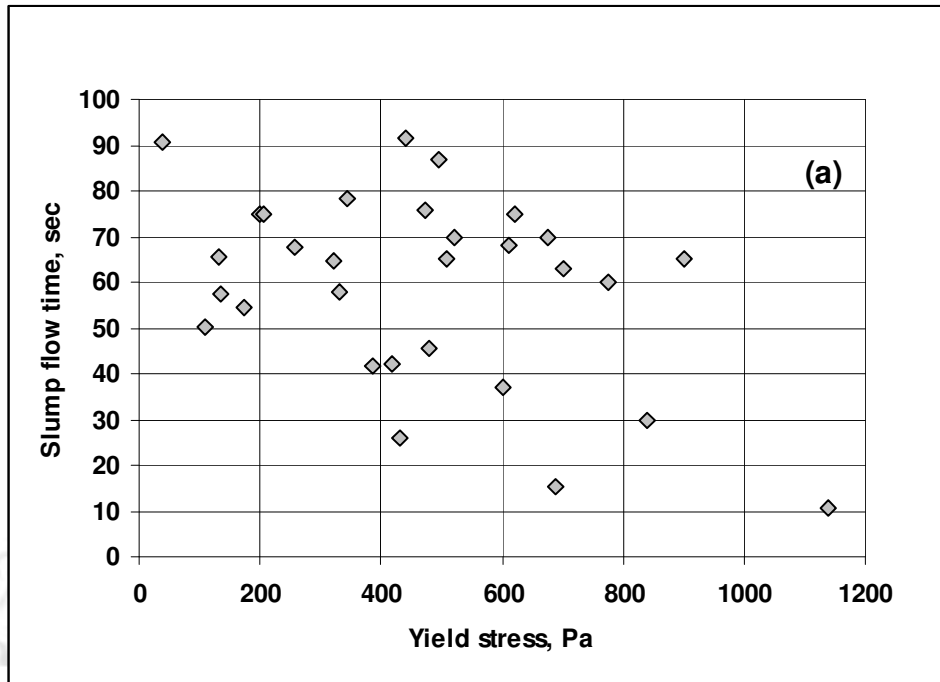


**Fig 3.15** Relationship between rheological parameters and slump flow time (a) yield stress (b) Plastic viscosity

## **CHAPTER 4**

### **RHEOLOGICAL BEHAVIOR OF HIGH PERFORMANCE CONCRETE WITH MINERAL ADMIXTURES AND STEEL FIBERS**

#### **4.1. INTRODUCTION**

In this chapter, the effect of mineral admixtures such as fly ash, condensed silica fume and rice husk ash and their blending on rheological behavior of high performance concrete has been presented. The effect of various parameters of round steel fibers such as fiber volume fraction, fiber diameter and fiber aspect ratio has also been presented. The correlation between conventional workability test methods such as Vebe, flow test and rheological parameters of steel fiber reinforced concrete has been investigated and presented.

#### **4.2. STUDY WITH MINERAL ADMIXTURES**

In this section, the experimental study to examine rheological behavior of HPC with different mineral admixtures has been presented. Admixtures are used individually first and then they are blended in suitable proportions to carry out further investigation. Classes F fly ash, condensed silica fume and rice husk ashes are the mineral admixtures used in the present investigation. The photograph of the samples of mineral admixtures is shown in **Fig 4.1**.

##### **4.2.1 Scanning Electron Microscopy**

Scanning electron microscopy (SEM) and its adjunct micro-analytical unit [**Fig 4.2**], energy dispersive X-ray analyzer (EDX), is relatively a new technique to investigate microstructure and morphology of cementitious materials. A finely focused electron beam scanned across the surface of the sample generates secondary electrons, backscattered electrons, and characteristic X-rays. These signals are collected by detectors to form images of the sample displayed on a cathode ray tube screen.



**Fig 4.1.** Mineral admixtures used in the present study (a) Condensed silica fume (b) Fly ash (c) Rice husk ash



**Fig 4.2.** Scanning electron microscope used in the present study

To understand effect of mineral admixtures on the rheological behavior of concrete, it is necessary to have an idea about the morphology and chemical composition. SEM and EDX have been, therefore, performed in the present study.

Class F fly ash collected by electrostatic precipitator, obtained from National Thermal Power Corporation at Farakka (India) was used in the present study. Images obtained from scanning electron microscope (SEM) at magnification 4 KX and 5 KX are presented in **Fig 4.3**. It may be observed that they appear as plain spherical particles of varying sizes. The surface of fly ash particles appears smooth and clean. Some cenospheres are also seen to be present.

Commercially available RHA supplied by Silicon India Limited, Kolkata, has been used in the present study. SEM photograph at magnifications 566X and 2 KX are shown in **Fig 4.4**. SEM images show that the particles are angular, elongated and flaky. Particles of different sizes and shapes are seen to be present.

CSF is not produced in India. However, Elkem microsilica (imported from Norway) and commercially available in the market as a building material, has been used throughout the investigation. SEM photographs at magnifications 4 KX and 30 KX are shown in **Fig 4.5**. Silica fume particles appear to be very fine, agglomerated and round. EDX can also be used to study a small spot in a constituent for its elemental composition. EDX analysis on CSF has been presented in **Fig 4.6**. It may be observed that higher peaks are shown by silicon, oxygen and iron. It may also be observed that the elemental compositions of CSF displayed in **Fig 4.6 (a)** and **Fig 4.6 (b)** are not the same. This is because of the fact that the analysis is made for some square micron meter of the material under investigation and does not necessarily represent the material as a whole. A regular criticism addressed towards EDX analysis is that results are based on examination of too small areas. EDX does not give compound composition. However, the element composition provides useful information for determining the compound composition by chemical analysis. The EDXA image of fly ash and RHA are also shown in **Fig 4.7** and **Fig 4.8**.

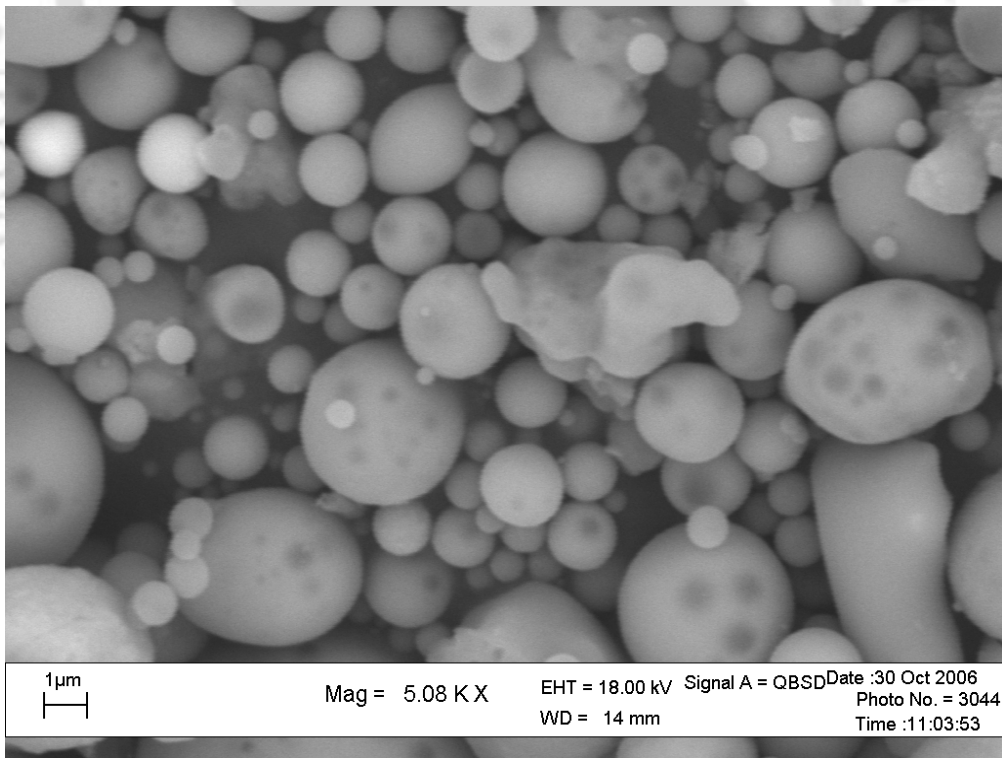
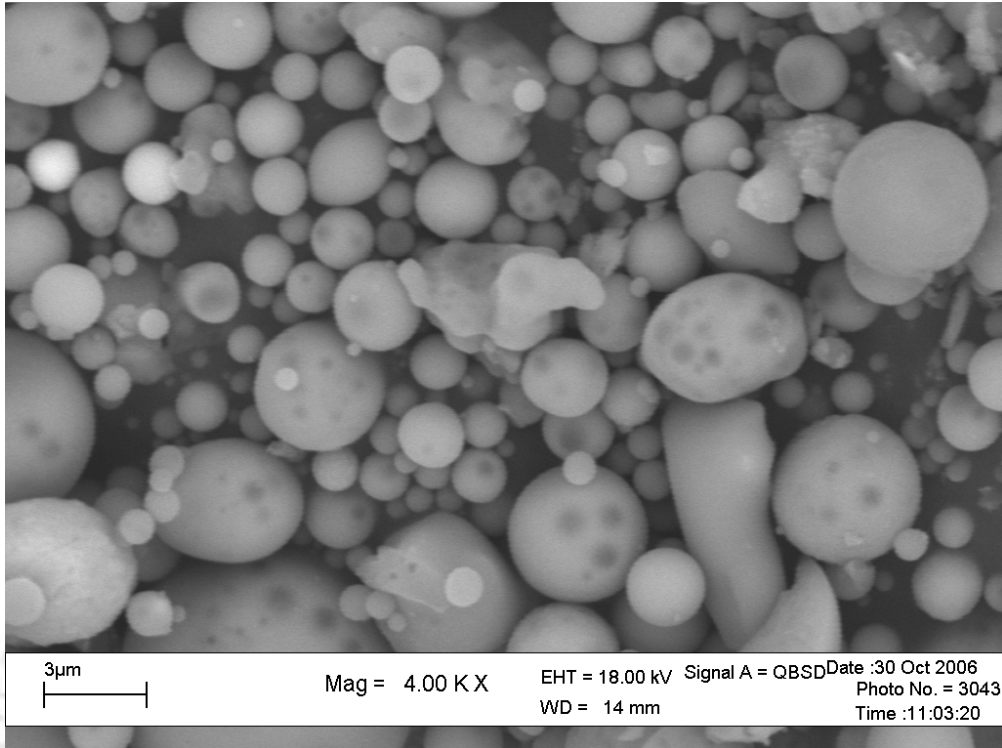


**Fig 4.3.** SEM images of fly ash

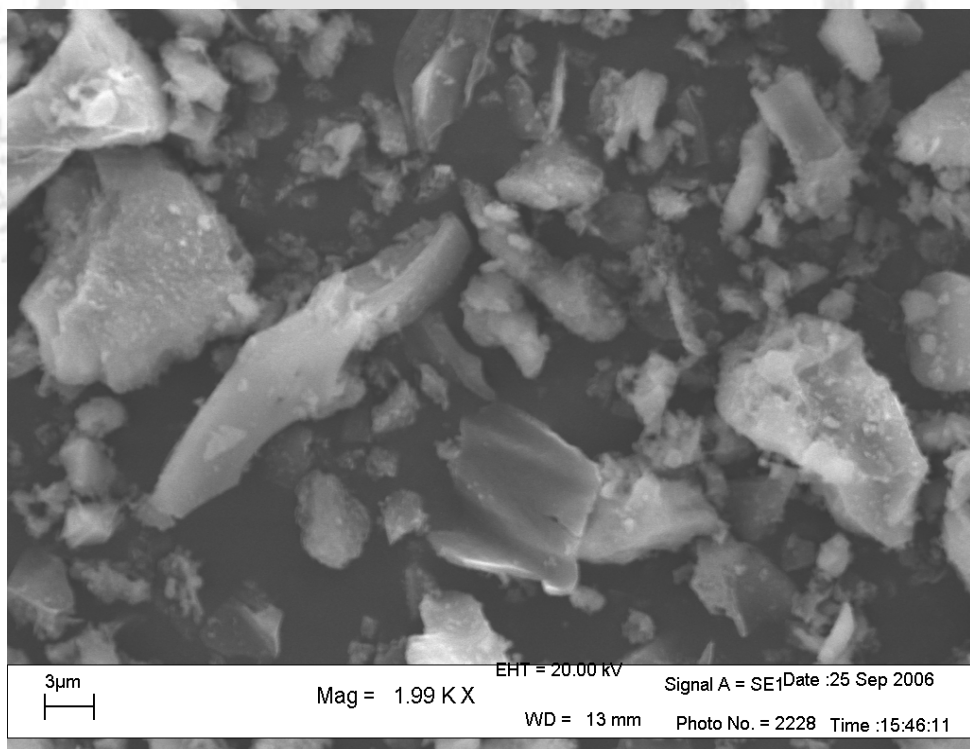
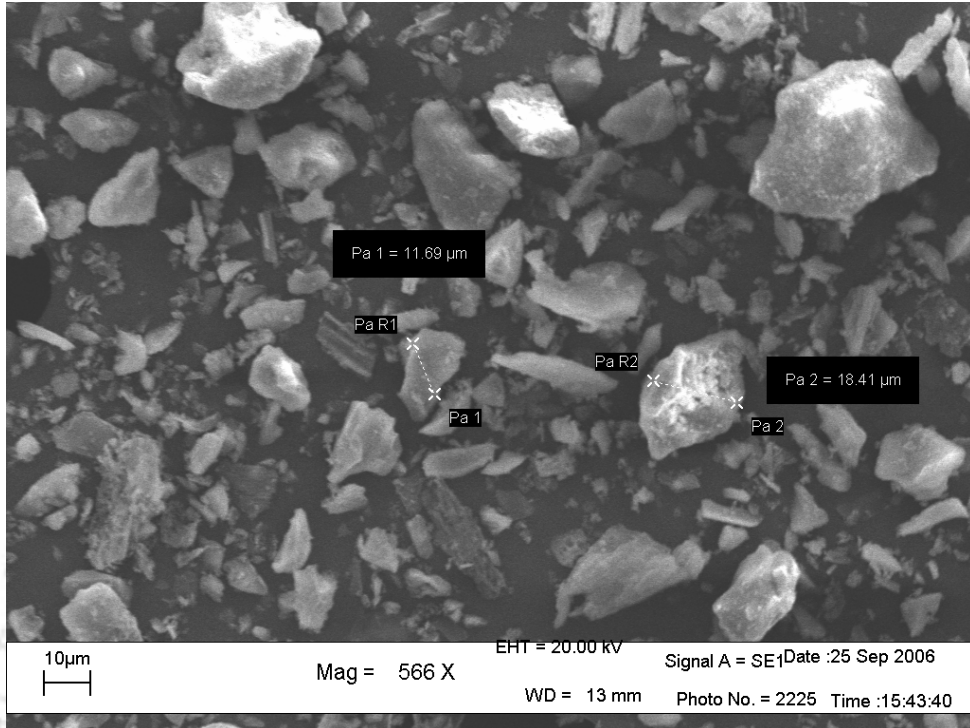


**Fig 4.4.** SEM images of RHA

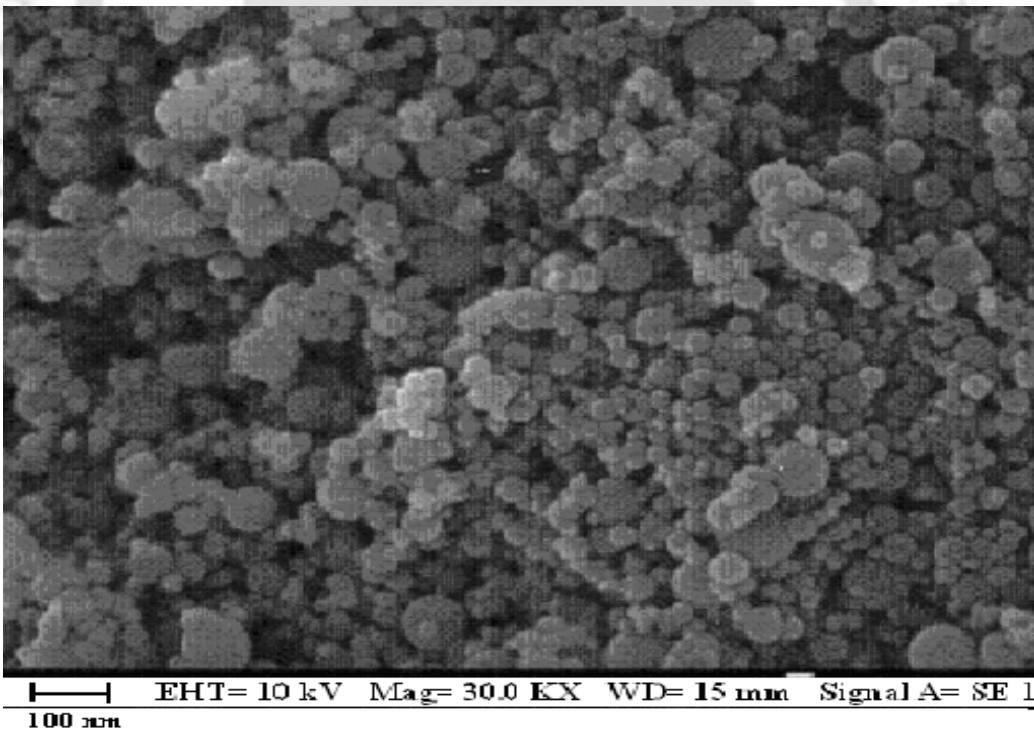
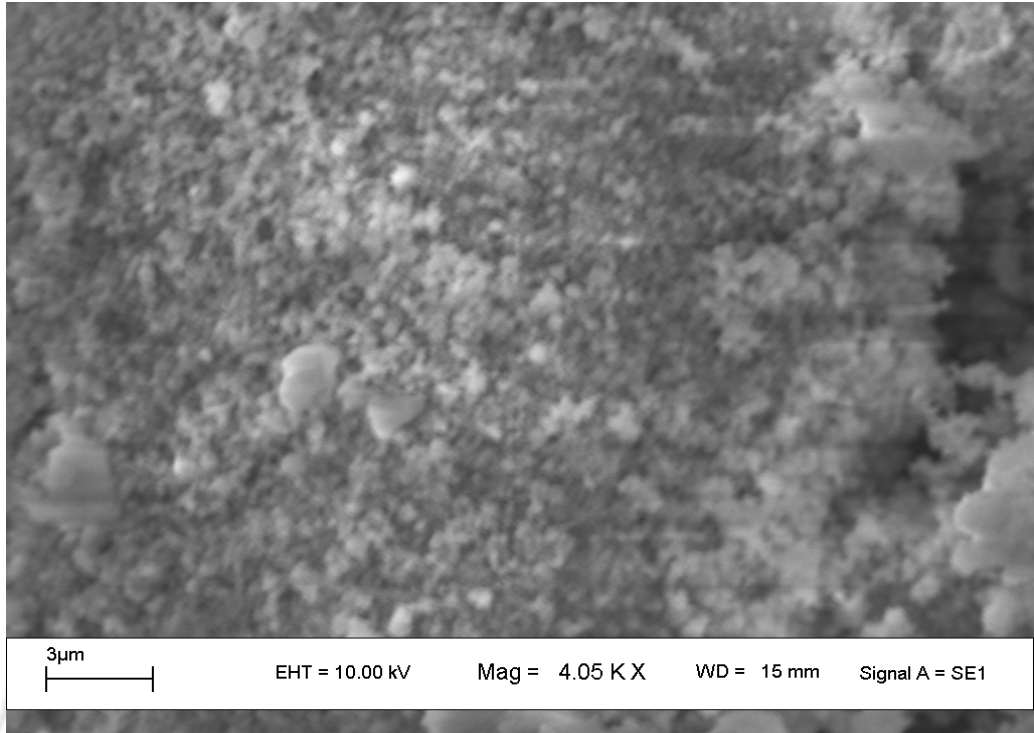


**Fig 4.5** SEM images of CSF

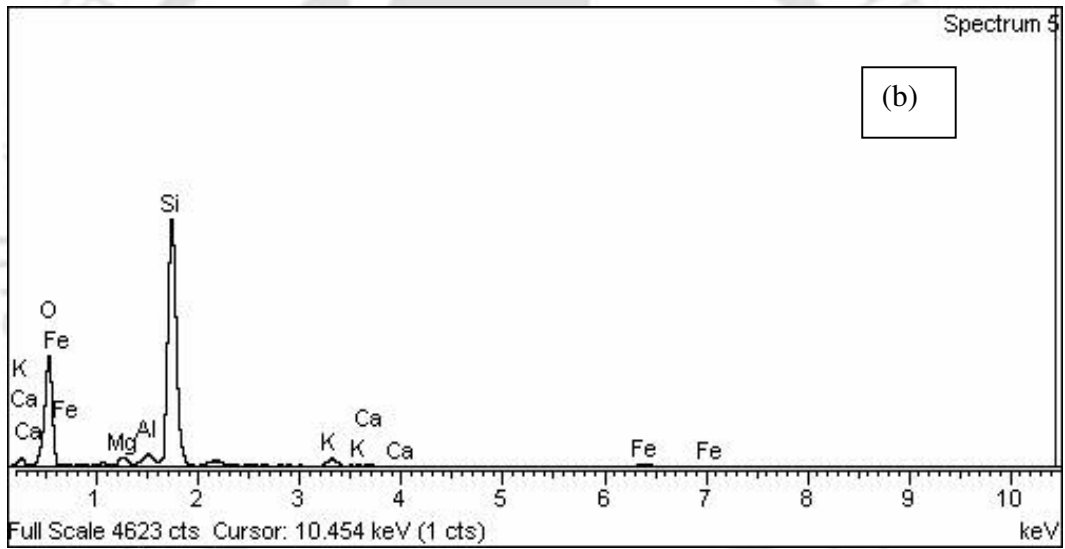
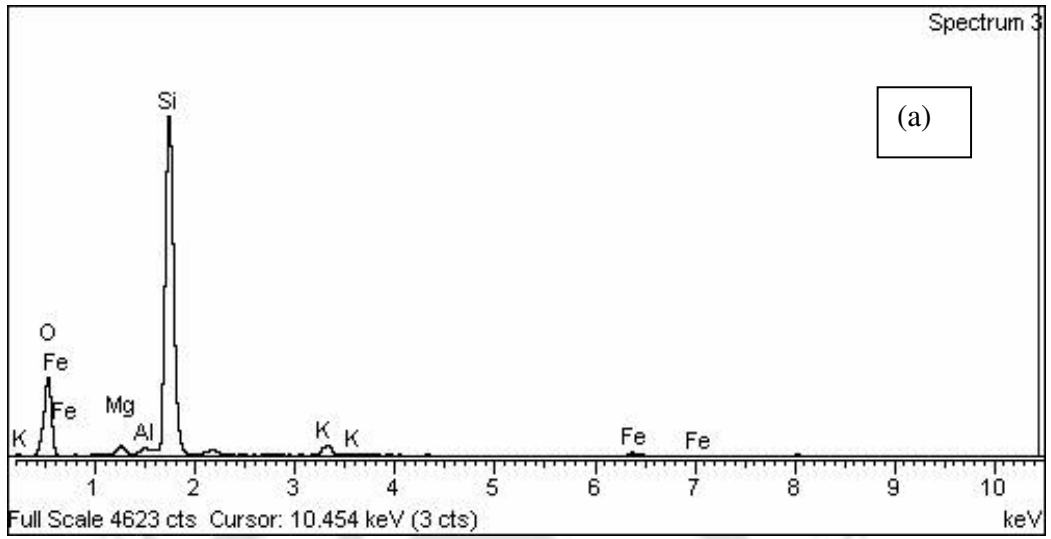


**Fig 4.6** EDX patterns of CSF at two spots

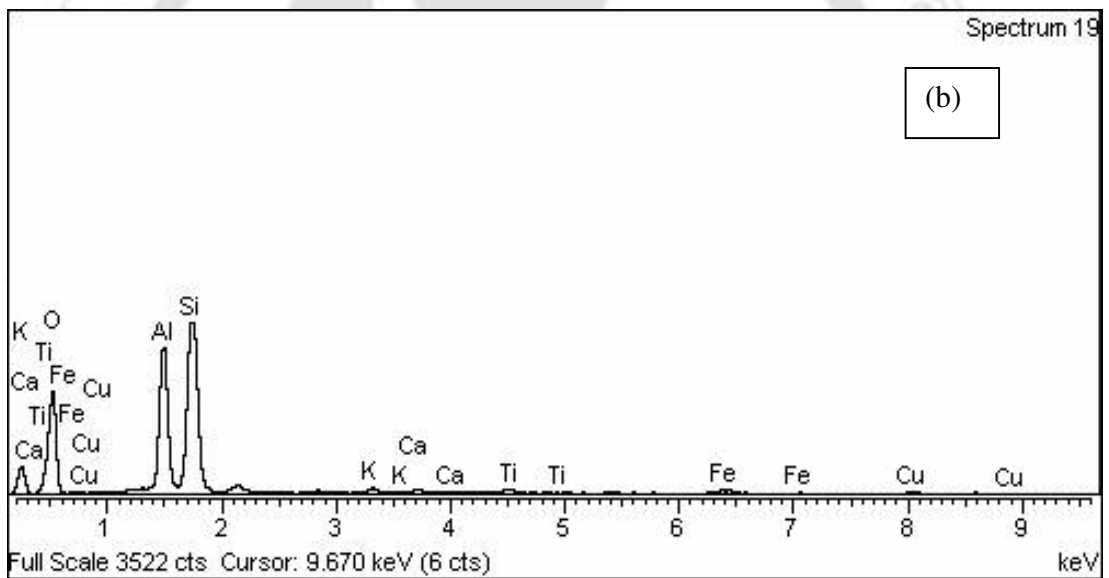
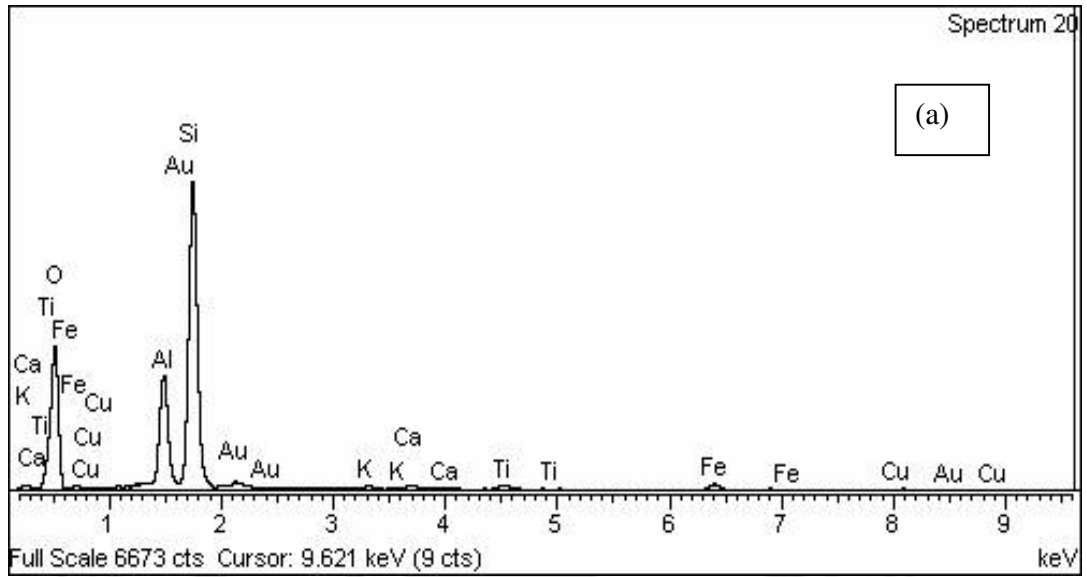


**Fig 4.7** EDX pattern of PFA at two spots

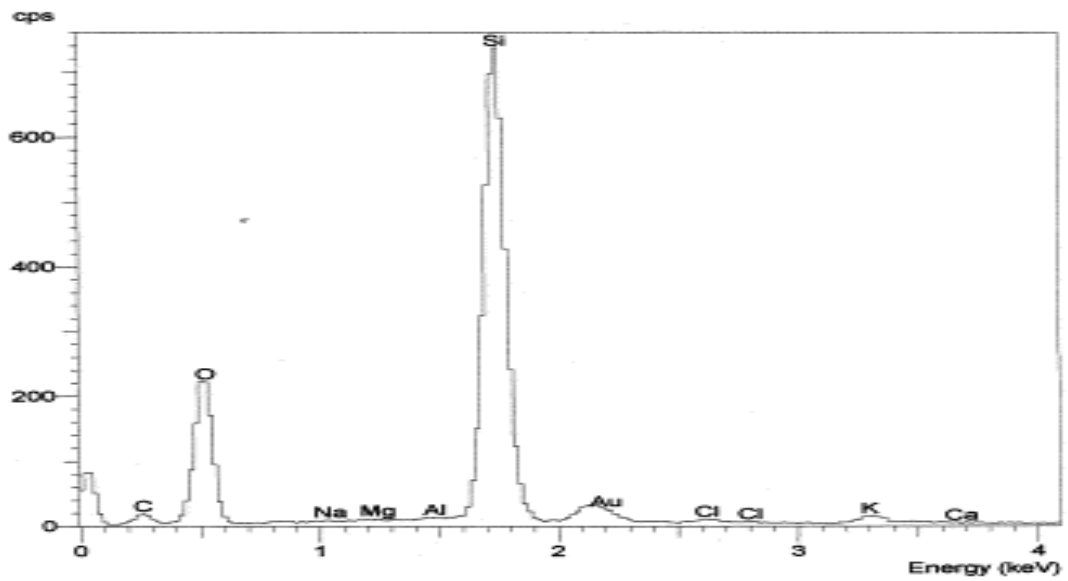


Fig 4.8 EDXA of RHA

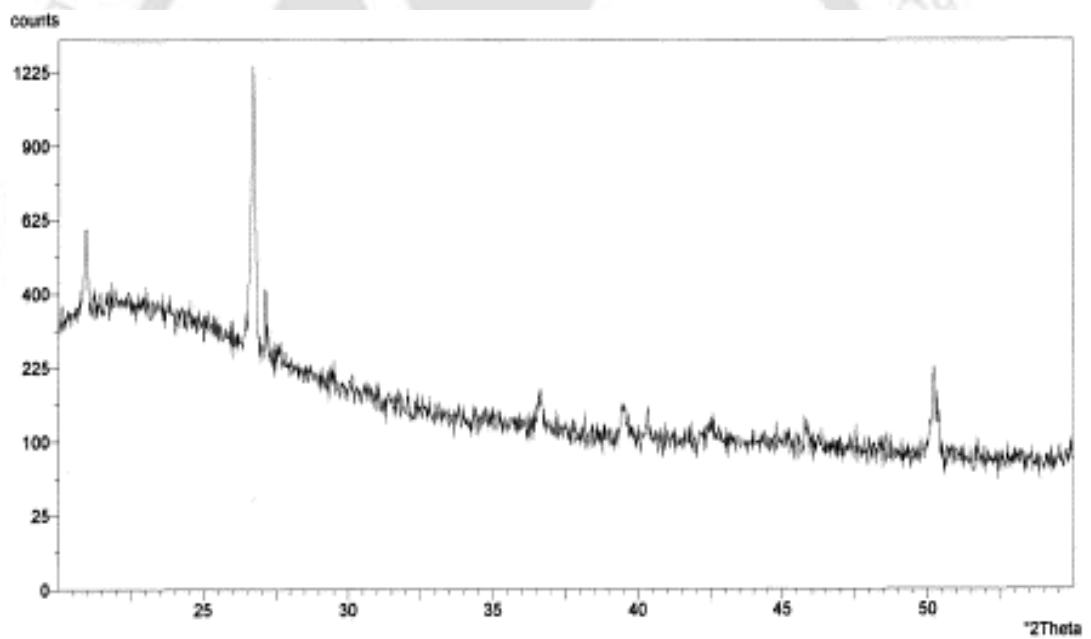


Fig 4.9 XRD pattern of RHA

#### 4.2.2 X-ray Diffraction Analysis (XRD)

XRD being a direct method for qualitative and quantitative characterization of poly-phase materials has turned out to be an indispensable tool in concrete technology. Each material

produces a unique diffraction pattern independent of others with the intensity of each pattern being proportional to concentration of materials in a mixture. In addition compositional and structural variations of each phase material in a mixture influence peak positions and relative intensities. The horizontal scale (diffraction angle) of a XRD pattern gives the crystal lattice and the vertical scale (peak intensities) gives the intensity of the diffracted ray. When the specimen being X-rayed contains more than one mineral, the intensity of characteristics peak from the individual minerals are proportional to their amount. For general purpose XRD of concrete making materials, normal focus X-ray tube with Cu target and Ni-filter with a monochromator system is widely used. The XRD measurements of RHA and CSF are presented in **Fig 4.9** and **Fig 4.10** respectively. It may be observed that all the mineral admixtures mainly consist of vitreous silica as shown by hump in XRD pattern. The flatter the hump observed, the more is the amorphous fume. The humps of XRD patterns is located near  $2\theta=20^\circ$  which means silica-tetrahedra in the vitreous particles are organized over a short distance range. The specific gravity and bulk density (dry-rodded) of cement and mineral admixtures was carried out as per IS: 1727-1967. Chemical properties of cement, fly ash, condensed silica fume and rice husk ash have been determined by XRD analysis. The results have been presented in **Table 4.1**

#### **4.2.3 Experimental Program**

Three different HPC mixes were prepared as control mixes with different mix proportions but with the same constituents such as cement, sand and coarse aggregates. The mix proportions and designations of control mixes are listed in **Table 4.2**. Mixing sequence and procedure for rheological measurements were the same as described in **section 2.6.3** and **section 2.5** of Chapter 2. Mineral admixtures were added as part replacement of cement in each mix at different replacement levels. Rheological tests were carried out as usual at each replacement level of mineral admixtures and the variation of rheological parameters was observed for replacement levels of mineral admixtures.

High range water reducing admixture (HRWRA) with set retarding effect was used as chemical admixture. Two types of HRWRA were used: Poly-carboxylic Ether Polymer

(PC) for Mixes C1, C2 and Sulfonated Naphthalene Polymer (SN) for Mixes C3. Ordinary tap water was used for all the mixes to prepare fresh concrete.

Particulars	Cement	Fly ash	Silica fume	RHA
Specific gravity	3.10	2.10	2.24	2.45
Bulk density (kg/ cum)	-	1080	810	585
SiO <sub>2</sub>	20.7%	57%	87.8%	91.6%
Al <sub>2</sub> O <sub>3</sub>	6.2%	27.1%	1.0%	0.37%
Fe <sub>2</sub> O <sub>3</sub>	3.1%	5.4%	4.4%	0.55%
CaO	64.9%	6.1%	0.4%	0.8%
MgO	0.82%	2.0%	0.24%	0.2%
K <sub>2</sub> O	0.53%	0.6%	0.5%	2.2%
SO <sub>3</sub>	2.7%	1.4%	-	2.9%
LOI	0.9%	0.8%	2.9%	3.4%

Particulars	Mix C1:PC	Mix C2:PC	Mix C3:SN
Cement	563	518	485
Sand	447	535	500
Coarse Aggregate	1093	1070	1140
Water	195	186	179
HRWRA	7.9	7.54	12.0
HRWRA Type	PC	PC	SN

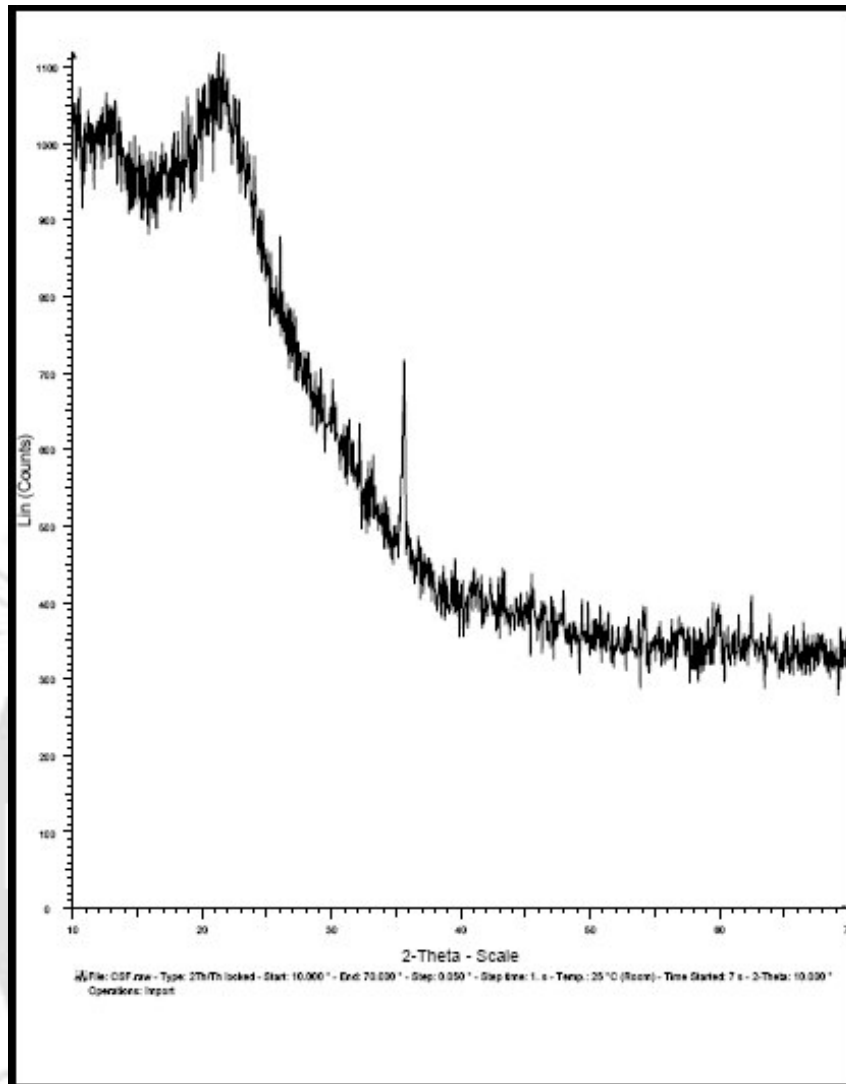


**Fig 4.10** XRD pattern of CSF

#### **4.2.4 Results and Discussion**

##### Use of Fly Ash

Fly ash was used as mass replacement for cement at rates 10%, 20%, 30%, and 50%. The 50% replacement level was incorporated to represent high volume fly ash concrete. The test results are shown in **Fig 4.11** [bwc refers to by weight of cement in all the figures]. As expected, addition of increasing levels of PFA resulted in a reduction of yield stress up to 30% level. Beyond this value, there is a slight increase in yield stress up to 50% level. The effect on plastic viscosity is peculiar for the mixes. Plastic viscosity increases

up to 10% and then gradually decreases up to 30%. The change in plastic viscosity beyond 30% is insignificant. Notably, the trend for yield stress and plastic viscosity are same for mixes containing PC and SN as HRWRA.

The spherical shape of PFA reduces frictional forces among the angular particles due to “ball bearing” effect. Slight increase in yield stress at high volume replacement level may be due active adsorption of HRWRA molecules by un-burnt carbons. Un-burnt carbons in PFA are known responsible for loss of workability because of adsorption of HRWRA molecules. The reason for initial increase in plastic viscosity is not clear.

#### Use of Condensed Silica Fume

CSF was used as mass replacement of cement at rates 5%, 10%, 15% and 20%. The test results are shown in **Fig 4.12**. Plastic viscosity increases steeply up to 10% level and then decreases again showing an optimum value for maximum plastic viscosity. The effect of CSF on yield stress is variable. In Mix#C1:PC and Mix#C2:PC, yield stress decreases up to optimum values then increases again. In case of Mix#C3:SN, yield stress increases up to 5% level, remains same up to 15% and then again increases.

CSF has very high fineness and surface area. CSF particles are chemically highly reactive and adsorb HRWRA molecules with multi-layers. Consequently, as replacement level increases, yield stress increases in Mix#C3:SN. In Mix#C1:PC and Mix#C2:PC, possibly improved gradation due CSF and lubricating effect reduce the yield stress initially. The decrease in plastic viscosity at higher replacement levels is more complex, even reaching a value equal to corresponding mix without CSF. In view of these results, the simple adage that CSF reduces concrete workability cannot be wholly justified.

#### Use of Rice Husk Ash

RHA was used to replace cement on mass basis at rates 5%, 10%, 15% and 20%. Results are presented in **Fig 4.13**. Yield stress decreases almost linearly up to 10% level beyond that it still decreases at lower decrement rates. This behavior is somewhat unexpected because RHA particles are flaky, elongated and angular as evident from SEM photograph. Plastic viscosity increases tremendously with the increase in replacement level.

RHA particles have the highest surface area and fineness and lower reaction ability than cement. RHA particles fill into the spaces made by larger cement particle, decrease frictional forces of RHA-OPC system and improve packing thereby reducing yield stress. The steep increase in plastic viscosity with the replacement levels suggests that fineness and shape of RHA play critical role. More the fineness more is the number of contacts among the particles and hence more is the resistance to flow. In addition, any deviation from a spherical shape implies an increase in plastic viscosity for the same phase volume.

#### Comparison of Rheological Parameters with Different Mineral Admixtures

Rheological parameters show different patterns with respect to different mineral admixtures. Yield stress shows that RHA and PFA act positively on workability whereas CSF acts negatively in this system i.e. yield value decreases with the increase in replacement level of RHA and PFA. With RHA as replacement material, workable mix beyond 20% replacement level is difficult to achieve. PFA keeps the mix workable over a very wide range of replacement level up to high volume replacement range. So, PFA may be a suitable option when low yield value is under consideration.

When low plastic viscosity values are desired, PFA seems to be the best option and RHA has the worst effect. In HPC, segregation of materials is an important factor since low plastic viscosity concretes are vulnerable to segregation. For designing HPC, therefore, moderate plastic viscosity is preferred. In view of this, CSF may be the suitable option.

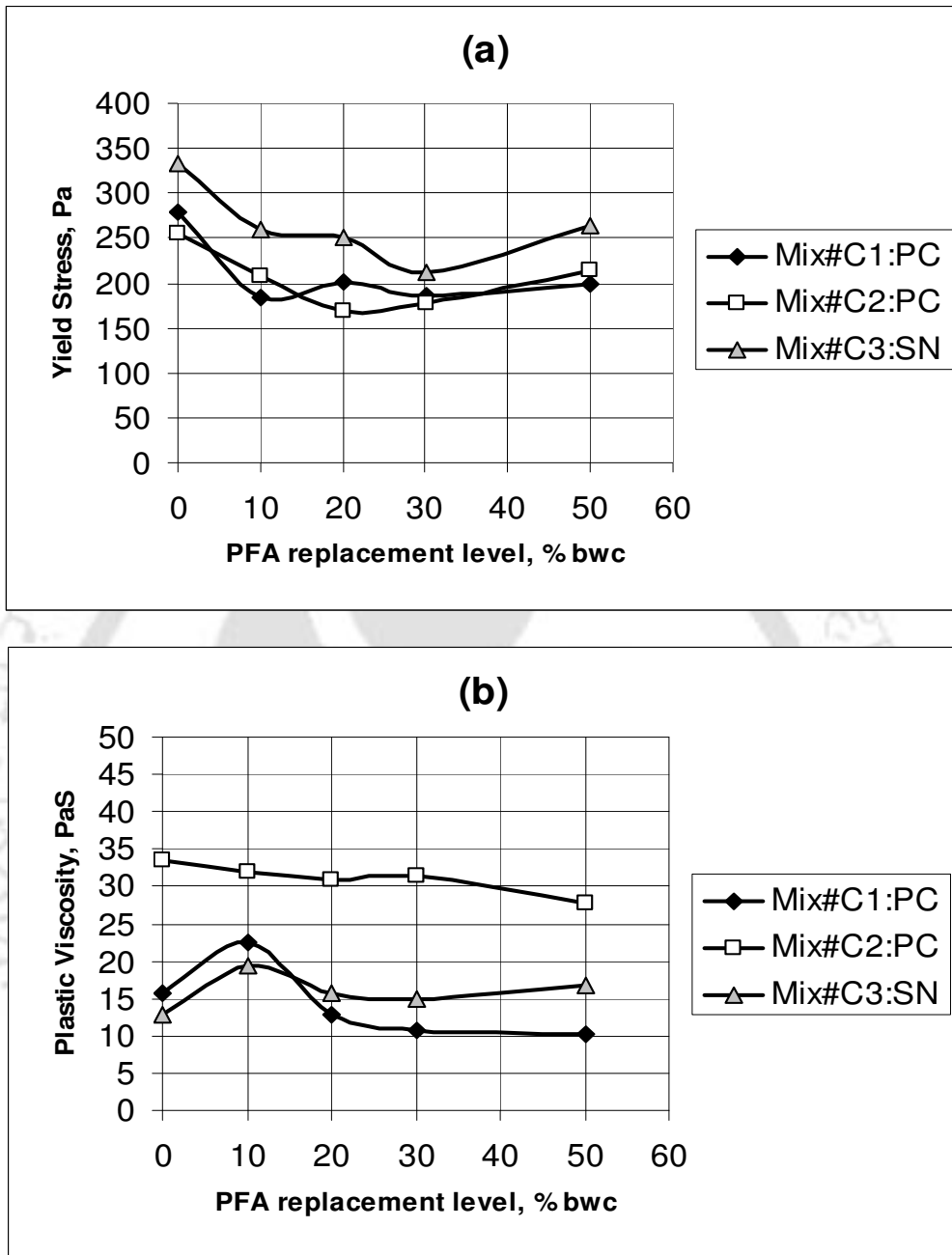


**Fig 4.11** Effect of PFA replacement on rheological parameters (a) Effect on yield stress  
(b) Effect on plastic viscosity

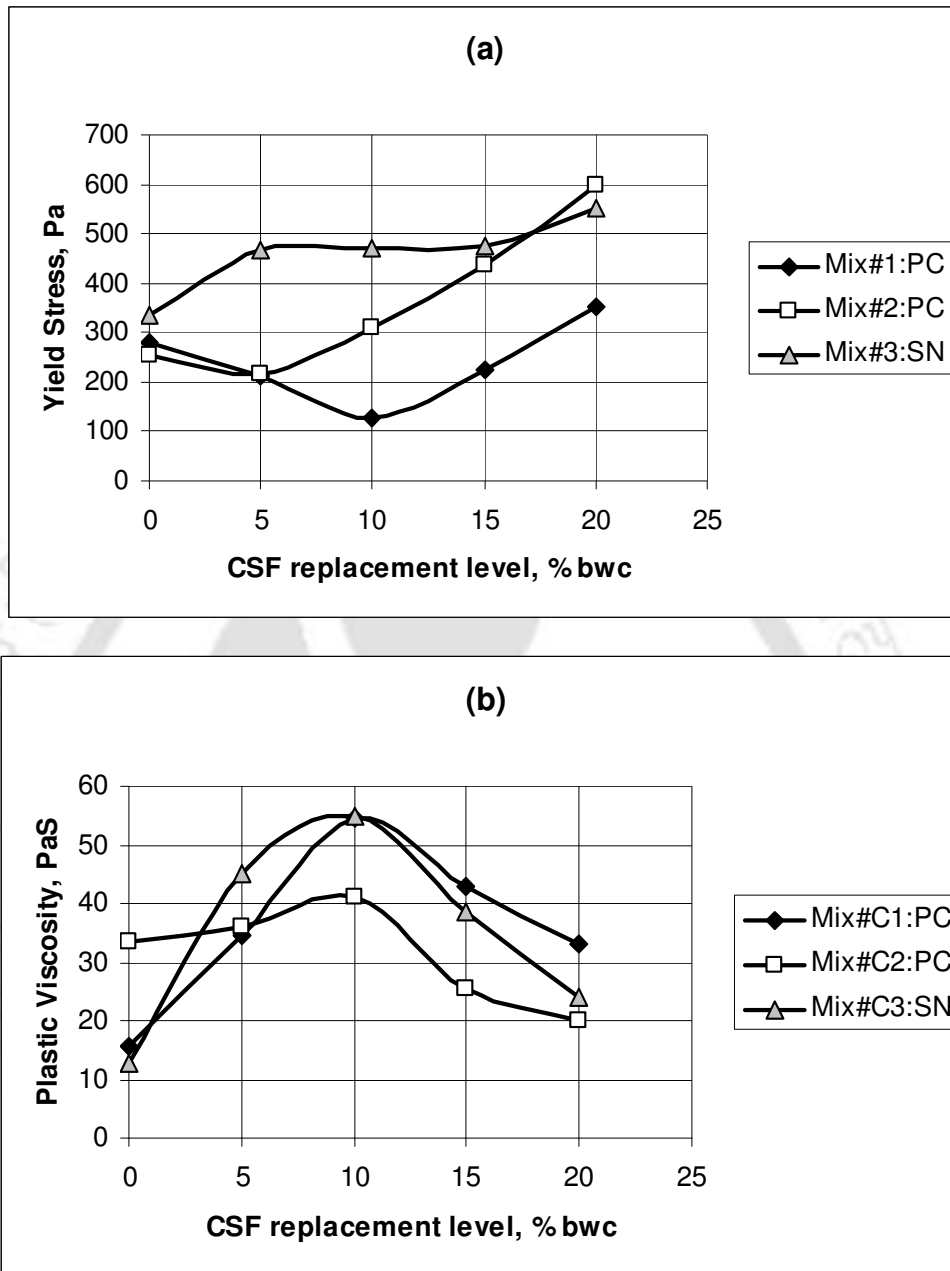


**Fig. 4.12** Effect of CSF replacement on rheological parameters (a) Effect on yield stress  
(b) Effect on plastic viscosity

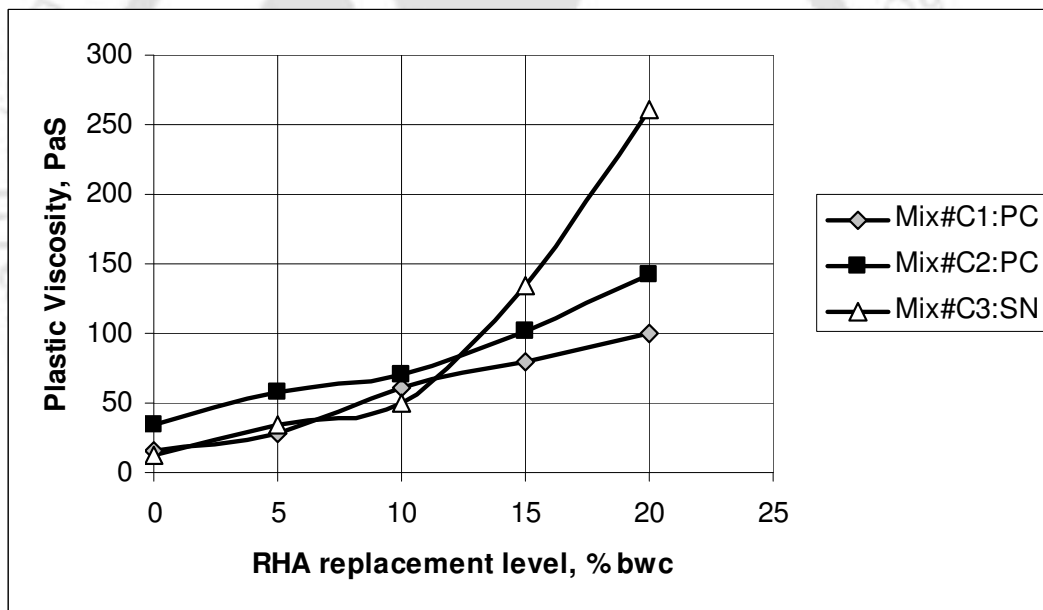
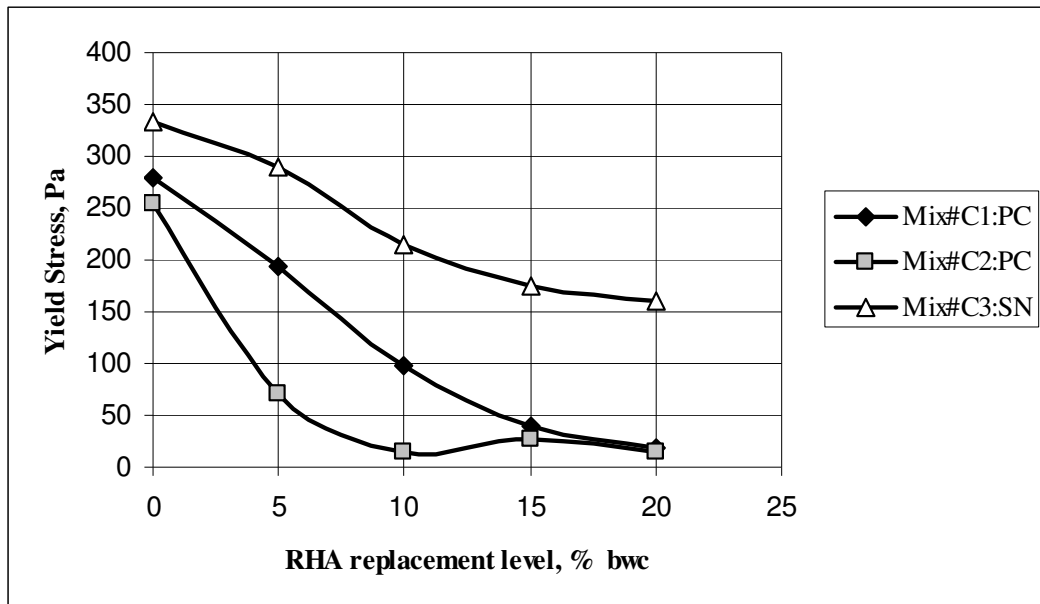


**Fig. 4.13** Effect of RHA replacement on rheological parameters (a) Effect on yield stress  
(b) Effect on plastic viscosity

### 4.3. STUDY OF TERNARY BLENDS

To take the advantage of different rheological parameters with various mineral admixtures, investigation has been carried out to examine the rheological behavior of concrete with ternary blends such as PFA-RHA, PFA-CSF and CSF-RHA. Mix#C2: PC was arbitrarily selected as control mix for this purpose. In each case of ternary blends, equal masses of respective mineral additives were mixed thoroughly before adding to cement.

The ternary blends were used to replace cement on mass basis at rates 5%, 10%, 15%, 20%, and 30%. The test results are shown in **Fig 4.14**. It is to be observed that yield stress and plastic viscosities of the concrete with ternary blends lie in between the values with the single mineral additive at each replacement values. For example,

$$\tau_o^{RHA} < \tau_o^{RHA+CSF} < \tau_o^{CSF}$$

$$\mu_{CSF} < \mu_{CSF+RHA} < \mu_{RHA}$$

where,  $\tau_o$  is the yield stress and  $\mu$  is the plastic viscosity. The rheological properties are thus improved with blending of admixtures. Least value of plastic viscosity is obtained in case of PFA-CSF whereas RHA-PFA still shows the highest values. When yield stress is under consideration, mixtures with PFA-RHA show least values whereas those with PFA-CSF have the highest values at different replacement levels. As evident from **Fig 4.14**, yield values of PFA-RHA and CSF-RHA are close indeed. Hence CSF-RHA may be considered as the best additive in the present case that has moderate plastic viscosity and very low yield stress. In general, proportions of RHA, CSF and PFA may be varied to have a large number of combinations of blended admixtures and the most suitable blended additive may be determined.

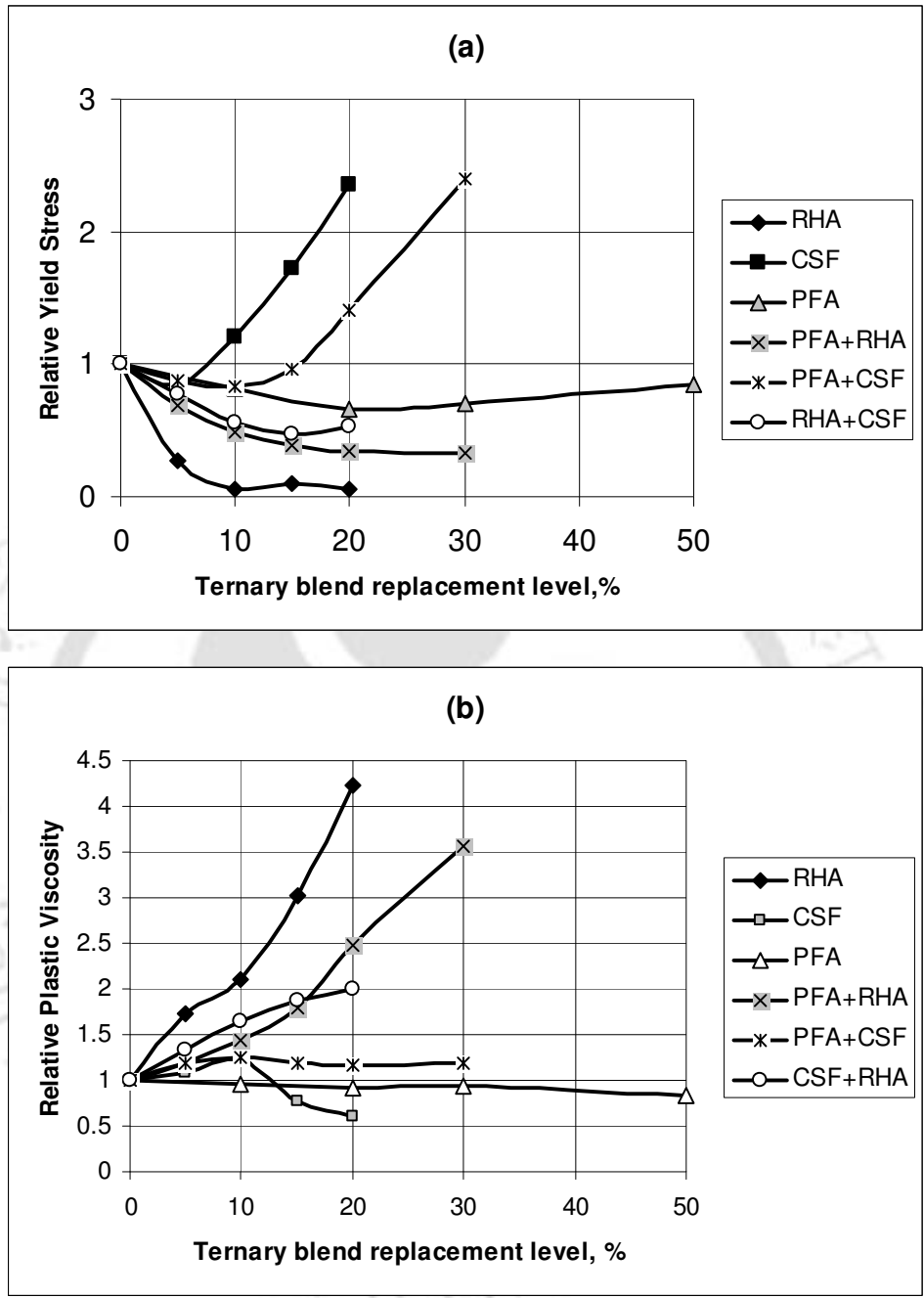


**Fig 4.14** Effect of ternary blends on rheological parameters (a) Effect on yield stress (b) Effect on plastic viscosity

#### 4.4. STUDY WITH ROUND STEEL FIBERS

Concrete incorporating steel fibers poses difficulty in mixing, transporting, placing and compacting that may lead to voids in hardened concrete. The determination of fresh fiber reinforced concrete properties is therefore, important for satisfactory performance in hardened state. Results of the experimental investigation of the effect of three fiber properties- volume fraction of fiber, aspect ratio of fiber and diameter of fiber- on the rheological properties of high performance concrete have been presented in this section.

##### 4.4.1. Experimental Program

Two different HPC mixes were prepared as control mixes with different mix proportions but with the same constituents such as cement, sand and coarse aggregates. The details of the material properties are mentioned in **section 2.6.2**. The mix proportions and designations are listed in **Table 4.3**. Polycarboxylic ether polymers (PC) were used as HRWRA.

Round steel fibers of different diameters such as 0.30mm, 0.50 mm, 0.70 mm, 1.0 mm with different aspect ratios for each size such as 25, 50, 75, 100, and 125 have been used in the present investigation. The physical properties of the fibers are as follows:

Specific gravity= 7.84;

Average tensile strength= 1.2 GPa;

Ultimate elongation= 2.5%.

Concrete was mixed in a tilting mixer (laboratory type). The weight of the materials was taken with a digital weighing balance. Mixing sequence was as follows:

- Mix coarse aggregate, fine aggregate cement and fibers for two minutes;
- Add water during mixing and mix for two minutes more;
- Stop mixing for one minute;
- Add HRWRA to the mix and mix for three minutes;
- Pour the concrete mix.

Rheological tests were carried out for fiber reinforced concrete for each parameter under consideration. The procedure for rheological test was same as described in **section 2.5**.

<b>Particulars</b>	<b>Mix C4</b>	<b>Mix C5</b>
Cement	518	485
Sand	535	505
Coarse Aggregate	1070	1140
Water	186	175
HRWRA	7.1	7.14

#### 4.4.2 Results and Discussion

##### Effect of Fiber Volume

Fibers were added to the control mixes at the rates 0.25%, 0.5%, 1.0%, 1.5% and 2.0% on volume basis keeping aspect ratio and diameter constant at each volume fraction level. The results are presented in **Fig 4.15**. In case of Mix#C4, yield stress increases almost linearly with the increase in volume of fibers. Plastic viscosity slightly decreases initially at small volume fraction showing an optimum point and again increases beyond the optimum value. In case of Mix#C5, the trend is different. Plastic viscosity increases linearly with the increase in volume of fibers without showing any optimum value. Yield stress initially decreases up to optimum value and then again increases almost linearly.

When fiber is added to concrete mix, the composite forms a relatively stable system due to interlocking of fibers that increase the effective cohesion in presence of fibers. Hence both the rheological parameters increase as volume of fibers increases in the mix. The initial reduction in yield stress in Mix#C5 and plastic viscosity in Mix#C4 is not fully understood. As cited earlier, Kuder et al [2007] observed similar trend in case of cement paste and mortar for both the parameters and concluded that initial decrease is due to thixotropic nature of cement. It was explained that stiff steel fibers might increase the amount of structural breakdown that occurs during mixing.

In the present study, concrete is pre-sheared in increasing strain rate sequence, allowing each step for sufficient duration for attaining equilibrium after complete structural breakdown that may be due to the consequence of thixotropy. Flow curve is drawn from

the downward sequence of strain rates. It is the down curve that follows the Bingham model. Therefore, once the Bingham parameters are determined, it obviously implies that the thixotropy can no longer play any role. Possibly, initial decrease in rheological parameters in some mixes might be due to improved packing of the mix due to small volume of fibers that is again dependent on the relative properties and proportions of other constituents of concrete. At higher volume fraction, interlocking phenomena dominate the flow behavior. It is to be mentioned here that Sundararajkumar et al [1997] also observed the same phenomena in case of fiber reinforced polymers.

#### Effect of Aspect Ratio

Fiber was added to the control Mix#C4 for constant volume concentration 0.25%, diameter equal to 0.5mm. In case of Mix#C5, volume concentration was 0.125% and diameter was 0.5mm. Aspect ratio was varied in each mix and rheological tests were performed. The test result is shown in **Fig 4.16**. Yield stress increases continuously with the increase in aspect ratio. Plastic viscosity also increases but the change is insignificant. At lower aspect ratios, the change in yield stress is less. This is due to the fact that short fibers cannot interlock the matrix effectively and can be dispersed easily by agitation. In case of very long fibers ( $l/d > 100$ ), the increase in yield stress is again less because of the fact that very long fibers tend to mat together. Thus, there is an aspect ratio range approximately between 50 and 100 where the rheological behavior of FRC is affected mostly.

#### Effect of Fiber Diameter

To investigate the effect of fiber diameter on rheological behavior of FRC, fiber was added at constant volume concentration 0.125% and aspect ratio 50. The test result is shown **Fig 4.17**. Yield stress is almost unchanged over the range of diameter studied. Plastic viscosity, however, increases slightly as the diameter increases. For a given aspect ratio and volume concentration, increase in diameter means the increase in fiber length and hence subsequent increase in effective mechanical interlocking.

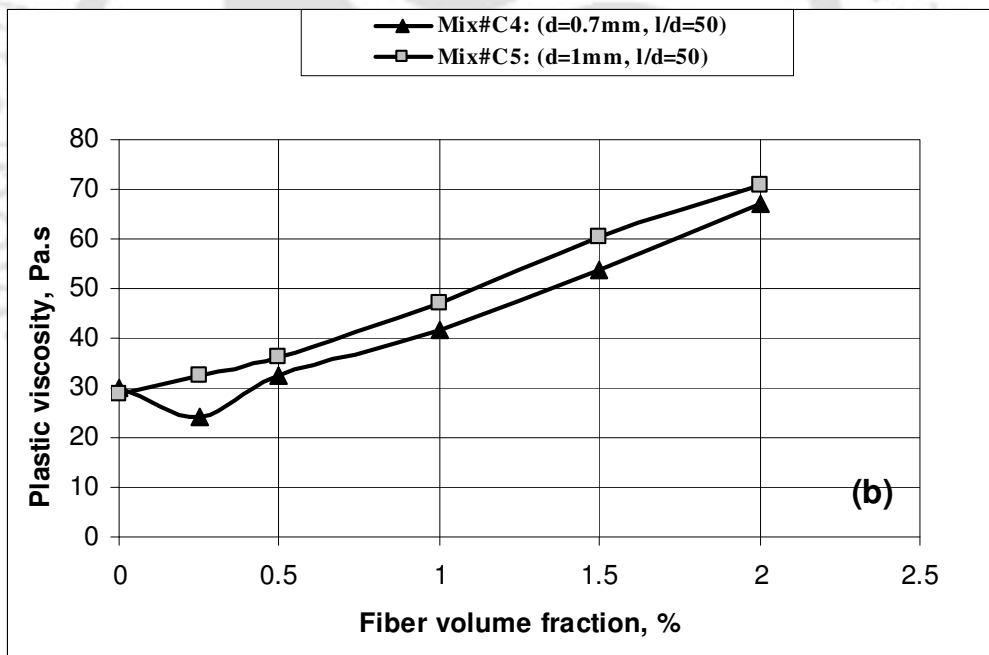
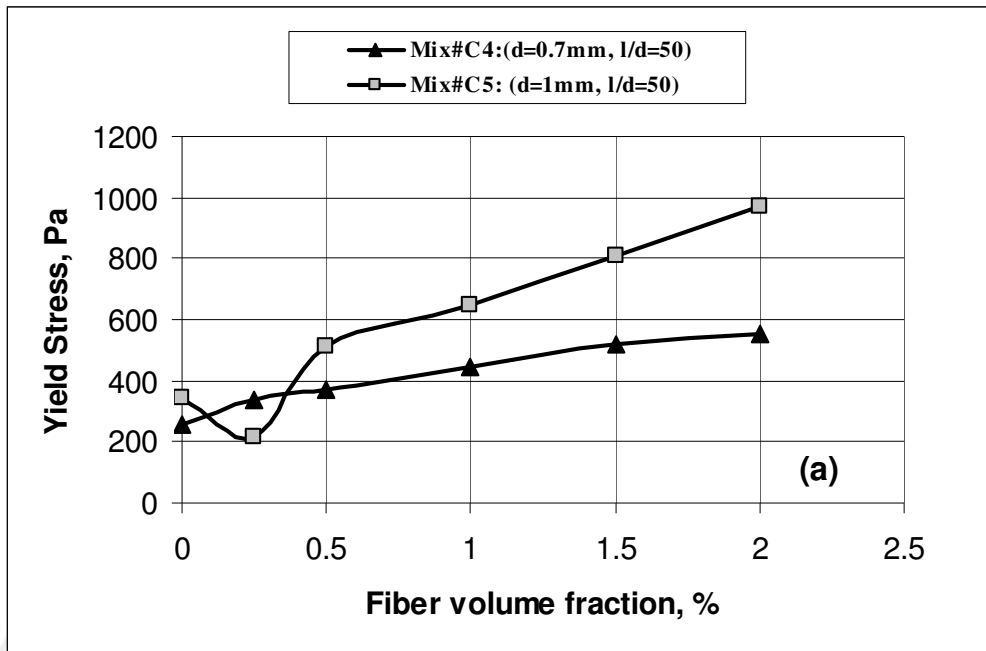


**Fig 4.15** Effect of fiber volume fraction on Bingham parameters (a) Effect on yield stress  
(b) Effect on plastic viscosity

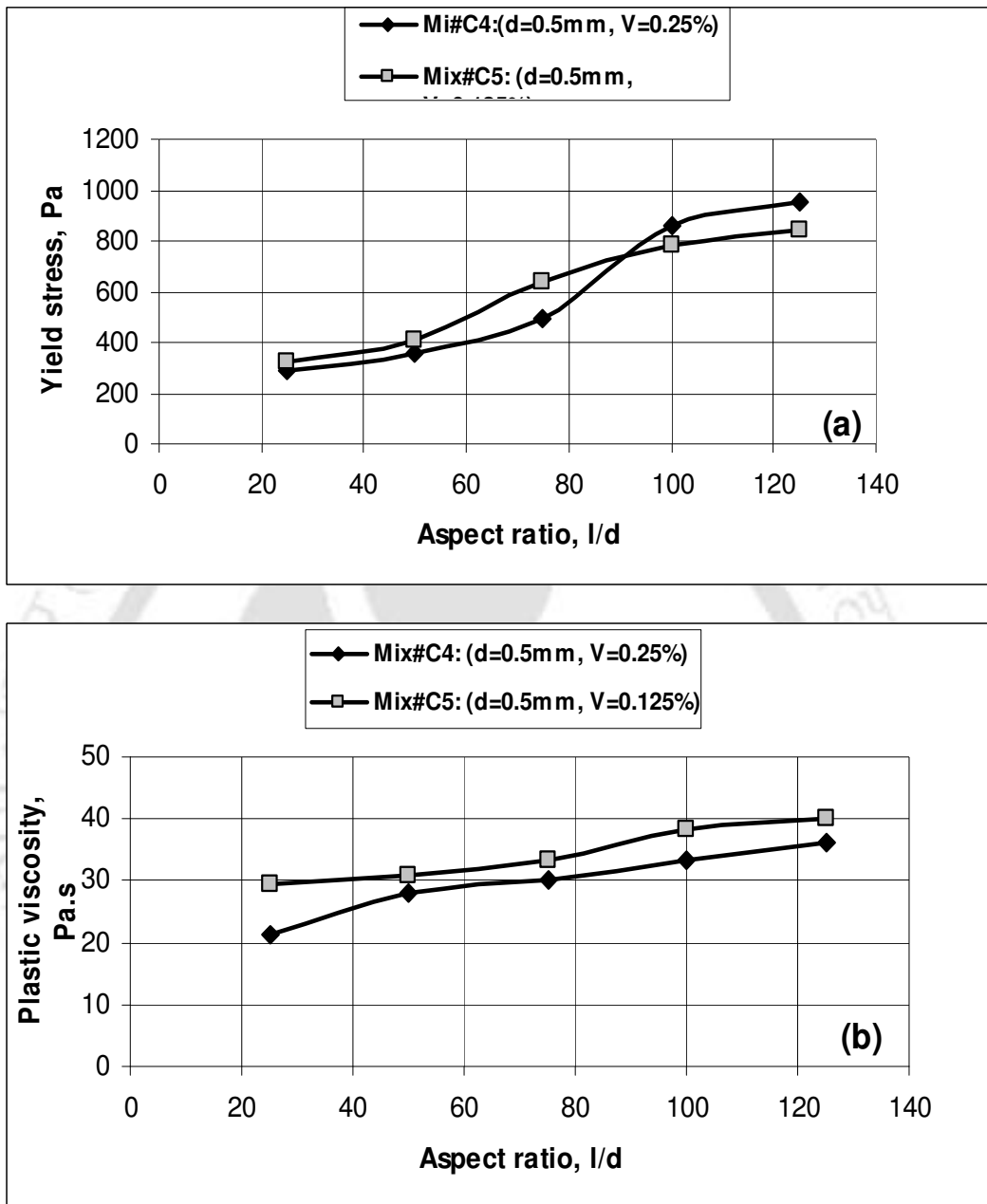


**Fig 4.16.** Effect of aspect ratio of fiber on rheological parameters (a) Effect on yield stress (b) Effect on plastic viscosity

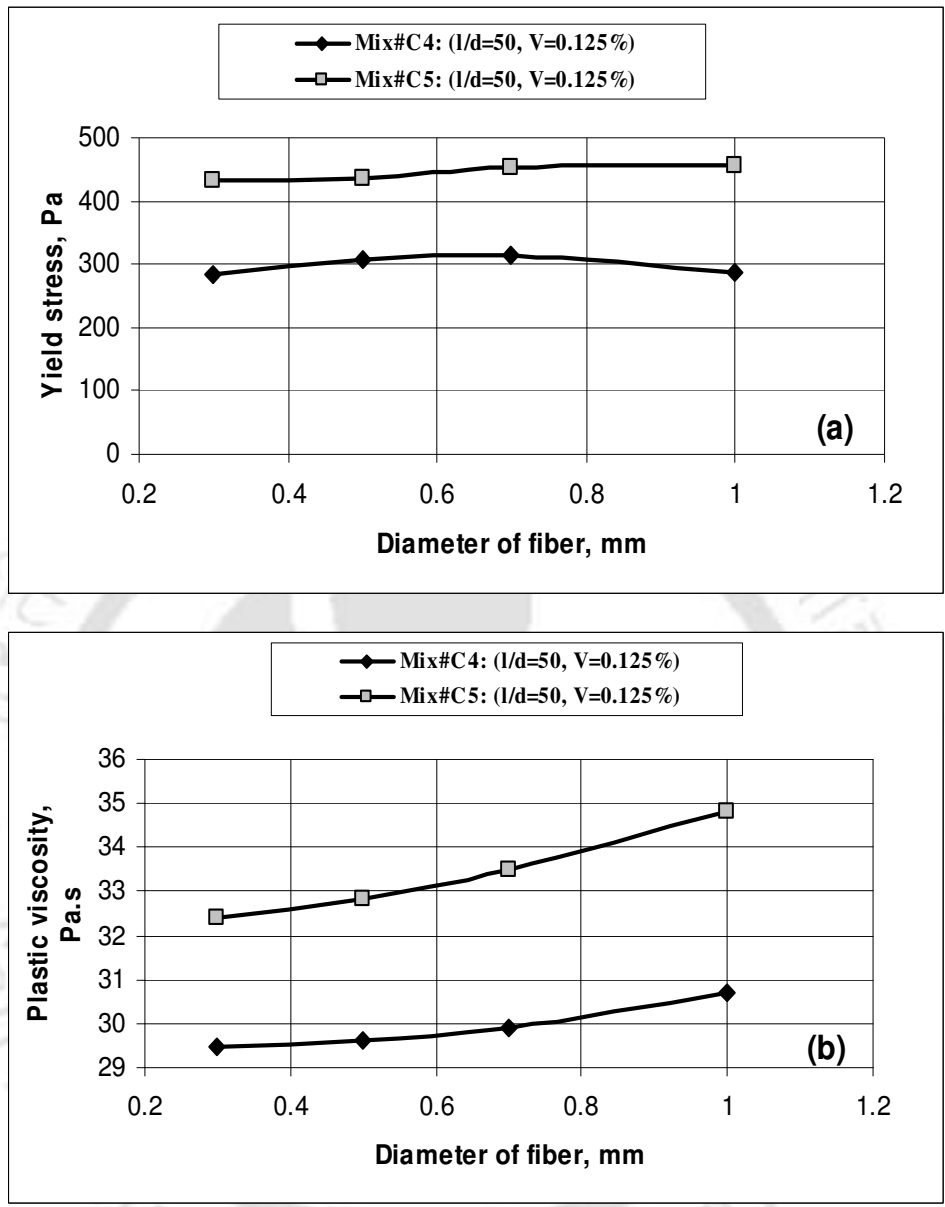


**Fig 4.17.** Effect of fiber diameter on Bingham parameters (a) Effect on yield stress (b) Effect on plastic viscosity

## **4.5 CORRELATION OF VEBE TIME AND PERCENT FLOW WITH RHEOLOGICAL PARAMETERS**

### **4.5.1 Vebe Test**

Vebe is a good laboratory test where condition of concrete during the test is comparatively closely related to the method of placing in practice [Neville, 2003]. The test actually measures the work needed to compact concrete. This test is recommended as workability test of FRC. A standard slump cone is placed in a cylinder 305 mm in diameter, the cylinder being mounted rigidly on a flow table, adjusted to give a drop [Fig 4.18]. The slump cone is filled in a standard manner, removed, and a disc-shaped rider is placed on the top of the concrete. The remolding is assumed complete when the glass plate rider is completely covered with concrete and all cavities in the surface of concrete have disappeared. It is assumed that input of energy required for compaction is a measure of workability of the mix, and this is expressed as the time in seconds, called Vebe time required for the remolding to be complete.

### **4.5.2 Flow Test**

Flow test has become more widely used in recent years as it is appropriate for concrete of high and very high workability including flowing concrete which would exhibit a collapse slump [Neville, 2003]. The apparatus consists of flow table over which concentric circles are marked. A standard mould made from smooth metal casting in the form of a frustum of a cone is kept on the centre of the table, firmly held and is filled in two equal layers, by compacting with a 16 mm rod [Fig 4.19]. Each layer is compacted 25 times as in slump test. After lifting the mould the table is jolted 15 times and the average diameter of the spread is noted. Flow of concrete is reported as the percentage increase in average diameter of the spread over the base diameter of the cone (250 mm in this case). The photograph of FRC before and after the flow test is shown in Fig 4.20.



**Fig 4.18** Vebe test apparatus

#### **4.5.3. Testing Procedure**

Rheological tests, Flow test and Vebe tests were carried out for concrete mixtures presented in **Table 4.4** with 0.50 mm diameter and 50 mm long round steel fibers at the rate of 1.5% by weight. For this purpose, fresh mixtures were prepared with the same materials described in **section 2.6.2** and mixing sequence mentioned in **section 2.6.3**. Rheological test, Vebe test and flow tests were performed at the end of 15 minutes from the addition of water, each time with a fresh concrete for each test. Vebe time was reckoned with a digital stop watch. Flow was reported as average of concrete diameter after spread at three horizontal directions.



**Fig 4.19** Flow test apparatus



**Fig 4.20.** Flow test of FRC (a) After lifting the cone (b) After jolting the flow table

#### **4.5.4 Results and Discussion**

The variations of yield stress and plastic viscosity with Vebe time are presented in **Fig 4.21**. It may be observed from **Fig 4.21** that Vebe time remains almost constant up to a value of 500 Pa for yield stress. Beyond this value, Vebe time increases linearly and steeply with the increase in yield stress. Vebe time also remains constant up to a value of

40 Pa.s for plastic viscosity beyond which there is a linear increase in Vebe time with further increase in plastic viscosity. Thus it may be concluded that Vebe test is not suitable for highly workable fiber reinforced concrete having  $\tau_o \leq 500$  Pa and  $\mu \leq 40$  Pa.s.

The variations of yield stress and plastic viscosity with % flow are shown in **Fig 4.22**. It may be observed from **Fig 4.22** that there is an excellent correlation ( $R^2 = 0.9947$ ) between yield stress and % flow. Percent flow decreases linearly with the increase in yield stress of fiber reinforced concrete. The correlation between plastic viscosity and % flow is also considered good [ $R^2 = 0.73$ ]. Percent flow in this case also decreases linearly with the increase in plastic viscosity. The following empirical relations may be derived by least square regression between percent flow ( $F$ ) and rheological parameters:

$$F = 104.73 - 0.114\tau_o \quad (4.1)$$

$$F = 109.58 - 1.41\mu; \quad (4.2)$$

**Table 4.4:** Mix proportions for studying Vebe and % flow (quantities in kg/cu.m)

Sl. No.	Cement	Sand	Coarse aggregate	HRWRA (PC)	Water	Remarks
1	503	660	1040	7.7	183	
2	558	444	1085	7.9	192	
3	532	516	1033	8.1	193	
4	505	491	1114	11.9	176	
5	423	677	1028	8.3	173	
6	300	647	1020	7.6	182	
7	343	637	1004	7.4	180	
8	385	627	988	7.3	177	
9	427	618	973	7.2	174	
10	466	610	960	7.0	171	
11	505	672	932	7.1	186	
12	588	590	930	8.8	202	

13	503	660	1040	2.78	209.8	
14	503	660	1040	13.9	198.7	
15	503	660	1040	7.7	183	Coarse sand
16	503	660	1040	7.7	183	Fine sand
17	503	660	1040	7.7	183	CA passing 12.5 mm
18	503	660	1040	7.7	183	CA passing 10 mm
19	503	660	1040	7.7	183	CA:10-6.3 mm
20	503	660	1040	7.7	183	CA: 12.5-10 mm
21	503	660	1040	7.7	183	CA: 16-12.5 mm
22	484	705	940	6.8	178	
23	514	452	1105	7.4	197	
24	471	460	1125	7.5	200	
25	600	440	1075	7.2	191	
26	570	453	1107	7.3	178	
27	563	448	1095	7.2	185	
28	560	536	996	7.2	183	
29	555	660	909	7.0	173	
30	518	535	1070	7.1	186	
31	485	505	1140	7.1	175	

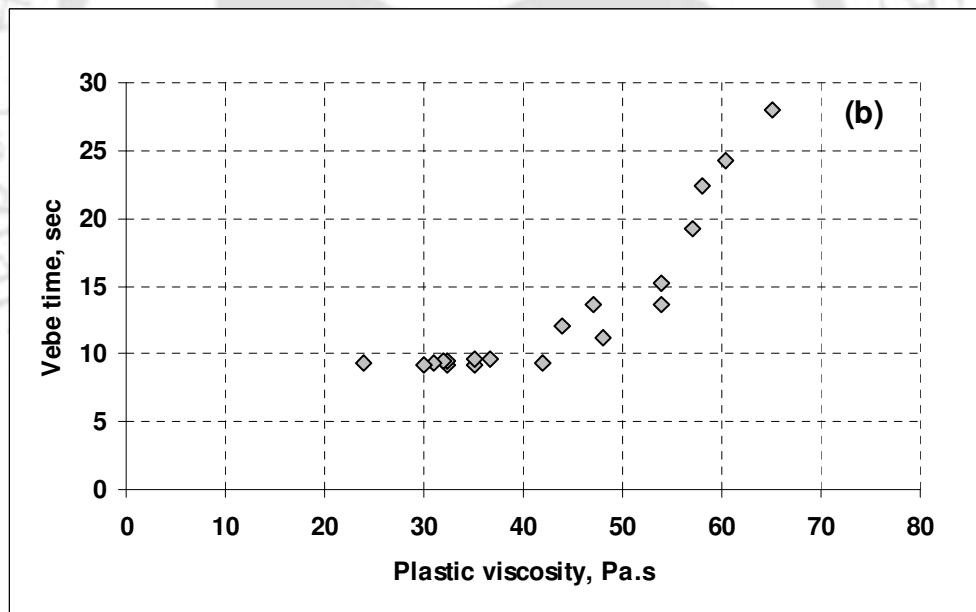
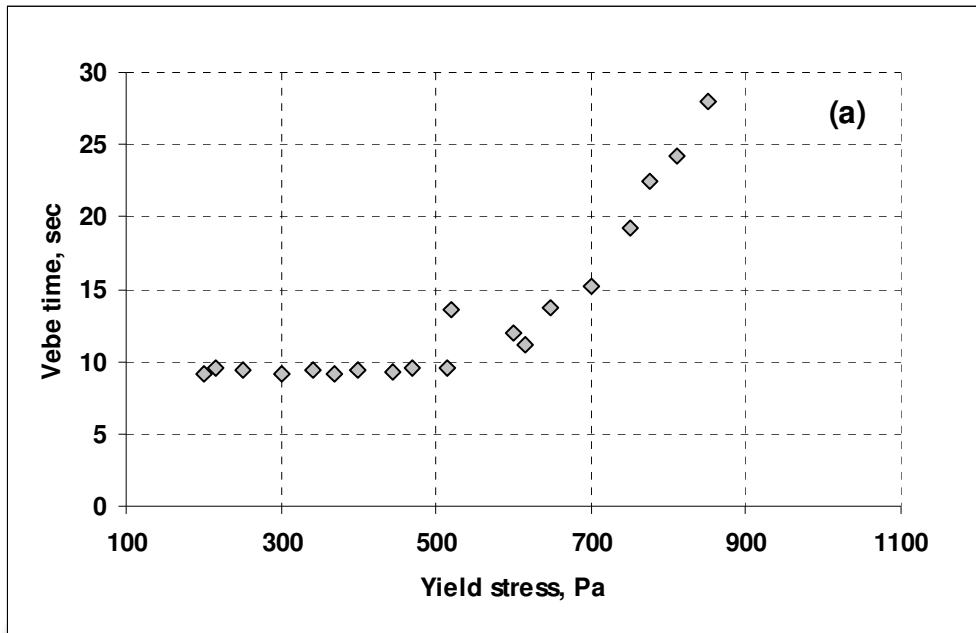


**Fig 4.21:** Variation of rheological parameters with Vebe time (a) Yield stress (b) Plastic viscosity

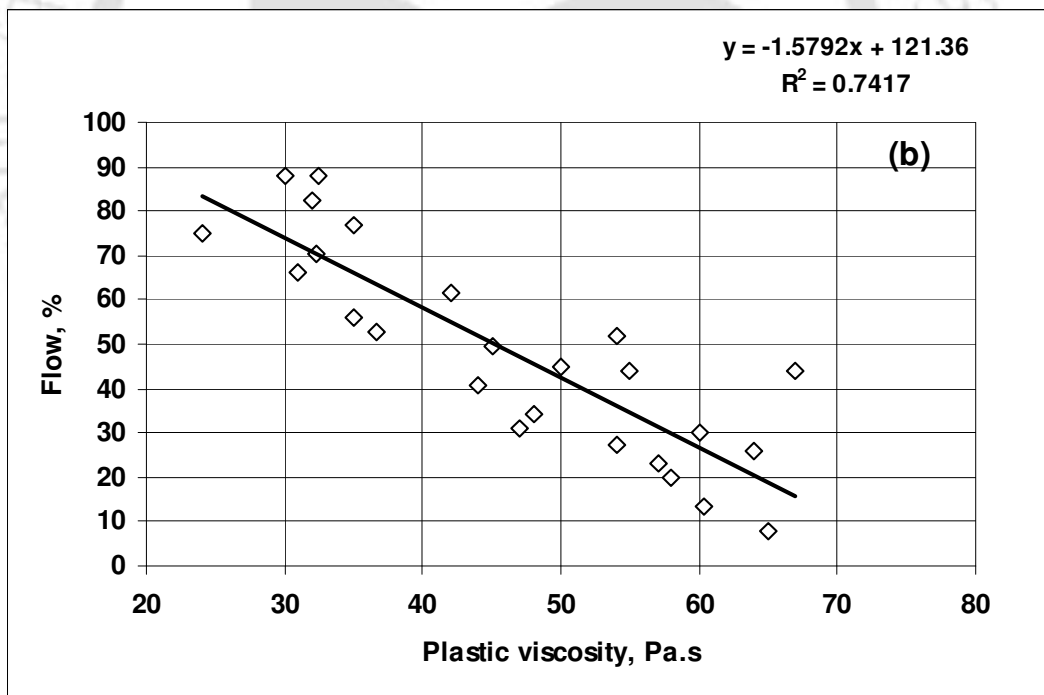
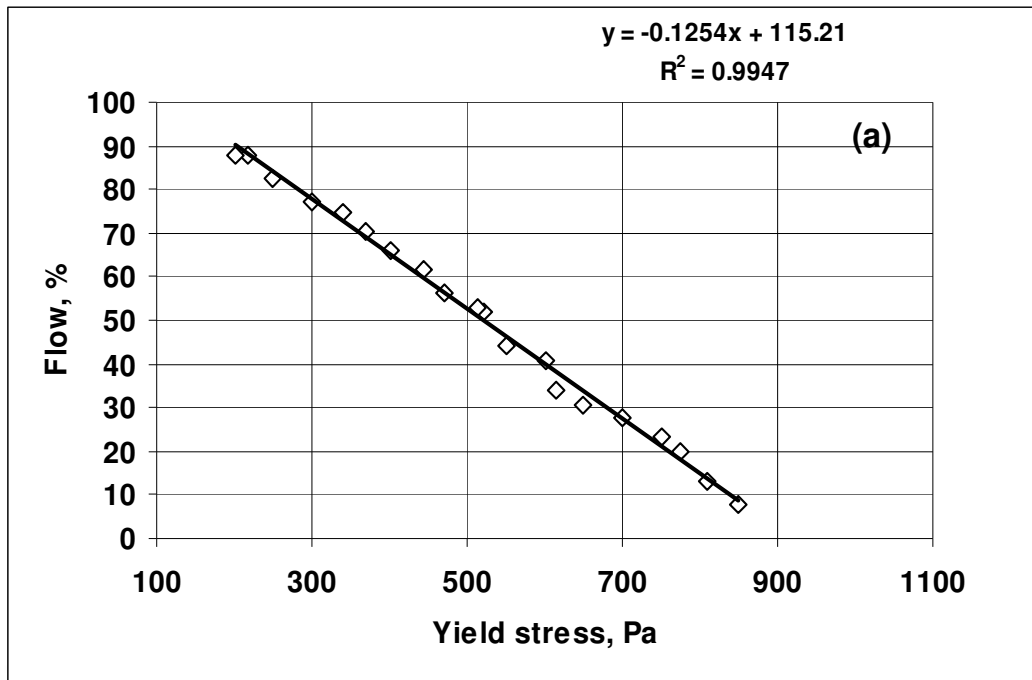


**Fig 4.22.** Variation of percentage flow with rheological parameters (a) yield stress (b) plastic viscosity

#### **4.6 CLOSURE**

Rheological properties of HPC were studied incorporating PFA, CSF and RHA and their blending. Cement was replaced on mass basis at different levels and rheological performances of concrete mixes were studied for individual additives. Effect of mineral admixtures on rheological parameters depends on various factors such as surface activity, particle size distribution, specific surface area, shape, surface features, type of cement and type of water reducers which are reflected on the observed parameters. The study also reveals improvement of rheological behavior with blending of different admixtures. Rheological measurements on fiber reinforced concrete were undertaken with round steel fibers. The effect of fiber volume concentration, aspect ratio and fiber diameter on the rheological behavior was investigated. The addition of fibers in concrete decreases the workability which is reflected in observed rheological parameters. In addition to rheological tests, Vebe and flow tests were also conducted to investigate the relationship between these tests and rheological parameters.

# **CHAPTER 5**

## **MIX DESIGN PROCEDURE OF HIGH PERFORMANCE CONCRETE**

### **5.1 OBJECTIVE OF MIX DESIGN OF HPC**

The objective of any mix design method is to determine an appropriate and economical combination of concrete ingredients that can be used for a first trial batch to produce a certain concrete which is capable of achieving a good balance between various desired properties of concrete at the minimum cost. A mixture proportioning only provides a starting mix design that will have to be more or less modified to meet the desired concrete characteristics. In spite of the fact that mix design is still something of an art, it is unquestionable that some essential scientific principles can be used as a basis for calculations. Mix design of high performance concrete (HPC) is different from that of usual concrete because of the following reasons:

- Water-binder ratio is very low.
- Concrete quite often contains cement replacement materials that drastically change the properties of fresh and hardened concrete.
- Slump or compaction factor can be adjusted using high range water reducing admixture (HRWRA) without altering water content.

For cementitious materials, rheological parameters help to describe workability of fresh state including mobility, placeability, compactability, pumpability and finishability. In existing mix design methods, there is no provision to have an idea of estimating workability or rheological parameters like yield stress and plastic viscosity. A new method of mix design procedure has been outlined in this chapter for design of high strength HPC taking into account of the rheological properties at the design stage itself.

### **5.2 BACKGROUND OF MIX DESIGN OF HPC**

Aitcin [1998], Mehta and Aitcin [1990] developed empirical procedures based on trial mixes for design of high performance concrete mix. According to Canadian Portland Cement Association, the trial mix approach is the best for selecting proportions for HPC

[Shah and Ahmad, 1994]. Some general guidelines for mix proportioning for HPC suggested by Aitcin [1998], Shah and Ahmad [1994] and Neville [2003] are as follows:

### **5.2.1 Water Binder Ratio**

For normal strength concrete (NSC), mix proportioning is based to a large extent on water-cement ratio law. For these concretes, in which aggregate strength is generally much greater than the paste strength, the w/c ratio does indeed determine the strength of concrete for any given set of raw materials. For HSC, however, in which aggregate strength or the strength of the cement-aggregate bond, are often the strength controlling factors, the role of w/c ratio is less clear. To be sure it is necessary to use very low w/c ratio to manufacture HSC. However, the relationship between w/c ratio and concrete strength is not straightforward as it is for NSC. The w/c ratio is a poor predictor of compressive strength in HSC [Aitcin, 1998; Shah and Ahmad, 1994].

### **5.2.2. Cementitious Materials Content**

For NSC, cement contents are typically in the range of 350- 550 kg/cu.m. For HSC, the content of cementitious materials is higher, ranging from 450-650 kg/cu.m [Neville, 2003; Nawy, 2001]. The quantity of supplementary materials may vary considerably depending upon workability, economy and heat of hydration considerations.

### **5.2.3. Mineral Admixtures**

It is possible to make HSC without using fly ash, slag or silica fume. For higher strength, supplementary cementing materials are generally necessary. In particular, the use of silica fume is required for strength much in excess of 98 MPa [Aitcin, 1998].

### **5.2.4. Super-plasticizers**

It is essentially impossible to make HSC at adequate workability in the field without the use of super-plasticizer. There are basically three principal types of super-plasticizers: (i) lingo-sulfonate based (ii) melamine sulfonate (iii) naphthalene based. In addition to the above, third generation of super-plasticizers are also used. These are polycarboxylate ester, acrylic polymer, multi-carboxylate ethers and others. The determination of SP

dosage is not easy. It greatly depends on what is the most critical issue for the particular HPC to be produced with a particular cementitious system. If the long term strength is the most critical without any problem on rheological side, it is preferable to work with the highest amount of SP and lowest amount of water possible. However, SP dosage should not be greater than saturation dosage to avoid segregation and set retardation. If the rheological properties are critical than the strength, it is the best to make the concrete with the highest water-binder ratio to achieve strength requirement and to adjust SP dosage in order to get desired rheology.

#### **5.2.5. Aggregates**

The aggregate properties that are most important with regard to HSC are particle shape, particle size distribution, mechanical properties of aggregates, possible chemical reaction between aggregate and cement paste which may affect the bond. Unlike their use in NSC, the aggregate may become the limiting factor in HSC. A number of different rock types have been used to make HSC; these include limestone, natural siliceous gravel, dolomite, granite, syenite, diorite, gabbro, andesite, diabase and so on. From strength and rheological point of view, the coarse aggregate must be roughly equi-dimensional, clean and should not be polished. It is commonly assumed that a smaller maximum size of coarse aggregate will lead to higher strength for two reasons. First, with increasing  $m_{sa}$  (maximum size of aggregates), the transition zone becomes larger and more heterogeneous and secondly, with most rock types, smaller particles of coarse aggregate are generally stronger than large particles. While Mehta and Aitcin (1990) recommend a maximum size of 10-12 mm, they report that 20-25 mm maximum size may be used for HPC.

Fine aggregate should consist of smooth rounded particles to reduce the water demand. It is recommended that the grading should lie on coarser side of the limit established by ACI 211.1 (1989) for Normal Strength Concrete. A fineness modulus 2.7-3.0 or greater is recommended to decrease water requirement and to improve workability of paste-rich mixes. The use of coarse sand is supported by the fact that HPC mixes are rich enough in fine particles because of their high cementitious content and it is not necessary to include fine aggregates from workability point of view. Natural sand is very often, but not

always, not very strong and can become the weakest link in concrete. Partial replacement of sand by crushed strong rock has been recommended by researchers. For NSC, ratio of coarse to fine aggregate is in the range of 0.9 to 1.4. However, for HSC, the coarse/fine ratio is much higher. A ratio between 1.5 and 1.8 is used in practice.

### **5.3. PROPOSED METHOD OF MIX DESIGN PROCEDURE**

Proposed method of mix design is a combination of empirical results and mathematical calculations based on absolute volume method. The water content is assumed to be inclusive of HRWRA content. The procedure is initiated by selecting different mix characteristics or material proportions in the following sequence:

- HRWRA dosage, sand content
- Estimation of yield stress and plastic viscosity
- Water-cement ratio
- Water content
- Cement content
- Aggregates content.

In laying down the design procedure, the reference is made to Indian Standard Code of Practice IS: 10262-1982 (Recommended Guidelines for Concrete Mix design). However, the difference between the proposed method and existing methods of mix design procedure such as IS code method is that corrections for sand zone, maximum size of coarse aggregate are applied from rheological point of view. And the rheological properties are only estimated from target strength criteria. In this section, some salient features of mix design method adopted in IS code is discussed in the following subsection.

#### **5.3.1. Some Salient Features of Mix Design Procedure in IS Code**

The following are steps for mix design procedure as per IS Code:

1. Calculate target mean strength taking standard deviation equal to 5 MPa for M45 and above.

2. Select the water-cement ratio from the standard graph corresponding to target mean strength. This will include the 28 day compressive strength of cement such as 33, 43 and 53 grade.
3. Estimate air content from the table given in the code depending on maximum size of aggregate.
4. Select water content and % sand per cu.m of concrete from the following table (**Table 5.1**) for w/c=0.35 and compaction factor (CF) =0.80 [approximate slump=30 mm].
5. Adjust water content and % sand obtained from **Table 5.1** for any deviation from w/c=0.35, CF=0.80 and sand zone 2 as per **Table 5.2**.
6. Calculate cement content as cement= water content/ water-cement ratio.
7. Calculate aggregate content from following relation

$$V = \left[ W + \frac{C}{S_c} + \frac{f_a}{S_{fa}p} \right] \frac{1}{1000} \quad \text{and} \quad C_a = \frac{1-p}{p} f_a \frac{S_{ca}}{S_{fa}}$$

where V=absolute volume of fresh concrete,

W=mass of water per cu.m,

C=mass of cement per cu.m ,

$S_c$ =specific gravity of cement,

p=% sand,

$f_a$  ,  $C_a$  are total masses of fine and coarse aggregates respectively,

$S_{fa}$  and  $S_{ca}$  are specific gravities of fine and coarse aggregates respectively.

8. Calculate actual quantities taking into consideration the water content and water absorption of the aggregates.

9. Calculated mix proportions shall be checked by means of trial batches for workability and strength.

The method given in IS code is applicable to a compressive strength of concrete up to 60 MPa and water-cement ratio up to 0.30. There is no provision of incorporating mineral and chemical admixtures. The workability of the mix so obtained will be very poor even though one may attain the high target strength. Thus, the mix design procedure cannot be

called a design for high performance concrete where high workability should also be achieved.

**Table 5.1: Approximate sand and water content for w/c=0.35; CF=0.80**

Maximum size of aggregate	Water content	%sand by volume
10	200	28
20	180	25

**Table 5.2: Adjustment of values in water content and %sand for other conditions**

Change in conditions stipulated for Tables	Adjustment required in	
	Water content	% sand
Sand conforming to zone 1, zone 3, zone 4	0	+1.5% for zone 1 -1.5% for zone 3 -3% for zone 4
Increase or decrease in CF by 0.1	$\pm 3\%$	0
Each 0.05 increase or decrease in w/c ratio	0	$\pm 1\%$

### 5.3.2 Steps to Arrive at Mix Proportions

#### HRWRA Dose and Sand Content

HRWRA dose can be determined from the dosage at the saturation point. If the saturation point is not known, it suggested to start with a HRWRA content of 1.5% by weight of cement. As can be seen from **section 3.3** in Chapter 3 that optimum dose of HRWRA is around 1.5% by weight of cement beyond which it does not significantly reduce yield stress and plastic viscosity. For yield stress, the optimum sand content is 30% for minimum yield strength; between 30%-40% sand, plastic viscosity is minimum

when HRWRA dose is approximately 1.5% by weight of cement. IS code also assumes sand content approximately equal to 28% when zone 2 sand is used.

#### Estimation of Yield Stress and Plastic Viscosity

Generally, determination of workability such as slump or Compacting Factor or Vebe time etc is the last step of any mix design procedure. After arriving at all the ingredients of concrete, trial batches are prepared in the laboratory and workability is measured. If the workability criterion is satisfied, cubes or cylinders are cast for compressive strength test. If desired level of workability is not obtained, adjustments of the constituents of concrete are again made and trial batch is prepared. The fact that rheological parameters are fundamental properties of fresh concrete and compressive strength is the most important hardened property of concrete, the correlation curves between rheological properties and compressive strength of concrete was developed in the present investigation and used in the mix design.

Correlation between compressive strength and rheological parameters were studied and curves were developed based on the data obtained from rheological tests on trial mixes shown in **Table 5.3** and **Table 5.4** and evaluating compressive strength of 15 cm cubes for the corresponding mixes. Two different categories of trial mixes have been considered: one with SN and other with PC as HRWRA. OPC was employed; local alluvial sand and crushed stone aggregate of 16 mm nominal size (unless otherwise stated in **Table 5.3** and **Table 5.4**) were used. Ordinary tap water was used to prepare the mixes. Rheological tests were performed with the present rheometer for each trial mix and cubes (3 sets) were cast. After 2 hours of casting, when the surface of concrete cubes were completely free of water, wax based curing compound was applied as per the instruction of the manufacturer. The cubes were de-molded after 24 hours and cured in water for 28 days. Compression testing was done after 28 days of curing in a standard manner.

The variation of compressive strength with respect to yield strength and plastic viscosity respectively for mixtures containing PC are shown in **Fig 5.1** and **Fig 5.2**. It may be observed that initially compressive strength increases steeply as yield stress increases.

Beyond 200 Pa, compressive strength increases at a slower rate but the increase is almost linear. Compressive strength increases as plastic viscosity increases up to a 60 Pa.s.

In mixtures containing SN as HRWRA, compressive strength also increases steeply up to yield stress equal to approximately 500 Pa and then remains unchanged with the increase in yield stress. It may also be observed that optimum values of plastic viscosity exist for both the categories of mixes. Compressive strength, however, decreases at a slower rate in mix with SN beyond optimum value.

Variation of compressive strength with yield stress and plastic viscosity are shown in **Fig 5.3- Fig 5.4** for mixture containing SN as HRWRA. For plastic viscosity between 50-75 Pa.s, and yield stress between 300-400 Pa, compressive strength is the highest in mix with PC, whereas in mixtures with SN, compressive strength shows highest value when plastic viscosity lies between 60-90 Pa.s and yield stress is greater than 500 Pa. It is to be mentioned here that concrete in these range of rheological parameters are very much workable.

In fact, complete rheological property of concrete is described by combination of yield stress and plastic viscosity simultaneously. The influence of mixture proportions and properties of ingredients are all contained in yield stress and plastic viscosity. Hence, for better representation, compressive strength should actually be plotted against yield stress and plastic viscosity as 3D surface. **Fig 5.5** shows such a surface for mixtures containing SN as HRWRA. Smooth surfaces could have been obtained with large number of data.

#### Water Cement Ratio

Since water-cement ratio is not a good predictor of strength in case of HPC, relationship between water-cement ratio and compressive strength has not been used. In fact, there may be various combinations of water-cement ratio and paste volume to aggregate volume ratio for a given rheological parameter and hence target strength.

#### Water Content

One difficult thing when designing HPC mixtures is to determine amount of water to be used to achieve a HPC mix with high slump after one hour of batching. This is because workability is controlled by several factors such as amount of initial water, reactivity of

the cement, amount of HRWRA dose, compatibility of HRWRA with cement. A high slump concrete can be achieved when batching the concrete with a low water dosage and a high HRWRA dose or with high water content and low HRWRA dose. Between the two options, the difference can be significant depending on the rheological reactivity of cement and the efficiency of HRWRA [Aitcin, 1998]. If the amount of mixing water selected is very low, mix can rapidly become sticky and a high HRWRA dose has to be used to achieve this high slump. Therefore, a simplified approach based on concept of saturation point may be used. Aitcin [1998] suggests that if saturation point of HRWRA is not known, one may start with water content of 145 liter/cu.m. In the present method, use of ratio of paste volume to total aggregate volume for a given water-cement ratio has been made. To do this, data presented in **section 3.3** of Chapter 3 has been used and the chart for finding aggregate volume to paste volume ratio against yield stress and plastic viscosity at different water-cement ratio has been prepared and presented in **Fig 5.6-Fig 5.7**. Extrapolation may be done to obtain values not presented as curve in the figure.

#### Aggregate Content

Coarse aggregate content depends on the particle shape. Aitcin [1998] suggests the coarse aggregate content as shown in **Fig 5.8**. In the present study, this has been adopted to find coarse aggregate content.

#### Cement Content

Cement content may simply be calculated once paste volume-aggregate volume ratio and water-cement ratio is known. Water content here is the free water content including HRWRA.

#### Correction Factors

Corrections are to be made in the mix design for different zones of sand and maximum size of coarse aggregates. These correction factors were derived from the experimental results of the variation of rheological parameters with sand gradation and maximum size of coarse aggregates of Chapter 3. To do this, a reference mix as per **Table 5.1** given in

IS: 10262-1982 has been considered and rheological parameters of this reference mix were obtained with the present rheometer. The reference mix is follows:

53 grade OPC= 571 kg/cu.m;

Indian Standard zone II sand= 436 kg/cu.m;

Coarse aggregate of nominal size 10 mm= 1083 kg/cu.m;

Water= 200 liters/cu. m inclusive of HRWRA;

PC as HRWRA= 7.7 kg/ cu. m;

Water-cement ratio= 0.35;

% sand= 28%.

Now, comparing the values of yield stress and plastic viscosity of the mixes presented in **Section 3.3** with the rheological parameters of the reference mix, correction factors for yield stress and plastic viscosity have been calculated and presented respectively in **Table 5.5** and **Table 5.6** respectively. It is to be noted from **Table 5.5** and **Table 5.6** that the correction factors for yield stress and plastic viscosity are  $K=k_1k_2$ ,  $K^* = k_1^* k_2^*$  respectively. The reason may be explained as follows:

Suppose it is required to find out the overall correction factor  $K$  for yield stress of concrete with 16 mm nominal maximum size of aggregate and zone- III sand (fine). With reference to Fig 3.6 of Chapter 3, for mixes with PC as HRWRA, there is a decrease in yield stress which may be expressed as  $k_1\tau_o$  where  $\tau_o$  is yield stress of reference mix with zone-II sand. With reference to Fig 3.7, there is again a decrease in yield stress from 10 mm to 16 mm nominal maximum size of coarse aggregate and suppose the decrement is  $k_2$ . Therefore the yield stress when 16 mm nominal maximum size coarse aggregate and zone-III sand are used will be given by  $k_1k_2\tau_o$ . Thus  $K$  is equal to the product of the correction factors  $k_1$  and  $k_2$ . The same is true for plastic viscosity.

From above discussions, steps for mix design are summarized as follows:

1. As per IS: 10262-1982, assume sand= 28% and take air content as follows:

For 10 mm nominal maximum size of aggregate (Msa): air= 3%

12.5 mm and 16 mm: air= 2.5%

20 mm: air= 2%.

2. Assume HRWRA dose= 1.5% by weight of cement.
3. From **Fig 5.1** and **Fig 5.2**, read  $\tau_o$ ,  $\mu$  for target given strength.

4. Calculate correction factors:  $K=k_1k_2$ ,  $K^*=k_1^*k_2^*$  from **Table 5.5** and **Table 5.6**.
5. Corresponding to  $K\tau_o$ , obtain aggregate volume- paste volume ratio from **Fig 5.6** and chosen water-cement ratio. Note down the aggregate volume- paste volume ratio from **Fig 5.7** for  $K\mu$ . Assume quantities of coarse aggregate from **Fig 5.8**, depending on particle shape.
6. Calculate cement and water content.

It may be mentioned that above mix proportion has been arrived at on the assumption that aggregates are saturated and surface dry. For any deviation from this condition, correction has to be applied on quantity of water as well as to the aggregate. The calculated mix proportions shall be checked by means of trial batches. Quantities of material for trial batch shall be enough for at least three 15 cm cubes. A minor adjustment in aggregate quantity may be made to improve the finishing quality or freedom from segregation and bleeding.

#### 5.4. EXAMPLES OF MIX DESIGN OF HPC USING PROPOSED METHOD

**Example 1:**Data: i) Cement: OPC, specific gravity (SG)=3.1, 53 grade as per IS: 12269-1987.

ii) Sand: zone II as per IS: 2386-1963, SG=2.6

iii) Coarse aggregate: crushed, 10 mm msa, SG=2.6

iv) HRWRA: Poly-carboxylic ether polymer, no mineral admixtures.

*To design a mix for target strength=70 MPa.*

- a) Assume air content=3.0 %, PC=1.5% bwc,
- b) From **Fig 5.1** and **Fig 5.2**, obtain values of yield stress and plastic viscosity for 70 MPa as  $\tau_o=310$  Pa;  $\mu=60$  Pa.s.
- c) Calculate  $K\tau_o=1.0 \times 1.0 \times 310= 310$  Pa and  $K^*\mu=1.0 \times 1.0 \times 60= 60$  Pa.s from **Table 5.5** and **Table 5.6**.
- e) Refer **Fig 5.6**, take w/c ratio=0.35;

Aggregate-paste volume ratio at w/c ratio=0.35 and  $K\tau_o=310$  Pa is approximately equal to 1.52.

f) Assume coarse aggregate content=1085 kg/cu.m and sand= 435 kg/cu.m so that sand= 28%.

g) Substitute sand and coarse aggregate content in the following expression:

$$\frac{V_{fine} + V_{coarse}}{V_{cement} + V_{water} + V_{air}} = 1.52$$

The final proportions of the ingredients (kg/cu.m) are as follows:

Cement= 573;

Sand= 435;

Coarse aggregate= 1085 kg/cu.m;

Water= 200.5 kg/cu.m including HRWRA;

HRWRA= 8.6 kg/cu.m

Water/cement ratio=0.35.

With the above mix proportion, rheological test was carried out and compressive strength (cube strength) was determined after 28 days of moist curing. Prior to curing by water, wax based curing compound was used after 2 hours from casting up to 24 hours. The laboratory results were as follows:

$\tau_o = 273$  Pa;  $\mu = 74$  Pa.s; Slump= 170 mm and 28 day cube strength=71.5 MPa.

When **Fig 5.7** is used, corresponding to plastic viscosity  $K^* \mu = 60$  Pa.s and aggregate volume/paste volume ratio=1.52, the value of w/c ratio is approximately 0.40. Therefore, mix proportioning has been done using yield stress criteria (w/c ratio being less). Value of plastic viscosity may be adjusted by trial.

**Example 2:** Data: i) Cement: OPC, SG=3.1, 53 grade as per IS: 12269-1987.

ii) Sand: zone III as per IS: 2386-1963, SG=2.6

iii) Coarse aggregate: crushed, 16 mm msa, SG=2.6

iv) HRWRA: Poly-carboxylic ether polymer, no mineral admixtures.

*To design a mix for target strength=60 MPa.*

As illustrated in example 1 above, estimated yield stress=230 Pa and plastic viscosity=59 Pa.s. Assuming coarse aggregate=1085 kg/cu.m and sand=29%, the final mix proportions are as follows:

Cement= 559;

Sand= 444;

Coarse aggregate= 1085 kg/cu.m;

Water= 200.7 kg/cu.m including HRWRA;

HRWRA= 7.2 kg/cu.m

Water/cement ratio=0.36.

With the above mix proportion, rheological test was carried out and compressive strength (cube strength) was determined after 28 days of moist curing. The laboratory results were as follows:

$\tau_o$  =289 Pa;  $\mu$  =56 Pa.s; Slump= 180 mm and 28 day cube strength=62.6 MPa.

**Example 3:** Data: i) Cement: OPC, SG=3.1, 53 grade as per IS: 12269-1987.

ii) Sand: zone III as per IS: 2386-1963, SG=2.6

iii) Coarse aggregate: crushed, 16 mm msa, SG=2.6

iv) HRWRA: Poly-carboxylic ether polymer, no mineral admixtures.

*To design a mix for target strength=45 MPa.*

Estimated yield stress=110 Pa and plastic viscosity=41 Pa.s. Assuming coarse aggregate=1035 kg/cu.m and sand=33%, the final mix proportions are as follows:

Cement= 545;

Sand= 516;

Coarse aggregate= 1035 kg/cu.m;

Water= 207 kg/cu.m including HRWRA;

HRWRA= 8.2 kg/cu.m

Water/cement ratio=0.38.

With the above mix proportion, rheological test was carried out and compressive strength (cube strength) was determined after 28 days of moist curing. The laboratory results were as follows:

$\tau_o$  =160 Pa;  $\mu$  =49 Pa.s; Slump= 170 mm and 28 day cube strength=46.2 MPa.

## 5.5. CLOSURE

A mix design procedure for HPC has been suggested. The proposed mix design procedure takes rheological parameters in to account to determine compressive strength,

water cement ratio and aggregate volume to paste volume ratio. Instead of using water-cement ratio and compressive strength relationship, relationship between compressive strength, paste volume-aggregate volume ratio, physical properties of aggregates and rheological parameters were used in mix design. Correlation charts for rheological parameters and compressive strength was developed based on cube test results of several trial mixes whose rheological parameters have also been found by the present rheometer. The ranges of Bingham parameters and compressive strength studied in the present investigation are as follows:

Yield stress: 40- 820 Pa;

Plastic viscosity: 15- 120 Pa.s;

Compressive strength (28 day): 40- 90 MPa.

It is always difficult to develop a mix design method that can be used universally because same properties of fresh and hardened concrete can be achieved in different ways from same materials. Since materials from different sources can vary widely in their composition and physical characteristics, a trend drawn from data for a single material source should not be extended to all material sources. Thus, generalization of the trend in concrete rheology and mix design involves complication. In fact, a broad range of data from various sources is desirable for drawing general conclusions. It is not the intention here to provide a mix design method. Rather, the principles on which such a mix design method should be based have been discussed. The method discussed in this chapter is related to calculation of the composition of non-air entrained concrete containing poly-carboxylic ether polymer as HRWRA without incorporating any mineral admixture.

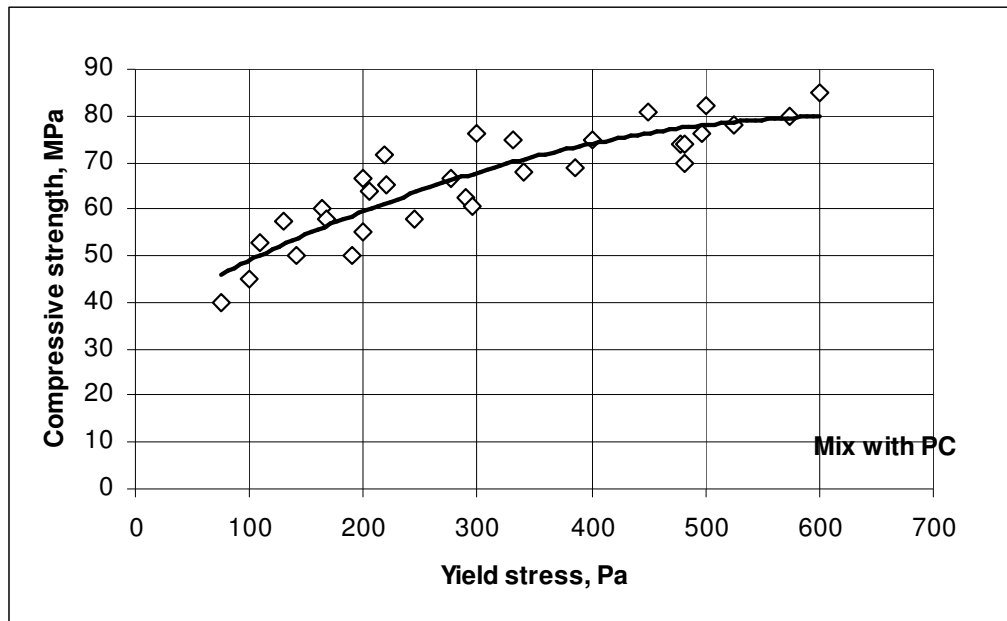


**Fig 5.1.** Variation of compressive strength with yield stress (Mixes with PC)

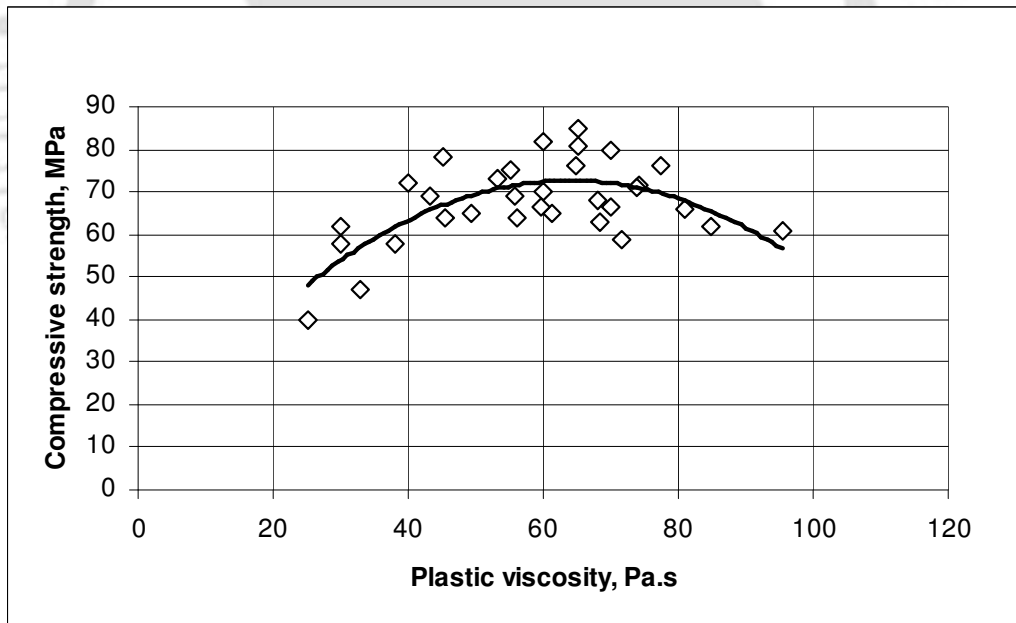


**Fig 5.2.** Variation of compressive strength with plastic viscosity (Mixes with PC)

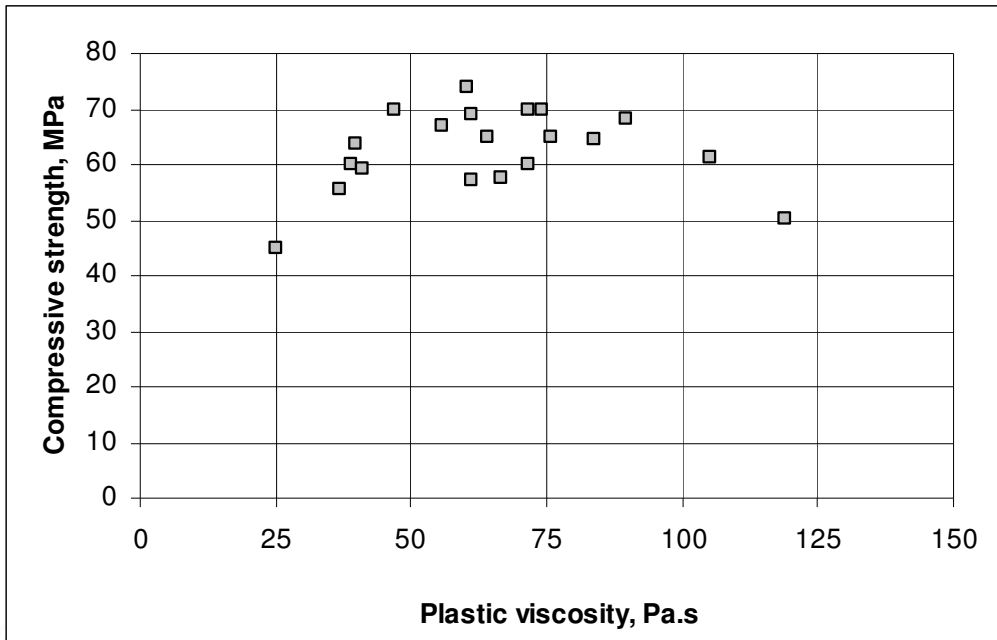


**Fig 5.3** Variation of compressive strength with plastic viscosity (Mixes with SN)

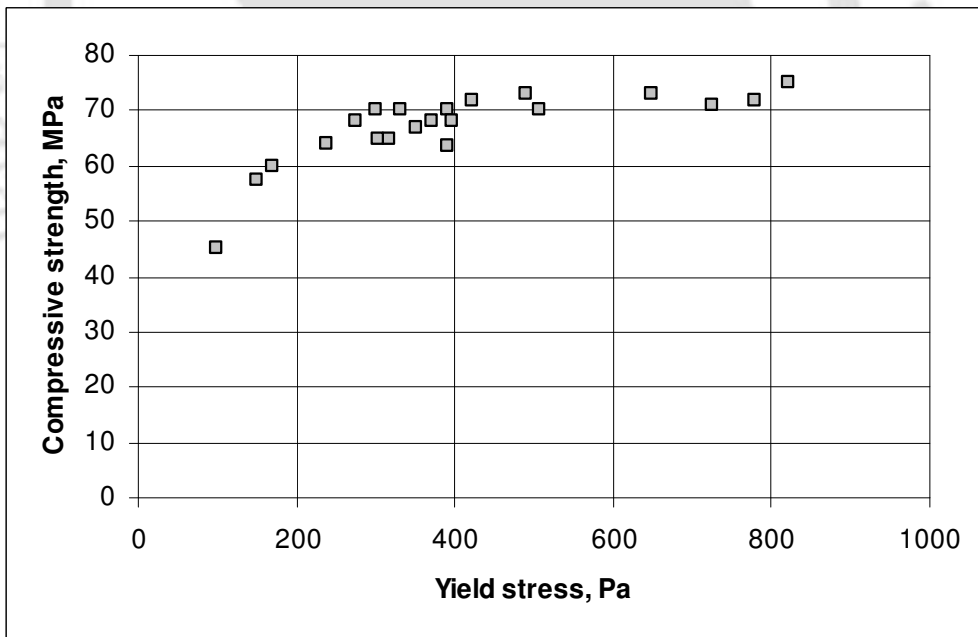


**Fig 5.4.** Variation of compressive strength with yield value (Mixes with SN)

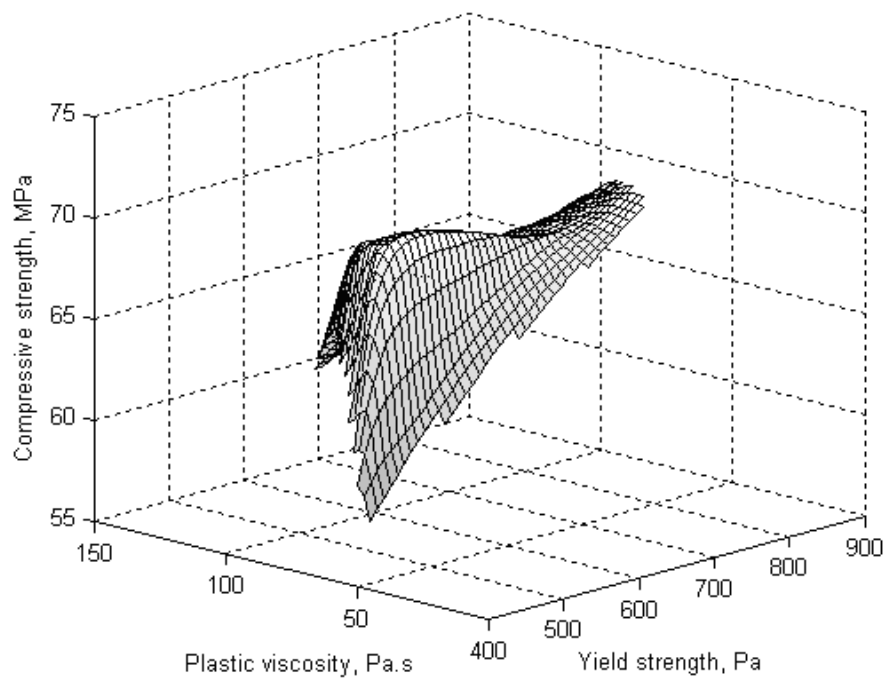


**Fig 5.5.** Variation of compressive strength with rheological parameters (with SN)

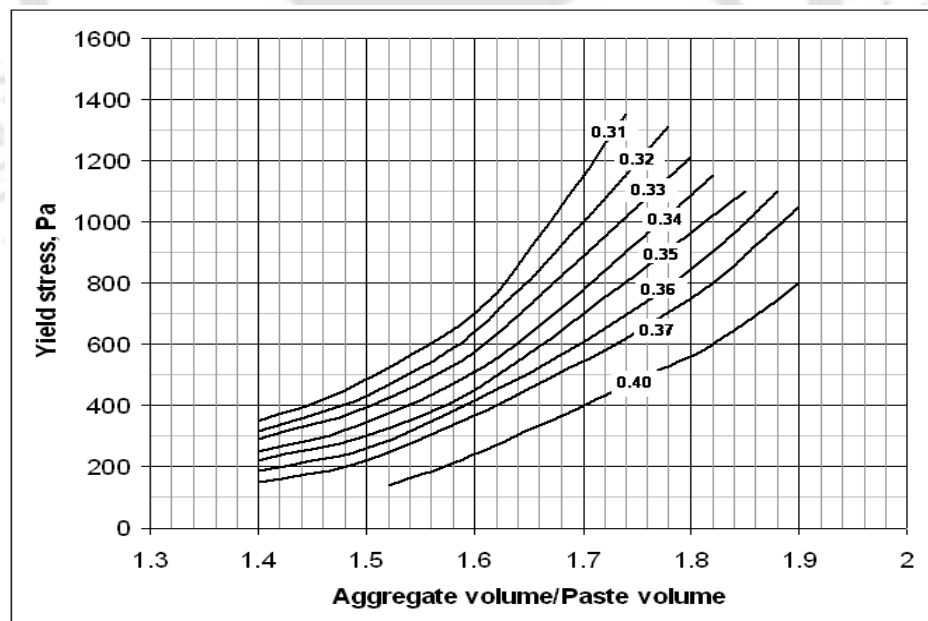


**Fig 5.6** Variation of aggregate volume/paste volume ratio with yield stress

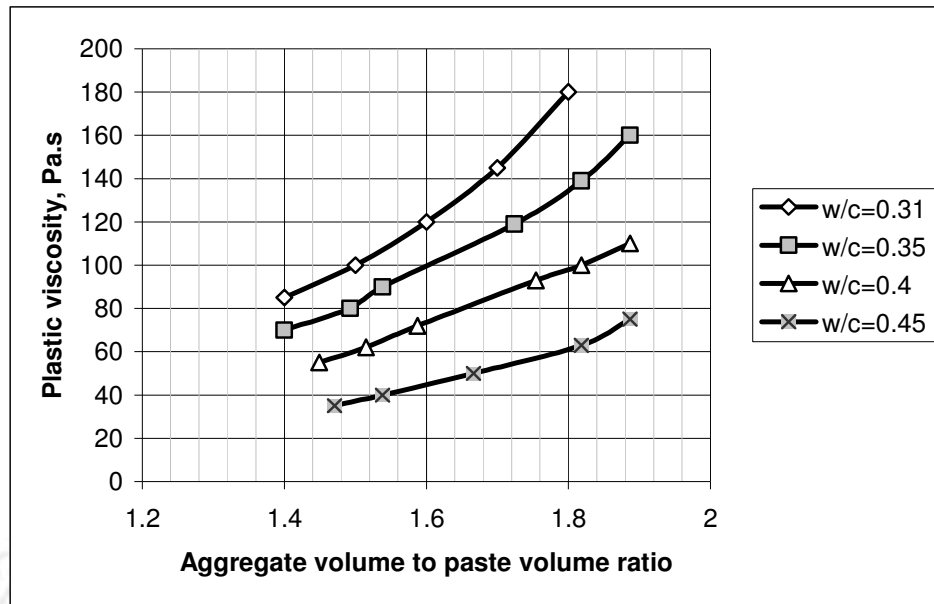


**Fig 5.7** Variation of aggregate volume/paste volume ratio with plastic viscosity

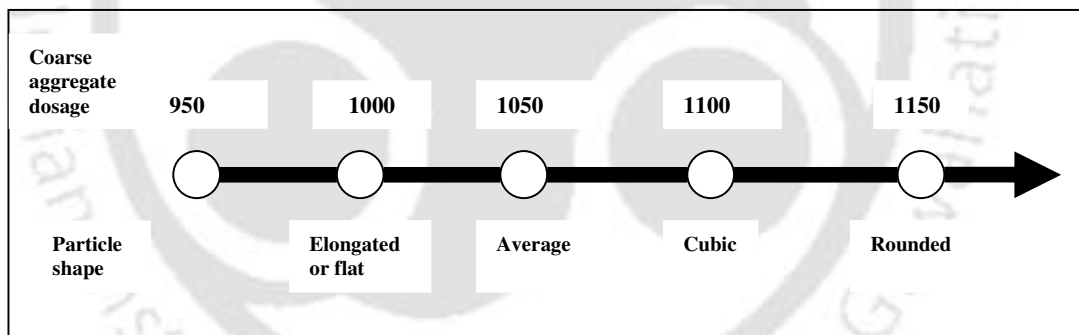


**Fig 5.8** Coarse aggregate content [Aitcin, 1998]

**Table 5.3:** Mixtures containing PC as HRWRA (Quantities in kg/cu.m)

Sl no.	Cement	Sand	Coarse aggregate	Water	HRWRA	28day strength,MPa	Remarks
1	471	460	1125	200.6	7.5	40	
2	487	709	946	179	6.8	62.6	
3	514	452	1105	197	7.4	45	
4	559	444	1085	193.5	7.7	80	
5	596	437	1068	190.5	7.1	85	
6	563	448	1095	186	7.3	81	
7	531	516	1033	196	7.4	75	
8	506	400	1206	186.5	7.1	64	
9	507	515	1094	187	7.1	67	
10	508	626	987	187	7.1	79	Zone 1 sand
11	508	626	987	187	7.1	74	Zone 2 sand
12	508	626	987	192	2.5	70	
13	508	626	987	182	12.7	76	
14	559	536	996	194	7.2	75	
15	549	655	901	190	7.1	68	
16	562	447	1093	195	7.3	74	Zone 2 sand
17	571	436	1083	193	7.2	72	Zone 2 sand
18	563	447	1093	195	7.3	66.4	CA passing 12.5mm
19	563	447	1093	195	7.3	63.1	CA passing 10mm
20	563	447	1093	195	7.3	66.5	CA: 16mm- 12.5mm
21	563	447	1093	195	7.3	60.8	CA: 12.5mm- 10 mm
22	508	626	987	187	7.1	66	CA passing 12.5mm
23	508	626	987	187	7.1	58	CA passing 10mm

(CA means coarse aggregate)



**Table 5.5:** Correction factors for  $\tau_o$  [Msa means maximum size of coarse aggregate]

Particulars	Yield stress
Sand zone II (Medium)	$k_1=1$
Sand zone I (Coarse)	$k_1=1.45$
Zone III (Fine)	$k_1=1.6$
Msa= 10 mm	$k_2=1$
Msa= 12.5 mm	$k_2=0.9$
Msa= 16 mm	$k_2=0.67$
Total:	<b><math>K= k_1, k_2</math></b>

**Table 5.6:** Correction factors for  $\mu$  [Msa means maximum size of coarse aggregate]

Particulars	Plastic viscosity
Sand zone II (Medium)	$k_1^*=1$
Sand zone I (Coarse)	$k_1^*=2.0$
Zone III (Fine)	$k_1^*=2.2$
Msa= 10 mm	$k_2^*=1$
Msa= 12.5 mm	$k_2^*=0.75$
Msa= 16 mm	$k_2^*=0.7$
Total:	<b><math>K^* = k_1^* .k_2^*</math></b>

## CHAPTER 6

### CHARACTERIZATION OF WORKABILITY OF HIGH PERFORMANCE CONCRETE

#### 6.1 INTRODUCTION

Monitoring of workability is a critical issue since high performance concrete is susceptible to small changes in mixture proportions that have a direct impact on hardened properties. Conventional workability tests are all empirical nature and are inadequate to characterize workability in a quantitative manner. These tests attempt to simulate a certain field placement condition and measure the distance or time that serves as an index of workability.

In the present chapter, method for quantitative characterization of workability of fresh HPC using the rheological parameters has been presented. Attempt has been made to correlate this quantitative scale to the various classes of workability such as medium, high and very high workability as determined by slump test.

#### 6.2 EXPERIMENTAL PROGRAM

For the purpose of workability characterization, HPC mixes with different combinations of the constituent materials were prepared for rheological testing. The mixes are presented in **Table 6.1** and **Table 6.2**.

Slump test was performed in a standard manner for each mix in addition to rheological tests. The reason for choosing slump test for characterizing workability is that slump test is the most widely accepted test of workability used by the engineers at sites. Secondly, recent research indicated that yield stress showed the same trend of the slump in concrete and plastic viscosity was associated with stickiness, placeability, pumpability, mixing, segregation and finishability of concrete. **Fig 1.1** and **Fig 1.2** of Chapter 1 show the relationship between rheology and workability of fresh concrete.

**Table 6.1:** Mixtures containing PC as HRWRA (Quantities in kg/cu.m)

Sl no.	Cement	Sand	Coarse aggregate	Water	HRWRA	Remarks
1	386	860	868	155	7.0	
2	445	673	953	179	8.0	
3	514	452	1105	197	7.4	
4	439	798	805	189	6.0	
5	596	437	1068	190.5	7.1	
6	563	448	1095	186	7.3	
7	531	516	1033	196	7.4	
8	506	400	1206	186.5	7.1	
9	507	515	1094	187	7.1	
10	445	809	815	178	8.0	
11	455	827	834	165	7.1	
12	508	626	987	192	2.5	
13	508	626	987	182	12.7	
14	559	536	996	194	7.2	
15	549	655	901	190	7.1	
16	504	756	763	202	6	
17	571	436	1083	193	7.2	
18	563	447	1093	195	7.3	CA passing 12.5mm
19	563	447	1093	195	7.3	CA passing 10mm
20	563	447	1093	195	7.3	CA: 16mm-12.5mm
21	563	447	1093	195	7.3	CA: 12.5mm- 10 mm
22	508	626	987	187	7.1	CA passing 12.5mm
23	508	626	987	187	7.1	CA passing 10mm
24	479	927	816	167	9.6	
25	412	868	932	185	6.2	
26	443	883	951	160	8.9	
28	492	949	835	170	7.4	
29	400	882	948	188	6.5	
30	438	851	917	175	8.0	

(CA means coarse aggregate)

**Table 6.2:** Mixtures containing SN as HRWRA (Quantities in kg/cu.m)

Sl no.	Cement	Sand	Coarse aggregate	Water	HRWRA	Remarks
1	460	780	1080	170	7.0	
2	490	576	1141	181	8.3	
3	485	662	1143	171	8.2	
4	416	834	898	197	8.3	
5	510	492	1118	182	5.1	
6	451	820	827	170	13	
7	505	491	1114	176.3	10.1	
8	495	657	998	168	8	
9	547	484	1099	174	10	
10	511	495	1124	171	10.2	
11	425	680	1033	178	4.3	
12	510	492	1118	174	12.7	
13	506	490	1112	183	7.1	
14	425	680	1033	174	8.3	CA passing 10mm
15	506	400	1208	176	10.1	
16	420	673	1019	179	8.2	
17	508	565	1048	177	10.8	
18	426	681	1034	167	8.3	
19	500	608	1068	178	7.5	
20	564	582	1100	168	11.3	
21	413	869	934	186	8.3	
22	407	857	922	183	8.1	
23	507	492	1118	177	10.1	CA : 16-12.5mm
24	390	819	881	175	7.8	

(CA means coarse aggregate)

The cement used throughout the experiment was Ordinary Portland Cement (OPC). The 28 day compressive strength and specific gravity of cement were  $50.2 \text{ N/mm}^2$  and 3.10 respectively. Locally alluvial sand (medium; specific gravity=2.6) inside the laboratory was used throughout the experimental investigation. Crushed stone aggregates (specific gravity=2.6) of nominal maximum size 16 mm were used as coarse aggregate. Ordinary tap water was used for all the mixes to prepare fresh concrete. Poly-Carboxylic Polymer

(PC) with set retarding effect was used as high range water reducing admixtures (HRWRA).

### 6.3 RESULTS AND DISCUSSION

The problem of assessing workability with rheological parameters is that it is difficult to define ranges of yield stress and plastic viscosity that produces good workability. The concept of rheology box as suggested by Tattersall [1991] was implemented in the present study. For this purpose, yield stresses were plotted against plastic viscosity values [Fig 6.1]. Keeping in mind the minimum recommended slump as 100 mm for HPC [Nawy, 2001], the workability were categorized for the present study as follows:

<i>50 mm &lt; slump &lt; 100 mm:</i>	<i>Medium workability</i>
<i>100 mm &lt; slump &lt; 200 mm:</i>	<i>High workability</i>
<i>Slump &gt; 200 mm:</i>	<i>Very high workability.</i>

It may be observed from Fig 6.1 that it is possible to draw a rectangle around a zone of rheological parameters of particular workability category based on slump values. It may also be observed from Fig 6.1 that the box for 'high workability' might include some 'medium' and 'very high workability' mixes. Similarly, some 'high workability' mixes might also be omitted. However, an approximate ranges of yield stress ( $\tau_o$ ) and plastic viscosity ( $\mu$ ) may be obtained for each class of workability from the rheology boxes which is as follows:

*High workability:  $200 Pa < \tau_o < 600 Pa$  and  $35 Pa.s < \mu < 70 Pa.s$ ;*

*Very high workability:  $\tau_o < 200 Pa$  and  $10 Pa.s < \mu < 40 Pa.s$ ;*

*Medium workability:  $\tau_o > 600 Pa$  and  $\mu > 70 Pa.s$ .*

It would be possible to combine rheology boxes for variety of criteria to improve and refine the ranges of rheological parameters. The use of rheology box is appealing because of its simplicity. However, engineers have a good sense of how concrete with certain

slump value should appear but they lack in practical idea of what a concrete with certain yield stress and plastic viscosity should look like. Moreover, appropriate range of yield stress and plastic viscosity need to be defined for specific use at construction site.

Characterization of workability is further complicated by the fact that different stages of workability such as mixing, transporting, compacting, and placing are all independent operations and there is no single stage available to combine the performances collectively. Effort required to manipulate fresh concrete in each stage of workability is dependent on the rheological properties in addition to shear rates. In other words, work done in each operation is influenced by yield stress, plastic viscosity and shear rate. Shear rate again is not same in different stages or operations. Maximum rate applied to concrete in mixer has been reported to be 10-60 per sec whereas rates for pumping and casting are estimated as 20-40 per sec and 10 per sec respectively [Roussel, 2006]. In case of mixing truck, shear rate is reported to be 10 per sec [Roussel, 2006]. Thus, complete characterization of workability requires knowledge of yield stress, plastic viscosity and shear rate. It is known that huge amount of energy is dissipated during viscous flow. In the present study, all the three parameters mentioned were combined to develop a single scale in terms of energy dissipation rate. Energy dissipation rate per unit volume for viscous flow is given by the following expression [Banfill, 1991]

$$\dot{E} = (\tau_o + \mu\dot{\nu})\dot{\nu} \quad (6.1)$$

where,  $\dot{E}$  is the energy dissipation rate per unit volume,  $\dot{\nu}$  is shear strain rate. Assuming that concrete flows at steady state at constant shear rate,  $\dot{E}$  values may be calculated for various shear stresses (combining yield stress and plastic viscosity) at different  $\dot{\nu}$  and the results may be presented as shown in **Fig 6.2**.

Corresponding to highest and lowest co-ordinates of each rheology box,  $\dot{E}$  values were calculated for a particular strain rate. Calculated  $\dot{E}$  for upper limit of “very high” class slightly overlaps with lower limit of “high” class of workability and the average was reported as boundary of two boxes. Thus, for different shear rates, upper and lower limits of different categories of workability were obtained. The results are shown in **Fig 6.3**. Points connecting upper and lower limits divide different categories of workability into different zones. It may be observed that for a given value of energy dissipation rate, a concrete may fall into the category of medium, high and very high workability depending

on shear strain. Hence, it may be emphasized that in addition to rheological parameters such as yield stress and plastic viscosity, shear rate plays a very critical role in workability characterization of high performance concrete.

Additional works are required to further divide this scale into narrow divisions such as low, medium, high, very high, and flowing. Extensive work can address the shortcomings to facilitate the application of rheological parameters to characterize workability of HPC.

#### **6.4 CLOSURE**

Rheological parameters were determined using the new parallel plate rheometer for high performance concrete mixtures containing poly-carboxylic polymer as HRWRA. Slump tests were performed for each individual mixes and rheology boxes were constructed based on slump values to categorize the workability. Upper and lower limits of rheology boxes were used to construct a power based scale of workability of HPC. This scale combines three parameters namely yield stress, plastic viscosity and shear strain rate into a single parameter. It is possible to assess the workability category with this new scale of energy dissipation rate of concrete flow. Also, shear rate plays a critical role in workability characterization of high performance concrete in addition to yield stress and plastic viscosity.

Since materials from different sources can vary widely in their composition and physical characteristics, a trend drawn from data for a single material source should not be extended to all material sources. Thus, generalization of the trend in concrete rheology involves complication. In fact, a broad range of data from various sources is desirable for drawing general conclusions.

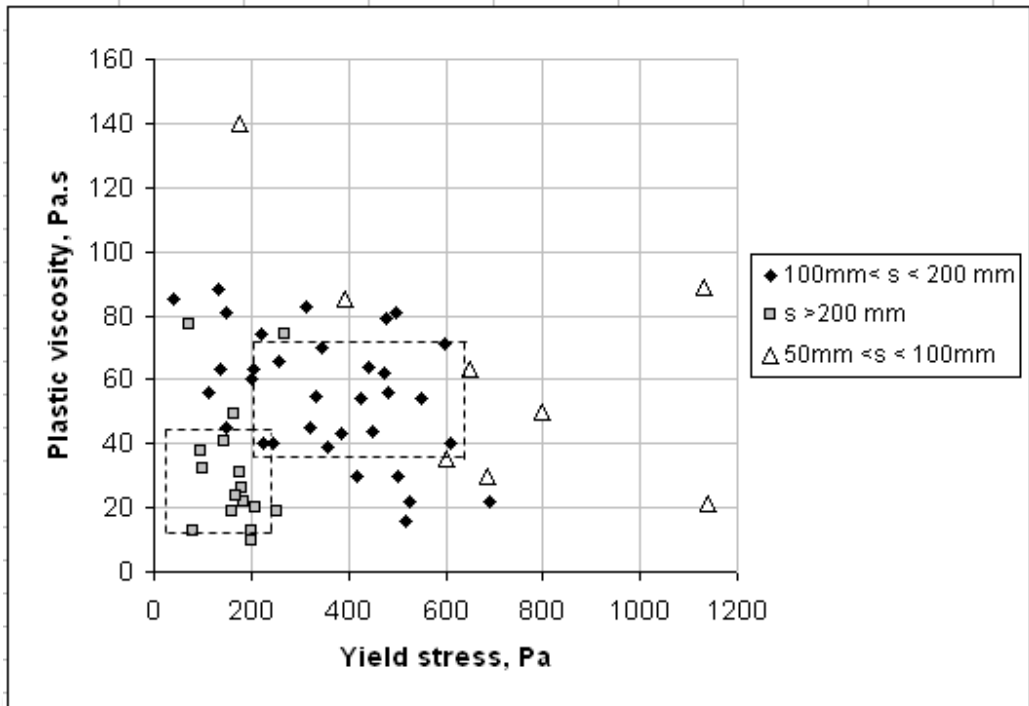


Fig 6.1 Construction of rheology box

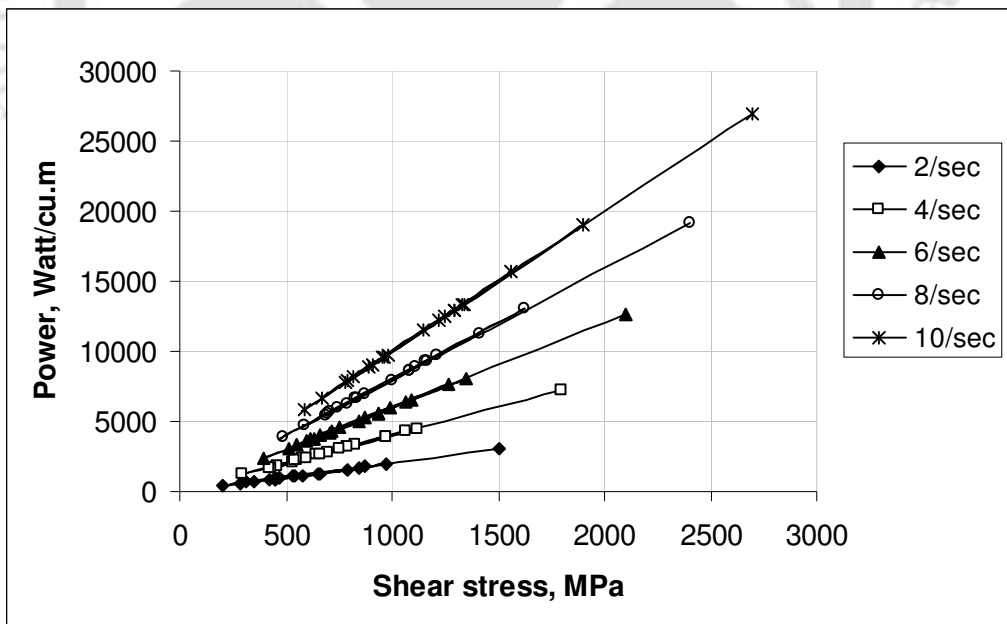
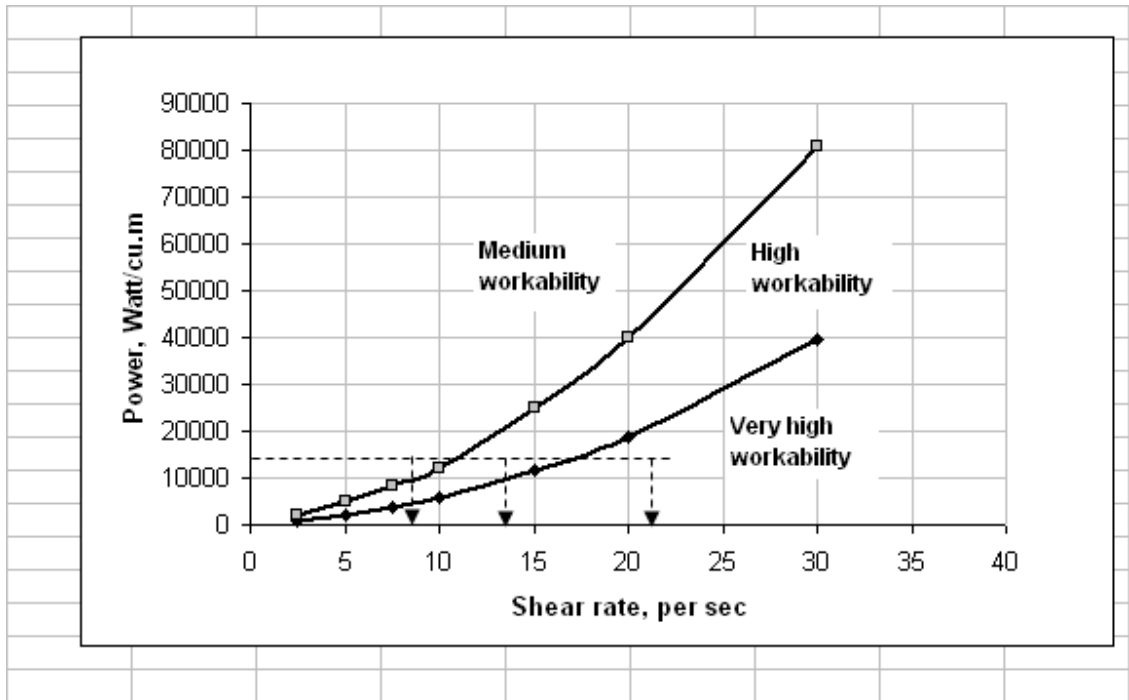


Fig 6.2 Power/cu.m versus shear stress at various shear rates



**Fig 6.3** Workability Characterization in terms of rheological parameters

## **CHAPTER 7**

### **SUMMARY AND CONCLUSIONS**

#### **7.1 SUMMARY OF INVESTIGATIONS**

In the present study, a parallel plate rheometer for concrete has been designed and fabricated. The present rheometer is a stress controlled rheometer that is capable of obtaining data that can be further used to draw flow curve. Rheometer was constructed with a vane plate of 150 mm diameter that is placed at the centre of 270 mm effective diameter cylindrical container where concrete is placed. Measures were taken to prevent wall slip. The rheometer is operated by varying input voltage with an AC variac and the speed of impeller is recorded with a non-contact laser tachometer. Calibration of torque was done by rotor blocking method.

In the present equipment, resistance offered by vertical wall of cylindrical container to concrete has been taken into consideration to represent actual flow condition of concrete during shearing. An expression for total shear stress has been derived from where shear stress versus torque and overall shear strain rate versus rotational frequency relationships have been established for the given geometry of the rheometer. A magneto-rheological fluid has been tested with the present rheometer and the results have been compared with the test results obtained by HAAKE RS1 rheometer to validate the present equipment. Repeatability tests were conducted with different concrete mixes and results were found to be reasonable.

After developing and validating the equipment, further studies have been undertaken to examine rheological behavior of High-Performance Concrete. The study incorporates concrete without mineral admixtures and with mineral admixtures. Condensed Silica Fume (CSF), Pozzolanic Fly Ash (PFA) and Rice Husk Ash (RHA) have been used. Experiments were also conducted to examine rheological behavior of steel fiber reinforced concrete. Conventional workability tests have been also conducted to find correlation between rheological parameters and workability test results. Attempts have also been made to correlate 28 days cube strength with rheological parameters. Finally, a procedure for mix design of high performance concrete has been outlined based on rheological parameters. Following the proposed method, proportions have been worked

out for three different mixes (Target strengths 45, 60 and 70 MPa). The strength has been verified from cube test results after 28 days of curing.

## 7.2 MAJOR FINDINGS

Some major findings from the present study are given below:

- Contribution of friction between concrete and side of the wall has been found to be significant in evaluating yield stress and plastic viscosity of fresh concrete. Neglecting such effect causes lower estimate of these parameters.
- Coarse and fine aggregate gradation and size have significant influence on yield stress and plastic viscosity. Optimum values exist for percentage sand, mean sand size, and HRWRA dosage. It was observed that in addition to water cement ratio, ratio of cement paste volume to aggregate volume affect yield stress and plastic viscosity significantly.
- Good correlation between yield stress and slump, yield stress and slump flow was observed in high performance concrete. Yield stress decreases linearly as either slump or slump flow increases.
- A relationship also exists between plastic viscosity and slump, plastic viscosity and slump flow, plastic viscosity and slump time. The optimum plastic viscosity is 60- 80 Pa.s for maximum slump, maximum slump flow and maximum slump time. No correlation exists between yield stress and slump flow time for the concrete studied.
- Optimum value of condensed silica fume (CSF) replacing cement has been found to exist for minimum yield stress and maximum plastic viscosity. However, the optimum values for yield stress and plastic viscosity are not necessarily the same. In concrete mix with SN as high range water reducer, yield stress is found to increase continuously.
- There is a decrease in yield stress and plastic viscosity of concrete when PFA replaces cement. Yield stress, however, slightly increases at higher replacement levels up to high volume level. The change in plastic viscosity is found to be insignificant.

- Experimental study using Rice Husk Ash (RHA) reveals that yield stress decreases due to increase in RHA replacement level. Plastic viscosity increases very steeply and the percentage increase in plastic viscosity is the highest among all the additives
- For two-component binder system such as cement-RHA, cement-CSF, cement-PFA, RHA gives the lowest value of yield stress whereas CSF produces concrete with the highest value of yield stress. When low value of plastic viscosity is under consideration, PFA shows the best effect while RHA shows the worst rheological performance of concrete.
- In case of ternary blends with equal masses, rheological properties are found to be lower compared to those of single mineral additives. CSF-RHA is found to yield the most suitable rheological performance with moderate plastic viscosity and low yield stress.
- Yield stress and plastic viscosity increase with the increase in fiber volume concentration. In some cases, rheological parameters may also decrease at low fiber volume concentration that can be explained with the coupling phenomena between improved packing density and mechanical interlocking. Mechanical interlocking dominates at higher volume concentrations. Only low and medium volume fraction of fibers was investigated because high volume fraction FRC is not workable and may not follow Bingham's equation.
- Rheological parameters increase with increasing fiber aspect ratio. The effect of this parameter on plastic viscosity is less significant. The change in yield stress at low aspect ratio and ratio greater than 100 is also less.
- The effect of fiber diameter on rheological parameters is less pronounced over the range of diameters studied. Among all the three fiber parameters investigated, volume fraction has the highest impact on the rheological behavior and diameter has the least.
- Vebe and flow tests results on FRC have been used to investigate the relationship between these tests results and rheological parameters. It was concluded that flow test may be a better test for FRC compared to Vebe test as it is found sensitive over all ranges of workability of concrete.

- Quantitative characterization of workability of fresh HPC has been outlined using rheological parameters. The quantitative scale has been correlated to the various classes of workability such as medium, high and very high workability as determined by slump test.
- Rheology box was used based on slump values to categorize the workability. Upper and lower limits of rheology boxes were utilized to construct a power based scale of workability of HPC. This scale combines three parameters namely yield stress, plastic viscosity and shear strain rate into a single parameter. It is possible to assess the workability category with this new scale of energy dissipation rate of concrete flow.
- Shear rate plays a critical role in workability characterization of high performance concrete in addition to yield stress and plastic viscosity.
- Rheological parameters have been used to outline a mix design procedure of HPC. Dependence of compressive strength on yield stress and plastic viscosity was studied. Study reveals that with the increase in yield stress, the compressive strength increases with non uniform rate. Compressive strength also increases up to certain level of plastic viscosity.
- It is found that superplasticizer type plays an important role in displaying the variation of compressive strength with yield stress and plastic viscosity. However, two types of superplasticizer viz. SN and PC shows an overlapping zone of plastic viscosity to attain the maximum compressive strength whereas compressive strength is the highest for larger yield stress in mixtures contain SN compared to the mixtures containing PC.
- From various experimental results, chart for finding aggregate volume to paste volume ratio corresponding to yield stress and plastic viscosity has been prepared for various water cement ratio. This was used to find cement content in the mix which avoids the water-cement ratio versus compressing strength relationship as used in design of conventional and high strength concrete mix.
- Correction factors to be used in yield stress and plastic viscosity for different sand zone and maximum size of aggregate have been suggested for working out the mix proportions.

- The mix design procedure is valid for yields stress value 40-820 Pa, Plastic viscosity 15-120 Pa.s and compressive strength 40-90 MPa.
- Laboratory trials have been given for three mixes of target strength 45 MPa, 60 MPa and 70 MPa and found successful with the worked out proportions adopting proposed method.

### **7.3. SCOPE FOR FUTURE WORK**

Additional work is needed in the following areas:

- To develop an automated version of the present rheometer. This can be done by including torque sensor, speed sensor, data acquisition system and software for computer interfacing.
- To conduct additional testing to supplement the findings of blended mineral admixtures. This will include blending of admixtures of varying proportions to arrive at appropriate ternary blend for minimum yield stress and moderate plastic viscosity.
- To develop a connection between workability and rheology and to develop guidelines for the use of rheology in concrete industry.
- Additional work can be done to correlate compressive strength and other hardened properties such as split tensile strength and flexural strength with rheological parameters for high strength, very high strength and ultra high strength concrete.
- Extensive experimental investigation can be carried out covering wide range of constituent materials for proper mix design method of concrete using rheological parameters for given target strength, incorporating supplementary cementitious materials, ternary blends and various super-plasticizers.

### **7.4. CONCLUDING REMARKS**

Concrete rheology presents several unique challenges due to the nature and composition of concrete. The main problem with properly characterizing the rheology of concrete is the large size of coarse aggregates. While concrete rheometers provide useful new information about workability, the use is very much limited for high equipment cost and

limited availability. Moreover, concrete which do not flow readily without vibration can not be evaluated by rheometer in fresh stage. However, it can be emphasized that for flowable concrete (with slump greater than 100 mm), rheological measurements better represent diverse requirement of workability compared to slump and other single point workability tests.

The prospect of characterizing concrete workability by measuring rheological properties is promising. If properly designed, rheometers are able to characterize the scientific flow properties of concrete. Despite the drawbacks, concrete rheometers provide important information about concrete flow properties. Additional development work can address these problems and further facilitate the application of fluid rheology to the fresh concrete.



## REFERENCES

- ACI 544 (1993): Guide for Specifying, Proportioning, Mixing, Placing, and Finishing Steel Fiber Reinforced Concrete, ACI Committee 544, ACI Materials Journal, Vol. 90, No. 1, Jan.-Feb. 1993, pp. 94-101.
- ACI 363 R-92 (1993). State-of- the art report on high strength concrete, ACI manual of concrete practice, part-I, American Concrete Institute.
- Ando T, Sakai H, Takahashi K, Hoshjima T, Awata M, Oka S. (1990). Fabrication and properties for a new carbon fibre reinforced cement product, Thin-Section Fiber Reinforced Concrete and Ferrocement, American Concrete Institute Special Publication SP-124, pp. 39-60.
- Aitcin PC (1998). High Performance Concrete, E & FN Spon, London.
- Bager DH, Geiker MR, Jensen RM (2001). Rheology of Self Compacting Mortars: Influence of Particle Grading, Nordic Concrete Research, 25.
- Bhattacharya SK (1990). Electrical Machines, Tata McGraw Hill Publishing Company Limited, New Delhi.
- Banfill PFG (1994). Rheological methods for assessing the flow properties of mortar and related materials, Construction and Building Materials, 8(1), 43-50.
- Banfill PFG (1991). Rheology of fresh cement and concrete, F & EN Spon, London.
- Banfill PFG, Saunders DC (1981). On the viscometric examination of cement paste, Cement and Concrete Research, 11, 363-370.
- Banfill PFG (2003). The Rheology of fresh cement and concrete-A review. Proceeding of 11<sup>th</sup> International Cement Chemistry Congress, Durban.
- Banfill PFG., (1990). The rheology of cement paste: Progress since 1973, Properties of fresh concrete, RILEM Proceeding, NY, 3-9.
- Banfill PFG (1982). An experimental study of the effect of pfa on the rheology of fresh concrete and cement paste, Proc International on the use of pfa in concrete, Leeds, 161-172.
- Barnes HA (1989). Shear thickening in suspensions of non-aggregating solid particles dispersed in Newtonian fluids, Journal of Rheology, 33(2), 329-366.
- Barnes, HA.(2000), A handbook of elementary rheology, Institute of Non-Newtonian Fluid Mechanics, University of Wales.

- Barnes HA., Hutton JF, Walters K. (1989). An Introduction to Rheology, New York: Elsevier.
- Beaupre D. (1994), Rheology of High Performance Shotcrete, PhD Tesis, University of British Columbia.
- Billberg P, Petersson O, and Norberg, J. (1996). New Generation of Superplasticizers, P.J.M.
- Brady JF, Bossis, G (1985). The rheology of concentrated suspension of spheres in simple shear flow by numerical simulation, Journal of Fluid Mechanics, 155, 105-129.
- Bui VK, Geiker MR, Shah SP (2003). Rheology of fibre reinforced cementitious materials, RILEM Pro 30, 4<sup>th</sup> International RILEM workshop on high performance fibre reinforced cement composites, Ann Arbor, USA, 221-231.
- Browne R, Bamforth P, (1977). Tests to establish concrete pumpability, ACI Materials Journal, 74(7), 4-19.
- Brown, RA. (1991). Fluid mechanics of the atmosphere, Academic Press Inc.
- Chapra SC, Canale RC(2002). Numerical Methods for Engineers, 4<sup>th</sup> Edition, Tata McGraw Hill Publishing Company, New Delhi.
- Chang PK, Peng, YN (2001). Influence of mixing techniques on properties of high performance concrete, Cement and Concrete Research, 31, 87-95.
- Chhabra RP, (1993). Bubbles, drops and particles in non-Newtonian fluids, C R C Press, Boca Raton, FL, p280.
- Christensen (1991). Modeling of Flow Properties of Fresh Concrete: The Slump Test, Ph.D. Thesis, Princeton University.
- Cyr M, Legrand C, Mouret M (2000). Study of shear thickening effect of super plasticizer on the Rheological behaviour of cement paste containing or not mineral additives, Cement and Concrete Research, 30, 1477-1483.
- Daczko, JA (2003). Stability of SCC-assumed or ensured? Proc 1<sup>st</sup> North American Conf on the design and use of SCC, Chicago, IL.
- de Larrard F, Sztikar JC, Hu C, Joly M (1996) et al, Evolution of the workability of superplasticized concrete: assessment with the BTRHEOM rheometer, RILEM

International Conference on Production methods and workability of concrete, RILEM Pro32, Glasgow, pp. 377-388.

de Larrard F (1999). Why Rheology Matters, Concrete International, 21(8), 79-81.

de Larrard F, Hu C, Sedran T, Sztikar JC, Joly M, Claux F, Derkx F.(1997). A New Rheometer for Soft-to-Fluid Fresh Concrete, ACI Materials Journal, 94(3), 234-243.

de Larrard F (1999). Concrete mixture proportioning, a scientific approach, E & FN Spon, New York.

Domone PLJ, Yongmo X, Banfill PFG (1999), Development of the two-point workability test for High Performance Concrete, Mag Con Res, 51(3), 171-179.

Diamond S, (1976). Cement paste microstructure- an overview of several levels, Proc Hydraulic cement paste: their structure and properties, CCA, Sheffield, 2-30.

Edgington J, Hannant DJ, Williams RIT. (1978): Steel fibre reinforced concrete, Fibre reinforced materials, The Construction Press, Lancaster, England, pp. 112-128.

Ellis C. (1982). The application of two-point workability and BS Tests to OPC/PFA concrete, Proc International on the use of pfa in concrete, Leeds, 121-131.

Esping O. (2003). Methods for characterization of fillers and fines for SCC, 3<sup>rd</sup> International Symposium on SCC, RILEM, Iceland, 208-219.

Faroug F, Szwabowski J, Wild S. (1999). Influence of Superplasticizers on Workability of Concrete, ASCE Journal of Materials in Civil Engineering, 11(2), 151-157.

Ferraris CF. (1999). Measurement of the Rheological Properties of High Performance Concrete: State of the Art Report, Journal of Research of the National Institute of Standards and Technology, 104(5), 461-478.

Ferraris CF. (1996), Measurement of rheological properties of High Performance Concrete: State of the art report, NIST Internal Report 5869.

Ferraris CF, de Larrard F. (1998), Testing and modeling of fresh concrete rheology, NIST Internal Report 6094.

Ferraris CF, Brower LE (Eds.). (2001). Comparison of concrete rheometers: International tests at LCPC (Nantes, France) in October 2000. (NIST IR 6819). Gaithersburg, MD: National Institute of Standards and Technology.

Ferraris CF, Browner LE. (Ed). (2004). Comparison of concrete rheometers: International Tests at LCPC, France, NIST Internal Report 7154, USA

Ferraris CF, Lobo C, (1998). Processing of HPC, *Concrete International*, 20(4), 61-64.

Geiker MR, Brandl M, Thrane LN, Nielsen LF. (2002). On the Effect of Coarse Aggregate Fraction and Shape on the Rheological Properties of Self-Consolidating Concrete, *Cement, Concrete, and Aggregates*, 24(1),3-6.

Geiker MR. (2003). On the Effect of Measuring Procedure and coagulation rate on apparent rheological Properties, 3rd International Symposium on Self Compacting Concrete, RILEM, Iceland.

Ghezal A, Khayat K. (2002). Optimizing Self-Consolidating Concrete with Limestone Filler by using Statistical Factorial Design Methods, *ACI Materials Journal*, 99(3), 264-272.

Grunewald S, Walraven JC. (2003). Rheological measurements on self compacting fibre reinforced concrete, 3<sup>rd</sup> International Conference on SCC, RILEM, 49-58.

Grzeszczyk S, Lipowski G. (1997). Effect of content and Particle size distribution of high Calcium fly ash on the rheological properties of cement paste, *Cement and Concrete research*, 27(6), 907-916.

Hackley V, Ferraris CF. (2001). The Use of Nomenclature in Dispersion Science and Technology. (Special Report 960-3). Gaithersburg, MD: National Institute of Standards and Technology.

Hoy CW. (1998): Mixing and Mix Proportioning of Fibre Reinforced Concrete, PhD-thesis, Advanced Concrete and Masonry Centre, University of Paisley.

Ho DWS, Sheinn AMM, Ng CC, Tam CT. (2002). The use of quarry dust for SCC applications, *Cement and Concrete Research*, 32(4), 505-511.

Hobbs DW. (1980). The effect of pfa upon the workability of cement and concrete, *Mag Con Res*, 37(113), 219-226.

Hoffman RL. (1998). Explanations for the cause of shear thickening in concentrated colloidal suspensions, *Journal of Rheology*, 42(1), 111-123.

Holton, JR. (1992). An introduction to dynamic meteorology, Academic Press Inc, California, 1992.

- Hope BB, Rose K. (1990). Statistical Analysis of the Influence of Different Cements on the Water Demand for Constant Slump, H.-J. Wierig, Ed., Properties of Fresh Concrete, Proc of the Coll. RILEM, Chapman and Hall, 179-186.
- Hu C de Larrard F.(1996). The rheology of fresh high performance concrete, Cement and Concrete Research, 26(2), 283-294.
- Hu C. (1995). Rheologie des betons fluides. Etudes et Recherches des Laboratoire des Ponts et Chaussees, OA16, Paris.
- Hu C, deLarrard F, Sedran T, Bonlag C, Bose F, Deflorenne F. (1996). Validation of BTRHEOM, the new rheometer for soft-to-fluid concrete, Materials and Structures, 29(194), 620-631.
- Ivanov Y, Zacharieva S. (1980). Influence of fly ash on rheology of cement paste, Proc 7<sup>th</sup> International Congress on Chemistry of Cement ,Paris, 103-107.
- IS: 2386-1963, Indian Standard Code of Practice for Methods of Test for Aggregate for Concrete, Indian Standard Institution, New Delhi.
- IS: 12269-1987, Indian Standard Specifications for 53 Grade Ordinary Portland Cement, Indian Standard Institution, New Delhi.
- IS: 10262-1982, Indian Standard Recommended Guidelines for Concrete Mix Design, Indian Standard Institution, New Delhi.
- IS: 7320-1974, Indian Standard Recommended Guidelines for slump test, Indian Standard Institution, New Delhi
- Jarney S, Roussel N, Roy RL, Coussot P, (2005). Steady state and transient behavior of fresh cement paste: MRI velocity measurement and simulation, Proc of 2<sup>nd</sup> North American Conf on design and use of SCC and 4<sup>th</sup> International RILEM Symposium of SCC, Chicago.
- JSCE-F503, (1990). Method of Test for Slump Flow of Concrete, Standards of Japan Soc of Civil Engineers.
- Johnston CD. (2001). Fiber-Reinforced Cements and Concretes, Gordon and Breach Science Publishers, Amsterdam, ISBN: 9056996940.
- Kaplan D (2000). Pumping of concrete. LCPC, France.
- Khayat K. (1998). Viscosity-Enhancing Admixtures for Cement-Based Materials—An Overview, Cement and Concrete Composites, 20(2-3), 171-188.

Koehler EP , Fowler DW. (2004). Development of a portable rheometer for fresh portland cement concrete, Report No.ICAR 105-3F International Center for Aggregates Research, The University of Texas at Austin

Koehler EP, Fowler DW. (2003). Summary of Concrete Workability Test Methods, (ICAR Report 105.1). Austin, TX: International Center for Aggregates Research.

Kosmatka SH, Panarese WC. (1994), Design and control of concrete mixtures, Portland Cement Association.

Kong HJ, Bike SG, Li VC. (2006). Effect of strong polyelectrolyte on the rheological properties of concentrated cementitious suspensions, *Cem Con Res*, 2006.

Kuder KG, Ozyurt N, Mu EB, Shah SP. (2007). Rheology of fiber-reinforced cementitious materials, *Cement and Concrete Research*, 37, 191-199.

Kwan AKH, Mora CF (2001). Effect of various shape parameters on packing of aggregate particles, *Magazine of Concrete Research*, 53(2), 91-100.

Leighton D, Acrivos A.(1987). The shear induced migration of particles in concentrated suspensions, *Journal of Fluid Mechanics*, 181, 415-439.

Li Z, Ohkhbo T, Tanigawa Y. (2004). Flow performance of high fluidity concrete, *ASCE Journal of Materials*, 16(6), 588-596.

Lin CC, Segel LA. (1988). Mathematics applied to deterministic problems in the natural science, SIAM, Philadelphia.

Mase, GE. (1970). Theory and problems of continuum mechanics: Schaums Outline series, McGraw Hill Inc.

Mehta PK, Monteiro, PJM. (2006). Concrete: microstructure, properties and materials, 3<sup>rd</sup> edition, Mc-Graw Hill Inc.

Mehta PK, Aitcin PC. (1990). Principles underlying the production of high performance concrete, *Cement, Concrete and Aggregate Journal*, 12(2), 70-78.

Mehta PK, Aitcin PC. (1990). Microstructural basis of selection of materials and mix proportion for high strength concrete, 2<sup>nd</sup> International Sym on High Strength Concrete, American Concrete Institute, Detroit, 265-286.

Mewis J. (1979), Thixotropy- a general review, *Journal of Non-Newtonian Fluid Mechanics*, 6, 1-20.

- Miller I, Freund JE. (1991), Probability and Statistics for Engineers, Prentice Hall of India.
- Mork JH. (1996). A Presentation of the BML Viscometer, P.J.M. Bartos, C.L.
- Mork JH, Gjoerv OE. (1997). Effect of Gypsum-Hemihydrate Ratio in Cement on Rheological Properties of Fresh Concrete, ACI Materials Journal, 94(2), 147-147.
- Morinaga J.(1973). Pumpability of concrete and pumping pressure in pipelines, Fresh Concrete: Important Properties and their measurement, Proc. of RILEM Conf., Leeds 7.3.1-7.3.39
- Murata J.(1984). Flow and Definitions of Fresh Concrete, Materials Construction 17(98) (1984) 117-129
- Narayanan R, Kareem-Palanjian AS. (1982). Factors influencing the workability of steel-fibre reinforced concrete, Concrete, Part 1: Vol.16, No. 10, pp.45-48, Part 2: Vol. 17, No. 2, pp. 43-44.
- Nawy EG. (2000). Reinforced Concrete: A fundamental approach, Prentice Hall Inc., N.J.
- Nawy EG. (2001). Fundamentals of high performance Concrete, John Wiley and Sons, Inc., 2<sup>nd</sup> Edition.
- Nehdi M, Rahman MA. (2004). Estimating rheological properties of cement paste using various rheological models for different test geometry, gap, and surface friction, Cem and Con Res, 34, 1993-2007.
- Neville AM. (March1973), Chairman's Summary, Fresh Concrete: Important properties and their measurement, Proc RILEM Seminar, University of Leeds.
- Neville AM. (2003). Properties of Concrete. ELBS Singapore Edition.
- Nguyen QD, Boger DV. (1985). Direct Yield Stress Measurement with the Vane Method, Journal of Rheology, 29(3), 335-347.
- Panton, RL. (1984). Incompressible flow, John Wiley and Sons, Inc, Singapore.
- Pashias N, Bogera DV, Summers J, Glenister DJ. (1996). A fifty cent rheometer for yield stress measurement, Journal of Rheology, 40(6), 1179-1189.
- Park CK, Noh MH, Park TH. (2005). Rheological properties of cementitious materials containing mineral admixtures, Cem and Con Res, 35, 842-849.
- Punkki J, Golaszewski J, Gjoerv OE, (1996). Workability loss of high strength concrete, ACI Materials Journal, 93, 427-431.

- Petit JY, Khayat KH, Wirquin E, (2006). Coupled effect of time and temperature on variation of yield value of highly flowable micromortars, *Cement and Concrete Research*, 36(5), 832-841.
- Quiroga PN. (2003). The Effect of Aggregate Characteristics on the Performance of Portland Cement Concrete, PhD Dissertation, The University of Texas at Austin, Austin, TX.
- Raynaud JS, Mouchernot P, Baudez JC et al. (2002). Direct determination by nuclear magnetic resonance of the thixotropic and yielding behavior of suspensions, *Journal of Rheology*, 46(3), 709-732.
- Ranganathan R. (1999). *Reliability Analysis and Design of Structures*, Jaico Publishing Company, Bombay.
- Roussel N. (2006), A thixotropy model for fresh fluid concretes: Theory, Validation and Applications, *Cement and Concrete Research*, 36, 1797-1806.
- Ramachandran VS, Beaudoin JJ. (2006). *Handbook of analytical techniques in concrete Science and Technology*, Williams Andrew, Inc, NY,(Indian Edition).
- Shetty MS. (2004). *Concrete Technology*, S. Chand and Company, New Delhi.
- Saak AW, Jennings HM, Shah SP. (2001). The influence of wall slip on yield stress and viscoelastic measurements of cement paste, *Cement and Concrete Research*, 31(2), 205-212.
- Scanlon JA. (1994). ASTM-STP 169C, American Society of Testing and Materials, 49-64.
- Schramm G. (1994). *A Practical Approach to Rheology and Rheometry*. Karlsruhe, Germany: Haake Rheometers.
- Shah SP, Ahmad SH, (1994). *High performance concrete: Properties and application*, McGraw Hill Inc.
- Shi, Y., Matsui, I., and Feng, N. (2002). Effect of compound mineral powders on workability and rheological property of HPC, *Cement and Concrete Research*, 32(1), 71-78.
- Smeplass S. (1994). Applicability of the Bingham Model to High Strength Concrete, P.J.M Bartos, Ed., *Proceedings, Special Concretes: Workability and Mixing*, Paisley, Scotland: RILEM, 145-151.

- Steel RGD, Torrie JH. (1980). Principles and Procedures of Statistics-A Biometrical Approach, McGraw Hill Book Company, NY.
- Sonebi M (2006). Rheological properties of grouts with viscosity modifying agents as diutan gum and welan gum incorporating pulverizing fuel ash, Cement and Concrete Research, 36, 1609-1618.
- Swamy RN. (1975). Fibre reinforcement of cement and concrete, Journal of Materials and Structure, 8(95), 235-254.
- Swamy RN. (1986). Cement replacement materials, Surrey University Press, London.
- Swamy RN. (1975). Fibre reinforcement of cement and concrete, Materials and Structures, Vol. 8, No. 45, pp. 235-254.
- Swamy RN, Mangat PS. (1974): Influence of fibre-aggregate interaction on some properties of steel fibre reinforced concrete, Materials and Structures, Vol. 7, No. 41, pp. 307-314.
- Szecszy RS. (1997). Concrete Rheology, PhD Dissertation, University of Illinois at Urbana-Champaign, Urbana, IL.
- Tanigawa Y, Mori H. (1989) Analytical Study of Deformation of Fresh Concrete, Journal of Engineering Mechanics 115(3), 493-508.
- Tanigawa Y, Mori H, Watanbe HK. (1991). Analytical and Experimental Studies on Casting of Fresh Concrete into Wallforms, Trans Japan Con Inst 13.
- Tattersall GH, Bloomer SJ. (1979), Further development of the two-point test for workability and extension of its range, Mag Con Res, 31(109), 202-210.
- Tattersall GH. (1976), The Workability of concrete, A Viewpoint Publication, Portland Cement Association.
- Tattersall GH. (1991). Workability and Quality Control of Concrete. London: E&FN Spon.
- Tattersall GH, Banfill PFG. (1983). The Rheology of Fresh Concrete. Marshfield, MA: Pitman Publishing.
- Tangtermsirikul S. (2004). Durability and mix design of concrete Sirindhorn International Institute of Technology, Thailand (1st edition).
- Vom Berg W. (1979). Influence of specific surface and concentration of solids upon the flow behavior of cement pastes, Magazine of Concrete Research, 31(109), 211-216.

- Wallewick OH, Gjorv OE. (1990). Development of a coaxial cylinder viscometer for fresh concrete. Properties of fresh concrete, Proceeding of RILEM Colloquium, Chapman and Hall, Hanover, 213-224.
- Wallewick OH, Gjorv OE. (1998). Rheology of fresh concrete. Advances in cement manufacture and use, Eng. Found. Conf., Potosi, MI.
- Wallewick JE. (2003). Rheology of Particle Suspension: Fresh Concrete, Mortar and Cement Paste with various Types of Lignosulfonates, Ph.D. Thesis, The Norwegian University of Science and Technology, Norway.
- Westerholm M, Lagerblad B. (2003). Influence of fines from crushed aggregate on micro mortar rheology, 3<sup>rd</sup> Internatioal Symposium on SCC, RILEM, Iceland, 165-173.
- Whorlow RW. (1992). Rheological Techniques. Chicheser, West Sussex, England: Ellis Horwood Limited.
- Yang G, Spencer BF, Carlson JD, Sain MK. (2002), Large scale MR fluid dampers: modeling and dynamic performance consideration, Engineering Structures, 24 (3), 309-323.
- Zhang M, Malhotra VM. (1996). High performance concrete incorporating rice husk ash as supplementary cementing materials, ACI Materials Journal, 93(6), 629-636.
- Zukoski CF, Struble LJ, (1993). Rheology of cementitious systems, Material Res Society Bulletin, 18, 39-42.

## LIST OF PUBLICATIONS FROM THESIS

### Journals:

1. Laskar AI, Talukdar S. Design of a new rheometer for concrete, **Journal of ASTM International**, American Institute of Physics, Vol. 5, No. 1, 2008.
2. Laskar AI, Talukdar S. Rheological behavior of high-performance concrete with mineral admixtures and their blending, **Construction and Building Materials, Elsevier**, 22 (2008) 2345-2354.
3. Laskar AI, Talukdar S. A new mix design method of high-performance concrete, **Asian Journal of Civil Engineering**, Vol. 9, No. 1, pp 31-39, 2008.
4. Laskar AI, Talukdar S. Rheology of steel fiber reinforced concrete, **Asian Journal of Civil Engineering**, Vol. 9, No. 1, pp 1-11, 2008.
5. Laskar AI, Talukdar S. Correlation between compressive strength and rheological parameters of high-performance concrete, **Research Letters in Materials Science**, Vol. 2007, article ID 45869.
6. Laskar AI, Talukdar S. Correlating slump, slump flow, Vebe, and flow test to rheological properties of high-performance concrete, **Construction and Building Materials, Elsevier**, 2008 (under review).
7. Laskar AI, Talukdar S. Rheology based approach for workability characterization of high-performance concrete, **Canadian Journal of Civil Engineering**, 2008 (under review).

### Conference Proceedings:

1. Laskar AI, Talukdar S. Is water-cement ratio a fundamental property of fresh concrete rheology?, **Proc of International Conf on Recent Developments in Structural Engineering**, Manipal, India, pp 707-715, 2007.
2. Laskar AI, S Talukdar. Rheological Behavior of High-Performance Concrete with Rice Husk Ash, **8th International Symposium on Utilization of High-Strength and High-Performance Concrete**, Japan, 2008.

# APPENDIX-I

## SOME BASIC PRINCIPLES OF STATISTICS

### **Sample and Population**

The word 'population' is used to refer any collection of objects, actual or conceptual and mainly set of numbers, observations or measurements. In some cases, population is finite and in other cases, it may be infinite.

The aim of statistical enquiry is to find out something about some specified population. If a population is infinite, it is possible to observe all its values, and even if it is finite, it may be impractical or uneconomical to observe all the values. Thus, it is usually necessary to study a selected number of individuals from population and infer from its results pertaining to entire population. This selected number of individuals is called a sample. The sampling should be random in order to apply theory of probability.

### **Sample Mean**

Sample mean of a variate  $x$  is defined as

$$\bar{x} = \frac{1}{n} \sum_{i=1}^n x_i \quad (\text{A1.1})$$

where  $x_1, x_2, \dots, x_n$  is the sequence of the of the observed values of the variate.

### **Standard Deviation**

Standard deviation is defined as the positive square root of the average of squared deviation from the mean given by

$$s = \sqrt{\frac{1}{n-1} \sum_{i=1}^n (x_i - \bar{x})^2} \quad (\text{A1.2})$$

### **Coefficient of Variation**

Coefficient of variation is defined as  $\delta = \frac{s}{\bar{x}}$  which is used as a measure of dispersion.

### **Sample Correlation**

A numerical summary of the tendency of the of the high values of one variable X pairing with the high values of other variable Y or, high values of X pairing with low values of Y is given by the sample covariance given by

$$s_{XY} = \frac{1}{N-1} \sum_{i=1}^N (x_i - \bar{X})(y_i - \bar{Y}) \quad (\text{A1.3})$$

If  $s_{XY} > 0$ , it means that high values of X pair with the high values of Y and if  $s_{XY} < 0$ , the low values of X pair with the high values of Y. The sample correlation coefficient is obtained by normalizing sample covariance with standard deviations. The sample correlation coefficient is given by

$$r_{XY} = \frac{s_{XY}}{s_X s_Y} \quad (\text{A1.4})$$

$r_{XY}$  is a dimensionless quantity and its value varies between  $\pm 1$ . If  $r_{XY} = 1$ , variables are perfectly positively correlated. If  $r_{XY} = -1$ , variables are perfectly negatively correlated. If  $r_{XY} = 0$ , there is no linear dependence between the two variable.

### **Normal Distribution**

Normal distribution is characterized by a single peak with the curve on either side of peak value being symmetrical. This distribution is very important because many random variables of practical interest are normal or can be transformed into normal in a relatively simple fashion. The density function of the normal distribution is given by

$$f(x) = \frac{1}{\sigma\sqrt{2\pi}} e^{-\frac{(x-\mu)^2}{2\sigma^2}}; \quad -\infty < x < \infty. \quad (\text{A1.5})$$

The area under the curve between ordinates, expressed as a fraction of total area under the curve measures the chance that the value of the random variable will lie between given limits.

### **Student's t-distribution**

Application of the theory of large samples requires knowledge of  $(\mu, \sigma)$ . If n is small, normal probability table will not be useful. Student resolved this difficulty by introducing a new distribution. He concerned himself with a variable given by

$$t = \frac{\bar{x} - \mu}{s / \sqrt{N}} \quad (\text{A1.6})$$

where  $s$  is the sample standard deviation.

It has been shown that  $t$ -distribution approaches normal distribution as  $(N-1)$ , called degree of freedom, approaches infinity.

### **Level of Confidence**

One can choose a probability  $p$  close to 100% and determine two quantities  $\theta_1$  and  $\theta_2$  such that probability that  $\theta_1$  and  $\theta_2$  include the exact unknown value of the parameter  $\theta$ , is equal to  $\beta$ . That is  $p(\theta_1 \leq \theta \leq \theta_2) = \beta$ .  $\beta$  is called level of confidence.

### **Level of Significance**

If we reject a hypothesis when it happens to be true, we say that a Type I error has been made. If we accept a hypothesis when it should be rejected, we say that a Type II error has been made. In either case a wrong decision or error in judgment has occurred. In order for any test of hypothesis or decision rules to be good, they must be designed so as to minimize errors of decision. The only way to reduce both type of error is to increase sample size which may or may not be possible.

In testing a given hypothesis, maximum probability with which we would be willing to risk a Type I error is called level of significance. This probability often specified before any samples are drawn, so that the results obtained will not influence the decision taken. In practice, a level of significance 5% or 1% is customary. 5% level of significance means there are about 5% chances that we would reject the hypothesis when it should be accepted i.e. we are about 95% confident that we would make the right decision.

### **Regression Analysis**

In regression analysis, standard error of estimate is used to quantify the spread of the data around the regression line. To do this, total sum of squares around the mean for the dependent variable is calculated and say this is  $S_t$ . This is the magnitude of residual error associated with the dependent variable prior to regression. After performing the regression, one can compute the sum of the squares of residual around the regression line

( $S_r$ ). The difference ( $S_t - S_r$ ) quantifies the error reduction or improvements due to describing the data. Because the magnitude of this quantity is scale dependent, the difference is normalized to  $S_t$  to yield

$$R^2 = \frac{S_t - S_r}{S_t} \quad (\text{A1.7})$$

where  $R^2$  is called coefficient of determination and  $R$  is the coefficient of correlation. For a perfect fit,  $S_r=0$  and  $R^2=1$ , signifying the curve explains 100% of the variability of the data. For  $R^2=0$ ,  $S_t= S_r$ , and the fit represents no improvement. Thus, departure of  $R^2$  from unity is a measure of departure from the relationship between the variables.

